

Wilfrid Laurier University

Scholars Commons @ Laurier

Theses and Dissertations (Comprehensive)

2019

Development and application of hydrological and limnological monitoring in lake-rich landscapes of Canada's subarctic National Parks

Hilary Emma White

Wilfrid Laurier University, whit6210@mylaurier.ca

Follow this and additional works at: <https://scholars.wlu.ca/etd>



Part of the [Environmental Monitoring Commons](#), and the [Hydrology Commons](#)

Recommended Citation

White, Hilary Emma, "Development and application of hydrological and limnological monitoring in lake-rich landscapes of Canada's subarctic National Parks" (2019). *Theses and Dissertations (Comprehensive)*. 2176.

<https://scholars.wlu.ca/etd/2176>

This Dissertation is brought to you for free and open access by Scholars Commons @ Laurier. It has been accepted for inclusion in Theses and Dissertations (Comprehensive) by an authorized administrator of Scholars Commons @ Laurier. For more information, please contact scholarscommons@wlu.ca.

**Development and application of hydrological and limnological
monitoring in lake-rich landscapes of Canada's
subarctic National Parks**

by

Hilary Emma White

B.Sc., Lafayette College, 2010
M.Sc., Acadia University, 2012

DISSERTATION

Submitted to the Department of Geography and Environmental Studies

in partial fulfilment of the requirements for

Doctor of Philosophy in Geography

Wilfrid Laurier University

© Hilary Emma White 2019

Declaration of Co-Authorship/Previous Publication

Co-Authorship Declaration

I hereby declare that I am the principal author of this thesis and that the research to which it refers is the product of my own work. Chapters 2, 3, and 4, which make up the body of this dissertation, contain material that is in preparation for publication. Brent Wolfe, Roland Hall, and Jason Venkiteswaran all contributed expertise and edits for the development of Chapters 2, 3, and 4.

Previous Publication

Appendices A, B, and C are licensed reprints of articles that I am a co-author on.

Abstract

Arctic and subarctic environments are being adversely influenced by human-caused climate change across our entire planet. Canada's northern freshwater ecosystems are influenced by a variety of environmental stressors and are particularly sensitive to climate change, since small shifts in climate have the potential to substantially alter their hydrological, limnological, and biogeochemical conditions. Some other indirect effects on northern freshwater landscapes are the expansion of vegetation as well as changes in wildlife and waterfowl populations and distribution. It is, therefore, critical to understand the observed and predicted influences of climate change and other environmental stressors on these northern freshwater environments dominant in arctic and subarctic landscapes, since they are considered productive northern "oases" and provide important habitat for wildlife and natural resources for indigenous communities.

Concerns have been increasing regarding climate change, rapidly changing lake levels, and the associated effects on aquatic ecological integrity within two of Canada's northern lake-rich national parks, Vuntut National Park (VNP), Yukon Territory, and Wapusk National Park (WNP), Manitoba. To address these issues, Park-led monitoring programs have been established to track status and trends of lake hydrological conditions using water isotopes, yet there remains a need to translate these data into a format that can be used by Parks Canada for their reporting requirements. Here, a novel water isotope-based lake hydrological monitoring program is applied that directly encompasses Parks Canada's long-term monitoring protocols and provides a sensitive way to detect hydrological change. Lake category (VNP - 'snowmelt-dominated', 'rainfall-dominated', or intermediate and WNP - coastal fen, interior peat plateau, or boreal spruce forest) and

season-specific (spring, summer, fall) water isotope-based hydrological thresholds were used to establish the condition ('good', 'fair', 'poor') of Parks Canada's hydrological 'Ecological Integrity Measure' for lakes within these two northern parks. Variability in the condition of VNP monitoring lakes exists between lake category ('rainfall-dominated', 'snowmelt-dominated', intermediate) as well as by season (spring, fall) from 2007 to 2015. However, rainfall-dominated lakes show the most variability in lake condition, spanning from lakes that fall entirely within the 'good' condition to lakes that are almost entirely in 'fair' to 'poor' conditions. In WNP, variability in lake condition exists between lake category (coastal fen, boreal spruce forest, interior peat plateau) and season (spring, summer, fall) from 2010 to 2013. However, during the spring and summer of 2014 and the entire ice-free season of 2015, these lakes improved to 'fair' or 'good' conditions, reflecting an increase in the precipitation/evaporation ratio. This research and monitoring-program development has bridged the gap between research science and Parks Canada monitoring by providing protocols and technical support to establish an effective long-term lake hydrological monitoring program for sensitive northern freshwater environments.

During the past ~40 years, WNP has experienced a rapid increase in Lesser Snow Goose (LSG) population and a corresponding expansion in the LSG-disturbed geographic region. This has raised concerns about environmental effects of their activities on WNP's aquatic ecosystems. Previous studies have found that using standard limnological measurements (e.g., specific conductivity) combined with carbon isotope variables ($\delta^{13}\text{C}_{\text{DIC}}$, $\delta^{13}\text{C}_{\text{PHYTOPOM}}$, $\Delta^{13}\text{C}_{\text{DIC-PHYTOPOM}}$) is informative and effectively captures differences in limnological and carbon behaviour in LSG-disturbed ponds compared to

unaffected ponds. This research compiles mid-summer limnological and carbon isotope data from 45 lakes during 2015 and 2016, which span a LSG disturbance gradient (undisturbed, actively-disturbed, severely-disturbed) across a portion of WNP. In 2015, higher mid-summer values of specific conductivity, pH, TP, TKN, DIC, DOC, and $\delta^{13}\text{C}_{\text{PHYTOPOM}}$ paired with lower mid-summer values of $\delta^{13}\text{C}_{\text{DIC}}$ and $\Delta^{13}\text{C}_{\text{DIC-PHYTOPOM}}$ values were characteristic of severely-disturbed ponds when compared to undisturbed and actively-disturbed ponds. Results from 2016 indicate a clear LSG disturbance gradient with increasing values of specific conductivity, pH, TP, TKN, DIC, DOC, and $\delta^{13}\text{C}_{\text{PHYTOPOM}}$ paired with decreasing values of $\delta^{13}\text{C}_{\text{DIC}}$ and $\Delta^{13}\text{C}_{\text{DIC-PHYTOPOM}}$, as LSG disturbance increased from undisturbed to actively-disturbed to severely-disturbed ponds. Reduced sensitivity to LSG disturbance during 2015 can be attributed to substantial rainfall that occurred during the month of July prior to and during sampling. These limnological trends can be explained by an array of processes including chemically-enhanced CO_2 invasion, elevated catchment runoff of nutrients, carbon and ions, as well as enhanced aquatic productivity, which increasingly influenced the nutrient and carbon balance of ponds along a LSG disturbance gradient. A numerical synthesis of the data identified established (by La Perouse Bay), active (the landscape to the north and northwest of Thompson Point), and emerging (the inland area in the southern portion of the study region) areas of LSG disturbance. Continued monitoring of LSG disturbance within WNP is critical to understand how freshwater environments in WNP will respond to historical, active, and new LSG disturbance. The analyses and interpretations presented in this research will serve as a useful tool for Parks Canada staff to monitor aquatic ecosystem trends and status as LSG population and migration patterns continue to evolve.

Monitoring and anticipating lake hydrological and limnological change is challenging in the north due to its remoteness and the sensitivity of shallow lakes and ponds to multiple environmental stressors. Often, due to the lack of alignment and effective communication of research priorities between southern researchers and northern agencies, the short duration of funding, as well as the high turnover rates of staff and graduate students, the science and training necessary to create the foundations for agency-led monitoring is not always feasible. However, by means of substantial efforts to augment relations with Parks Canada staff, a long-term lake monitoring program within Wapusk National Park (the ‘Hydroecology Monitoring Program’) was successfully established in 2015. These efforts included instilling the significance of our research to Park’s staff and the local community of Churchill, providing the necessary training and knowledge transfer, as well as offering ongoing assistance and guidance. This monitoring program has been developed in a format that aligns with Parks Canada’s mandate, can be utilized for their reporting requirements, and is designed to focus on two major threats to aquatic ecosystems: 1) Pond Water Dynamics/Lake Hydrology monitoring and 2) Goose Aquatic Impact monitoring. Several key contributions transformed this research science into action and application. These include operationalizing agency-led monitoring (e.g., creation of training schematics and standard operating procedures), communicating monitoring results with science practitioners (e.g., scientific reports and open-access data), and communicating research with the general public (e.g., news articles, public presentations, and the Expedition Churchill interactive platform). In summary, research presented here is a contribution to the new research paradigm in northern Canada, where

collaborative, interdisciplinary, and community-driven research reflects northern priorities and leads to action.

Acknowledgements

I am grateful for the generous financial support that I have received during my graduate program from Wilfrid Laurier University and through a NSERC scholarship. My research has been financially supported by the NSERC grants (Discovery, Northern Research Supplement, Discovery Frontiers), the Polar Continental Shelf Program, Parks Canada, the Churchill Northern Studies Centre, and the Polar Knowledge Canada. I would like to thank the University of Waterloo Environmental Isotope Laboratory, the Macrae Lab, and the National Laboratory for Environmental Testing, especially Xiaowa Wang, for analyzing samples included in this thesis.

I would like to thank Chantal Ouimet, Melissa Gibbons, and Matthew Webb from Parks Canada for their support, advocacy, and hard work to operationalize our research methods into Wapusk National Park's monitoring program. It has been an incredible experience to work alongside you all through both the challenges and successes of creating the monitoring program! Thank you to all of the Parks Canada bear monitors I have had over the years as well as Joan Brauner and her team of Hudson Bay Helicopter pilots; I appreciate that you were dedicated to looking out for me, always lending a helping hand, and making field work the best possible experience.

I would also like to give a huge shout out to the Churchill Northern Studies Centre and everyone who works there. Not only have you made the many years of fieldwork logistically easy and enjoyable, but you have all been a tremendous support for me personally. In particular, I want to thank LeeAnn Fishback; your mentorship, support, and friendship have been some of the most valuable things that I have received

throughout my Ph.D. I am so incredibly grateful for the opportunities you have provided me and would not be the person I am today without you.

I would also like to thank the following people who have made the completion of this thesis possible, specifically my supervisor, Brent Wolfe. Thank you for the opportunity to complete this thesis, conduct fieldwork in amazing locations, and present my research at many conferences. I have appreciated all of the knowledge you have passed on to me, the help you have provided, and the patience and many edits you have given me throughout the years. Roland, thank you for all your edits, comments, and suggestions. My thesis would not be where it is today without your guidance. Jason, thank you for getting me through the last hurdles of this Ph.D. process. Thank you for putting up with all of my statistics and R questions and for teaching me about the passive voice and how water samples really should not be collected by zombies! Thank you to Lauren MacDonald, Stephanie Roy, and all those who helped with lab and fieldwork for this thesis.

Finally, I would like to thank my family and friends for their unfailing love and encouragement and for always believing in me. Mom and Dad, there have been some hard times throughout my Ph.D. and I know that I would not have made it through the process without your constant support and belief that I could achieve this. I love you both so much. Meghan, thank you for being my role model, for encouraging me to pursue my goals, and for always editing anything I needed, no matter what. Jessey, thank you for keeping me sane and for all the love, support, and laughter every single day.

Statement of Originality

I declare that the work presented here is original and the result of my own research, except as acknowledged, and has not been submitted, either in part or whole, for a degree as this or any other University. Ideas taken from other sources are cited as such.

Table of Contents

Declaration of Co-Authorship/Previous Publications	ii
Co-Authorship Declaration	ii
Previous Publication	ii
Abstract	iii
Acknowledgements	viii
Statement of Originality	x
Table of Contents	xi
List of Figures	xiv
List of Tables	xvii
Chapter 1: Introduction	1
1.1 Objectives and Approach	5
1.2 Outline of Thesis	6
Chapter 2: Establishing water isotope-derived thresholds to assess the hydrological condition of lake-rich landscapes of Canadian subarctic National Parks	8
2.1 Introduction	8
2.2 Study Areas	11
Old Crow Flats – Vuntut National Park	11
Meteorological Conditions	13
Western Hudson Bay Lowlands – Wapusk National Park	15
Meteorological Conditions	16
2.3 Methods	17
Water isotope sampling and framework development	17
E/I ratios and hydrological threshold development	20
2.4 Results and Interpretations	22
Old Crow Flats – Vuntut National Park	22
Developing an isotope framework	22
Lake hydrological variability	22
Monitoring lake hydrological conditions using bootstrapped E/I thresholds	23
Western Hudson Bay Lowlands – Wapusk National Park	25
Developing an isotope framework	25
Lake hydrological variability	25
Monitoring lake hydrological conditions using bootstrapped E/I thresholds	26

2.5 Discussion	29
Development of novel hydrological thresholds using water isotopes to monitor the Ecological Integrity of northern shallow lakes	29
Integration of novel thresholds to assess the hydrological ‘Ecological Integrity Measure’ condition within two subarctic Canadian National Parks	32
2.6 Conclusions and Recommendations	34
2.7 Figures	37
2.8 Tables	52
2.9 Chapter 2 Appendix	57
Isotope framework	57
Bootstrapping statistical analysis	61
Chapter 3: Use of water chemistry and carbon isotopes to assess effects of Lesser Snow Geese disturbance on lakes in Wapusk National Park, northern Manitoba	67
3.1 Introduction	67
3.2 Study Area	70
Lake locations and LSG disturbance classification	70
Meteorological Conditions	71
3.3 Methods	72
Hydrology	72
Limnology and carbon behaviour	72
Numerical and statistical analyses	74
Spatial interpolation	75
3.4 Results	77
Hydrology	77
Comparison of limnological conditions and carbon behaviour among LSG-disturbance categories	77
Spatial interpolation	80
3.5 Discussion	82
Variation of limnological conditions and carbon behaviour in relation to LSG disturbance	83
Spatial patterns of LSG disturbance	86
3.6 Conclusions and Recommendations	89
3.7 Figures	92
3.8 Tables	101
3.9 Chapter 3 Appendix	106
Chapter 4: Translating science into a sustainable, long-term monitoring program	110
Operationalizing agency-led monitoring	113

4.A. Sample of generated SOPs for Parks Canada	117
Communicating monitoring results with science practitioners	131
4.B. 2018 Pond Water Dynamics/Lake Hydrology Report	132
4.C. 2017 Goose Aquatic Impact Report	163
4.D. Open access data	179
1. Pond Water Dynamics/Lake Hydrology public data	179
2. Goose Aquatic Assessment public data	180
Communicating research with the general public	181
4.E. Wapusk News, Issue 7, 2014	182
Chapter 5: Conclusions and Recommendations	183
5.1 Synthesis of key contributions	184
5.2 Final Comments and Recommendations	188
References	191
Appendix A	204
Bouchard et al., 2013	204
License	210
Appendix B	211
MacDonald et al., 2017	211
License	243
Appendix C	244
Hadley et al., 2019	244
License	260

List of Figures

Figure 2.1: Study site map of Old Crow Flats, Yukon Territory	37
Figure 2.2: Vuntut National Park meteorological data	38
Figure 2.3: Study site map of Wapusk National Park	39
Figure 2.4: Wapusk National Park meteorological data	40
Figure 2.5: A schematic $\delta^{18}\text{O}$ - $\delta^2\text{H}$ diagram illustrating two hypothetical lakes, from Tondu et al. (2013), p. 601	41
Figure 2.6: Three-year mean Local Evaporation Line for Vuntut National Park	42
Figure 2.7: Isotope composition of Vuntut National Park monitoring lakes (δ_{L}) superimposed on the 3-year monitoring isotope framework for each sampling year (2007-2015)	43
Figure 2.8: Vuntut National Park E/I results for the spring sampling period	44
Figure 2.9: Vuntut National Park E/I results for the fall sampling period	45
Figure 2.10: Evolution of water d18O sampled from Churchill evaporation pan	46
Figure 2.11: Three-year mean Local Evaporation Line for Wapusk National Park	47
Figure 2.12: Isotope composition of Wapusk National Park monitoring lakes (δ_{L}) superimposed on the 3-year monitoring isotope framework for each sampling year (2010-2015)	48
Figure 2.13: Wapusk National Park E/I results for the spring sampling period	49
Figure 2.14: Wapusk National Park E/I results for the summer sampling period	50
Figure 2.15: Wapusk National Park E/I results for the fall sampling period	51
Figure 2.A1: Sample of a bootstrapped dataset (Wapusk National Park June Coastal Fen)	61

Figure 2.A2: Figures depicting that the three-year threshold calculations are accurate representations of the data for Vuntut and Wapusk National Parks	62
Figure 3.1: Study site map of Wapusk National Park and corresponding information regarding Lesser Snow Geese	92
Figure 3.2: Photographs depicting the gradient of LSG disturbance within Wapusk National Park	93
Figure 3.3: Wapusk National Park meteorological data	94
Figure 3.4: $\delta^{18}\text{O}$ - $\delta^2\text{H}$ graphs showing lake water isotope values for July 2015 and 2016	95
Figure 3.5: Principal components analysis ordination biplot comparing limnological conditions among lakes in the three categories of Lesser Snow Goose disturbance for July 2015 and 2016	96
Figure 3.6: Boxplots depicting 2015 and 2016 data for limnological parameters; a) conductivity, b) pH, c) TP, d) TKN, e) DIC, f) DOC, g) $\delta^{13}\text{C}_{\text{DIC}}$, h) $\delta^{13}\text{C}_{\text{PHYTOPOM}}$	97
Figure 3.7: a) Boxplots depicting $\Delta^{13}\text{C}_{\text{PHYTOPOM}}$ values for 2015 and 2016, b) $\delta^{13}\text{C}_{\text{DIC}}$ vs. $\delta^{13}\text{C}_{\text{PHYTOPOM}}$ depicting the 20‰ offset representing the theoretical value of photosynthetic isotopic fractionation	98
Figure 3.8: Maps showing the 2015 and 2016 inverse-distance-weighted interpolation values of conductivity, TP, TKN, $\delta^{13}\text{C}_{\text{DIC}}$, and $\delta^{13}\text{C}_{\text{PHYTOPOM}}$	99
Figure 3.9: Map showing the inverse-distance-weighted interpolations of scaled values for 2016	100
Figure 4.1: Schematic depicting hydrological processes that influence lake water isotope composition	114

Figure 4.2: Schematic depicting the difference in nutrient concentrations, carbon isotope compositions of dissolved inorganic carbon, and pond conductivity resulting from catchment erosion, in response to LSG disturbance	115
Figure 4.3: Schematic showing the organization of Wapusk National Park's Hydroecology Monitoring Program Standard Operating Procedures	116

List of Tables

Table 2.1: Vuntut National Park precipitation values	52
Table 2.2: Wapusk National Park precipitation values	53
Table 2.3: Vuntut and Wapusk National Parks three-year E/I ratio thresholds	54
Table 2.4: Summary of Vuntut National Park E/I values per lake per season from 2007 to 2015	55
Table 2.5: Summary of Wapusk National Park E/I values per lake per season from 2010 to 2015	56
Table 2.A1: Select lake characteristics for Vuntut National Park	63
Table 2.A2: Select lake characteristics for Wapusk National Park	64
Table 2.A3: Modified from Tondu et al. (2013), flux weighted ice-free season temperatures and relative humidity based on data from the Old Crow Airport weather station, as well as parameters used to construct the three-year average isotope framework for Vuntut National Park lakes	65
Table 2.A4: Flux weighted ice-free season temperatures and relative humidity based on Environment and Climate Change Canada Historical Weather data from the Churchill Airport weather station, as well as parameters used to construct the three-year average isotope framework for Wapusk National Park lakes	66
Table 3.1: Field-based classification used to distinguish the three categories of Lesser Snow Goose disturbance to lakes in Wapusk National Park	101
Table 3.2: Wapusk National Park precipitation values compared to 1971-2000 climate normals	102
Table 3.3: Results of the analysis of similarity (ANOSIM) pairwise test between the three Lesser Snow Goose disturbance categories for 2015 and 2016	103

Table 3.4: P-values from Kruskal-Wallis tests that compared values of limnological variables among lakes within the Lesser Snow Goose disturbance categories for 2015 and 2016	104
Table 3.5: P-values from post-hoc Dunn’s test to determine which specific lake categories were significant from the others in 2015 and 2016	105
Table 3.A1: Key July 2015 field observations and conductivity values of Lesser Snow Goose disturbance for the 45 sampling lakes within Wapusk National Park	106
Table 3.A2: Key July 2016 field observations and conductivity values of Lesser Snow Goose disturbance for the 45 sampling lakes within Wapusk National Park	108

Chapter 1: Introduction

Globally, arctic and subarctic environments are being adversely influenced by human-caused climate change. In these northern regions, feedbacks between the loss of snow and ice and the absorption of solar radiation regionally amplify the global warming signal, resulting in warming trends four or more times greater than the global average (IPCC, 2014; Bush and Lemmen, 2019). During the past century, the circumpolar North has experienced some of the greatest regional warming compared to other areas of the world, which has substantial impacts on hydrological conditions, permafrost dynamics, and the overall stability of arctic and subarctic landscapes (ACIA, 2004; IPCC, 2014). Freshwater resources within Canada's North, although relatively isolated from direct human activity, are influenced by a variety of environmental stressors and are particularly sensitive to climate change. Small shifts in climate have the potential to substantially alter their hydrological, limnological, and biogeochemical conditions (Rouse et al., 1997; ACIA, 2004; Prowse et al., 2006; Schindler and Smol, 2006; IPCC, 2014). Recent studies have predicted that climate warming will have the greatest effects on the limnological and biogeochemical processes of northern freshwater environments (e.g., wetlands as well as lakes and ponds, hereafter referred to as lakes) through the modification of hydrological processes, not just through the temperature rise itself (Rouse et al., 1997; Prowse et al., 2006; Schindler and Smol, 2006). Some other indirect effects on northern freshwater landscapes are the expansion of vegetation (e.g., Tape et al., 2006; Mamet and Kershaw, 2012) and changes in wildlife and waterfowl populations and distribution (e.g., Abraham et al., 2005a; Luoto et al., 2014). It is, therefore, critical to understand the observed and predicted influences of climate change and other environmental stressors on

these northern freshwater environments dominant in arctic and subarctic landscapes, since they are considered productive northern “oases” and provide important habitat for wildlife and natural resources for indigenous communities (Rouse et al., 1997; Prowse et al., 2006).

Northern freshwater ecosystems remain among the least studied due to the scarcity of long-term monitoring data (Smol, 2002). This is critical since one of the predominant concerns for these freshwater ecosystems is the current and future state of water quality and quantity, especially in relation to climate change. Some key climate drivers of hydrological change include permafrost thaw as well as changes in the duration and amount of snow and ice cover, the proportions of rain and snow, and thaw season evaporation-to-precipitation ratios (Rouse et al., 1997; Prowse et al., 2006; Schindler and Smol, 2006). Scientists have recently begun to examine the responses of northern freshwater ecosystems to climate change across the subarctic and Arctic (e.g., MacDonald et al., 2017), as well as in Siberia (e.g., Smith et al., 2005), Nunavut (e.g., Smol and Douglas, 2007), Northwest Territories (e.g., Brock et al., 2010), Alaska (e.g., Riordan et al., 2006), Yukon Territory (e.g., Labrecque et al., 2009; Turner et al., 2010), and the Hudson Bay Lowlands (Bouchard et al., 2013; Rühland et al., 2013, MacDonald et al., 2015). They find that northern freshwater landscapes are reacting differently to climate change forcing and are becoming increasingly dynamic, with lake expansion increasing in some regions and lake-water levels decreasing in other locations (Yoshikawa and Hinzman, 2003; Smith et al., 2005; Riordan et al., 2006; Smol and Douglas, 2007; Labrecque et al., 2009; MacDonald et al., 2017). Many of these freshwater ecosystems have also shown an increase in lake productivity in response to

longer ice-free seasons and a corresponding increase in lake evaporation (e.g., Rühland et al., 2003; Antoniadou et al., 2005, Rühland and Smol, 2005). However, as previously mentioned, there is a paucity of long-term monitoring programs and many of the existing programs that monitor northern freshwater lakes rely on labour-intensive and expensive techniques that are generally not feasible on large spatial scales in remote landscapes (i.e., gauged inflow and outflow, lysimeters; Gilvear and Bradley, 2000; Karlsson et al., 2011). These long-term data are critical to better understand how hydrological and limnological conditions have and will continue to respond to climate change and there is need to translate southern scientists and researchers' priorities into sustainable monitoring programs that can be carried out by northern science practitioners (e.g., Parks Canada, community members).

To address complexities of climate change, concerns about rapidly changing lake levels, and associated effects on ecological integrity, ongoing multi-disciplinary lake monitoring projects have been initiated in collaboration with Parks Canada staff from two subarctic Canadian National Parks: Vuntut National Park (VNP) and Wapusk National Park (WNP). Both VNP and WNP contain abundant shallow lakes, which are dominant features in these northern freshwater landscapes. Substantial lake water isotope hydrology datasets have now been generated for both national parks (since 2007 in VNP; since 2010 in WNP). The legacy of these datasets is evidenced by Parks Canada staff-led water isotope sampling of a subset of lakes in VNP (since 2012) and WNP (since 2015), in partnership with university-based researchers. These complete hydrological datasets are important components of this thesis and help translate our research priorities into

long-term, sustainable monitoring programs to track the hydrological and limnological conditions of northern freshwater ecosystems in response to climate change.

Long-term monitoring datasets for northern freshwater ecosystems are also increasingly critical due to the mounting concerns regarding multiple and interacting environmental stressors. One of these concerns is related to the environmental consequences of changes in wildlife and waterfowl populations and distributions. Waterfowl population expansions in particular, can act as an environmental stressor and change the functioning and structure of northern freshwater ecosystems through eutrophication brought on by changes in vegetation, nutrient sources and cycling (Rühland et al., 2003; Gregory-Eves et al., 2004; Abraham et al., 2005a; Smol and Douglas, 2007; Côté et al., 2010; MacDonald et al., 2014; 2015). The effects of waterfowl in northern freshwater ecosystems lead to varying degrees of disturbance associated with changes in productivity and nutrient concentrations (Michelutti et al., 2009; 2010; Côté et al., 2010; Sun et al., 2013; MacDonald et al., 2014). The supply of nutrients due to waterfowl disturbance has the potential to increase these freshwater ecosystems' productivity and alter the role that they play in the global carbon cycle. Very few studies have examined the dual effects of climate warming and waterfowl expansion, which could have drastic impacts on the integrity of northern freshwater ecosystems. Thus, a major component of this thesis is to address lake monitoring needs stemming from recent exponential growth of Lesser Snow Goose (LSG; *Chen caerulescens caerulescens*) populations within WNP. During the past ~40 years, there has been a rapid increase (5-14% per year) in the population density and nesting area range of the Lesser Snow Goose within Wapusk National Park (Batt et al., 1997; Jefferies et al., 2006;

Alisauskas et al., 2011; Peterson et al., 2013). This region has also experienced some of the greatest warming in the circumpolar North during the past ~50 years (Smith and Burgess, 2004; Kaufman et al., 2009; Hochheim et al., 2010), which has the potential to exacerbate LSG-disturbance on the Hudson Bay Lowlands landscape. Parks Canada (2011) acknowledged that the combination of expanding LSG population and climate warming may drastically alter the ecological integrity of lakes in WNP, emphasizing the need for effective aquatic ecosystem monitoring.

1.1 Objectives and Approach

To understand future environmental (hydrological, limnological, carbon behaviour) changes in northern freshwater ecosystems in response to multiple environmental stressors (e.g., climate change and waterfowl expansion), current research and continued monitoring is required. As identified, there are research gaps that require new knowledge to fully assess and monitor the effects of climate warming and waterfowl population expansion within Canada's northern subarctic National Parks. Additionally, there is a need to adopt a new research paradigm, where collaborative, interdisciplinary, and community-driven research reflects northern priorities and leads to action. This research focuses on work completed within Vuntut National Park, northern Yukon Territory and Wapusk National Park, northern MB. Using a variety of approaches that are outlined in detail within each chapter (e.g., field observations, water isotopes, limnological and carbon isotope data, and spatial interpolation), my research addresses through the following objectives:

- 1) To track hydrological conditions within two of Canada's subarctic National Parks by developing and applying novel lake hydrological thresholds in order to establish hydrological 'Ecological Integrity Measure' conditions (good, fair, poor) in a manner congruent with Parks Canada's established 'Ecological Integrity Indicator' system.
- 2) To characterize how lake hydrology, limnology, and carbon behaviour vary spatially across a gradient of Lesser Snow Goose disturbance within a portion of Wapusk National Park and to identify spatial patterns and degree of Lesser Snow Goose disturbance within Wapusk National Park's freshwater ecosystems.
- 3) To ensure that the research results generated to address the previous objectives are translated into sustainable, collaborative, long-term monitoring programs and to advocate the importance of fostering relationships and communicating science with local science practitioners (e.g., Parks Canada), local community organizations, and the general public.

1.2 Outline of Thesis

This thesis is organized into chapters that correspond to several distinct scientific studies. The introduction, Chapter 1, provides a broad overview of themes discussed throughout the thesis; specifically, the hydrology and limnology of subarctic freshwater systems in response to climate change and other environmental stressors (e.g., waterfowl disturbance). Chapters 2 through 4 are the results, exploration, and application of direct field and laboratory-based research focused on the hydrology and limnology of several lakes within Canada's subarctic. The assessment of hydrological conditions of lake-rich landscapes within two of Canada's subarctic National Parks (Vuntut National Park and

Wapusk National Park) in response to climate change is presented in Chapter 2, addressing objectives 1 and 3. Chapter 3 focuses on the use of water chemistry and carbon isotopes to assess the effects of another environmental stressor, Lesser Snow Geese disturbance, on lakes in Wapusk National Park, addressing objectives 2 and 3. Chapter 4 addresses objective 3 and discusses the importance of translating science into action and the various ways I have achieved this goal; through operationalizing agency-led monitoring, communicating monitoring results with science practitioners, and communicating research with the general public. The final chapter, Chapter 5, contains concluding remarks, synthesizes the key contributions of this research, and includes general recommendations for the future.

Chapter 2: Establishing water isotope-derived thresholds to assess the hydrological condition of lake-rich landscapes of Canadian subarctic National Parks

2.1 Introduction

Shallow lakes, many of which are thermokarst in origin, are often abundant within arctic and subarctic landscapes. These landscapes are considered highly productive northern oases, providing necessary resources and habitat for a variety of wildlife as well as supporting the traditional lifestyles of Indigenous cultures (Rouse et al., 1997; Prowse et al., 2006). However, these freshwater resources are particularly sensitive to climate change, which is causing pronounced variation in hydrological conditions (Smith et al., 2005; Smol et al., 2005; Schindler and Smol, 2006; Prowse et al., 2006; Riordan et al., 2006; Labrecque et al., 2009; Avis et al., 2011; Carroll et al., 2011). Declines have been observed in both the abundance and size of lakes due to warmer temperatures, longer ice-free seasons, and increased evaporation (Labrecque et al., 2009; Turner et al., 2010; Bouchard et al., 2013). These climatological changes have also led to increasing permafrost thaw with the potential of rapid lake drainage events (Wolfe and Turner, 2008; Marsh et al., 2009; Jones et al., 2011). However, increases in lake surface area have been reported, also driven by permafrost thaw (Payette, 2004; Smith et al., 2005). Additionally, below average snow accumulation has been documented in lake-rich subarctic landscapes (Schindler and Smol, 2006; Bouchard et al., 2013). If snowmelt supply is diminished and prolonged dry conditions become more frequent due to

pronounced climate warming and longer ice-free seasons, widespread mid-summer landscape drying, reduced water levels, and lake desiccation may occur.

Detecting and anticipating the varying hydrological responses to climate warming are challenging in northern landscapes due to the rapid rate of changes and remoteness, which impedes conventional monitoring approaches. Large-scale, northern hydro-ecological monitoring programs are few in number and many existing long-term programs monitoring freshwater lakes rely on labour-intensive and expensive techniques that are generally not feasible on large spatial scales in remote landscapes (e.g., gauged inflow and outflow, lysimeters; Gilvear and Bradley, 2000; Karlsson et al., 2011). Alternatively, previous research has successfully demonstrated the use of water isotopes ($\delta^{18}\text{O}$, $\delta^2\text{H}$) to characterize variations in lake water balance within remote locations (e.g., Gibson and Edwards, 2002; Tondu et al., 2013, MacDonald et al., 2017). The oxygen and hydrogen isotope compositions of water vary in a systematic and predictable manner as water passes through the hydrological cycle (Clark and Fritz, 1997; Edwards et al. 2004). Water isotopes can be used as a practical and affordable monitoring tool to track hydrological conditions and drivers at the landscape scale since samples can be easily collected in the field, and the analyses are broadly applicable, sensitive, and diagnostic of changes in lake water balance and the source of input waters (Gibson and Edwards, 2002; Brock et al., 2007; Wolfe et al., 2007b; Turner et al., 2010; Tondu et al., 2013; Anderson et al., 2013; Brooks et al., 2014).

To address complexities of climate change, concerns about rapidly changing lake levels, and associated effects on ecological integrity, ongoing multi-disciplinary lake monitoring projects have been initiated in collaboration with Parks Canada staff from two

subarctic Canadian National Parks: Vuntut National Park (VNP) and Wapusk National Park (WNP). Both VNP and WNP contain abundant shallow lakes, which are dominant features in these thermokarst landscapes. Components of water isotope hydrological monitoring in VNP and WNP, such as lake selection and frequency of sampling, were based on a suite of lake isotope hydrology studies designed to identify the range of lake water balances and their sensitivity to catchment characteristics and meteorological conditions (Turner et al. 2010, 2014; Bouchard et al. 2013; Tondu et al. 2013; MacDonald et al. 2017). The legacy of these studies are evidenced by Parks Canada staff-led water isotope sampling of a subset of lakes in VNP (since 2012) and WNP (since 2015), in partnership with university-based researchers. Substantial lake water isotope hydrology datasets have now been generated for both national parks (since 2007 in VNP; since 2010 in WNP).

In 2011, Parks Canada established a greater emphasis on developing sustainable monitoring programs with a commitment to maintain or restore ecological integrity in national parks (Parks Canada, 2011). Evaluation of ecological integrity centers on the assessment of approved park ‘Ecological Integrity Indicators’ that represent the major ecosystems in each park, park approved ‘Ecological Integrity Measures’ within each major park ecosystem (e.g., water quality, hydrology), and the condition of each ‘Ecological Integrity Measure’ (‘good’, ‘fair’, ‘poor’). Although prior lake isotope hydrology studies have been conducted in VNP and WNP, with Parks Canada listed as a partner and co-author (e.g., Tondu et al., 2013; MacDonald et al., 2017), research has yet to align the science outcomes to directly encompass Parks Canada’s long-term monitoring protocols and terminology. Therefore, effort is still required to bridge the gap

between scientific research results and sustainable government-led monitoring programs at a more operational level. This study advances the application of previous isotope-based lake hydrological studies by reporting and evaluating data in a manner that is congruent with Parks Canada's established 'Ecological Integrity Indicator' system.

The three main objectives of this research are to 1) develop novel lake hydrological thresholds using evaporation/inflow ratios determined from measurement of lake water isotopes, 2) apply these novel thresholds to establish the condition ('good', 'fair', 'poor') of the hydrological 'Ecological Integrity Measure' for lakes within two subarctic Canadian national parks, and 3) suggest improvements to ensure this approach meets the goals of an effective, collaborative, long-term hydrological monitoring program for these subarctic Canadian national parks.

2.2 Study Areas

OLD CROW FLATS – VUNTUT NATIONAL PARK

The Old Crow Flats (OCF; 68°N, 140°W), located in northern Yukon Territory, is a vast freshwater landscape (5600 km²) containing over 2,500 shallow thermokarst lakes that are considered an important refuge for arctic wildlife while also supporting the lifestyle of the Vuntut Gwitchin First Nation (VGFN) (Figure 2.1). OCF was a large region of Beringia that remained unglaciated and was inundated by Glacial Lake Old Crow during the Last Glacial Maximum. This ancient lake deposited a thick layer of fluvial and glaciolacustrine sediments (Hughes, 1972; Lauriol et al., 2002; Zazula et al., 2004). The glacial lacustrine plain has been incised by the meandering Old Crow River and has left the river valley 40-50 m below a plateau of "perched" mainly thermokarst

lakes underlain by continuous permafrost (Yukon Ecoregions Working Group, 2004; Labrecque et al., 2009; Roy-Léveillé and Burn, 2011; Tondu et al., 2013).

Spatially complex patterns due to topographic variability and ongoing thermokarst cycles including lake formation, expansion, and drainage have been identified (Yukon Ecoregions Working Group, 2004). Vegetation and land cover have been broadly categorized using Landsat imagery by Turner et al. (2014). OCF is characterized by 37% dwarf shrub tundra vegetation (e.g., Labrador tea, arctic marsh grass, water sedges, horsetails, sphagnum mosses and lichens) located mainly in drained lake beds and polygonal peatlands. Well-drained areas made up of coniferous and deciduous forests (e.g., black and white spruce) account for 13% of the landscape, and 25% of the landscape is covered by tall shrub tundra species (e.g., willows and shrub birch). The remaining area consists of abundant shallow lakes that provide habitat for communities of aquatic vegetation (Yukon Ecoregions Working Group, 2004).

Vuntut National Park (VNP) was established in 1995 to conserve and protect a portion of the North Yukon Natural Region as part of the Vuntut Gwitchin First Nation (VGFN) Final Agreement and is co-managed by Parks Canada, the Vuntut Gwitchin Government, and the North Yukon Renewable Resources Council (Parks Canada, 2009). Observations and traditional knowledge of the VGFN indicate that the OCF has been undergoing rapid changes in temperature, precipitation, vegetation cover, lake and river water levels, along with changes in the diversity and distribution of wildlife (Wolfe et al., 2011b). To address the complexities of climate change in northern landscapes and the concerns about rapidly changing lake levels with the associated effects on ecological integrity, a multidisciplinary project supported by the Government of Canada

International Polar Year program was initiated in 2007 to study the physical and biological components of the OCF. An important outcome was the development of a hydrological monitoring program based on five years of water isotope data (2007-2011) from 14 lakes (Tondu et al., 2013). These 14 lakes (Table 2.A1) are situated in catchments that are representative of OCF land-cover and hydrological diversity and have been categorized as: ‘rainfall-dominated’, ‘snowmelt-dominated’, and ‘intermediate’ based on the main source of input water (Turner et al., 2010; Tondu et al., 2013). Eleven of these lakes are situated within VNP and the rest are located within the VGFN Special Management Area; however, hereafter the data set will be referred to as VNP for ease and consistency in reporting (Figure 2.1). Note that prior publications have listed these lakes as ‘OCF XX’ (e.g., Turner et al., 2010, 2014, Tondu et al. 2013).

Meteorological Conditions

Meteorological conditions for this region have been monitored at the Old Crow airport and show marked seasonal variations in temperature and precipitation (Figure 2.2; Table 2.1; Environment Canada, 2019). A sampling ‘year’ has been defined as October to September to capture full winter and summer records. Based on 1971-2000 climate normals, average annual temperature is -9.0°C and temperature fluctuates substantially between summer and winter seasons. Average annual precipitation is 265.5 mm, 62% of which falls as rain between May and September (165.5 mm), while the remainder falls as snow between October and April (100 mm). The monthly mean temperatures during the study period (2007-2015) were comparable to the 1971-2000 climate normals. Maximum

monthly summer temperatures were, on average 0.4°C warmer during the study period, while maximum monthly winter temperatures were, on average, 0.3°C cooler.

Total annual precipitation records (Figure 2.2; Table 2.1) were not consistently recorded over the study period, with some missing data between 2006 and 2014, thus hampering comparisons. Total annual precipitation was variable between 2007 and 2015 with several years comparable to climate normals (2006-2007: 230.6 mm; 2008-2009: 239.5 mm; 2012-2013: 223.7 mm; and 2014-2015: 250.9 mm). There were also two wet years in 2009-2010 and 2010-2011 (320.6 mm and 388.5 mm, respectively) and two dry years in 2007-2008 and 2011-2012 (189.2 mm and 185.8 mm, respectively).

Seasonal precipitation was divided into 1) winter precipitation, defined as predominantly snowfall between the months of October and April and 2) summer precipitation, consisting of predominantly rainfall between the months of May and September. Winter precipitation during 2006-2007 (115.9 mm), 2008-2009 (91.8 mm), and 2014-2015 (81.7 mm) were comparable to climate normals (100 mm). However, except for one wet winter (2010-2011; 183.9 mm), the remaining winters, 2007-2008 (27.2 mm), 2009-2010 (50.4 mm), 2011-2012 (70.1 mm), and 2012-2013 (64.1 mm), had drier winter conditions as compared to climate normals. Summer precipitation during 2007-2008 (162.0 mm), 2008-2009 (147.4 mm), 2012-2013 (159.6 mm), and 2014-2015 (169.2 mm) were comparable to climate normals (165.5 mm). There were two wet summers (2009-2010 – 270.2 mm; 2010-2011 – 204.2 mm) and two dry summers (2006-2007 – 114.7 mm; 2011-2012 – 115.7 mm) compared to the climate normals.

WESTERN HUDSON BAY LOWLANDS – WAPUSK NATIONAL PARK

The western Hudson Bay Lowlands (HBL) is a low-relief landscape between the latitudes of 51° and 65° North and spans the transition from boreal forest in the south to Arctic tundra vegetation in the north (Rouse, 1991; Griffis et al., 2000; Duguay and Lafleur, 2003). The landscape developed following the end of the Wisconsinan Glaciation and the retreat of the Laurentide Ice Sheet (Dredge and Nixon, 1992; Klinger and Short, 1996). As deglaciation took place, the formation of prehistoric Hudson Bay, the Tyrrell Sea, occurred and fine-grained glaciolacustrine sediment was deposited above the dolomitic limestone bedrock. Upon retreat of the ice sheet, the ice-free land began to rebound. This isostatic rebound led to the recession of the Tyrrell Sea and development of the current landscape with visible beach ridges near the coast. Rates of isostatic rebound are ~1.3 m per century (Lambert et al., 2001).

Since this region is underlain by continuous and discontinuous permafrost and impermeable silt-clay soils (post-glacial Tyrrell Sea deposits), water infiltration is impeded, which leads to water pooling at the surface, creating extensive wetlands as well as thousands of lakes (Rouse, 1991; Griffis et al., 2000). Wapusk National Park (WNP) was established in 1996 to protect a representative portion of the western HBL (~11,475 km²), which contains the world's second largest contiguous wetland (Figure 2.3). The park has been divided into six unique physiographic ecotypes: coastal fen, coastal ridges and fen, transitional fen, coastal forested fen, interior peat plateau, and forested peat plateau (Parks Canada, 2000). This ecotype designation is used for lake classification and has been simplified to three unique ecotypes that encompass the lakes across the landscape and within our sample set: coastal fen, interior peat plateau, and boreal spruce

forest. The coastal fen ecotype is dominated by sedge and rush vegetation. The lakes within this ecotype are formed in depressions between beach ridges exposed by isostatic rebound or in depressions caused by the thawing of permafrost in organic-rich terrain. The interior peat plateau ecotype contains moss, lichen, and small shrubs as the dominant vegetation types. This ecotype has 2-3 m of peat underlain by ~70 cm of continuous permafrost (Dredge and Nixon, 1992; Parks Canada, 2000). The lakes in this ecotype are mainly thermokarst in origin and ice-wedge peat polygons are dominant features. The boreal spruce forest ecotype is dominated by lichens, sphagnum moss, black spruce, tamarack, shrub willow, and birch. The lakes within this ecotype are predominantly thermokarst in origin.

Since this area has experienced some of the greatest warming in the circumpolar North (Smith and Burgess, 2004; Kaufman et al., 2009; Hochheim et al., 2010), ongoing multi-disciplinary research has taken place since 2010 to address the concerns regarding the effects of climate change on the hydrological conditions of WNP lakes. In collaboration with Parks Canada, a long-term hydrological monitoring program was established in 2015 that includes water isotope sampling since 2010 from 16 lakes, spanning the three main ecotypes in WNP (Figure 2.3; Table 2.A2).

Meteorological Conditions

Meteorological conditions for this region have been monitored at the Churchill airport since 1943 and temperature and precipitation exhibit marked seasonal variations (Station #5060608; Environment Canada, 2016; Figure 2.4; Table 2.2). A sampling ‘year’ has been defined as October to September to capture full winter and summer records.

Based on 1971-2000 climate normals, average annual temperature is -6.9°C and fluctuates substantially between summer and winter seasons. Average annual precipitation is 431.6 mm, 61% of which falls as rain between May and September (263.9 mm), while the remainder falls as snow between October and April (167.7 mm). The mean monthly temperatures during the study period (2010-2015) were comparable to the 1971-2000 climate normals. However, monthly maximum temperatures during the summer were, on average, 1.6°C warmer than climate normals during the entire study period and maximum monthly temperatures during winter were, on average, 3.3°C warmer between 2010 and 2012 and 1.2°C cooler between 2013 and 2015 as compared to climate normals.

Total annual precipitation (Figure 2.4; Table 2.2) was variable between 2010 and 2015 with two dry years in 2010-2011 and 2012-2013 (253.1 mm and 257.7 mm, respectively). While summer precipitation during the entire study period was, on average, comparable to climate normals (260.2 mm), winter precipitation was very low for four of the six study years (2009-2010, 2010-2011, 2012-2013, and 2013-2014; 4 yr. mean = 87.1 mm).

2.3 Methods

Water Isotope Sampling and Framework Development

Monitoring lakes were sampled for water isotopes in the spring, summer, and fall from 2007-2009 in VNP and from 2010-2015 for WNP. From 2010-2014, VNP monitoring lakes were sampled during the spring and fall. In 2015, the VNP monitoring lakes were sampled in the spring due to poor weather conditions in the fall.

Water samples were collected and stored in 30 mL high density polyethylene bottles until analysis. Between 2010 and 2012, all water samples were analyzed by conventional continuous flow isotope ratio mass spectrometry (CF-IRMS) at the University of Waterloo Environmental Isotope Laboratory (UW-EIL), whereas water samples from 2013 to 2015 were measured by off-axis integrated cavity output spectroscopy (O-AICOS) at UW-EIL. Isotope compositions are expressed as variations in the relative abundance of rare, heavy (^{18}O , ^2H) isotope species of water with respect to the common, light (^{16}O , ^1H) isotope species. These compositions are conventionally reported in delta (δ) notation as per mil (‰) values. Reported values reflect the deviation between the ratio of the sample and the ratio of a known standard (Vienna Standard Mean Ocean Water [VSMOW]) such that $\delta^{18}\text{O}$ or $\delta^2\text{H} = [(R_{\text{sample}}/R_{\text{standard}}) - 1] \times 1000$ ‰, where R is the $^{18}\text{O}/^{16}\text{O}$ or $^2\text{H}/^1\text{H}$ ratio in the sample and standard. Results of $\delta^{18}\text{O}$ and $\delta^2\text{H}$ analyses are normalized to -55.5 ‰ and -428 ‰, respectively, for Standard Light Antarctic Precipitation (Coplen, 1996). Analytical uncertainties are standard deviations based on the in-run standards and are ± 0.2 ‰ for $\delta^{18}\text{O}$ and ± 2.0 ‰ for $\delta^2\text{H}$ for water samples analyzed by CF-IRMS, and ± 0.2 ‰ for $\delta^{18}\text{O}$ and ± 0.8 ‰ for $\delta^2\text{H}$ for those analyzed by O-AICOS.

A Class-A evaporation pan was deployed and maintained by Vuntut Gwitchin Government (VNP) and Parks Canada (WNP) staff during the ice-free season from 2007-2010 (Tondu et al., 2013) and 2010-2015, respectively, to simulate the isotopic and hydrological behaviour of a steady-state terminal lake (e.g., closed-basin) where inflow is equal to evaporation (δ_{SSL}). Water within both evaporation pans was maintained at a constant volume, and water samples were collected weekly for isotopic analysis.

Lake hydrological conditions were evaluated using an isotope framework in $\delta^{18}\text{O}$ - $\delta^2\text{H}$ space (Figure 2.5; Appendix). A critical feature of an isotope framework is the Global Meteoric Water Line (GMWL), which is represented by the linear function: $\delta^2\text{H} = 8\delta^{18}\text{O} + 10$ (Craig, 1961). The slope of the GMWL (slope = 8) represents the temperature-dependant fractionation (partial separation between two or more isotopes) during condensation of atmospheric vapour, while the linearity of the GMWL reflects that atmospheric moisture primarily originates from one large water source (e.g., subtropical ocean surface) and undergoes progressive distillation during atmospheric transport from the tropics to the poles (Rayleigh distillation; Rozanski et al., 1993; Edwards et al., 2004; Yi et al., 2008). Consequently, decreasing temperature at the site of condensation and increasing continentality (e.g., latitude, altitude, and distance from moisture source) will result in progressively decreasing $\delta^{18}\text{O}$ and $\delta^2\text{H}$ values in precipitation. Therefore, snow typically has lower δ values and plots lower along the GMWL while rain typically has higher δ values, plotting higher along the GMWL (Rozanski et al., 1993; Wolfe et al., 2001).

When surface water undergoes evaporation, the isotope composition diverges from the GMWL in a systematic way due to mass-dependant fractionation (i.e., preferential evaporation of water molecules containing lighter isotopes). Consequently, lake water isotope compositions will plot in a linear trend to form the Local Evaporation Line (LEL; Edwards et al., 2004) (Figure 2.5). The LEL is controlled by local atmospheric conditions during the thaw season including flux-weighted temperature (T) and relative humidity (h; as per recommendations by Gibson et al. (2016) for lakes that experience seasonal ice cover), as well as the isotope composition of atmospheric

moisture (δ_{AS} ; Appendix). The LEL typically has a slope between 4 and 6 (Yi et al., 2008). Additionally, the relative position of an individual lake (δ_L) along the LEL is strongly associated with the water balance of each lake (Gonfiantini, 1986; Gibson and Edwards, 2002; Edwards et al., 2004; Yi et al., 2008). Key reference points that make up the LEL include the mean annual isotope composition of precipitation (δ_P ; at the GMWL-LEL intersection), the limiting steady-state isotope composition (δ_{SSL}), and the theoretical limiting isotopic enrichment (δ^*) of a desiccating basin during ice-free conditions (Figure 2.5; Appendix).

E/I Ratios and Hydrological Threshold Development

Lake water isotope compositions were used to derive the isotope composition of lake-specific input water (δ_I) and to then calculate evaporation-to-inflow ratios (E/I; Appendix). These values were derived using the Yi et al. (2008) coupled isotope tracer method that assumes conservation of mass and isotopes during evaporation and quantitatively assesses the relative influence of evaporation on lake water balances. Since E/I ratios are a quantitative expression of the relative influence of lake-specific input water and evaporative flux, they are useful indicators of the hydrological status of each monitoring lake. An E/I value of 1 occurs when lake water isotope composition is at terminal basin steady-state limiting composition (δ_{SSL}), which is when inflow is equal to evaporation. Therefore, an E/I ratio greater than 1 indicates that the lake has a negative water balance and is experiencing net evaporative drawdown.

Hydrological thresholds of E/I ratios were established to provide a quantitative assessment of hydrological condition. Here, a hydrological threshold is defined as a

critical value past which a water body faces an increasing risk of evaporative loss. We consider that elevated E/I ratios and consequent water-level drawdown potentially impair aquatic habitats. To align with Parks Canada's ecological reporting requirements, these generated E/I ratio hydrological thresholds have been categorized into three conditions ('good', 'fair', and 'poor'). 'Fair' and 'poor' thresholds were established using the statistical representations of the 68th and 95th percentiles on the average gamma distribution of the bootstrapped E/I ratios of long-term monitoring lakes, which are analogous to 1 and 2 standard deviations above the mean for normally distributed data, as per protocol commonly employed by Parks Canada. 'Good' thresholds are a description of central tendency, representing the middle 68% of the data. To estimate the error for each threshold, we used a bootstrapping technique where individual seasonal hydrological thresholds were calculated based on bootstrapping (random sampling and resampling of the dataset with replacement) gamma distributions of E/I ratios for each sample lake category. Gamma distributions were used since the E/I ratios are not distributed normally, are continuous, and cannot be negative. Since our sample sizes are small ($n = 6-88$), bootstrapping was applied to allow inferences to be made about the population. We bootstrapped, or 'resampled', each seasonal lake category dataset 1,000 times and calculated the mean of the 68th and 95th percentiles for each (Appendix Figure 2.A1).

For monitoring lakes in VNP, unique E/I thresholds were established for spring and fall for each lake category using results from 2007-2009. This generated two thresholds per lake category and six thresholds in total (Table 2.3). For monitoring lakes in WNP, unique E/I thresholds were established for spring, summer, and fall for each

lake category using results from 2010-2012. This generated three thresholds per lake category and nine thresholds in total (Table 2.3). E/I results were evaluated in the context of these thresholds for 2007-2015 in VNP and for 2010-2015 in WNP. Further statistical analysis (bootstrapping) identified that generating thresholds using only the first three years of data for both parks is comparable to using the entire dataset (Appendix Figure 2.A2).

2.4 Results and Interpretations

OLD CROW FLATS – VUNTUT NATIONAL PARK

Developing an Isotope Framework

Key meteorological and isotope parameters for VNP were obtained directly from Tondu et al. (2013) and are reported in Table 2.A3. Here, we utilize 3-year averaged values (2007-2009) to generate the isotope framework (Figure 2.6) and to ensure consistency with all other calculations throughout this study (WNP 3-year framework as well as both WNP and VNP 3-year E/I threshold calculations). δ_{SSL} , δ^* , and δ_P values are similar for years 2007 to 2009, reflecting that temperature and relative humidity values were consistent among the three years.

Lake Hydrological Variability

Lake water isotope compositions (δ_L) measured during 2007-2015 field seasons were superimposed on the 3-year average isotope framework (Figure 2.7). Inter-annual differences in the flux and isotope compositions of inputs (snowmelt, rainfall) and outputs (evaporation) cause each year to have its own isotopic footprint in $\delta^2\text{H}-\delta^{18}\text{O}$

space. δ_L values span the δ_P - δ_{SSL} segment of the LEL and occasionally beyond, indicating a broad range of hydrological conditions are captured by the monitoring lakes ($\delta^{18}O_L = -25.8\text{‰}$ to -8.7‰ , $\delta^2H_L = -200.3\text{‰}$ to -99.9‰). Distinct seasonal trends are evident with lower δ_L values in the spring and higher δ_L values in the fall. This change is typical of high-latitude lakes due to input from isotopically-depleted snowmelt in spring and subsequent evaporative enrichment throughout summer. This pattern is evident in all years where sampling occurred more than once (2007-2014). Typically, rainfall-dominated lakes plot above the LEL and closer to δ_{SSL} reflecting greater influence from evaporation in comparison to snowmelt-dominated lakes which fall below the LEL and closer to δ_P . Due to well-below average snowfall in the winter that preceded 2008 (27.2 mm), δ_L values are higher in the summer and fall with multiple lakes plotting beyond δ_{SSL} compared to other years. Additionally, heavy rain during 2010 and 2011 caused δ_L values to plot above the LEL in both fall seasons. It should also be noted that 2007-2009 are the only years with summer data.

Monitoring Lake Hydrological Conditions using Bootstrapped E/I Thresholds

The importance of evaporation on lake water balances was quantitatively assessed by evaporation-to-inflow (E/I) ratios estimated for each lake and then examined as time-series in relation to bootstrapped thresholds (Table 2.3; Figures 2.8, 2.9). Overall, E/I values vary substantially among lakes and over time ranging from 0.03 to 0.78 in the spring (mean = 0.33) and from 0.05 to 1.08 in the fall (mean = 0.50). This variability can be attributed to snowmelt-dominated lakes having lower E/I ratios due to high input of isotopically-depleted snowmelt, whereas rainfall-dominated lakes are more prone to

evaporation and have higher E/I ratios (see also Turner et al., 2010, 2014 and Tondu et al., 2013).

The bootstrapped E/I thresholds for spring and fall seasons of each lake category reveal the vulnerability of each lake to inter-annual meteorological variations (Figures 2.8, 2.9). In the spring, rainfall-dominated lakes show the most variability in E/I ratios during the nine-year period (Figure 2.8). VNP 06, 19, 29, 46, 49 and 58 appear to be most prone to evaporation with multiple E/I values falling within the ‘fair’ to ‘poor’ conditions. VNP 34, 35, 37 and 38 show less influence of evaporation, with most if not all of their E/I values falling within the ‘good’ condition. E/I ratios for intermediate lakes, lakes with input close to δ_p (VNP 26 and 48), mostly fall within the ‘fair’ condition while E/I ratios for snowmelt-dominated lakes (VNP 11 and 55) also mostly fall within the ‘good’ condition, although these lakes occasionally approach the ‘poor’ threshold.

In the fall, individual lake variability in E/I ratios increased relative to spring (Figure 2.9). Rainfall-dominated lakes VNP 19, 46 and 49 had E/I values in both the ‘fair’ and ‘poor’ conditions from 2007-2012, but during the latter three years (2013-2015) values are mostly within the ‘good’ condition. Rainfall-dominated lakes VNP 29 and 58 were prone to evaporation during spring, but during fall most if not all E/I values are ‘good’. Rainfall-dominated lakes VNP 34, 35, 37 and 38 continue to show less influence from evaporation during the fall season. VNP 06 is the only rainfall-dominated lake that has several E/I values within the ‘fair’ and ‘poor’ conditions for both sampling seasons and E/I ratios tend to be high during these years, implying that this lake is highly prone to evaporative water loss.

WESTERN HUDSON BAY LOWLANDS – WAPUSK NATIONAL PARK

Developing an Isotope Framework

During the three years used for isotope framework calculations (2010-2012), isotopic enrichment of evaporation pan water occurred initially with increasing cumulative evaporation until equilibrium with atmospheric conditions was reached (Figure 2.10). Once equilibrium was estimated to be established, mean δ_{SSL} values were calculated for each year. The decline in $\delta^{18}\text{O}$ (and $\delta^2\text{H}$) values during the fall of most sampling years is due to rainfall influencing the water in the evaporation pan. To establish the 3-year LEL, 2010-2012 evaporation pan-generated δ_{SSL} values were averaged for the isotope framework (Figure 2.11). These and other values for calculating and constructing the isotope framework are reported in Table 2.A4. δ_{SSL} and δ^* values are similar for 2010-2012, reflecting similar temperature and relative humidity during the three years.

Lake Hydrological Variability

Similar to the VNP dataset, WNP lake water isotope compositions (δ_L) acquired during 2010-2015 field seasons are shown superimposed on the 3-year average isotope framework (Figure 2.12). Strong seasonal and spatial variability in lake hydrological conditions also exist ($\delta^{18}\text{O}_L = -14.7\text{‰}$ to -0.9‰ , $\delta^2\text{H}_L = -122.4\text{‰}$ to -48.8‰) with isotope compositions spanning the δ_P - δ_{SSL} segment of the LEL and sometimes beyond. This can be attributed to variable meteorological conditions and catchment characteristics, as described below, indicating that a broad range of hydrological conditions are captured by the 16 monitoring lakes.

Most δ_L values, regardless of season, tend to plot above the LEL, suggesting a persistent greater relative influence of rainfall relative to snowmelt. This interpretation aligns well with the meteorological conditions during the monitoring years in which rainfall accounted for 60-85% of the annual precipitation (Table 2.2). Seasonally, distinct trends are evident with lower δ_L values in spring due to the influence of snowmelt, higher δ_L values during the summer due to warmer temperatures and evaporation, and intermediate δ_L values during the fall due to late summer rainfall. Due to well-below average snowfall in the 2012-2013 winter (45.2 mm), low summer rainfall (212.5 mm), and temperatures $\sim 2^\circ\text{C}$ warmer than climate normals in 2013, δ_L values are high in the summer and several plot beyond δ_{SSL} (Figure 2.12d). In 2014 and 2015, δ_L values show contrastingly less evaporative enrichment due to large rainfall events (representing 30-50% of all summer precipitation) directly prior to summer sampling, which dampen the influence of evaporation.

The three main ecotypes within WNP also display different patterns of hydrological variability. Boreal spruce forest lakes consistently have the lowest δ_L values with some values plotting below the LEL, reflecting an influence from snowmelt which offsets the influence of evaporation. In contrast, δ_L values of lakes in the interior peat plateau and coastal fen are higher and reflect stronger influences of evaporation during the summer sampling period.

Monitoring Lake Hydrological Conditions Using Bootstrapped E/I Thresholds

Time-series of E/I ratios were calculated for the 16 monitoring lakes from WNP and plotted in relation to bootstrapped thresholds determined for lakes in coastal fen,

interior peat plateau, and boreal spruce forest ecotypes (Table 2.3; Figures 2.13, 2.14, & 2.15). Seasonal variability exists in WNP's E/I ratios with a spring average of 0.08, summer average of 0.24, and fall average of 0.14. This seasonal pattern corresponds to the trends observed in the $\delta^2\text{H}-\delta^{18}\text{O}$ plots, where spring values tend to be lower due to the influence of snowmelt, summer values are higher due to warmer temperatures and the influence of evaporation, and fall values are intermediate due to late summer and fall precipitation.

Bootstrapped thresholds calculated for spring, summer, and fall seasons of each lake category are utilized here to show responses of each lake to temporal variations in meteorological conditions (Figures 2.13, 2.14, and 2.15). In spring, coastal fen lakes show the greatest amount of variability in E/I ratios with WNP 05, 12, and 21 having several values within the 'fair' and 'poor' conditions, while E/I ratios for WNP 07, 15, and 20 are mostly within the 'good' condition (Figure 2.13). Interior peat plateau lakes WNP 32 and 34 E/I values mostly fall within the 'fair' to 'poor' condition indicating that these lakes start the ice-free season off in a relatively vulnerable state. WNP 37 and 39 E/I values are within the 'good' condition and are less vulnerable to evaporation. E/I ratios for boreal spruce forest lakes mostly fall within 'good' and 'fair' conditions, due to the strong snow trapping ability of the forest. However, the E/I ratio for WNP 23 plots within the 'poor' condition during 2013, indicating that the low snow accumulation in the preceding winter was enough for a typically resilient boreal spruce forest lake to cross the 'poor' threshold.

In summer, coastal fen lakes WNP 05, 12, and 21 have multiple E/I values in the 'fair' and 'poor' conditions during 2010-2013 and E/I ratios are high, implying that

evaporation has a large effect on these lakes (Figure 2.14). However, during the wet summers of 2014 and 2015, E/I ratios for these lakes correspondingly transitioned to falling within the ‘good’ condition. WNP 07, 15 and 20, similarly to E/I results from spring, continue to show less influence of evaporation. Interior peat plateau lakes WNP 32 and 34 continue to be strongly influenced by evaporation with most E/I values falling within the ‘fair’ to ‘poor’ condition during 2010-2013 summers. However, similar to the vulnerable coastal fen lakes, E/I values for these lakes decreased during the wet 2014 and 2015 seasons into the ‘good’ condition. WNP 33, 37, and 39 continue to be resilient to evaporation and most E/I values fall within the ‘good’ condition. E/I ratios for the boreal spruce forest lakes also continue to stay within the ‘good’ to ‘fair’ conditions, indicating more resistance to evaporative drawdown as compared to lakes in other ecotypes. However, as previously mentioned, when dry winters occur prior to sampling (e.g., 2010, 2012, and 2013), boreal spruce forest lakes approach the ‘poor’ condition, but E/I ratios remain low and therefore these lakes remain far from experiencing extensive lake-level drawdown.

During fall, coastal fen lakes WNP 05, 12, and 21 show comparable patterns to the spring and summer with ‘poor’ E/I values during the dry 2011 summer season and then mostly ‘good’ to ‘fair’ values during 2012-2015, reflecting the influence of high amounts of rainfall at the end of the ice-free season (Figure 2.15). WNP 07, 15, and 20 also show similar patterns as compared to the earlier seasonal intervals with ‘fair’ / ‘poor’ E/I values during the 2013 dry year but then lower E/I values for 2014 and 2015 due to the influence of fall precipitation. Most interior peat plateau lakes return to E/I values within the ‘fair’ to ‘good’ conditions due to the end of summer and fall precipitation.

Boreal spruce forest lakes also continue to show little influence from evaporation, with most E/I values staying within the ‘good’ to ‘fair’ conditions, with WNP 23 showing the strongest influence preceding low winter precipitation.

2.5 Discussion

Development of novel hydrological thresholds using water isotopes to monitor the Ecological Integrity of northern shallow lakes

Rapid and dramatic climate-induced shifts in freshwater ecosystems are of major concern across the arctic and subarctic, leading to the need for increased understanding and monitoring of the impacts of such change (Smith et al., 2005; Smol et al., 2005; Schindler and Smol, 2006; Prowse et al., 2006; Riordan et al., 2006; Labrecque et al., 2009; Avis et al., 2011; Carroll et al., 2011). Thresholds have been used as a critical tool in successful environmental management, where measurements can be made in an environment as a motivation for management decisions, and defined thresholds, once crossed, will move the system away from a ‘desired’ or baseline state (Groffman et al., 2006). Yet, thresholds used in environmental research are difficult to define and quantify since they represent a complex series of interacting variables, not just distinct boundaries in time and space (Briske et al., 2005; Revenga et al., 2005; Capon et al., 2015).

Inadequate temporal and spatial resolution often prevents change from being accurately quantified since ecosystem variability is not measured or addressed (Capon et al., 2015).

Parks Canada has identified that the hydrological condition of the freshwater resources within both VNP and WNP are a crucial ‘Ecological Integrity Measure’, since freshwater resources are essential for entire ecosystem health. Detecting and anticipating

the varying hydrological responses to climate warming is challenging in northern landscapes, however, both VNP and WNP have now adopted thresholds as points of management concern within their ‘Ecological Integrity’ monitoring program (Parks Canada, 2011). Previous isotope-based studies in VNP and WNP have used a static and universal model to designate E/I thresholds (e.g., where E/I values > 0.5 represents the threshold for defining lakes that are more influenced by evaporation versus inflow; Turner et al., 2010, 2014; Tondu et al., 2013; MacDonald et al., 2017). Additionally, MacDonald et al. (2017) used static E/I thresholds to compare lake water balances across multiple northern lake-rich landscapes. However, our research focuses on monitoring individual northern lake-rich landscapes to identify changes in the local hydrology of lakes *over time* in response to varying meteorological conditions. Since hydrology (e.g., ‘snowmelt-dominated’ vs. ‘rainfall-dominated’ or coastal fen vs. boreal spruce forest) and seasonality (spring vs. summer vs. fall) influence lakes in a variety of ways, this study provides an alternative to the static E/I threshold of > 0.5 and defines thresholds specific to lake categories and seasons. Operationally, this facilitates a more sensitive approach to detect lake hydrological change.

An excellent example of the utility of this lake category and season-specific threshold approach is that two boreal spruce forest lakes in WNP (WNP 23 and 25) approach and cross the ‘poor’ threshold every ice-free season from 2010-2013. The E/I ratios for boreal spruce forest lakes during the summer are so low and consistent among all lakes in all years that the thresholds are very close together and very low. This results in very small variations in lake E/I values leading to a change in condition (‘poor’, ‘fair’, ‘good’), even if the water balance has shifted only subtly. Additionally, lakes in the

boreal spruce forest category are the most consistent. However, it should be noted that while several boreal spruce forest lakes fall into ‘fair’ and ‘poor’ conditions, their E/I values never exceed 0.26, which represents a lake that is experiencing a strongly positive water balance (i.e., not undergoing drying and potentially growing in size). While these boreal spruce forest lakes are resilient to evaporative loss, they are still shown to be somewhat sensitive to changes in meteorological conditions (e.g., low amount of snow in the preceding winter). Thus, the lake category and season-specific approach to defining thresholds is a more sensitive way to detecting hydrological change, but it may not always signal aquatic ecosystem impairment.

Based on statistical analysis of the current datasets, generating thresholds using only the first three years of data for both parks is comparable to using the entire dataset (Figure 2.A2). Additionally, these three-year hydrological thresholds encompass meteorological variability that span both above and below the climate normals of temperature and precipitation. Therefore, it would appear to be justifiable to continue to use the bootstrapped thresholds reported in this study for future monitoring (Table 2.3). This is an extremely useful aspect to the monitoring program since it has long-term applicability and thus, time consuming, yearly recalculation of specific thresholds may not be necessary. Once a more sufficient baseline (~10 years, as preferred by Parks Canada) has been determined, re-evaluation of hydrological thresholds should take place.

Integration of novel thresholds to assess the hydrological 'Ecological Integrity Measure' condition within two subarctic Canadian National Parks

A key contribution of this work is the establishment of hydrological thresholds to align with Parks Canada's usage of thresholds as 1) a tool to evaluate 'Ecological Integrity' and 2) to establish the 'condition' of an individual ecosystem (Parks Canada, 2011). This contribution is critical to parlay scientific research into metrics that serve Parks Canada and their reporting requirements. The lake status designations ('good,' 'fair,' and 'poor') have been generated for each lake category and season to represent easily quantifiable Ecological Integrity conditions, which Parks Canada can then incorporate into their 'State of the Park' report to quantify fluctuations in the hydrological status of lakes in response to climate change. Two summary tables (Tables 2.4 and 2.5) have been generated to enable a more efficient assessment of lake hydrological conditions across both Parks.

Variability in the condition ('good', 'fair', 'poor') of VNP monitoring lakes exists between lake category (rainfall-dominated, snowmelt-dominated, intermediate) as well as by season (spring, fall). However, rainfall-dominated lakes show the most variability in lake condition, spanning from lakes that fall entirely within the 'good' condition to lakes that are almost entirely in 'fair' to 'poor' conditions. Within VNP, rainfall-dominated lakes occupy poorly drained and sparsely vegetated areas that are not effective in promoting snow accumulation as compared to other lake categories (Turner et al., 2010, 2014; Bouchard et al. 2013; Tondu et al., 2013). Five rainfall-dominated lakes (VNP 06, 19, 29, 46, 49, and 58) in particular are more prone to evaporation with multiple E/I values falling within the 'fair' to 'poor' conditions (Table 2.4). This implies that some

rainfall-dominated lakes will be more sensitive to changes in precipitation than others. Also, VNP 06 & 19 E/I ratios are mostly within the ‘fair’ and ‘poor’ conditions, implying that these lakes are the most sensitive within the VNP monitoring lakes to evaporation (Table 2.4). Additionally, in 2007, VNP 06 experienced a thermokarst lake drainage event and has since stabilized as a shallow, residual waterbody prone to eutrophication and lake level drawdown (Turner et al., 2010; Tondu et al., 2017). Since the frequency of thermokarst lake drainages has increased during recent decades in response to changing climatic conditions, this landscape will likely see a corresponding increase in remnant shallow waterbodies that will be prone to increased evaporation and higher E/I ratios (Lantz and Turner, 2015; Tondu et al., 2017).

In WNP, variability in lake condition exists between lake category (coastal fen, boreal spruce forest, interior peat plateau) and season (spring, summer, fall) from 2010 to 2013. However, during the spring and summer of 2014 and the entire ice-free season of 2015, these lakes improved to ‘fair’ or ‘good’ conditions, reflecting an increase in the precipitation/evaporation ratio and a strong sensitivity to meteorological conditions. There was a large amount of rainfall during the month of July prior to and during sampling (117.9 mm) in 2014. This rainfall likely caused the homogenization of hydrological conditions between the lakes. Although there were no large rain events prior to the other sampling periods in 2014 and 2015, precipitation/evaporation ratios were evidently sufficient for lakes to maintain ‘good’ or ‘fair’ status. Most interior peat plateau lakes fall within ‘good’ and ‘fair’ conditions, however, WNP 32 and 34 mostly fall within the ‘fair’ to ‘poor’ conditions from 2010-2013, indicating that these lakes are more vulnerable to evaporation as compared to other lakes within the same ecotype. WNP 32

and 34 are the smallest (by both depth and surface area; Appendix Table 2.A2) compared to the rest of the interior peat plateau lakes, implying that smaller (by depth and/or surface area) lakes may be the most affected by factors that lead to increased evaporation. Many boreal spruce forest lakes fall within ‘good’ and ‘fair’ conditions due to the stronger snow trapping ability of the forest, indicating more resistance to evaporative drawdown compared to lakes in other ecotypes. However, the extreme low snow amount in 2009-2010, 2010-2011, and 2012-2013 did lead several boreal spruce forest lakes (WNP 23, 25, 27) to approach or cross the ‘poor’ threshold, despite snow-trapping effects of their forested catchments. While their E/I ratios remain low, boreal spruce forest lakes may become more vulnerable to evaporation under a climate change scenario of low snowfall as previously discussed. Several studies have recently documented and predicted that decreasing snowfall as well as warming climate and longer ice-free seasons will potentially lead to increased lake desiccation as well as having a profound influence on wildlife habitat, carbon behaviour and overall aquatic ecosystem function (van der Molen et al., 2007; Abnizova et al., 2012; Derksen and Brown, 2012; Bouchard et al., 2013; MacDonald et al., 2017).

2.6 Conclusions and Recommendations

Through this research, a common approach for a sustainable hydrological monitoring program has been developed and applied within VNP and WNP. This approach can be readily adapted and applied to other northern lake-rich parks. However, a key component for the sustainability of this monitoring program is the commitment from both researchers and Parks Canada that future water isotope monitoring will

continue to provide critical hydrological information for Parks Canada ‘State of the Park’ reports. Four major recommendations have been established to ensure that this approach continues to be an effective, collaborative, and long-term hydrological monitoring program within VNP and WNP. Firstly, if financially feasible, water isotope sampling should be completed every spring and fall with summer sampling added every three years to capture a broad spectrum of hydrological conditions. Water isotope samples were only consistently collected during the spring and fall at VNP since 2010. While this was reported to capture the full scope of seasonal isotope evolution by Tondu et al. (2013), our recommendation is to sample during the summer ever three years, since mid-ice-free season (summer) is when the most evaporation typically occurs as shown by 2007-2009 VNP and 2010-2015 WNP records. Not including the summer sampling period within VNP means that the maximum influence of evaporation on the lakes may not be captured. However, with the difficulties in securing reliable funding sources every year in mind, spring and fall sampling may be deemed sufficient since there was only one lake isotope value (δ_L) from the summer during 2007-2009 that fell outside the range captured by the spring and fall seasons.

Secondly, an evaporation pan should be maintained every ice-free season if it is easily accessible for Parks Canada staff. The evaporation pan is helpful to simulate the isotopic and hydrological behaviour of a steady-state terminal lake where inflow is equivalent to evaporation (δ_{SSL}). This value is an important component of the Local Evaporation Line and helps to constrain δ_{AS} (the isotopic composition of the ice-free season atmospheric moisture) which is an important component for calculating E/I ratios, the basis of our lake thresholds.

Thirdly, the partnership between Parks Canada staff and researchers needs to remain strong and long-term. Funding needs to be secured, field collection and processing needs to be carried out efficiently and accurately, data collection and the corresponding isotope framework calculations need to be completed, and E/I values plotted within the Ecological Integrity thresholds is necessary. This seems like an obvious recommendation, however without this partnership commitment, this monitoring program would not be viable.

Lastly, a yearly report and a complete data file should be created by both researchers and Parks Canada staff to ensure the science is understandably portrayed and can inform policy and land-management decisions. Summary figures, similar to Tables 2.4 and 2.5, should be included as data continues to accumulate, since they are a quick and easy way to explore the temporal and spatial hydrological trends. This report and the corresponding data should be made public as government open files so this research and monitoring on the effects of climate change can be viewed by the general public as well.

As a final comment, it has been predicted that large summer storms/precipitation events will increase in frequency and magnitude (Sauchyn and Kulshreshtha, 2008; Kaufman et al., 2009). This could lead to these subarctic landscapes becoming inundated with water and therefore lake water levels would rise above 'normal'. Our use of thresholds within this study has solely focused on the concern of lake desiccation and therefore our methodology would need to be modified to address concerns of increasing lake water levels if the need arises.

2.7 Figures

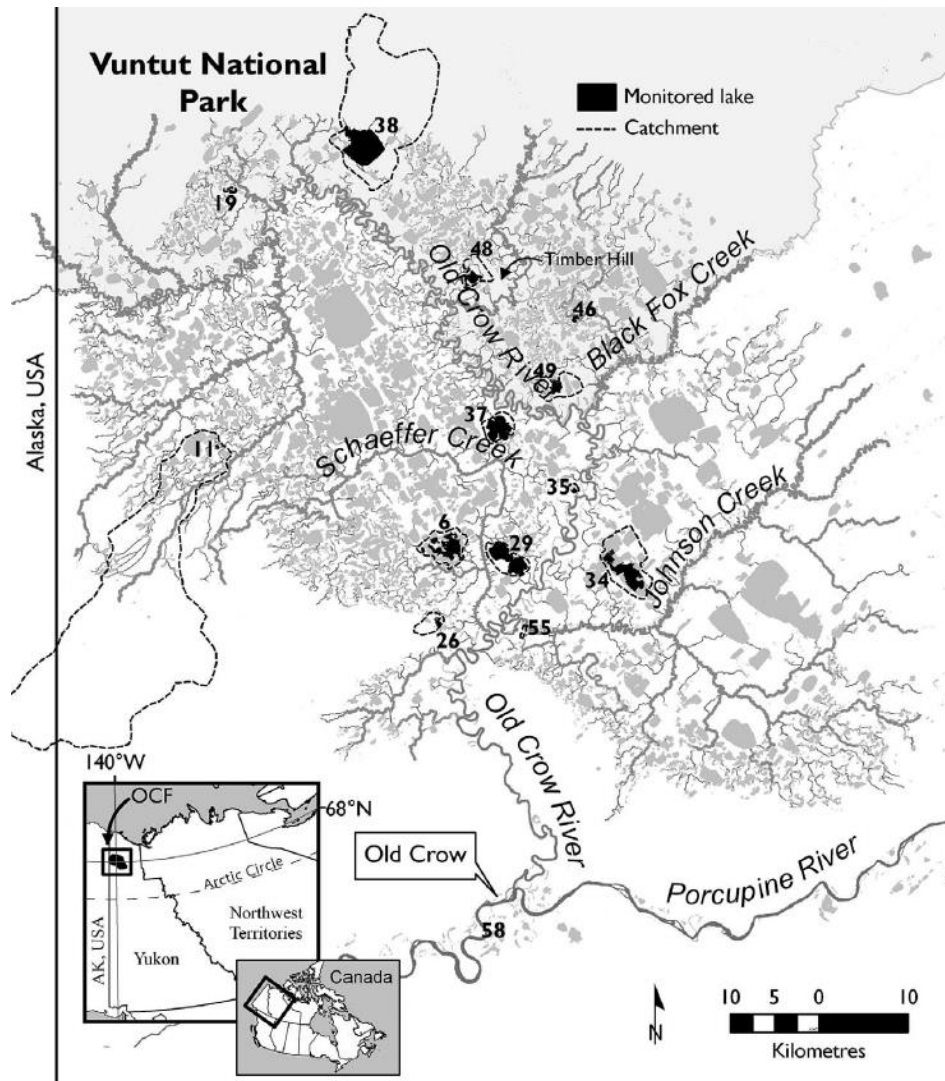


Figure 2.1 Map showing locations of the 14 lakes selected for hydrological monitoring within the Old Crow Flats (Tondou et al., 2013, p. 596). The grey-shaded area north of Old Crow River represents Vuntut National Park, while the southern portion represents the Vuntut Gwitchin First Nation Special Management Area.

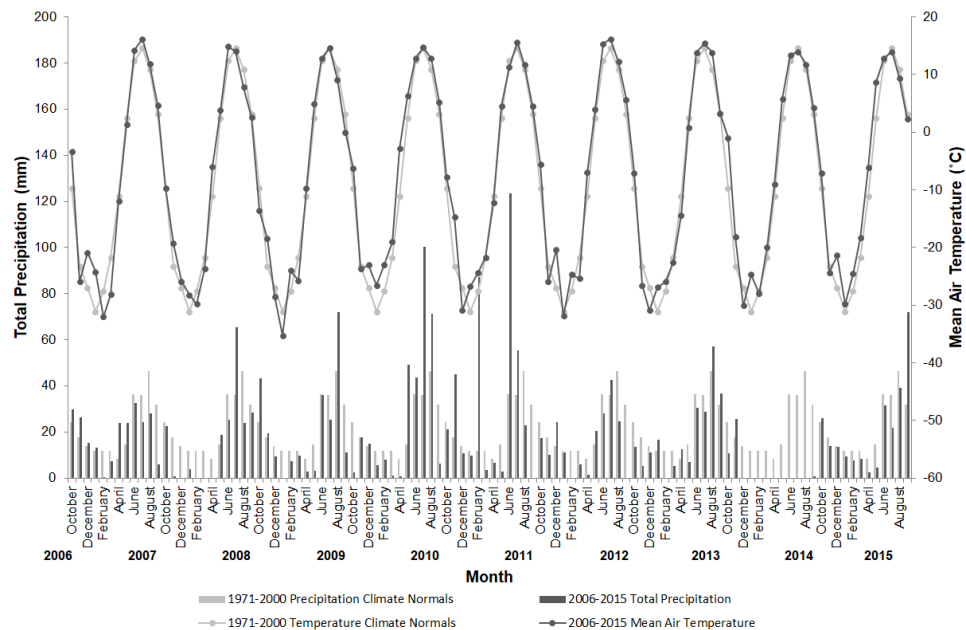


Figure 2.2 VNP meteorological data from a weather station at the Old Crow Airport Station (Station ID 2100800 and 2100805; Environment Canada, 2019); a) mean monthly air temperature from 2006-2015 compared to climate normals (1971-2000) and b) total monthly precipitation from 2006-2015 compared to climate normals (1971-2000). No precipitation data were missing from 2006-2007, 2007-2008, 2011-2012 and 2012-2013 sampling years. Less than 1% of the precipitation data were missing from 2008-2009, 2009-2010, and 2014-2015 sampling years. Less than 10% of the precipitation data were missing from the 2010-2011 sampling year. For 2013-2014, > 85% of the precipitation data were missing; therefore, no data for this year are displayed. Annual and seasonal precipitation totals are the sum of all observations.

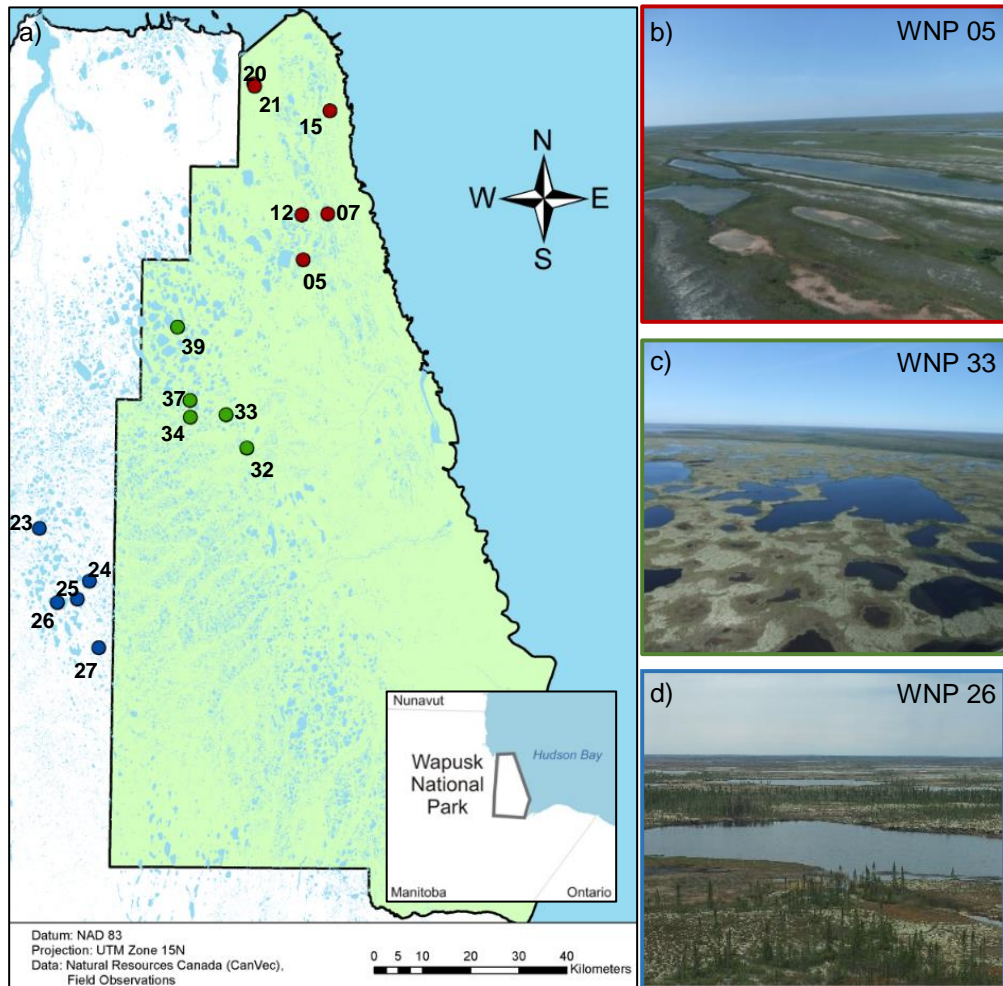


Figure 2.3 a) Map showing the locations of 16 lakes selected for the WNP hydrological monitoring program. Red circles represent lakes within the coastal fen ecotype, green circles represent lakes within the interior peat plateau ecotype, and blue circles represent lakes within the boreal spruce forest ecotype. Photographs show b) WNP 5 within the coastal fen ecotype, c) WNP 33 within the interior peat plateau ecotype, and d) WNP 26 within the boreal spruce forest ecotype.

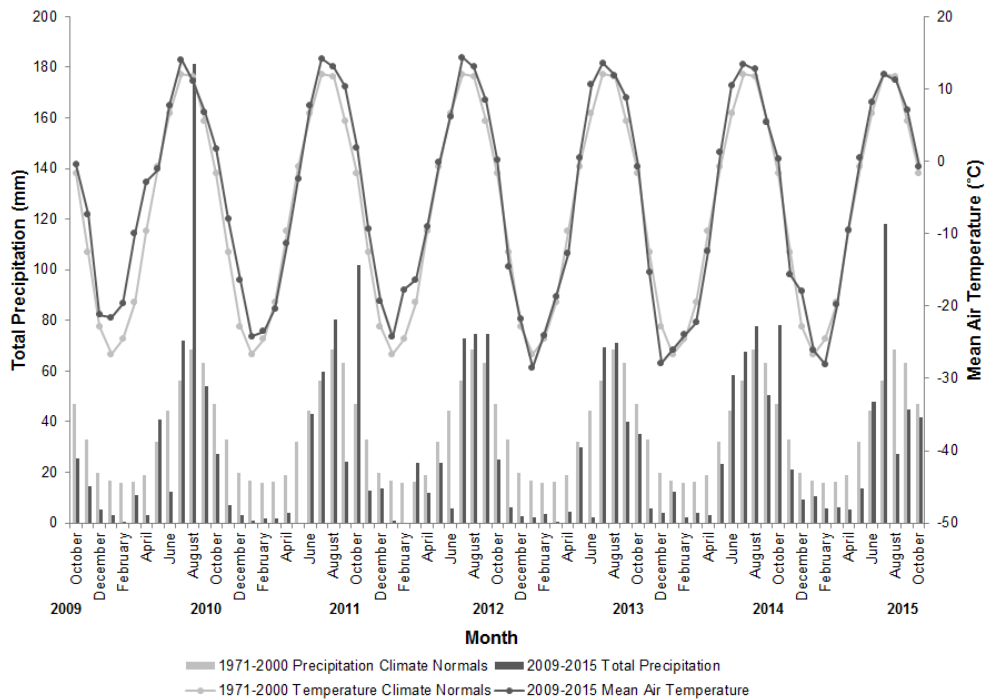


Figure 2.4 WNP meteorological data based on Environment and Climate Change Canada Historical Weather data from the Churchill Airport weather station (Station ID 5060608; Environment Canada, 2019); a) mean monthly air temperature from 2009-2015 compared to climate normals (1971-2000) and b) total monthly precipitation from 2009-2015 compared to climate normals (1971-2000). Annual totals are the sum of all observations.

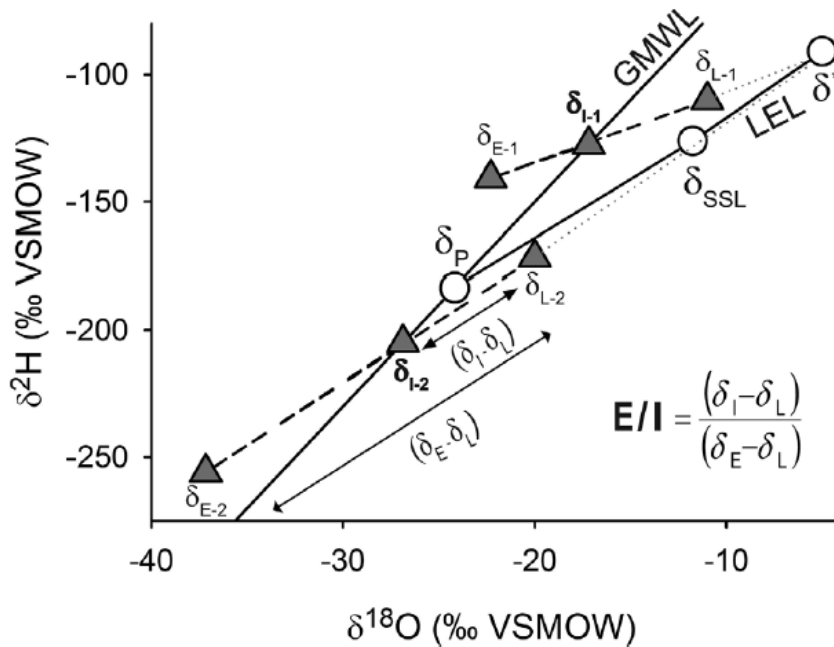


Figure 2.5 A schematic $\delta^{18}\text{O}$ - $\delta^2\text{H}$ diagram illustrating two hypothetical lakes (lake 1 and lake 2; from Tondu et al., 2013, p. 601). Each lake plots along a lake-specific evaporation line and intersects the Global Meteoric Water Line (GMWL). Key reference points in relation to the Local Evaporation Line (LEL) include mean annual isotope composition of precipitation (δ_P), the limiting steady-state isotope composition (δ_{SSL}), and the limiting isotopic enrichment of a desiccating lake (δ^*). Evaporation to inflow (E/I) ratios are calculated using isotope mass-balance models of lake water isotope compositions (δ_L), input water isotope compositions (δ_I), and isotope compositions of evaporated vapour from each lake (δ_E ; see Appendix for calculations). VSMOW represents the Vienna Standard Mean Ocean Water.

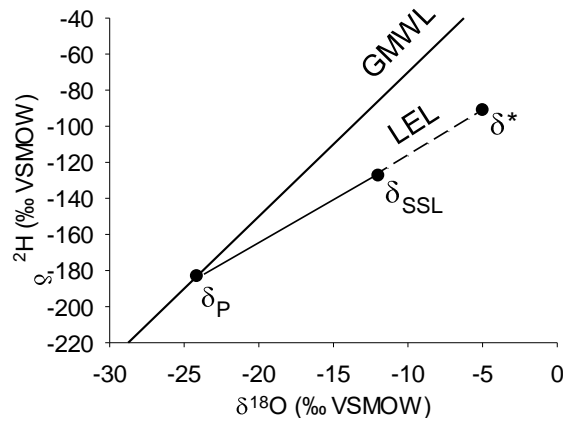


Figure 2.6 Three-year mean Local Evaporation Line (LEL; $\delta^2\text{H} = 4.8\delta^{18}\text{O} - 68.7$) for VNP using 2007-2009 values from Tondu et al. (2013; Table 2.A3), (δ_P = isotope composition of mean annual precipitation, δ_{SSL} = isotope composition of a terminal lake at steady-state, δ^* = limiting isotopic enrichment of a desiccating basin).

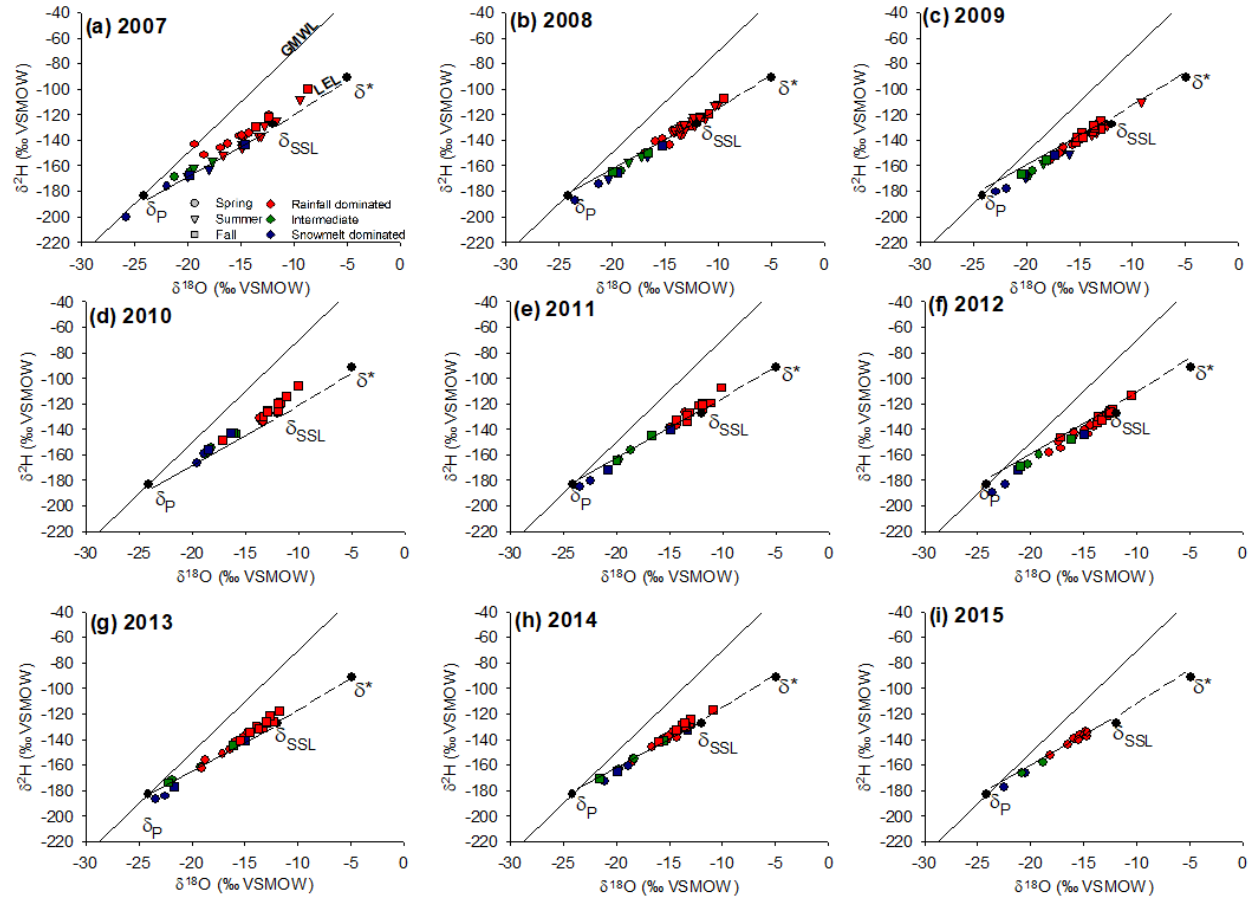


Figure 2.7 Isotope composition of VNP monitoring lakes (δ_L) superimposed on the 3-year monitoring isotope framework for each sampling year: (a) 2007, (b) 2008, (c) 2009, (d) 2010, (e) 2011, (f) 2012, (g) 2013, (h) 2014, and (i) 2015. Seasonal differences are denoted by shapes and lake type is denoted by colour (GMWL = Global Meteoric Water Line, LEL = Local Evaporation Line, δ_P = mean annual isotope composition of precipitation, δ_{SSL} = isotope composition of a terminal lake at steady-state, δ^* = limiting isotopic enrichment of a desiccating basin).

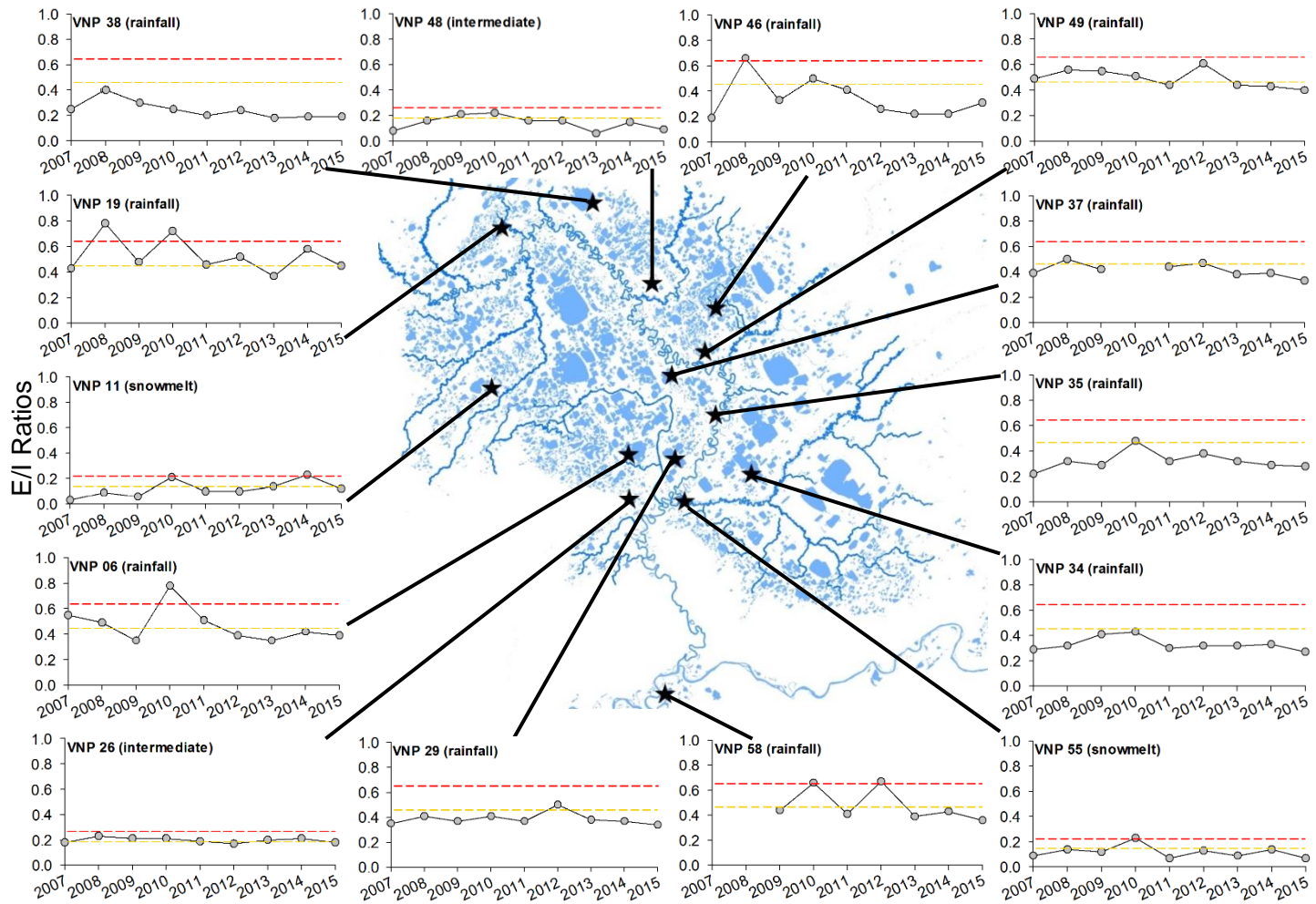


Figure 2.8 VNP E/I results for the spring sampling period. Red dash line represents 'poor' threshold and the yellow dash line represents 'fair' threshold.

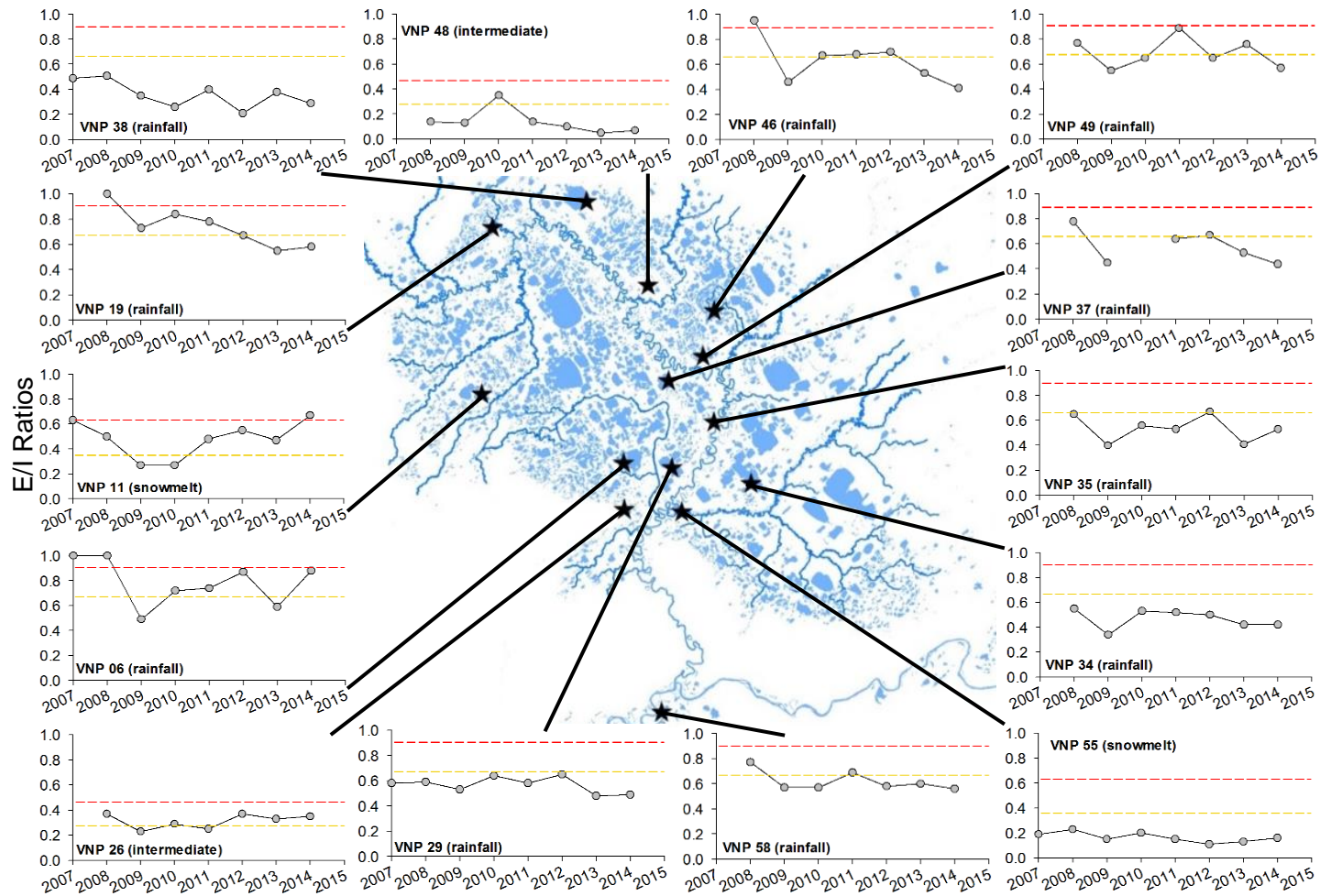


Figure 2.9 VNP E/I results for the fall sampling period. Red dash line represents 'poor' threshold and the yellow dash line represents 'fair' threshold. The monitoring lakes were not sampled in the fall of 2015 due to poor weather conditions.

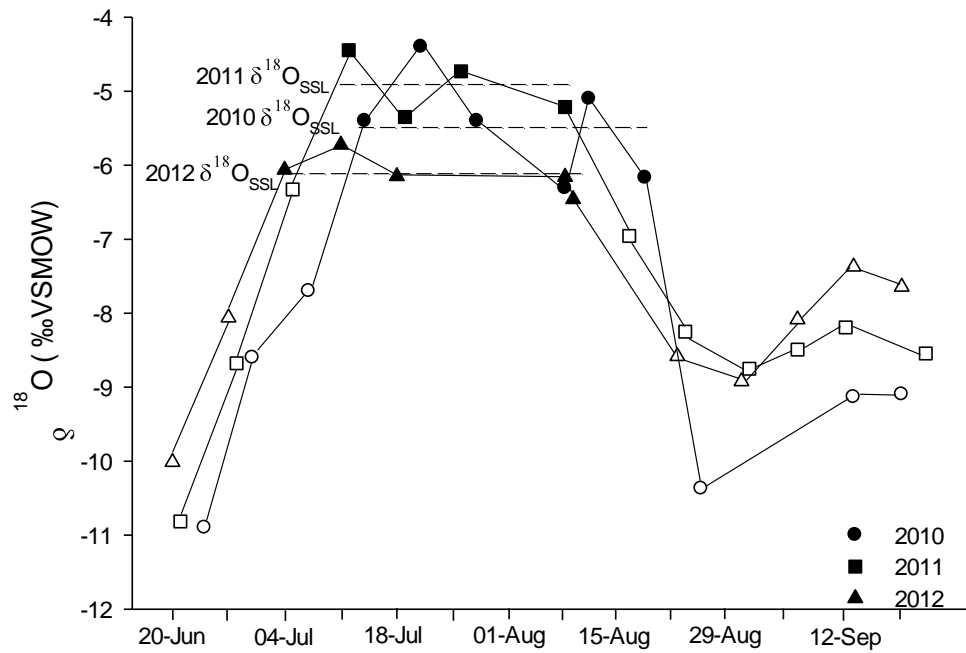


Figure 2.10 Evolution of water $\delta^{18}\text{O}$ sampled from an evaporation pan maintained at the Parks Canada office in Churchill from June to September of 2010 to 2012. Solid shapes represent values used for estimating δ_{SSL} . Dashed lines are the mean $\delta^{18}\text{O}_{\text{SSL}}$ values used for calculating the 3-year isotope framework.

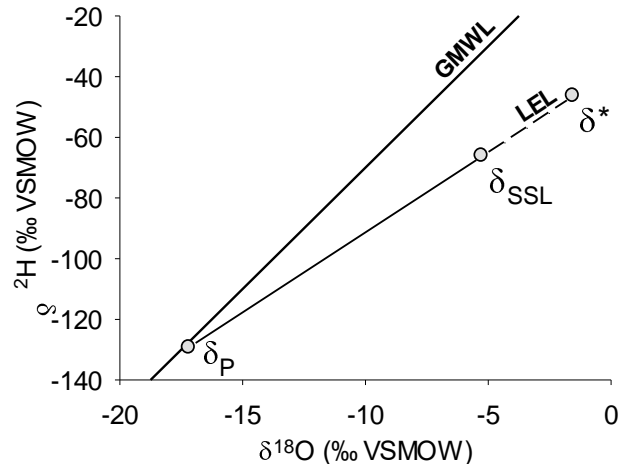


Figure 2.11 Three-year mean Local Evaporation Line (LEL; $\delta^2\text{H} = 5.1\delta^{18}\text{O} - 41.6$) for WNP using 2010-2012 values reported in Table 2.5 (δ_P = isotope composition of mean annual precipitation, δ_{SSL} = isotope composition of a terminal lake at steady-state, δ^* = limiting isotopic enrichment of a desiccating basin).

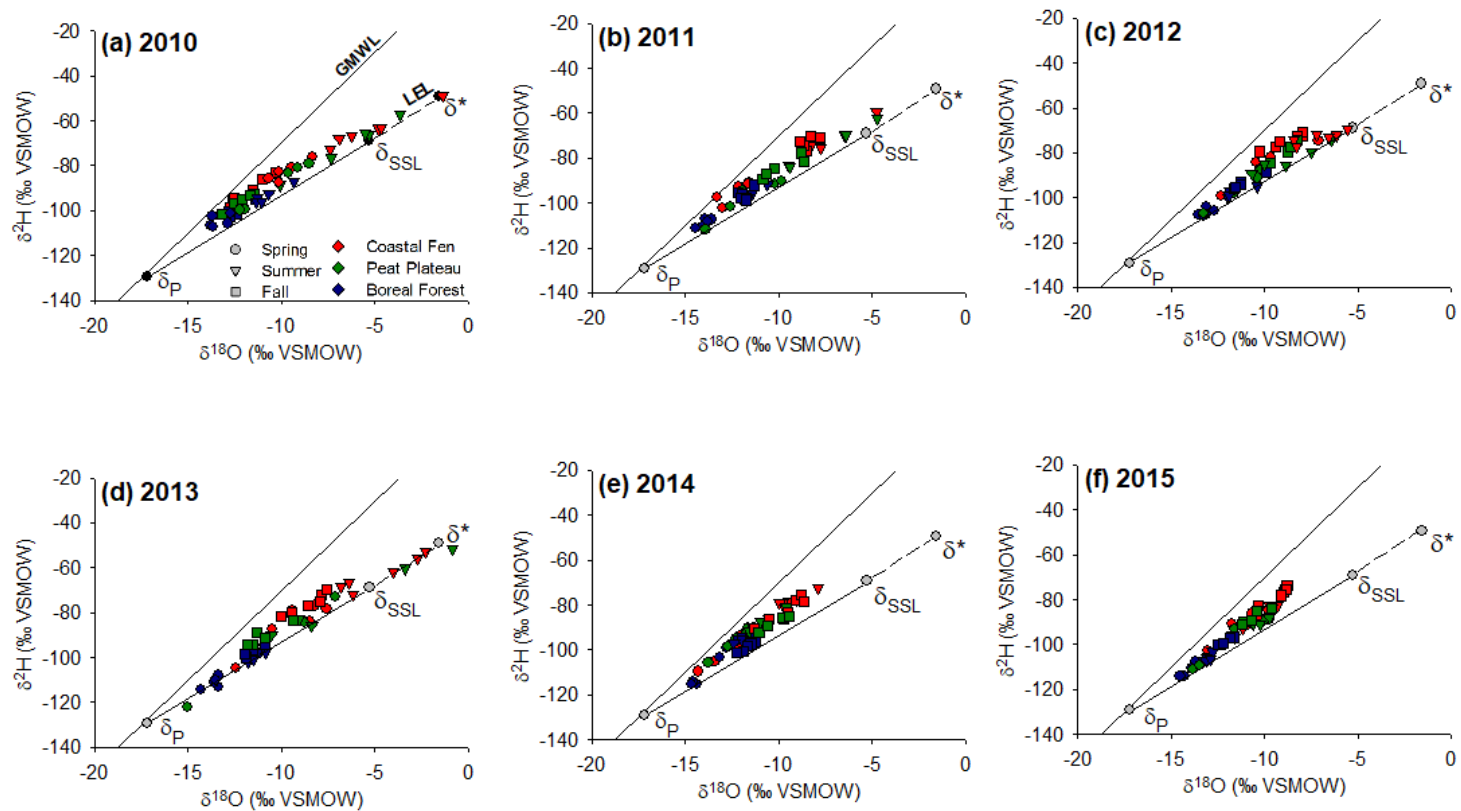


Figure 2.12 Isotope composition of WNP monitoring lakes (δ_L) superimposed on the 3-year monitoring isotope framework for each sampling year: (a) 2010, (b) 2011, (c) 2012, (d) 2013, (e) 2014, and (f) 2015. Seasonal differences are denoted by shapes and ecotype is denoted by colour (GMWL = Global Meteoric Water Line, LEL = Local Evaporation Line, δ_P = mean annual isotope composition of precipitation, δ_{SSL} = isotope composition of a terminal lake at steady-state, δ^* = limiting isotopic enrichment of a desiccating basin).

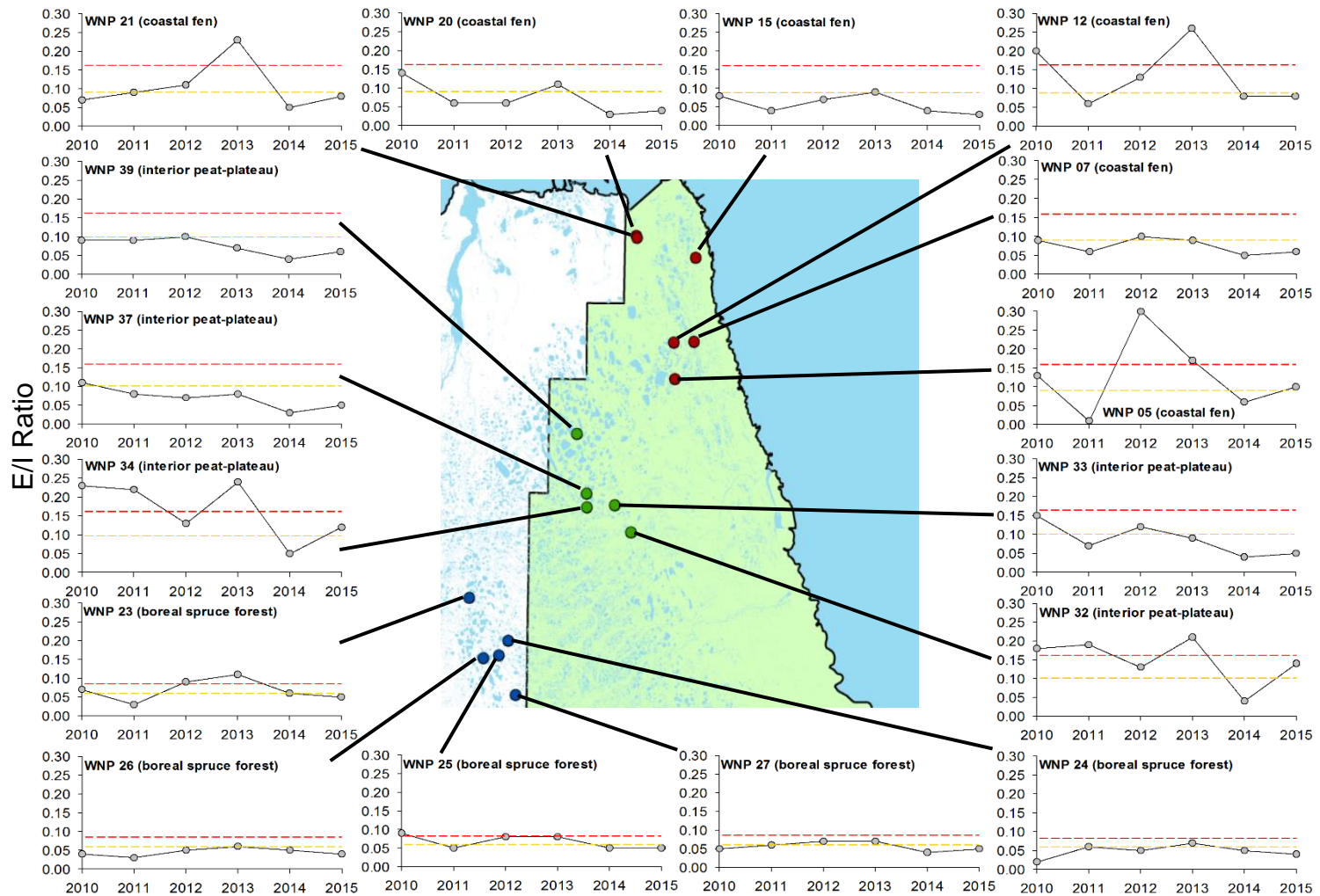


Figure 2.13 WNP E/I results for the spring sampling period. Red dash line represents 'poor' threshold and the yellow dash line represents 'fair' threshold. Note that the y-axis scale is from 0.00-0.30.

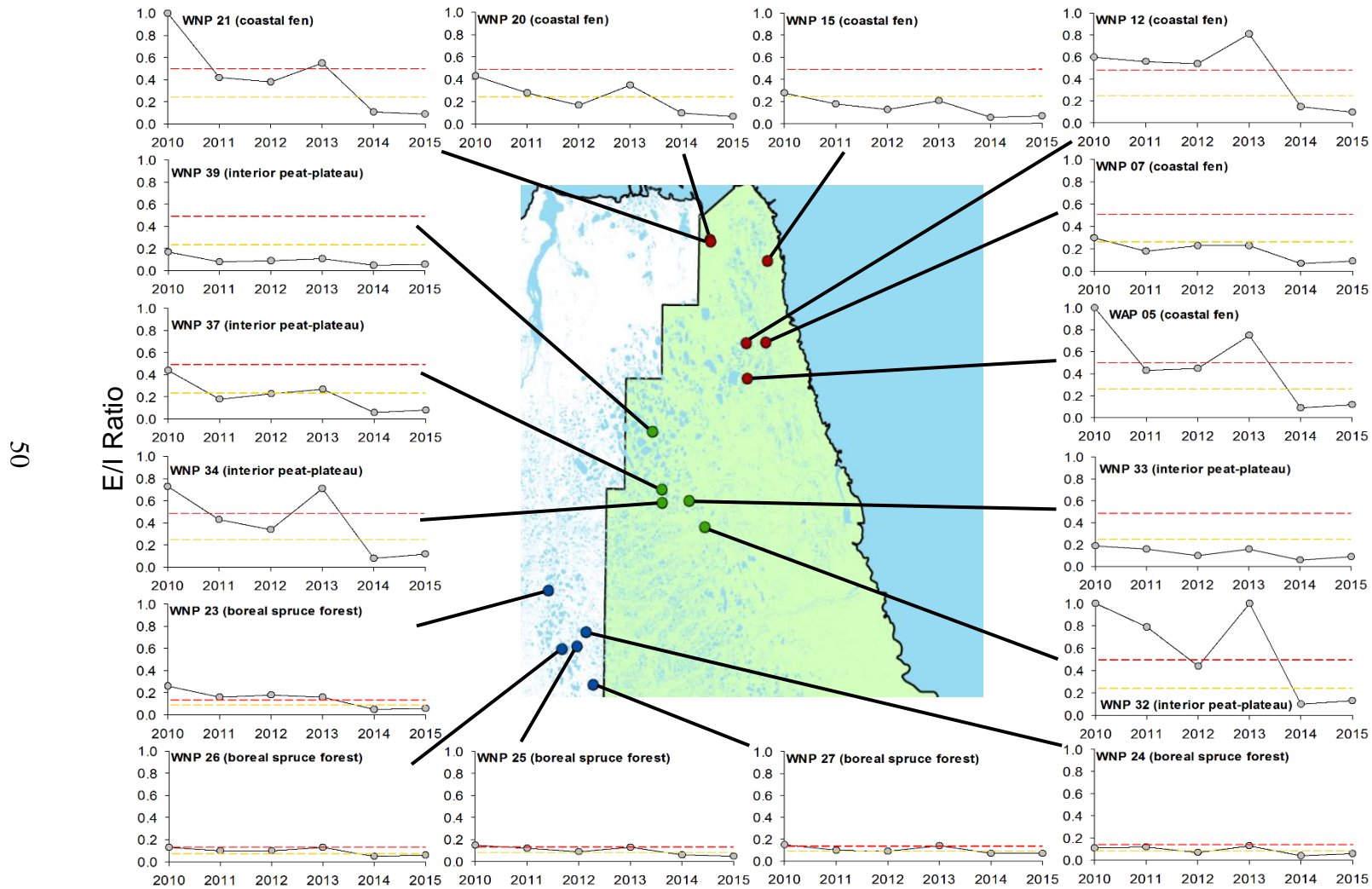


Figure 2.14 WNP E/I results for the summer sampling period. Red dash line represents 'poor' threshold and the yellow dash line represents 'fair' threshold. Note that the y-axis scale is from 0.00-1.00.

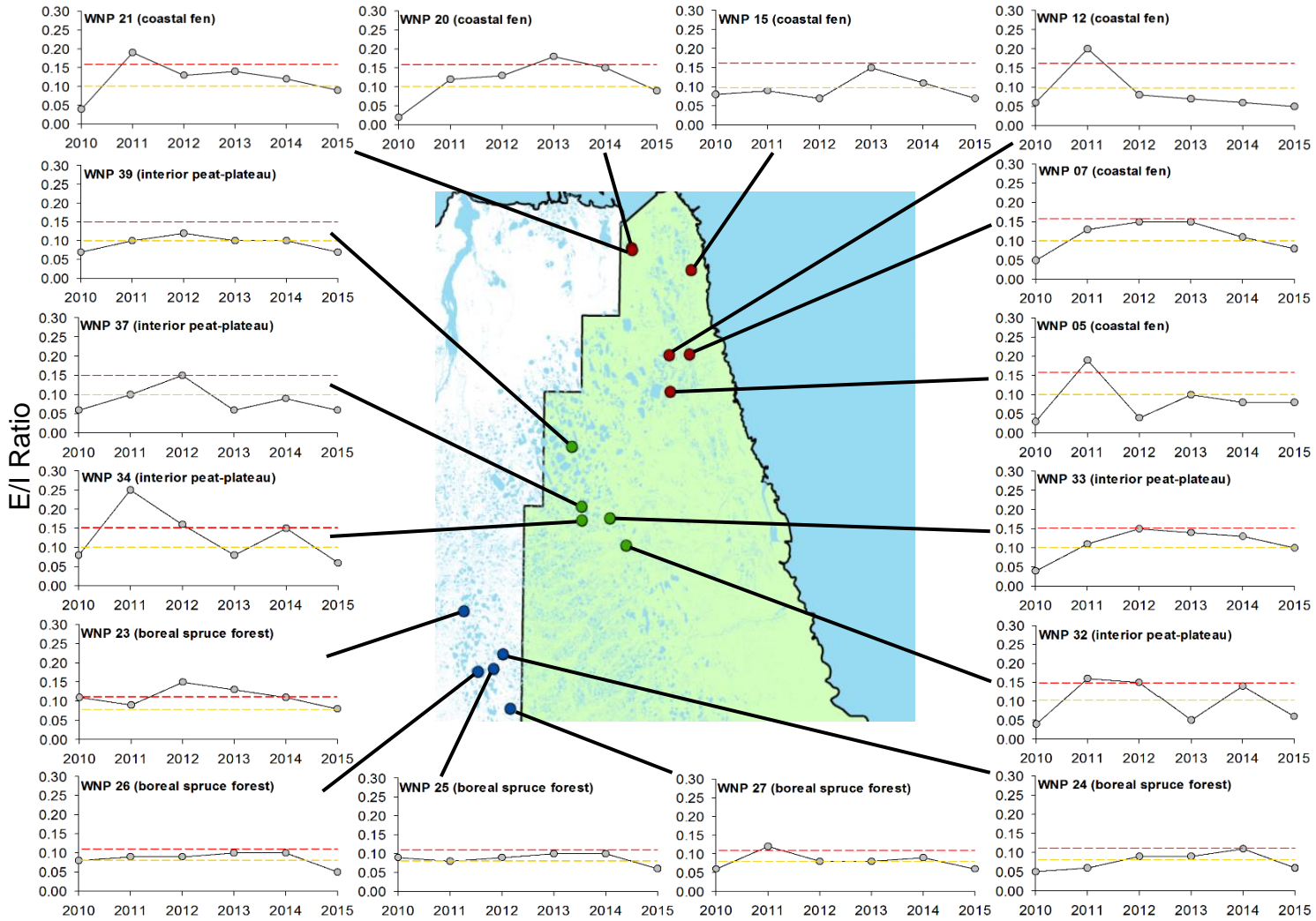


Figure 2.15 WNP E/I results for the fall sampling period. Red dash line represents 'poor' threshold and the yellow dash line represents 'fair' threshold. Note that the y-axis scale is from 0.00-0.30.

2.8 Tables

Table 2.1 VNP precipitation values from the Old Crow Airport weather station (Station ID 2100800 and 2100805; Environment Canada, 2019) listed along with the 1971-2000 climate normals. A sampling ‘year’ has been defined as October to September in order to capture full winter and summer records. No precipitation data were missing from 2006-2007, 2007-2008, 2011-2012 and 2012-2013 sampling years. Less than 1% of the precipitation data were missing from 2008-2009, 2009-2010, and 2014-2015 sampling years. Less than 10% of the precipitation data were missing from the 2010-2011 sampling year. For 2013-2014, > 85% of the precipitation data were missing. Annual totals are the sum of all observations.

Year (winter-winter)	Total Precipitation (mm)	Winter (Oct-Apr) Precipitation (mm)	Summer (May-Sept) Precipitation (mm)
Climate Normals (1971-2000)	265.5	100.0	165.5
2006-2007	230.6	115.9	114.7
2007-2008	189.2	27.2	162.0
2008-2009	239.5	91.8	147.4
2009-2010	320.6	50.4	270.2
2010-2011	388.5	183.9	204.6
2011-2012	185.8	70.1	115.7
2012-2013	223.7	64.1	159.6
2013-2014	-	-	-
2014-2015	250.9	81.7	169.2

Table 2.2 WNP precipitation values based on Environment and Climate Change Canada Historical Weather data from the Churchill Airport weather station (Churchill Climate, #5060608; Environment Canada, 2019) listed along with the 1971-2000 climate normals. A sampling ‘year’ has been defined as October to September to capture full winter and summer records. Annual and seasonal totals are the sum of all observations.

Year (winter-winter)	Total Precipitation (mm)	Winter (Oct-Apr) Precipitation (mm)	Summer (May-Sept) Precipitation (mm)
Climate Normals (1971-2000)	431.6	167.7	263.9
2009-2010	423.8	62.9	360.9
2010-2011	253.1	46.0	207.1
2011-2012	417.0	164.9	252.1
2012-2013	257.7	45.2	212.5
2013-2014	344.1	66.9	277.2
2014-2015	387.7	136.5	251.2

Table 2.3 VNP and WNP 3-year E/I ratio thresholds. ‘Fair’ and ‘poor’ thresholds are statistical representations of the 68th and 95th percentiles, respectively, on the mean, and are analogous to 1 and 2 standard deviations above the mean for normal data. Separate thresholds are set for the three lake categories in VNP (rainfall-dominated, snowmelt-dominated, and intermediate) and the three lake categories in WNP (coastal fen, interior peat plateau, and boreal spruce forest).

	Lake Category	Season	‘Good’	‘Fair’	‘Poor’
VNP	Rainfall-dominated (R-D)	Spring	< 0.45	0.45 – 0.63	> 0.63
		Fall	< 0.66	0.66 – 0.91	> 0.91
	Snowmelt-dominated (S-D)	Spring	< 0.14	0.14 – 0.21	> 0.21
		Fall	< 0.36	0.36 – 0.63	> 0.63
	Intermediate (I)	Spring	< 0.19	0.19 – 0.26	> 0.26
		Fall	< 0.27	0.27 – 0.46	> 0.46
WNP	Coastal fen (CF)	Spring	< 0.09	0.09 – 0.16	> 0.16
		Summer	< 0.26	0.26 – 0.51	> 0.51
		Fall	< 0.10	0.10 – 0.16	> 0.16
	Interior peat plateau (IPP)	Spring	< 0.10	0.10 – 0.16	> 0.16
		Summer	< 0.23	0.23 – 0.49	> 0.49
		Fall	< 0.10	0.10 – 0.15	> 0.15
	Boreal spruce forest (BSF)	Spring	< 0.06	0.06 – 0.08	> 0.08
		Summer	< 0.09	0.09 – 0.13	> 0.13
		Fall	< 0.08	0.08 – 0.11	> 0.11

Table 2.4 Summary of VNP E/I values per lake and season from 2007 to 2015. Green values represent lake E/I ratios that fall within the ‘good’ condition, yellow represents lake E/I ratios that fall within the ‘fair’ condition, and red values represents lake E/I ratios that are within the ‘poor’ condition.

		2007		2008		2009		2010		2011		2012		2013		2014		2015
Lake #	Lake Category	Spring	Fall	Spring	Fall	Spring	Fall	Spring	Fall	Spring	Fall	Spring	Fall	Spring	Fall	Spring	Fall	Spring
06	R-D	0.55	1.02	0.49	1.04	0.35	0.49	0.78	0.72	0.51	0.74	0.39	0.87	0.35	0.59	0.42	0.88	0.39
19	R-D	0.43	-	0.78	1.08	0.48	0.73	0.72	0.84	0.46	0.78	0.52	0.67	0.37	0.55	0.58	0.58	0.45
29	R-D	0.35	0.58	0.41	0.59	0.37	0.53	0.41	0.64	0.37	0.58	0.50	0.65	0.38	0.48	0.37	0.49	0.34
34	R-D	0.29	-	0.32	0.55	0.41	0.34	0.43	0.53	0.30	0.52	0.32	0.50	0.32	0.42	0.33	0.42	0.27
35	R-D	0.22	-	0.32	0.65	0.29	0.40	0.48	0.56	0.32	0.53	0.38	0.67	0.32	0.41	0.29	0.53	0.28
37	R-D	0.39	-	0.50	0.78	0.42	0.45	-	-	0.44	0.64	0.47	0.67	0.38	0.53	0.39	0.44	0.33
38	R-D	0.25	0.49	0.40	0.51	0.30	0.35	0.25	0.26	0.20	0.40	0.24	0.21	0.18	0.38	0.19	0.29	0.19
46	R-D	0.19	-	0.66	0.95	0.33	0.46	0.50	0.67	0.41	0.68	0.26	0.70	0.22	0.53	0.22	0.41	0.31
49	R-D	0.49	-	0.56	0.77	0.55	0.55	0.51	0.65	0.44	0.89	0.61	0.65	0.44	0.76	0.43	0.57	0.40
58	R-D	-	-	-	0.77	0.44	0.57	0.66	0.57	0.41	0.69	0.67	0.58	0.39	0.60	0.43	0.56	0.36
26	I	0.18	-	0.23	0.37	0.21	0.23	0.21	0.29	0.19	0.25	0.17	0.37	0.20	0.33	0.21	0.35	0.18
48	I	0.08	-	0.16	0.14	0.21	0.13	0.22	0.35	0.16	0.14	0.16	0.10	0.06	0.05	0.15	0.07	0.09
11	S-D	0.03	0.63	0.09	0.50	0.06	0.27	0.21	0.27	0.10	0.48	0.11	0.55	0.14	0.47	0.23	0.67	0.12
55	S-D	0.09	0.19	0.14	0.23	0.12	0.15	0.23	0.20	0.07	0.15	0.13	0.11	0.09	0.13	0.14	0.16	0.07

Table 2.5 Summary of WNP E/I values per lake and season from 2010 to 2015. Green values represent lake E/I ratios that fall within the ‘good’ condition, yellow represents lake E/I ratios that fall within the ‘fair’ condition, and red values represents lake E/I ratios that are within the ‘poor’ condition.

Lake #	Lake Category	2010			2011			2012			2013			2014			2015		
		Spring	Summer	Fall	Spring	Summer	Fall	Spring	Summer	Fall	Spring	Summer	Fall	Spring	Summer	Fall	Spring	Summer	Fall
05	CF	0.13	1.28	0.03	0.01	0.43	0.19	0.30	0.45	0.04	0.17	0.75	0.10	0.06	0.19	0.08	0.10	0.12	0.08
07	CF	0.09	0.30	0.05	0.06	0.18	0.13	0.10	0.23	0.15	0.09	0.23	0.15	0.05	0.07	0.11	0.06	0.09	0.08
12	CF	0.20	0.60	0.06	0.06	0.56	0.20	0.13	0.54	0.08	0.26	0.81	0.07	0.08	0.15	0.06	0.08	0.10	0.05
15	CF	0.08	0.28	0.08	0.04	0.18	0.09	0.07	0.13	0.07	0.09	0.21	0.15	0.04	0.06	0.11	0.03	0.07	0.07
20	CF	0.14	0.43	0.02	0.06	0.28	0.12	0.06	0.17	0.13	0.11	0.35	0.18	0.03	0.10	0.15	0.04	0.07	0.09
21	CF	0.07	1.52	0.04	0.09	0.42	0.19	0.11	0.38	0.13	0.23	0.55	0.14	0.05	0.11	0.12	0.08	0.09	0.09
32	IPP	0.18	2.75	0.04	0.19	0.79	0.16	0.13	0.44	0.15	0.21	0.99	0.05	0.04	0.10	0.14	0.14	0.13	0.06
33	IPP	0.15	0.19	0.04	0.07	0.16	0.11	0.12	0.10	0.15	0.09	0.16	0.14	0.04	0.06	0.13	0.05	0.09	0.10
34	IPP	0.23	0.73	0.08	0.22	0.43	0.25	0.13	0.34	0.16	0.24	0.71	0.08	0.05	0.08	0.15	0.12	0.12	0.06
37	IPP	0.11	0.44	0.06	0.08	0.18	0.10	0.07	0.23	0.15	0.08	0.27	0.06	0.03	0.06	0.09	0.05	0.08	0.06
39	IPP	0.09	0.17	0.07	0.09	0.08	0.10	0.10	0.09	0.12	0.07	0.11	0.10	0.04	0.05	0.10	0.06	0.06	0.07
23	BSF	0.07	0.26	0.11	0.03	0.16	0.09	0.09	0.18	0.15	0.11	0.16	0.13	0.06	0.05	0.11	0.05	0.06	0.08
24	BSF	0.02	0.11	0.05	0.06	0.12	0.06	0.05	0.07	0.09	0.07	0.13	0.09	0.05	0.04	0.11	0.04	0.06	0.06
25	BSF	0.09	0.15	0.09	0.05	0.12	0.08	0.08	0.09	0.09	0.08	0.13	0.10	0.05	0.06	0.10	0.05	0.05	0.06
26	BSF	0.04	0.13	0.08	0.03	0.10	0.09	0.05	0.10	0.09	0.06	0.13	0.10	0.05	0.05	0.10	0.04	0.06	0.05
27	BSF	0.05	0.15	0.06	0.06	0.10	0.12	0.07	0.09	0.08	0.07	0.14	0.08	0.04	0.07	0.09	0.05	0.07	0.06

2.9 Chapter 2 Appendix

ISOTOPE FRAMEWORK

Meteorological Calculations

Temperature (T) and relative humidity (h) were calculated as the average evaporation-flux-weighted values for VNP from 2007 to 2009 and for WNP from 2010 to 2012. In both cases utilized climate data was from Environment Canada (VNP: Station ID 2100800 and 2100805; WNP: 5060608; Environment Canada, 2019). The average ice-free season T and h values were flux-weighted based on estimates of potential evapotranspiration following Thornthwaite (1948):

$$T_{flux} (\text{°C}) = \Sigma (T_a \times E_t) / (E_t) \quad [\text{E.1}]$$

$$h_{flux} (\%) = \Sigma (h \times E_t) / (E_t) \quad [\text{E.2}]$$

where T_a represents the monthly average temperature and h represents the monthly average humidity. The value of E_t represents the monthly potential evapotranspiration for ice-free months using:

$$E_t (\text{cm}) = 1.6 \times (L/12) \times (N/30) \times ((10 \times T_a) / I)^a \quad [\text{E.3}]$$

where L represents average day length in hours in a month and N represents the number of days in the month. I represents the thaw season heat index and a is a calculated coefficient. I was calculated as:

$$I (\text{°C}) = \Sigma ((T_a^{1.5}) / 5) \quad [\text{E.4}]$$

and the coefficient a is calculated as:

$$a = 0.49239 + 0.01792 \times I - 7.7 \times 10^{-5} \times I^2 + 6.75 \times 10^{-7} \times I^3 \quad [\text{E.5}]$$

Isotopic Framework Calculations

The isotopic framework parameters were calculated based on the linear resistance model of Craig and Gordon (1965) as well as the approaches outlined in detail in Gonfiantini (1986), Gibson and Edwards (2002), Edwards et al. (2004) and Yi et al. (2008).

The LEL for both VNP and WNP was determined using a 3-year average (2007-2009 and 2010-2012, respectively) of environmental conditions as well as calculated flux-weighted values and pre-existing isotopic data. The LEL was determined as a regression of the mean annual isotope composition of precipitation (δ_P), the limiting steady-state isotope composition (δ_{SSL}), and the theoretical limiting non-steady-state composition of a water-body approaching complete desiccation (δ^*). For VNP calculations, δ_P was estimated from the intersection of the evaporation pan-predicted LEL and the GMWL (Turner et al., 2010, 2014; Tondu et al., 2013). For WNP calculations, δ_P was obtained from the Canadian Network for Isotopes in Precipitation (CNIP). Mean δ_{SSL} was determined once equilibrium was estimated to be established within the deployed evaporation pan for each year (refer to Figure 5a in Tondu et al., 2013 for VNP and Figure 7 for WNP). δ^* was calculated from Gonfiantini (1986):

$$\delta^* = (h\delta_{AS} + \epsilon_K + \epsilon^* / \alpha^*) / (h - \epsilon_K - \epsilon^* / \alpha^*) \quad [\text{E.6}]$$

where δ_{AS} is the isotope composition of atmospheric moisture for the ice-free season, ϵ_K is the kinetic enrichment factor, ϵ^* is the equilibrium enrichment factor and α^* is the equilibrium liquid-vapour isotope fractionation factor.

α^* for $\delta^{18}\text{O}$ and $\delta^2\text{H}$ were derived using equations reported in Horita and Wesolowski (1994):

$$1000\ln\alpha^* = -7.685 + 6.7123 (10^3/T) - 1.6664 (10^6/T^2) + 0.35041 (10^9/T^3)$$

for $\delta^{18}\text{O}$ and [E.7]

$$1000\ln\alpha^* = 1158.8 (T^3/10^9) - 1620.1 (T^2/10^6) + 794.84 (T/10^3) - 161.04 + 2.9992 (10^9/T^3)$$
[E.8]

for $\delta^2\text{H}$, where temperature (T) represents flux-weighted temperature in Kelvin. The equilibrium (ϵ^*) enrichment factor was calculated as:

$$\epsilon^* = \alpha^* - 1$$
[E.9]

and the kinetic (ϵ_K) enrichment factor was calculated as:

$$\epsilon_K = 0.0142 (1 - h)$$
[E.10]

for $\delta^{18}\text{O}$ and

$$\epsilon_K = 0.0125 (1 - h)$$
[E.11]

for $\delta^2\text{H}$ (Gonfiantini, 1986). Isotope composition of the ice-free season atmospheric moisture (δ_{AS}) was calculated using the equation from Gibson et al. (1999):

$$\delta_{AS} = [(\delta_{SSL} - \epsilon^*) / \alpha^* - \epsilon_K - \delta_P(1 - h + \epsilon_K)] / h$$
[E.12]

Results of the isotope framework calculations are reported in Table 2.A3 for VNP and Table 2.A4 for WNP.

Calculating Evaporation to Inflow Ratios

The isotope compositions of individual lake input water and evaporative flux were derived based on isotope mass-balance equations and the Yi et al. (2008) coupled isotope tracer method. This includes balancing the volume of evaporative flux (δ_E) with outflow (δ_L) to input water (δ_I). δ_L is isotopically equivalent to lake water since liquid outflow does not fractionate (Gibson and Edwards, 2002). Therefore, utilizing an isotope-mass balance, isotope data can be quantified in terms of an evaporation to inflow (E/I) ratio:

$$E/I = (\delta_I - \delta_L) / (\delta_E - \delta_L) \quad [E.13]$$

where δ_I can then be estimated by determining the point of intersection between the GMWL and the lake-specific LEL (consisting of δ_E , δ_L , and δ^*) and where δ_E represents the isotope composition of the vapour derived from an evaporating lake. δ_E was calculated using Craig and Gordon (1965):

$$\delta_E = [((\delta_L - \epsilon^*) / \alpha^*) - h\delta_{AS} - \epsilon_K] / (1 - h + \epsilon_K) \quad [E.14]$$

BOOTSTRAPPING STATISTICAL ANALYSIS

Since the sample size for each category is relatively small, the random sampling and resampling of a dataset with replacement, or bootstrapping, was applied to gamma distributions of E/I ratios to establish ‘good’, ‘fair’, and ‘poor’ hydrological thresholds. We bootstrapped or ‘re-sampled’ each seasonal lake category dataset 1,000 times and calculated the mean 68th and 95th percentiles for each (Figure 2.A1).

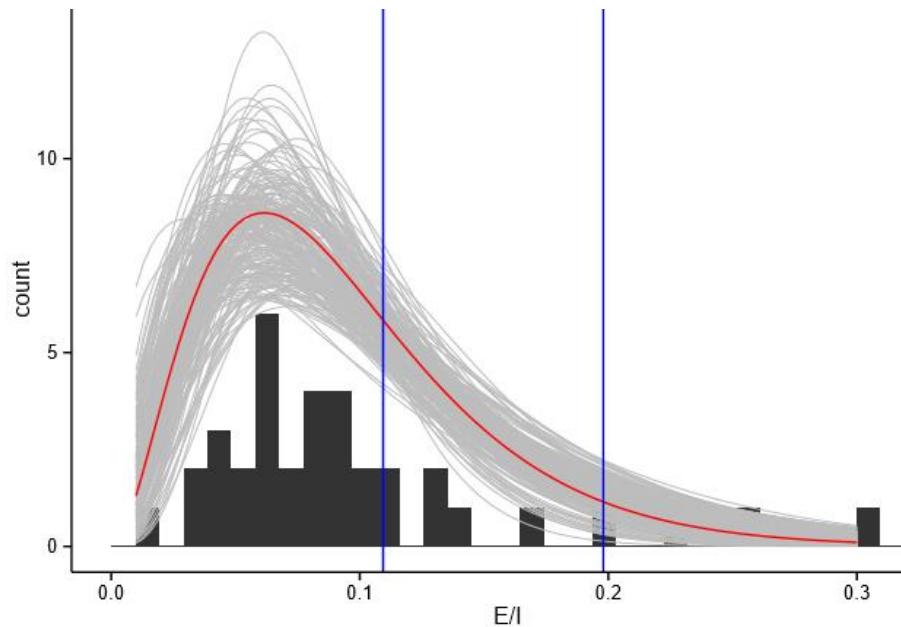


Figure 2.A1 Sample of a bootstrapped dataset (WNP June Coastal Fen) where 200/1000 bootstrapped models are shown in grey, the red line represents the mean of all bootstrapped models, and the blue lines represent the 68th and 95th percentiles used to generate the thresholds.

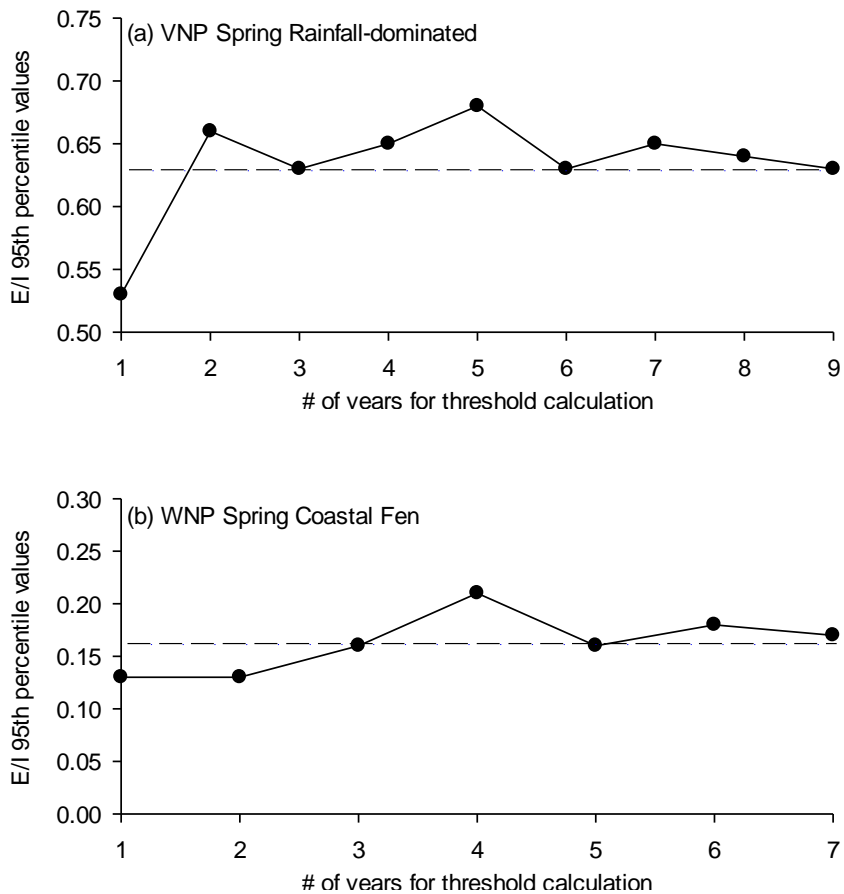


Figure 2.A2 The 3-year threshold calculations used for this research are accurate representations of the data for both VNP and WNP. (a) Threshold calculations based on 1 to 9 years of data for spring samples of rainfall-dominated lakes in VNP. Dashed line represents the mean threshold value (mean E/I = 0.63). (b) Threshold calculations based on 1 to 7 years of data for spring samples of coastal fen lakes in WNP. Dashed line represents the mean threshold value (mean E/I = 0.16).

Table 2.A1 Select lake characteristics for VNP, modified from Tondu et al. (2013, p. 598). Lake categories were defined by Turner et al. (2010) and Tondu et al. (2013).

Lake ID	Lake Category	Latitude	Longitude	Approximate Depth (cm)	Surface Area (km²)
VNP 06	Rainfall	67°55'N	139°56'W	33	5.01
VNP 11	Snowmelt	68°01'N	140°34'W	78	0.07
VNP 19	Rainfall	68°17'N	140°31'W	86	0.11
VNP 26	Intermediate	67°50'N	139°59'W	169	0.42
VNP 29	Rainfall	67°54'N	139°48'W	118	6.86
VNP 34	Rainfall	67°53'N	139°27'W	154	6.11
VNP 35	Rainfall	67°58'N	139°37'W	116	0.14
VNP 37	Rainfall	68°05'N	139°81'W	119	5.14
VNP 38	Rainfall	68°19'N	140°08'W	105	12.67
VNP 46	Rainfall	68°09'N	139°36'W	48	0.12
VNP 48	Intermediate	98°11'N	139°52'W	70	1.31
VNP 49	Rainfall	68°04'N	139°39'W	124	1.15
VNP 55	Snowmelt	67°50'N	139°45'W	>500	0.02
VNP 58	Rainfall	67°32'N	139°51'W	255	-

Table 2.A2 Select lake characteristics for WNP. Surface area was calculated by Farquharson (2013). WNP 12 surface area is not reported due to low-resolution satellite imagery. Lake depths are average values estimated from multiple field season (2010-2015) observations.

Lake ID	Lake Category	Latitude	Longitude	Approximate Depth (cm)	Surface Area (km²)
WNP 05	Coastal fen	58.34223	-93.2645	15	2.29
WNP 07	Coastal fen	58.42721	-93.1782	30	25.84
WNP 12	Coastal fen	58.42558	-93.2689	15	-
WNP 15	Coastal fen	58.62001	-93.1710	30	93.72
WNP 20	Coastal fen	58.66995	-93.4437	40	23.06
WNP 21	Coastal fen	58.66515	-93.4409	25	0.70
WNP 23	Boreal forest	57.83547	-94.1827	>200	1,087.51
WNP 24	Boreal forest	57.73882	-94.0051	>200	98.20
WNP 25	Boreal forest	57.70476	-94.0465	>300	2,686.41
WNP 26	Boreal forest	57.69803	-94.1149	>200	177.37
WNP 27	Boreal forest	57.61421	-93.9695	>300	1,196.03
WNP 32	Interior peat plateau	57.99007	-93.4593	60	0.53
WNP 33	Interior peat plateau	58.05161	-93.5329	60	12.61
WNP 34	Interior peat plateau	58.04637	-93.6592	10	0.13
WNP 37	Interior peat plateau	58.0782	-93.6610	100	1,366.13
WNP 39	Interior peat plateau	58.21463	-93.7076	>500	7,613.78

Table 2.A3 Modified from Tondu et al. (2013), flux weighted ice-free season temperature and relative humidity based on data from the Old Crow Airport weather station (Station ID 2100800 and 2100805; Environment Canada, 2019) as well as parameters used to construct the 3-year average isotope framework for VNP lakes.

Parameter	2007	2008	2009	3-yr average
T (K)	287.7	286.3	285.8	286.6
h (%)	62.6	64.0	66.5	64.4
α^* (^{18}O , ^2H)	1.0103, 1.0910	1.0104, 1.0927	1.0105, 1.0934	1.0104, 1.0924
ε^* (^{18}O , ^2H) ‰	10.3, 91.0	10.4, 92.7	10.5, 93.4	10.4, 92.4
ε_K (^{18}O , ^2H) ‰	5.3, 4.7	5.1, 4.5	4.8, 4.2	5.1, 4.5
δ_{AS} (^{18}O , ^2H) ‰	-28.8, -216	-29.5, -220	-27.8, -216	-28.7, -217
δ_{SSL} (^{18}O , ^2H) ‰	-11.8, -127	-12.4, -129	-11.7, -127	-12.0, -128
δ^* (^{18}O , ^2H) ‰	-4.1, -87	-5.6, -93	-5.2, -94	-5.0, -91
δ_P (^{18}O , ^2H) ‰	-24.1, -183	-24.2, -184	-24.1, -183	-24.1, -183

Table 2.A4 Flux weighted ice-free season temperature and relative humidity based on Environment and Climate Change Canada Historical Weather data from the Churchill Airport weather station (Churchill Climate, #5060608; Environment Canada, 2019) as well as parameters used to construct the 3-year average isotope framework for WNP lakes.

Parameter	2010	2011	2012	3-yr average
T (K)	283.3	284.4	283.7	283.8
h (%)	80.2	77.4	78.1	78.6
α^* (^{18}O , ^2H)	1.0107, 1.0968	1.0106, 1.0952	1.0107, 1.0963	1.0107, 1.0961
ε^* (^{18}O , ^2H) ‰	10.7, 96.8	10.6, 95.2	10.7, 96.3	10.7, 96.1
ε_K (^{18}O , ^2H) ‰	2.8, 2.5	3.2, 2.8	3.1, 2.7	3.0, 2.7
δ_{AS} (^{18}O , ^2H) ‰	-20.0, -183	-19.8, -185	-21.2, -200	-20.3, -189
δ_{SSL} (^{18}O , ^2H) ‰	-5.4, -66	-4.8, -63	-5.7, -70	-5.3, -66
δ^* (^{18}O , ^2H) ‰	-1.9, -41	-0.9, -43	-2.0, -55	-1.6, -46
δ_P (^{18}O , ^2H) ‰	-17.2, -129	-17.2, -129	-17.2, -129	-17.2, -129

Chapter 3: Use of water chemistry and carbon isotopes to assess effects of Lesser Snow Geese disturbance on lakes in Wapusk National Park, northern Manitoba

3.1 Introduction

Shallow lakes are abundant within many arctic and subarctic landscapes. These aquatic ecosystems are considered highly productive northern oases, providing necessary resources and habitat for wildlife and the traditional practices of indigenous cultures (Rouse et al., 1997; Prowse et al., 2006; Schindler and Smol, 2006). However, they are particularly responsive to environmental changes since small shifts in climate and wildlife populations can substantially alter their hydrological, limnological, and biogeochemical conditions via changes in water balance, nutrient cycling, and aquatic habitat (Handa et al., 2002; Gregory-Eaves et al., 2004; Lim et al., 2005; Van Geest et al., 2007; Côté et al., 2010; Sun et al., 2013; MacDonald et al., 2014). For example, shallow lakes of Wapusk National Park (WNP) within the western Hudson Bay Lowlands (HBL) of northern Manitoba provide important habitat and resources for a variety of wildlife, particularly waterfowl populations, yet are considered vulnerable to environmental stressors (Parks Canada, 2011; Wolfe et al., 2011a; Bouchard et al., 2013; MacDonald et al., 2015).

During the past ~40 years, there has been a rapid increase (5-14% per year) in the population density and nesting area range of the Lesser Snow Goose within WNP (LSG; *Chen caerulescens caerulescens*; Batt et al., 1997; Jefferies et al., 2006; Alisauskas et al., 2011; Peterson et al., 2013). This rapid population growth has been attributed to several

factors that increase the amount of energy LSG can allocate to reproduction and survival including: 1) nutrient subsidies at their wintering grounds and stopover locations due to modifications in agricultural practices, 2) the creation of conservation refuges along migratory flyways (e.g., Western Central and Mississippi flyways), and 3) warmer nesting locations within Canada's central Arctic and subarctic, adjacent to southern Hudson Bay during the past ~50 years (Boyd et al., 1982; Batt, 1997; Abraham et al. 2005b; Jefferies et al., 2006; Peterson et al., 2013). This region has experienced some of the greatest warming in the circumpolar North during the past ~50 years (Smith and Burgess, 2004; Kaufman et al., 2009; Hochheim et al., 2010), which has the potential to exacerbate LSG-disturbance on the HBL landscape. Parks Canada (2011) acknowledged that the combination of expanding LSG population and climate warming may drastically alter the ecological integrity of lakes in WNP, emphasizing the need for effective aquatic ecosystem monitoring.

Due to the recent population growth, grubbing, nesting, and defecating activities of LSG have increased in spatial coverage from <5 km² in 1969 to >300 km² in 2008, extending farther inland from the coastal fen into the interior peat plateau ecotype of WNP (Parks Canada, 2011). LSG arrive in WNP during early spring and alter the landscape by extensive removal of vegetation cover through grubbing (the removal of plant roots and rhizomes), therefore eliminating the important root system that binds soil (Hik et al., 1992; Jefferies et al., 2003, Peterson et al., 2013). Between 1973 and 1993, LSG activities led to the loss of >2,000 ha of coastal habitat along the northern La Perouse Bay portion of WNP and >35,000 ha of habitat within the HBL (Jefferies et al., 2006; Peterson et al., 2013).

Removal of catchment vegetation and deposition of feces substantially alters the limnology of affected lakes in WNP (MacDonald et al., 2014; 2015). Based on the analysis of water chemistry from one lake disturbed by LSG compared to 15 undisturbed lakes, MacDonald et al. (2014; 2015) identified a suite of limnological and carbon isotope variables sensitive to catchment disturbance by LSG including specific conductivity, $\delta^{13}\text{C}_{\text{Dissolved Inorganic Carbon (DIC)}}$, and $\Delta^{13}\text{C}_{\text{DIC-Phytoplanton Particulate Organic Matter (PHYTOPOM)}}$. Results indicated that high values of specific conductivity were likely due to the influx of dissolved ions from LSG-disturbed catchments (MacDonald et al., 2014; 2015). Additionally, high dissolved inorganic carbon demand and increased aquatic productivity were inferred from the carbon isotope data (MacDonald et al., 2014). These variables have been recommended for use in a long-term monitoring program for tracking effects of LSG disturbance over a broader landscape within WNP. Here, we apply these approaches to assess the effects LSG have on the WNP lakes within an $\sim 1,800 \text{ km}^2$ sector of the coastal fen and interior peat plateau landscapes where LSG disturbance is clearly evident from field observations in portions of this landscape. This research focuses on limnological and carbon isotope lake data collected in July 2015 and July 2016 and specifically aims to 1) characterize how lake hydrology, limnology, and carbon behaviour vary spatially across a gradient of LSG disturbance within a portion of WNP, 2) assemble and synthesize data to identify spatial patterns and degree of LSG disturbance to lakes within WNP, and 3) provide recommendations for continued monitoring of LSG disturbance to lakes within WNP.

3.2 Study Area

Wapusk National Park (WNP) was established in 1996 to protect a representative portion of the western HBL. The park spans approximately 11,475 km², containing the transition between discontinuous and continuous permafrost and the boundary between boreal forest and arctic tundra vegetation (Parks Canada, 2000). While WNP is covered extensively by wetlands (~80%), the park includes six physiographic ecotypes: coastal fen, coastal ridges and fen, transitional fen, coastal forested fen, interior peat plateau, and forested peat plateau (Parks Canada, 2000). This study focuses on lakes located within the coastal fen and interior peat plateau ecotypes since LSG population has expanded in size, density and geographic location within these ecotypes (Figure 3.1). The fen ecotypes are dominated by sedge and rush vegetation, with sparse terrestrial plant cover. The interior peat plateau ecotype contains moss, lichen, and small shrubs.

Lake Locations and LSG Disturbance Classification

Forty-five lakes (WNP 42-86) were chosen to provide a spatial assessment of LSG disturbance in the northern portion of WNP (Figure 3.1), which included 40 lakes in the coastal fen and 5 lakes in the interior peat plateau. Lakes of similar size (average area = 0.5 km²) and depth (< 1 m) with limited inflow and outflow were selected across the study area to avoid confounding influence of lake size and basin hydrology. In 2016, Parks Canada staff deemed that lake WNP 76A was too close to the coast since it was experiencing salt water inundation and a replacement lake was selected farther inland (WNP 76B; Figure 3.1a). Based on observations and specific conductivity values from previous field campaigns (2010-2014), a preliminary gradient of LSG disturbance was

identified across the WNP landscape from undisturbed (little to no LSG presence) to actively-disturbed (LSG present, evidence of feces, nesting, and grubbing) to severely-disturbed (barren landscape and lack of vegetation, potential past LSG presence) (Table 3.1, Figures 3.1, 3.2, Table 3.A1, and 3.A2). From these data, 29% of the study lakes were considered disturbed (eight lakes were classified as actively-disturbed and five lakes were classified as severely-disturbed), while the remainder (32, 71%) were considered undisturbed.

Meteorological Conditions

Meteorological conditions for this region have been monitored at the Churchill airport (Meteorological Service of Canada Station #5060608) since 1943, and air temperature and precipitation values show marked seasonal variations (Environment Canada, 2019; Figure 3.3). Based on 1971-2000 climate normals, annual mean air temperature is -6.9°C . Monthly mean air temperature fluctuates substantially between summer and winter seasons during the study period (2014-2016), comparable to the 1971-2000 climate normals (Figure 3.3a). However, maximum monthly summer and winter temperatures were on average $\sim 1.0^{\circ}\text{C}$ warmer during the entire study period.

Average annual precipitation is 431.6 mm, 61% of which falls as rain between May and September (263.9 mm), while the remainder falls as snow between October and April (167.7 mm). Total annual precipitation was comparable between 2014-2015 and 2015-2016 seasons, with total winter and summer precipitation values below climate normals (Table 3.2). However, almost 50% of summer rainfall (117.9 mm) in 2015 occurred in July prior to sampling (Figure 3.3b).

3.3 Methods

Water samples were collected from each of the 45 study lakes via helicopter once per summer (July 29-31, 2015, July 27-28, 2016) to characterize processes influencing hydrology, limnology, and carbon behaviour of lakes undisturbed and disturbed by LSG activities.

Hydrology

Water samples were collected at the edge of all 45 lakes at ~10 cm below the water surface and stored in 30 mL high density polyethylene bottles for oxygen and hydrogen stable isotope analysis. Samples were analyzed at the University of Waterloo Environmental Isotope Laboratory (UW-EIL) via off-axis integrated cavity output spectroscopy (O-AICOS). Isotope compositions are expressed as δ -values of ^{18}O and ^2H in per mil (‰) relative to the Vienna Standard Mean Ocean Water (VSMOW) standard ($\delta_{\text{sample}} = [(R_{\text{sample}}/R_{\text{VSMOW}}) - 1] \times 10^3$ ‰, where R is the $^{18}\text{O}/^{16}\text{O}$ or $^2\text{H}/^1\text{H}$ ratio in sample and VSMOW). Values of $\delta^{18}\text{O}$ and $\delta^2\text{H}$ are normalized to -55.5 ‰ and -428 ‰, respectively, for Standard Light Antarctic Precipitation (Coplen, 1996). Analytical uncertainties are standard deviations based on the in-run standards and are ± 0.2 ‰ for $\delta^{18}\text{O}$ and ± 0.8 ‰ for $\delta^2\text{H}$ (See Section 2.9 Chapter 2 Appendix for more details).

Limnology and Carbon Behaviour

In-situ measurements of water temperature, pH, and specific conductivity were made at ~15 cm water depth using a YSI 600QS multiparameter probe. Water samples were collected from the edge of each lake and stored in a 5 L carboy for nutrient

analyses. After sample collection, all lake water samples for nutrient analyses were transported by helicopter to the Churchill Northern Studies Centre (CNSC) for initial processing, where water was passed through an 80 μm mesh to remove large particles that can interfere with concentration estimates and then stored in the dark at 4°C until further analysis. The concentration of total Kjeldahl nitrogen (TKN, preserved with 0.02% H_2SO_4) and total phosphorus (TP) were measured at the Biogeochemistry Lab, University of Waterloo, following standard methods (TKN = Bran Luebbe, Method No. G-189-097; TP = Bran Luebbe, Method No. G-188-097; Seal Analytical, Seattle). For the determination of dissolved inorganic carbon (DIC) and dissolved organic carbon (DOC), water was filtered within 12 hours of collection (cellulose acetate filters: 0.4 μm pore size, 47 mm diameter) and stored in the dark at 4°C until analysis at Environment Canada's National Laboratory for Environmental Testing (NLET), Burlington, Ontario, using standard methods (Environment Canada, 1994).

The carbon isotope ratio of dissolved inorganic carbon ($\delta^{13}\text{C}_{\text{DIC}}$) was measured from samples collected while in the field in 125 mL glass serum bottles with rubber stoppers and needles to expel any excess air. Samples were then transported by helicopter to the Churchill Northern Studies Centre (CNSC) and stored in the dark and at 4°C prior to analysis at the UW-EIL. Samples for measurement of the carbon isotope ratio of phytoplanktonic particulate organic matter ($\delta^{13}\text{C}_{\text{PHYTOPOM}}$) were collected by multiple horizontal tows of a phytoplankton net (mesh size of 25 μm). Water samples were then passed through a 63 μm mesh net to remove zooplankton and other large particles, filtered onto pre-ashed Whatman[®] (GE Healthcare UK Limited, Little Chalfont, UK) quartz filters (CAT no. 1851-047), and dried at 60 °C for 24 h in an oven, following

MacDonald et al. (2014, 2015). HCl (12N) fumes were then used to remove carbonates from the filters (Lorrain et al., 2003). The acidified filters were analyzed for $\delta^{13}\text{C}_{\text{PHYTOPOM}}$ at the UW-EIL. Stable carbon isotope ratios are reported as $\delta^{13}\text{C}$ (‰) relative to the Vienna-PeeDee Belemnite (VPDB) standard. Additionally, the carbon isotope fractionation was approximated by the difference between $\delta^{13}\text{C}_{\text{DIC}}$ and $\delta^{13}\text{C}_{\text{PHYTOPOM}}$ as per MacDonald et al. (2015) and is reported as $\Delta^{13}\text{C}_{\text{DIC-PHYTOPOM}}$ (Fry, 2006; Coplen, 2011).

Numerical and Statistical Analyses

Multivariate ordinations by principal components analysis (PCA) were used to assess variation among lakes in limnological conditions and carbon isotope values of water and particulate organic matter during 2015 and 2016 (pH, TP, TKN, DIC, DOC, $\delta^{13}\text{C}_{\text{DIC}}$, and $\delta^{13}\text{C}_{\text{PHYTOPOM}}$). To accomplish this, the ‘prcomp’ function in R Statistical Environment was used (R Core Team, 2015). In the resulting ordination biplots, sample scores for the study lakes were colour-coded according to their LSG-disturbance categories (undisturbed, actively-disturbed, severely-disturbed) to explore for limnological differences among the categories. Then, a series of ANOSIM tests, a multivariate equivalent to 1-way ANOVA tests, with associated pairwise comparisons, were run to determine if limnological conditions differed among the three LSG disturbance categories. ANOSIM tests were performed separately for the 2015 and 2016 sampling years and were run using a function of the ‘vegan’ package in R Statistical Environment (Oksanen et al., 2019). The ANOSIM test statistic, global R, ranges from 0 to 1 and represents the observed differences between groups of samples compared with

the differences among replicates within each group. A test statistic (R value) of 0 indicates that the similarity between and within LSG disturbance categories is on average the same, whereas a value of 1 indicates that replicates within a LSG disturbance category are more similar to each other than to replicates of the other LSG disturbance categories. P-values were generated by comparing the distribution within and across LSG disturbance category rank (999 permutations) to the initial rank similarity (reported by the global R value). Then, using univariate Kruskal-Wallis tests, we tested if each limnological variable differed among the three LSG-disturbance categories. For Kruskal-Wallis tests that produced a significant p-value, Dunn's post-hoc pairwise comparisons were run, which do not assume equal variances of limnological variables among the LSG disturbance categories. For all statistical tests, alpha was set to 0.05. For both sampling years, boxplots were used to compare the distribution of lake limnological variables among lakes in the three LSG-disturbance categories. The Kruskal-Wallis tests and Dunn's post-hoc-tests and boxplots were all performed using SigmaPlot version 14.0 software (Systat Software Inc., San Jose, California).

Spatial interpolation

The level of spatial association among limnological results (specific conductivity, pH, $\delta^{13}\text{C}_{\text{DIC}}$, $\delta^{13}\text{C}_{\text{PHYTOPOM}}$, $\Delta^{13}\text{C}_{\text{DIC-PHYTOPOM}}$, and concentrations of TP, TKN, DIC, and DOC) in 2015 and 2016 was assessed through calculation of Moran's I coefficient, a local indicator of spatial association expressed on a scale from 0 (weakest) to 1 (strongest) (Anselin, 1995). To explore spatial patterns of LSG disturbance across WNP, inverse-distance-weighted (IDW) interpolated contour prediction maps of selected

limnological data (variables with Moran's I > 0.5) were generated following methods of Turner et al. (2010, 2014).

To synthesize the spatial data into a single metric of LSG disturbance, minimum and maximum values of variables with Moran's I > 0.5 (specific conductivity, $\delta^{13}\text{C}_{\text{DIC}}$, $\delta^{13}\text{C}_{\text{PHYTOPOM}}$, and concentrations of TP and TKN) were individually scaled from 0 to 1 per lake using the following equation:

$$x_{scaled} = \frac{x - x_{min}}{x_{max} - x_{min}} \quad [\text{eq. 1}]$$

The scaled data for these five measures were then averaged at each lake to obtain a single integrated measure of LSG disturbance for every sampling lake, where values approaching 1 represent areas of higher LSG disturbance and values approaching 0 represent areas undisturbed by LSG. The averaged scaled value for each lake was calculated using the following equation:

$$x_{scaled_WNP\#} = \frac{(x_{scaled_cond} + x_{scaled_TP} + x_{scaled_TKN} + x_{scaled_delta13CDIC} + x_{scaled_delta13CPHYTOPOM})}{5} \quad [\text{eq. 2}]$$

Finally, an inverse-distance-weighted (IDW) interpolated contour prediction map of these scaled limnological data was generated following methods of Turner et al. (2010, 2014). The ArcGIS (ESRI) suite as well as the Spatial Statistics and Spatial Analyst toolboxes were used for all spatial interpolations (ESRI, 2017).

3.4 Results

Hydrology

Water isotope values for July 2015 do not show substantial variability among the study lakes. Instead, values narrowly range from -11.5 to -8.1‰ and -95.3 to -80.4‰ for $\delta^{18}\text{O}$ and $\delta^2\text{H}$, respectively, and values for several lakes plot above the Local Evaporation Line (LEL; Figure 3.4a). Both the low variability and positioning of lake water isotope compositions above the LEL in 2015 are most likely due to a large amount of rainfall during the month of July, just prior to and during sample collection (117.9 mm; Figure 3.3b). This rainfall likely caused a lowering of lake water isotope compositions, homogenizing the hydrological conditions among the lakes. In July 2016, water isotope compositions show considerably greater variability of values among lakes and values are generally higher than in 2015 (-9.4 to -4.9‰ and -86.6 to -65.8‰ for $\delta^{18}\text{O}$ and $\delta^2\text{H}$, respectively; Figure 3.4b). Greater influence of evaporation led to several lakes partially desiccating in 2016 (WNP 51-56). Less rainfall occurred in summer 2016 compared to 2015 and no major rainfall events took place prior to sampling, yet some influence of rainfall is evident because several of the lake water isotope compositions plot above the LEL.

Comparison of limnological conditions and carbon behaviour among LSG-disturbance categories

In 2015, the first two PCA axes explain 66.8% of the total variation in the measured variables. Axis 1 explained 45.8% and separated sample scores based mainly on pH, concentrations of nutrients (TP, TKN, DIC, DOC), and $\delta^{13}\text{C}_{\text{PHYTOPOM}}$ (Figure

3.5a). Axis 2 captured 21.0% of the variation and separated samples based on carbon isotope values ($\delta^{13}\text{C}_{\text{DIC}}$). PCA axis 1 separated lakes in the severely-disturbed category from those in the actively- and undisturbed categories (Figure 3.5a). Lakes in the severely-disturbed category possessed relatively higher pH and concentrations of nutrients (TP, TKN, DIC, DOC) than lakes in the other two categories. ANOSIM tests on the 2015 limnological data identified that limnological conditions differ significantly between at least one the three LSG disturbance categories ($R = 0.649$, $P = 0.001$). Pairwise ANOSIM tests identify that limnological conditions within severely-disturbed lakes differ significantly from conditions in the other two categories (undisturbed, actively-disturbed; Table 3.3). However, the difference between undisturbed and actively-disturbed lake categories are not significant (Table 3.3).

Univariate Kruskal-Wallis tests (Table 3.4) and Dunn's post-hoc tests (Table 3.5) identified that distributions of all the limnological variables (pH, $\delta^{13}\text{C}_{\text{DIC}}$, and concentrations of TP, TKN, DIC, and DOC), except $\delta^{13}\text{C}_{\text{PHYTOPOM}}$, differ significantly between severely-disturbed lakes and lakes in the other two categories, but they do not differ significantly between actively-disturbed and undisturbed lakes (Figure 3.6, Table 3.5). The distribution of $\delta^{13}\text{C}_{\text{PHYTOPOM}}$ differs significantly between severely-disturbed lakes and undisturbed lakes, but it does not differ significantly between lakes in the actively-disturbed and undisturbed categories (Table 3.5).

In 2016, the first two PCA axes explain 70.7% of the total variation in the measured limnological variables (Figure 3.5b). Axis 1 captured most of the total variation (58.5%). Lakes with relatively high pH, nutrient concentrations (TP, TKN, DIC, DOC), and $\delta^{13}\text{C}_{\text{PHYTOPOM}}$ were positioned to the right along axis 1, whereas lakes with lower

values of these variables and relatively higher values of $\delta^{13}\text{C}_{\text{DIC}}$ were positioned to the left along axis 1. Sample scores were distinctly separated by the PCA ordination for lakes in the three LSG-disturbance categories. The severely-disturbed lakes were positioned farthest to the right along axis 1, associated with relatively high concentrations of nutrients and high pH, and the highest $\delta^{13}\text{C}_{\text{PHYTOPOM}}$ values, as well as the lowest values of $\delta^{13}\text{C}_{\text{DIC}}$. In contrast, the undisturbed lakes possessed the highest values of $\delta^{13}\text{C}_{\text{DIC}}$ and the lowest values of pH, nutrient concentrations (TP, TKN, DIC, DOC), and $\delta^{13}\text{C}_{\text{PHYTOPOM}}$. The lakes in the actively-disturbed category were characterized by intermediate values of all the limnological variables. Sample scores for only two lakes plot outside the range of the others in their disturbance category. ANOSIM tests on the 2016 limnological data identified that limnological conditions differ significantly among the three LSG disturbance categories ($R = 0.879$, $P = 0.001$). Pairwise ANOSIM tests identify that limnological conditions differ significantly among all three LSG disturbance categories (Table 3.3).

Univariate Kruskal-Wallis tests (Table 3.4) and Dunn's post-hoc tests (Table 3.5) identified that distributions of all the limnological parameters (pH, TP, TKN, DIC, DOC, $\delta^{13}\text{C}_{\text{DIC}}$, and $\delta^{13}\text{C}_{\text{PHYTOPOM}}$) differ significantly among all three LSG-disturbance categories in 2016 (Figure 3.6, Table 3.5). Interestingly, boxplots illustrate that concentrations of TP, TKN, DIC and DOC span a much larger range in the severely-disturbed lakes than the lakes in the other two categories (Figure 3.6).

$\Delta^{13}\text{C}_{\text{DIC-PHYTOPOM}}$ values for the severely-disturbed category are lower than both undisturbed and actively-disturbed lakes during both 2015 and 2016 (Figure 3.7a). Comparable to limnological trends observed for 2015, there is no significant difference

between the undisturbed and actively-disturbed categories (Figure 3.7a). However, $\Delta^{13}\text{C}_{\text{DIC-PHYTOPOM}}$ values during 2016 sequentially decrease along the gradient of increasing LSG disturbance and show a significant difference between all three LSG disturbance categories. C-isotope fractionation values around -20‰ are expected when there is sufficient dissolved CO_2 to support aquatic photosynthesis (Rau, 1978; Herczeg and Fairbanks, 1987; Bade et al., 2004; Fry, 2006; MacDonald et al., 2014). In a scatterplot of $\delta^{13}\text{C}_{\text{DIC}}$ versus $\delta^{13}\text{C}_{\text{PHYTOPOM}}$, severely-disturbed lake values fall above the $\Delta = -20\text{‰}$ line, signifying isotope fractionation under conditions where dissolved CO_2 concentrations are not in excess. In contrast, lakes in the undisturbed category and many actively-disturbed categories fall below the $\Delta = -20\text{‰}$ line, signifying isotope fractionation where dissolved CO_2 concentrations are in excess (Figure 3.7b).

Spatial Interpolation

All water chemistry parameters were explored for spatial associations, but only those that achieved high Moran's I levels (values above 0.5) are considered here (Figure 3.8). In 2015 and 2016, lakes with high specific conductivity located in the northern portion of WNP, by La Perouse Bay, have been identified using inverse-distance-weighted interpolation (Figure 3.8b, c). This area corresponds to lakes within actively- and severely-disturbed LSG categories. Since the severely-disturbed lakes (WNP 52-56) have substantially higher specific conductivity (2-year range = 3,872 to 7,066 $\mu\text{S}/\text{cm}$) compared to other lakes (2-year range = 94 to 1,727 $\mu\text{S}/\text{cm}$), their signal is particularly dominant within the inverse-distance-weighted interpolation. However, during the

summer of 2016, lakes north/northwest of Thompson Point also had relatively high specific conductivity values (average = 1,514 $\mu\text{S}/\text{cm}$; Figure 3.8c).

Three areas of elevated nutrient (TP, TKN) concentrations can be identified (Figure 3.8d, e, f, g): 1) the northern region by La Perouse Bay, 2) north/northwest of Thompson Point, and 3) the southern inland portion of the sampling area. The spatial distribution of TP values is similar for 2015 and 2016 with elevated concentrations in lakes close to La Perouse Bay (WNP 52-56; severely-disturbed), two lakes closer to Thompson Point (WNP 72, actively-disturbed and 74, undisturbed), and two lakes in the southern portion of our study area (WNP 85 and 86) both of which fall into the undisturbed category (Figure 3.8d, e). TKN concentrations show similar spatial patterns as TP concentrations, however, the three areas of elevated nutrient levels are more pronounced in 2016 (Figure 3.8g) compared to 2015 (Figure 3.8f). Severely-disturbed and actively-disturbed lakes within the La Perouse Bay area (WNP 52-46, 48, 50, and 51), an actively-disturbed lake north of Thompson Point (WNP 72) and several undisturbed lakes located within the southern inland portion of our study area (WNP 78-81, 85, and 86) all have elevated TKN concentrations.

In 2015, $\delta^{13}\text{C}_{\text{DIC}}$ values do not show much spatial variability across the study area (Moran's $I = 0.589$, Figure 3.8h). However, spatial trends are more evident in 2016 with lower $\delta^{13}\text{C}_{\text{DIC}}$ values near La Perouse Bay (severely-disturbed lakes WNP 52-56 and actively-disturbed lakes WNP 48, 50, 51, 57, 58, 59), by Thompson Point (actively-disturbed lake WNP 72), and in the southern inland portion of the study area (undisturbed lakes WNP 79, 80, 85, 86; Figure 3.8i).

$\delta^{13}\text{C}_{\text{PHYTOPOM}}$ values during 2015 also do not show much spatial variability across the study area (Moran's $I = 0.586$), except for elevated values in lakes near La Perouse Bay (actively-disturbed lakes, WNP 52-56; Figure 3.8j). However, spatial trends are clearly visible in 2016 with higher $\delta^{13}\text{C}_{\text{PHYTOPOM}}$ values especially by La Perouse Bay (severely-disturbed lakes WNP 52-56 and actively-disturbed lakes WNP 48, 50, 51, 57, 59) and also along the coast, north/northwest of Thompson Point (actively-disturbed lake WNP 72 and undisturbed lakes WNP 69, 70; Figure 3.8k).

3.5 Discussion

During the past ~40 years, WNP has experienced a rapid increase in LSG population and a corresponding expansion in the LSG-disturbed geographic region (Batt et al., 1997; Jefferies et al., 2006; Alisauskas et al., 2011; Peterson et al., 2013; Figures 3.1, 3.2). Previous studies have found that using standard limnological measurements (e.g., specific conductivity) combined with carbon isotope variables ($\delta^{13}\text{C}_{\text{DIC}}$, $\delta^{13}\text{C}_{\text{PHYTOPOM}}$, $\Delta^{13}\text{C}_{\text{DIC-PHYTOPOM}}$) is very informative and effectively captures differences in limnological and carbon behaviour in LSG-disturbed lakes compared to unaffected lakes (MacDonald et al., 2014, 2015). This research compiles two years of mid-summer limnological and carbon isotope data from 45 lakes that span a LSG disturbance gradient (undisturbed, actively-disturbed, severely-disturbed; Figure 3.2) across a portion of WNP (Figures 3.1, 3.6, & 3.7). Spatial variability was found for several of the limnological and carbon isotope variables corresponding to differing degrees of LSG disturbance. As discussed below, three different areas of LSG disturbance were found representing established, active, and emerging areas of LSG disturbance. Therefore, continued

monitoring of LSG disturbance within WNP is critical to understand how freshwater environments in WNP will respond to historical, active, and new LSG disturbance.

Variation of limnological conditions and carbon behaviour in relation to LSG disturbance

Previous research on LSG disturbance within WNP compared results during an entire ice-free season (summer) between 15 lakes that had minimal to no LSG disturbance and one lake that had been subject to substantial LSG activity (MacDonald et al., 2014). Results identified that carbon isotope measurements (e.g., $\delta^{13}\text{C}_{\text{DIC}}$) were more informative than the standard water chemistry measurements (e.g., pH, concentrations of TP, TKN, DOC) and captured marked differences in carbon behaviour between the undisturbed lakes and the LSG-disturbed lake. In their study, lakes with little to no LSG activity had mid-summer increases in $\delta^{13}\text{C}_{\text{DIC}}$ values, as expected, due to increasing primary productivity and the preferential uptake of ^{12}C by algae during photosynthesis (Quay et al., 1986; Keeley and Sandquist, 1992; Wachniew and Rożański, 1997; MacDonald et al., 2014). However, the lake exposed to LSG disturbance showed a marked difference in dissolved inorganic carbon behaviour with mid-summer declines in $\delta^{13}\text{C}_{\text{DIC}}$ values. MacDonald et al. (2014) attributed this difference in carbon behaviour to chemically-enhanced CO_2 invasion, where LSG disturbance promoted high algal production, high inorganic carbon demand, and high pH – conditions that led to strong kinetic carbon isotope fractionation and a subsequent decrease in $\delta^{13}\text{C}_{\text{DIC}}$ values as reported elsewhere for lakes under similar conditions (Wanninkhof, 1985; Herczeg and Fairbanks, 1987; Takahashi et al., 1990; Wanninkhof and Knox, 1996; Bade et al., 2004; Bade and Cole, 2006). It remained unknown, however, if this difference in carbon

behaviour at the one LSG disturbed lake was typical or representative of other lakes subjected to LSG disturbance.

In this study, higher mid-summer values of specific conductivity, pH, concentrations of TP, TKN, DIC, and DOC, and $\delta^{13}\text{C}_{\text{PHYTOPOM}}$ paired with lower mid-summer values of $\delta^{13}\text{C}_{\text{DIC}}$ and $\Delta^{13}\text{C}_{\text{DIC-PHYTOPOM}}$ values were characteristic of severely-disturbed lakes when compared to undisturbed and actively-disturbed lakes (Figures 3.6, 3.7). However, results from 2016 indicate a clear LSG disturbance gradient with increasing values of specific conductivity, pH, concentrations of TP, TKN, DIC, and DOC, and $\delta^{13}\text{C}_{\text{PHYTOPOM}}$ paired with decreasing values of $\delta^{13}\text{C}_{\text{DIC}}$ and $\Delta^{13}\text{C}_{\text{DIC-PHYTOPOM}}$, as LSG disturbance increased from undisturbed to actively-disturbed to severely-disturbed lakes (Figures 3.6, 3.7). Reduced evidence of sensitivity to LSG disturbance during 2015 can be attributed to substantial rainfall that occurred during the month of July prior to and during sampling (117.9 mm; Figure 3.3). This high amount of rainfall not only caused lowering of lake water isotope compositions and homogenized the hydrological conditions of the lakes (Figure 3.4a), but it also homogenized the limnological conditions, evidently dampening the signal of LSG disturbance on the sampling lakes (Figures 3.6, 3.7). As observed, substantial precipitation is ineffective at influencing the limnological conditions and carbon behaviour at the severely-disturbed lakes (Figures 3.6, 3.7)

Even with the dampening effect of heavy rainfall prior to sampling in 2015, this study has identified clear differences in nutrient concentrations between severely-disturbed lakes and the remaining sampled WNP lakes (undisturbed and actively-disturbed lakes). Furthermore, in 2016, a stronger gradient in nutrient concentrations is

observed between all three LSG-disturbance categories. Previous studies did not find differences in the concentrations of major nutrients (e.g., TKN, TP) when comparing one sampled LSG-disturbed lake with non-LSG disturbed sites. However, in this study, observed higher nutrient levels in LSG-disturbed lakes can likely be attributed to the input of nutrients derived from feces and soil erosion/runoff from the catchment. We speculate that the one LSG-disturbed lake chosen by MacDonald et al. (2014) was not indicative of all LSG-disturbed lakes and did not capture the full spectrum of limnological differences caused by LSG disturbance.

In contrast to the nutrient concentration results, patterns in the carbon isotope data align with the findings of MacDonald et al. (2014). Lower $\delta^{13}\text{C}_{\text{DIC}}$, higher $\delta^{13}\text{C}_{\text{PHYTOPOM}}$, and lower $\Delta^{13}\text{C}_{\text{DIC-PHYTOPOM}}$ values were observed with increasing LSG-disturbance (Figure 3.6, 3.7). These patterns, paired with high pH (>9) and high aquatic productivity, indicate demand for CO_2 exceeds rates of supply, consistent with the hypothesis of MacDonald et al. (2014) of chemically-enhanced CO_2 influencing carbon behaviour in the severely disturbed lakes.

Another possible explanation for the lower $\delta^{13}\text{C}_{\text{DIC}}$ values within LSG-disturbed lakes is an elevated supply of soil-derived isotopically-depleted DIC from the catchment (Figure 3.6). This hypothesis was previously discounted by MacDonald et al. (2014) due to dry climate conditions during their 2010 mid-summer sampling period (e.g., lake desiccation, no surface inflow). However, desiccation was not observed during the 2015 and 2016 mid-summer sampling periods and a large amount of rainfall occurred directly prior to 2015 sampling (~50% of summer rainfall). Indeed, runoff could provide an overarching mechanism that explains the observed decrease in $\delta^{13}\text{C}_{\text{DIC}}$ values, increase in

DIC concentrations, increased nutrient (TP, TKN) concentrations, as well as increased specific conductivity (Figure 3.6, 3.8). This increase in specific conductivity is likely associated with increased erosional input of dissolved ions caused by LSG grubbing and the removal of catchment vegetation and root systems within the saline HBL soils (Jefferies and Rockwell, 2002; Parks Canada, 2011; MacDonald et al., 2014, 2015). Despite the increasing supply of carbon from the catchment, intense aquatic productivity likely accounts for the low $\Delta^{13}\text{C}_{\text{DIC-PHYTOPOM}}$ values in the LSG-disturbed lakes. Thus, based on our results, both chemically-enhanced CO_2 invasion and catchment runoff may explain observed patterns in the limnological and carbon isotope data among LSG-disturbance categories.

Spatial patterns of LSG disturbance

From a spatial perspective, the limnological and carbon isotope variables collectively identify three distinct areas of LSG disturbance: 1) the area by La Perouse Bay, 2) the landscape to the north and northwest of Thompson Point, and 3) the inland area in the southern portion of the study region (Figure 3.8). Both La Perouse Bay and Thompson Point are areas that have been previously identified by researchers and Parks Canada staff as regions of extensive LSG nesting and disturbance (Jefferies and Rockwell, 2002; Rockwell et al., 2009; Parks Canada, 2011). The La Perouse Bay region has sustained the longest and most intense disturbance by LSG (Jefferies and Rockwell, 2002; Parks Canada, 2011; Rockwell et al., 2009; Koons et al., 2014). This region is characterized by elevated concentrations of specific conductivity and nutrients as well as low values of $\delta^{13}\text{C}_{\text{DIC}}$. The coastal region near Thompson Point was the location of a

LSG short-stop in 2001, caused by harsh weather. Consequently, a large number of geese were forced to nest at Thompson Point (Parks Canada, 2011; Rockwell et al., 2009). The offspring of these geese now consider this location home and have increasingly nested there since 2003 with >10,000 nesting pairs returning to this location every spring (Parks Canada, 2011; Rockwell et al., 2009). This area is characterized by slightly elevated specific conductivity (compared to the La Perouse Bay region), low values of $\delta^{13}\text{C}_{\text{DIC}}$, and elevated concentrations of nutrients.

Field observations in the third area of apparent LSG disturbance located within the southern portion of the study area indicated the presence of LSG feces and feathers, but no signs of grubbing. These lakes are designated as undisturbed lakes since they did not show elevated specific conductivity levels and there was minimal goose presence. This area did, however, have elevated concentrations of nutrients and low values of $\delta^{13}\text{C}_{\text{DIC}}$ in 2016 (Figure 3.8e, g). These elevated nutrient concentrations, coupled with low $\delta^{13}\text{C}_{\text{DIC}}$ values, could be the first indication that LSG disturbance is expanding from the traditional LSG nesting locales (e.g., La Perouse Bay, Thompson Point) and these lakes could potentially be transitioning from undisturbed to actively-disturbed. LSG disturbance is a plausible explanation for the high nutrient concentrations in this southern portion of our study area, especially since field observations detected the presence of geese.

To synthesize the spatial patterns of LSG disturbance, scaled specific conductivity, TP, TKN, $\delta^{13}\text{C}_{\text{DIC}}$, and $\delta^{13}\text{C}_{\text{PHYTOPOM}}$ values from 2016 were aggregated using equations 1 and 2. Results are displayed using inverse-distance-weighted interpolations (Figure 3.9). Note that 2015 data were not used for this synthesis due to the

reduced sensitivity to LSG disturbance attributed to substantial rainfall prior to and during sampling. Based on this metric, La Perouse Bay, the area north/northwest of Thompson Point, and the southern portion of our study area all show elevated scaled values and indicate areas of LSG disturbance within our study area (Figure 3.9). The oldest, established location of LSG disturbance by La Perouse Bay is characterized by the highest scaled values, which approach 1. The location of the 2001 LSG short-stop, where LSG are known to be currently active, is indicated by elevated scaled values north/northwest of Thompson Point. Finally, the newly emerging area of LSG can be identified by elevated scaled values in the inland area in the southern portion of the study area. From a monitoring perspective, Figure 3.9 on its own depicts the compilation of effects of all limnological and carbon isotope variables that are deemed sensitive to LSG disturbance and identifies old, current, and emerging areas of LSG disturbance (La Perouse Bay, north/northwest of Thompson Point, and inland area in the southern portion of study area, respectively).

Two important assumptions for this technique are 1) that each variable is equally responsive to LSG disturbance, and 2) outliers can exert control on the final product. Additionally, it is important to note that a suite of limnological and carbon isotope variables (specific conductivity, TP, TKN, $\delta^{13}\text{C}_{\text{DIC}}$, $\delta^{13}\text{C}_{\text{PHYTOPOM}}$) was critical to identify these three different areas of LSG disturbance. Specific conductivity, while perhaps the easiest variable to measure more frequently, would not, on its own, capture the other two areas of supposed disturbance (Thompson Point and the southern portion of our study area).

3.6 Conclusions and Recommendations

This research aimed to track and identify the degree of LSG disturbance on the freshwater lakes within an ~1800 km² sector of WNP. A suite of limnological and carbon isotope variables supported a gradient of LSG disturbance where increasing LSG disturbance corresponds to increasing values of specific conductivity, pH, nutrient concentrations (TP, TKN), DIC and DOC concentrations, and $\delta^{13}\text{C}_{\text{PHYTOPOM}}$ as well as decreasing values of $\delta^{13}\text{C}_{\text{DIC}}$ and $\Delta^{13}\text{C}_{\text{DIC-PHYTOPOM}}$, representing increased productivity, chemically-enhanced CO₂ invasion, and catchment runoff. These patterns were more evident in 2016 as compared to 2015 because of reduced sensitivity to LSG disturbance attributed to substantial rainfall that occurred prior to and during the 2015 sampling trip. Through spatial analysis, three distinct areas affected by LSG disturbance were identified that represent established (La Perouse Bay), current (north/northwest of Thompson Point), and emerging (inland area in the southern portion of the study region) areas of LSG disturbance. Baldwin et al. (2018) recently reported that the growth rate of the LSG population has decreased simultaneously with static or increasing adult survival, implying that recruitment rates themselves must be decreasing. While this is good news for the landscape, Baldwin et al. (2018) also mentioned that there is incomplete knowledge regarding the carrying capacity of arctic habitats as well as how much habitat has been negatively affected by the influences of LSG disturbance. Results presented here provide other researchers as well as Parks Canada with improved knowledge of areas and degree of aquatic disturbance from LSG activities and will aid in determining how these LSG-affected freshwater habitats evolve through ongoing monitoring. Recommendations for LSG disturbance monitoring within WNP are described below.

Sampling lakes once per season

We propose that one sampling of water chemistry as well as carbon isotope compositions of DIC and phytoplankton at peak primary productivity (e.g., mid-summer) is sufficient to delineate a range of conditions and influence of LSG disturbance on WNP lakes. Although sampling multiple times during the ice-free season, as suggested by MacDonald et al. (2014), would be ideal for tracking seasonal variability, it is not always sustainable and feasible (e.g., financial, time, available personnel constraints). The results of this research were able to capture major differences in limnology and carbon behaviour among three unique LSG-disturbance categories (when not masked by the effects of rainfall, as occurred in 2015). This finding is important considering the desire to sustain a cost-efficient and long-term LSG-disturbance monitoring program led by WNP (Parks Canada, 2011; Baldwin et al., 2018).

A suite of limnological variables are necessary to measure the degree of LSG disturbance

This study substantiates the utility of a suite of limnological variables sensitive to catchment disturbance by LSG including pH, specific conductivity, total phosphorus (TP), total Kjeldahl nitrogen (TKN), and carbon isotope measures ($\delta^{13}\text{C}_{\text{Dissolved Inorganic Carbon (DIC)}}$, $\delta^{13}\text{C}_{\text{Phytoplanktonic Particulate Organic Matter (PHYTOPOM)}}$, and $\Delta^{13}\text{C}_{\text{DIC-PHYTOPOM}}$). Previous research found differing nutrient concentration trends than our own research and suggested that they may not be as important to monitor (MacDonald et al., 2014). However, our research across 45 lakes found that increasing nutrient concentrations paired with decreasing $\delta^{13}\text{C}_{\text{DIC}}$ values corresponded with increasing LSG disturbance and can identify potential early stages of disturbance within WNP lakes.

For a sustainable, long-term monitoring program, we propose obtaining specific conductivity and field observations from all 45 lakes annually since they are simple and cost-effective measures and then sampling the full suite of water chemistry and carbon isotope variables from all lakes every other or every three years depending on funding. We also suggest the incorporation of yearly water isotope measurements given the potential confounding effects of rainfall on detecting limnological consequences of LSG disturbance, as occurred in 2015.

Spatial monitoring of LSG disturbance within WNP: A work in progress

It should be noted that these 45 lakes were chosen as part of a preliminary assessment of the spatial extent of LSG disturbance. It is not unreasonable to add new lakes to the sampling list as LSG disturbance continues to shift and change across the WNP landscape. However, repeated sampling over several years of the same lakes provide the basis for examining LSG disturbance trends over time and the potential to identify new areas of disturbance, areas of increasing disturbance, or perhaps even the first signs of post-disturbance recovery, especially since LSG populations may be stabilizing (Baldwin et al., 2018). Finally, one of the most important contributions of this work is the generation of a single map that synthesizes data to identify areas and the degree of LSG disturbance. This synthesis map can be used as a management tool to address and track LSG disturbance within WNP, especially after multiple years of data have been compiled. Trends in the cumulative scaled data could then be compared over time as well as spatially.

3.7 Figures

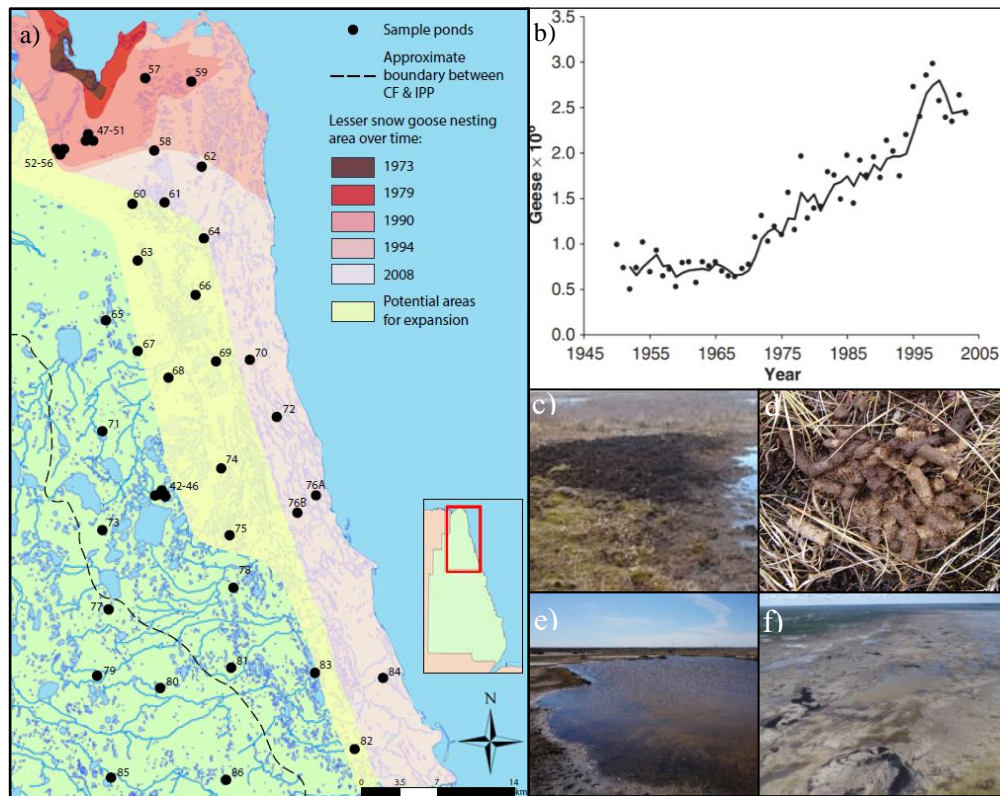


Figure 3.1 a) Map showing the location of sampling sites within Wapusk National Park. Black circles represent sampling lakes spanning the coastal fen (CF) and interior peat plateau-palsa bog (IPP) ecotypes. The approximate boundary between these two ecotypes is represented by the black dashed line. Shaded areas represent the area of Lesser Snow Goose (LSG) nesting habitat over time and include potential areas for LSG nesting location expansion (Parks Canada, 2009). b) An estimate of WNP LSG population over time based on surveys; the solid line represents a 3-year running average (modified from Abraham et al., 2005b pg. 843). Photographs showing evidence of LSG disturbance: c) LSG grubbing (photo credit: L. MacDonald), d) LSG feces, e) vegetation removal adjacent to a sampling lake, and f) large-scale vegetation removal in a LSG-disturbed area.

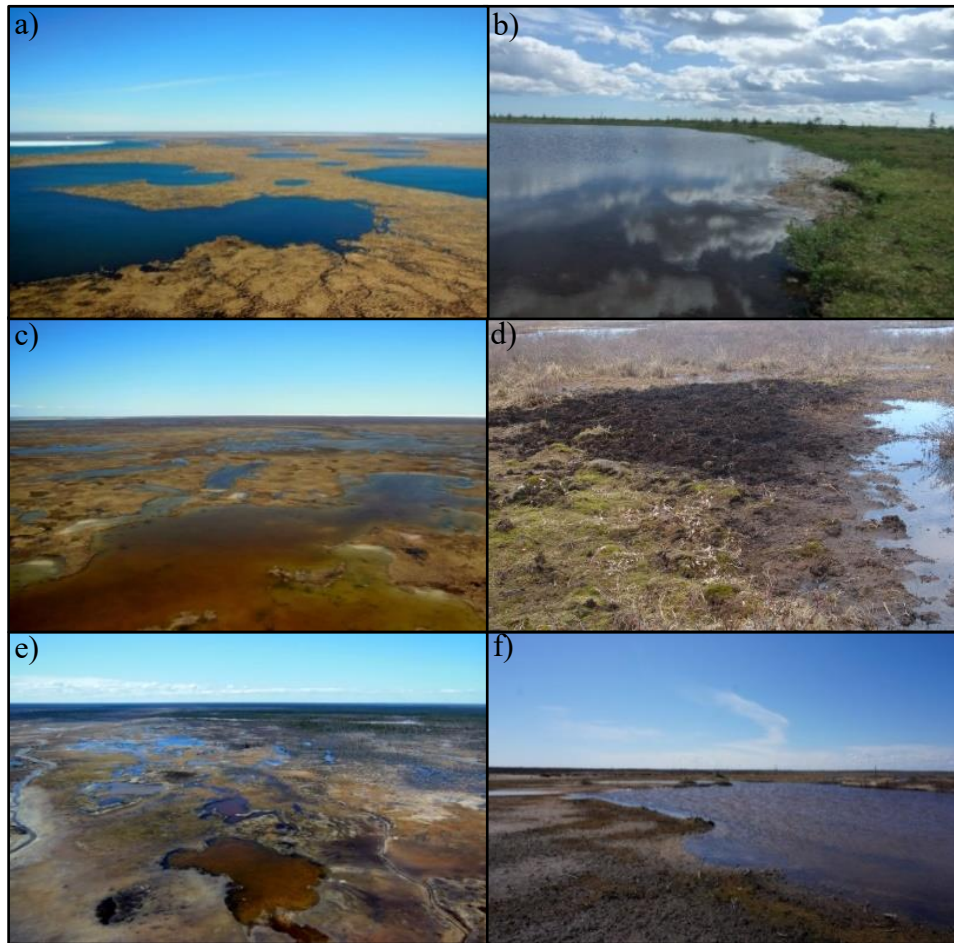


Figure 3.2 Gradient of LSG disturbance within WNP based on extensive observations and conductivity values from 2010-2014 field campaigns: a) undisturbed landscape; b) undisturbed lake (photo credit: L. MacDonald); c) actively-disturbed landscape; d) actively-disturbed landscape adjacent to a sampling lake, depicting grubbing (photo credit: L. MacDonald); e) severely-disturbed landscape; f) severely-disturbed landscape, no vegetation adjacent to a sampling lake.

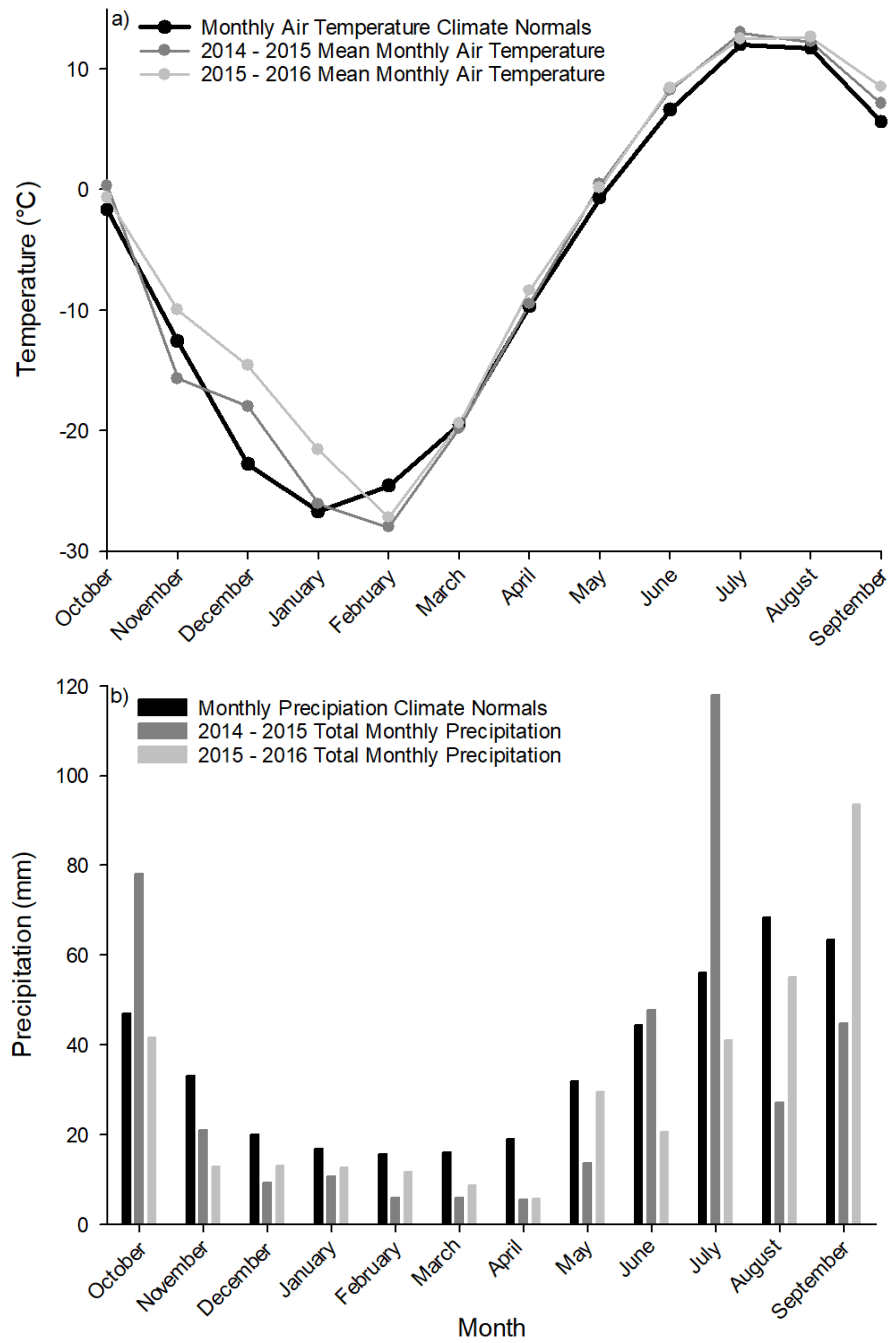


Figure 3.3 Wapusk National Park meteorological data compared to 1971-2000 climate normal; a) 2014-2015 sampling year and b) 2015-2016 sampling year. Data were compiled using Environment and Climate Change Canada Historical Weather data from the Churchill Airport weather station (Churchill Climate, #5060608).

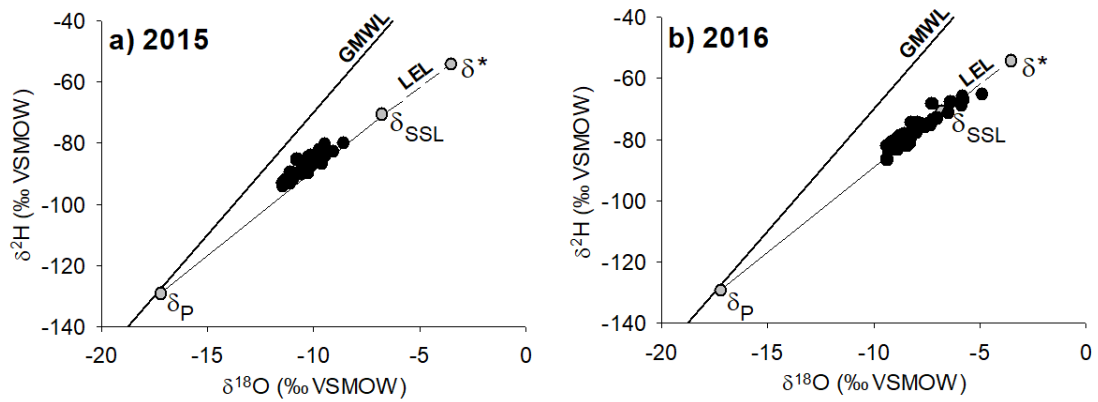


Figure 3.4 $\delta^{18}\text{O}$ - $\delta^2\text{H}$ graphs showing the lake water isotope values (black circles) for a) July 2015 and b) July 2016. Isotope values are plotted with the Global Meteoric Water Line (GMWL; Craig, 1961) and the Local Evaporation Line, which is comprised of δ_P (mean annual isotope composition of precipitation), δ_{SSL} (steady-state limiting - isotope value of lake water where inputs equal outputs), and δ^* (the theoretical isotope value of the last drop of water in a lake prior to desiccation). Refer to Chapter 2 for the methodology on how these values are calculated.

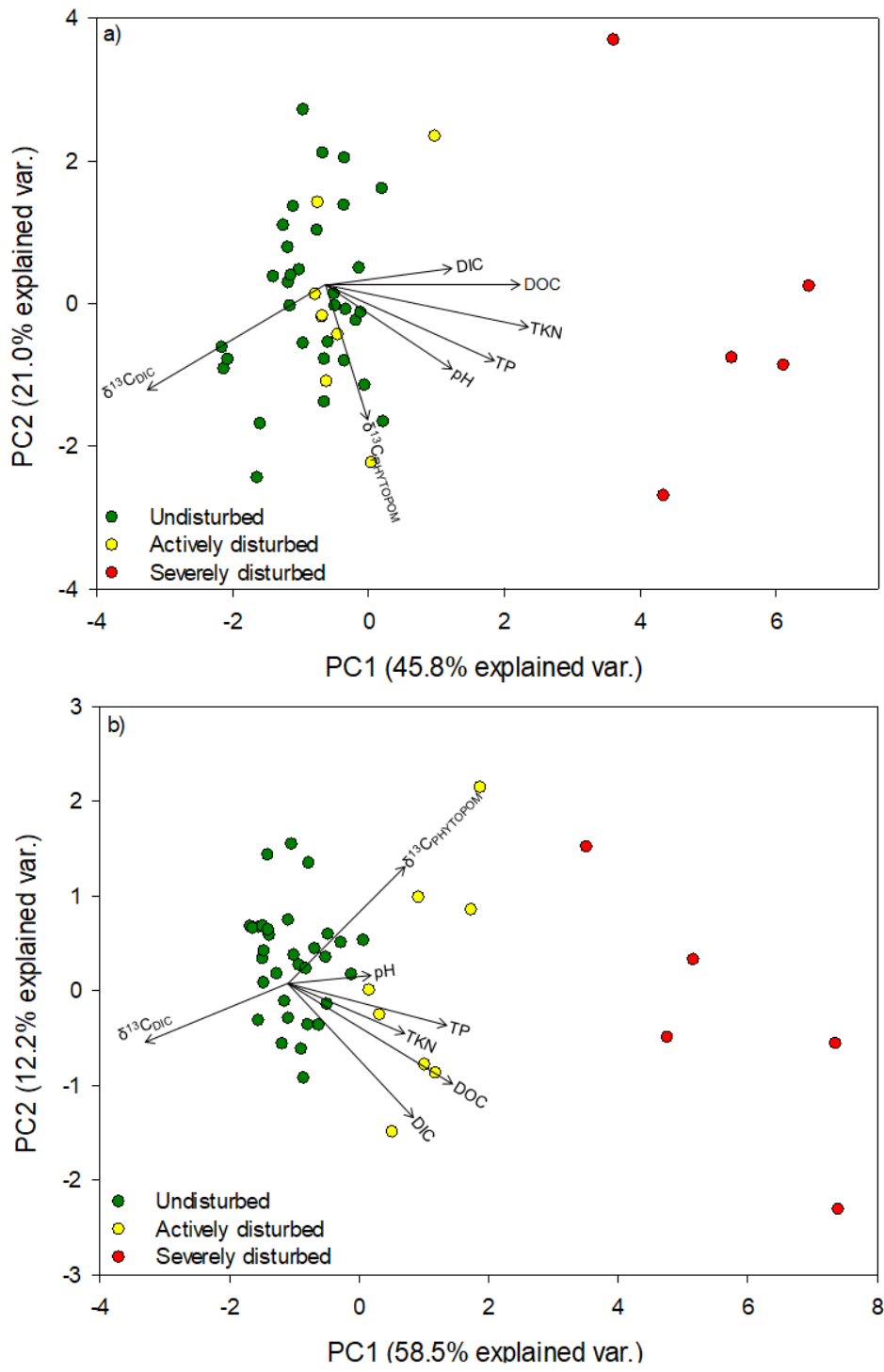


Figure 3.5 Principal components analysis (PCA) ordination biplot comparing limnological conditions among lakes in the three categories of Lesser Snow Goose disturbance: a) July 2015 and b) July 2016.

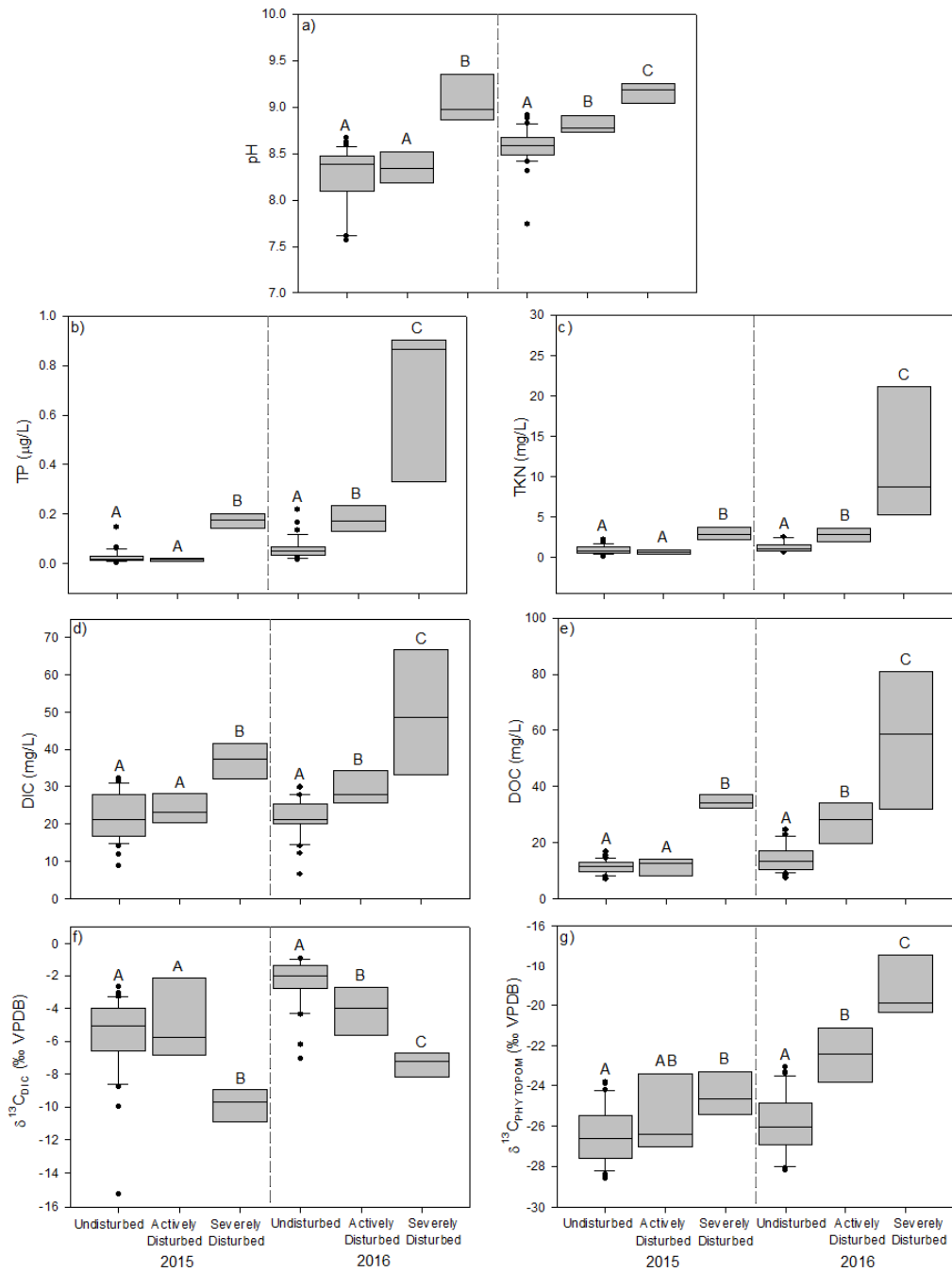


Figure 3.6 Boxplots depicting data for limnological parameters; a) pH, b) TP, c) TKN, d) DIC, e) DOC, f) $\delta^{13}\text{C}_{\text{DIC}}$, and g) $\delta^{13}\text{C}_{\text{PHYTOPOM}}$. Each plot contains data from all three categories of Lesser Snow Goose disturbance: undisturbed (n = 32), actively disturbed (n = 8), and severely disturbed (n = 5) for the two sampling years (2015-2016). Capital letters are used to present results of the Dunn's post-hoc tests that display statistically significant differences or not between LSG-disturbance categories.

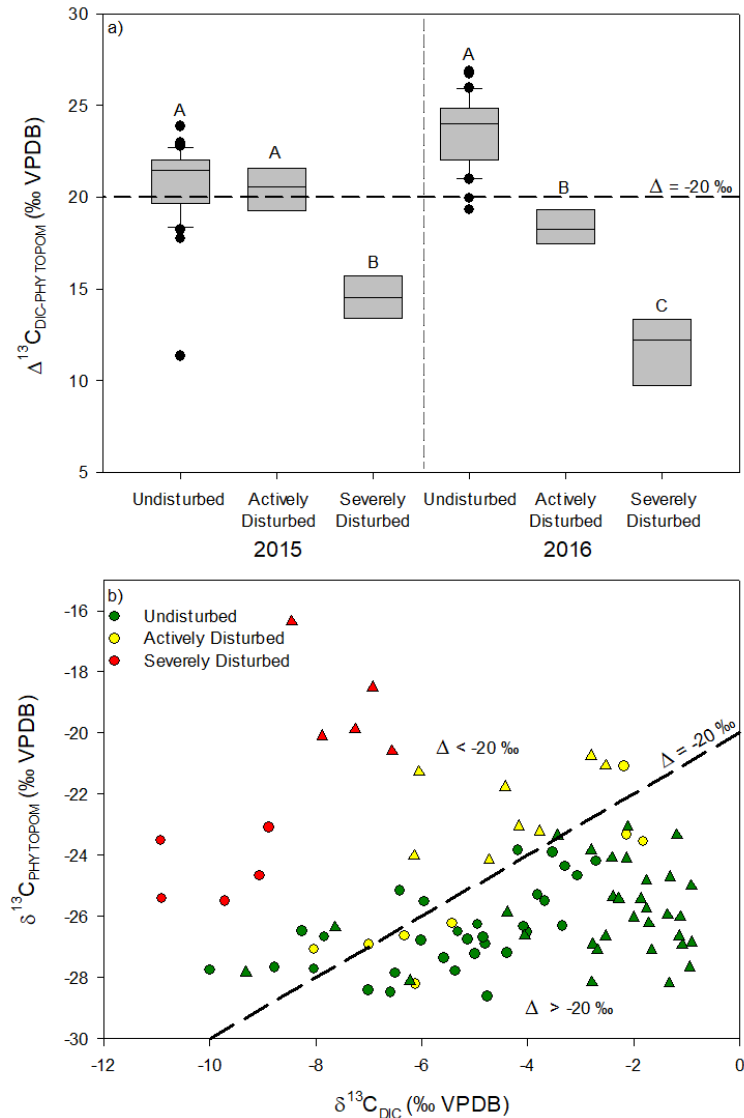


Figure 3.7 a) Boxplots depicting $\Delta^{13}\text{C}_{\text{DIC-PHYTOPOM}}$ values for 2015 and 2016. Data are from all three categories of Lesser Snow Goose (LSG) disturbance; undisturbed ($n = 32$), actively disturbed ($n = 8$), and severely disturbed ($n = 5$). Horizontal dashed line represents the photosynthetic isotope fractionation of -20‰ , representing sufficient dissolved CO_2 concentrations (Rau, 1978; Herczeg and Fairbanks, 1987; Bade et al., 2004; Fry, 2006; MacDonald et al., 2014). Letters A, B, and C represent statistically defined groupings. b) $\delta^{13}\text{C}_{\text{DIC}}$ versus $\delta^{13}\text{C}_{\text{PHYTOPOM}}$ depicting the 20‰ offset representing the theoretical value of photosynthetic isotopic fractionation (dashed line represents $\Delta = -20\text{‰}$). Lake values are separated by defined LSG disturbance category; green = undisturbed, yellow = actively disturbed, red = severely disturbed. Circles represent 2015 and triangles represent 2016 values.

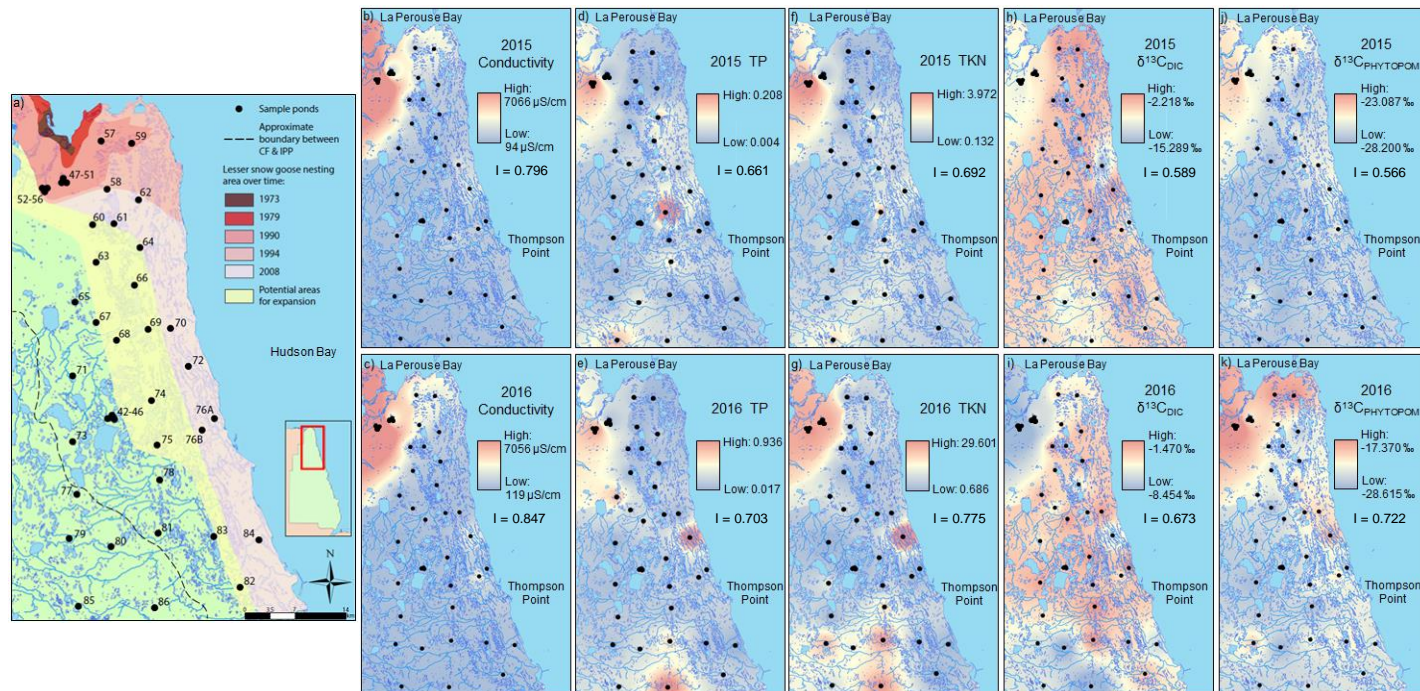


Figure 3.8 a) From Figure 1, the location of sampling sites within WNP. Maps showing the inverse-distance-weighted interpolation values of b) 2015 conductivity (range = 94 to 7,066 $\mu\text{S/cm}$), c) 2016 conductivity (range = 119 to 7,056 $\mu\text{S/cm}$), d) 2015 total phosphorus (TP; range = 0.004 to 0.208 $\mu\text{g/L}$), e) 2016 TP (range = 0.017 to 0.936 $\mu\text{g/L}$), f) 2015 total Kjeldahl nitrogen (TKN; range = 0.132 to 3.972 mg/L), g) 2016 TKN (range = 0.686 to 29.601 mg/L), h) 2015 $\delta^{13}\text{C}_{\text{DIC}}$ (range = -15.29 to -2.22 ‰ VPDB), i) 2015 $\delta^{13}\text{C}_{\text{PHYTOPOM}}$ (range = -28.22 to -23.09 ‰ VPDB), and j) 2016 $\delta^{13}\text{C}_{\text{PHYTOPOM}}$ (range = -28.62 to -17.37 ‰ VPDB). Lower values are represented by blue and higher values represented by red.

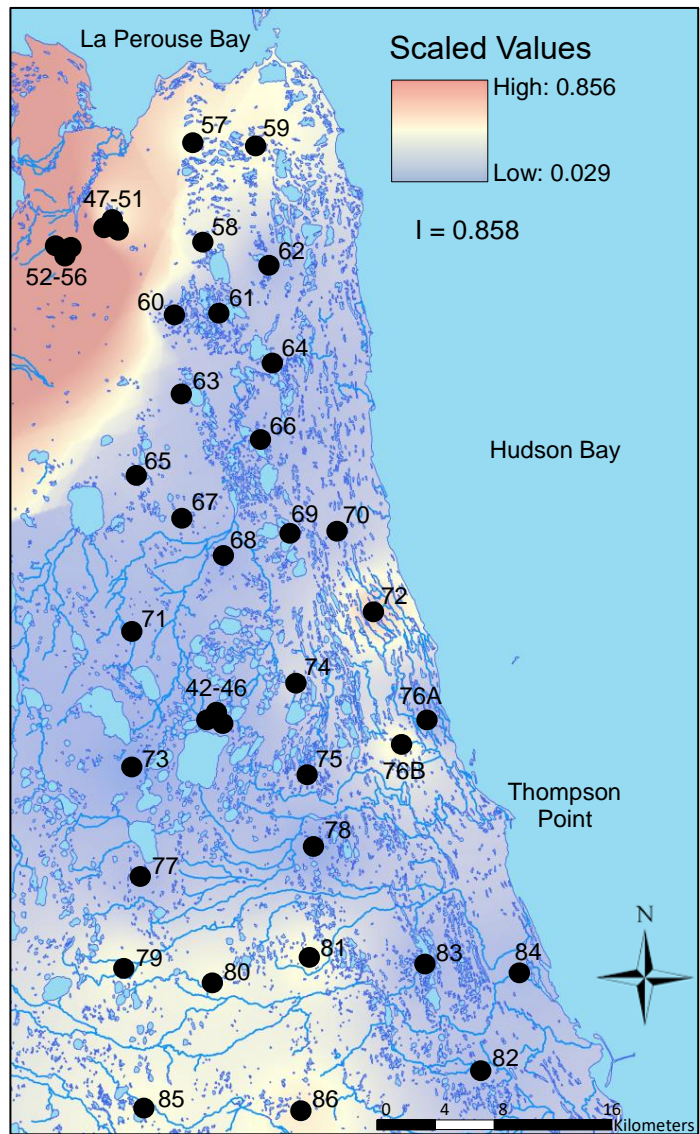


Figure 3.9 Map showing the inverse-distance-weighted interpolations of scaled values (conductivity, TP, TKN, $\delta^{13}\text{C}_{\text{DIC}}$ and $\delta^{13}\text{C}_{\text{PHYTOPOM}}$; range = 0.029 to 0.856) for 2016. Lower values are represented by blue and higher values represented by red.

3.8 Tables

Table 3.1 Field-based classification used to distinguish the three categories of Lesser Snow Goose disturbance to lakes in WNP (See Appendix Table A1 for a complete list of lakes and field observations).

	Undisturbed	Actively Disturbed	Severely Disturbed
Visual indicators	Pristine landscape, lack of LSG on-site	LSG on-site, actively using the landscape, some dead vegetation (grubbing)	Barren landscape, soil visible, few LSG on-site but less than Actively Disturbed sites
Conductivity Values	<500 $\mu\text{S}/\text{cm}$	500-3000 $\mu\text{S}/\text{cm}$	>3000 $\mu\text{S}/\text{cm}$

Table 3.2 Wapusk National Park precipitation values compared to 1971-2000 climate normals. Data were compiled using Environment and Climate Change Canada Historical Weather data from the Churchill Airport weather station (Churchill Climate, #5060608; Environment Canada, 2019).

Year (winter-winter)	Total precipitation (mm)	Winter (Oct-Apr) Precipitation (mm)	Summer (May-Sept) Precipitation (mm)
Climate Normals (1971-2000)	431.6	167.7	263.9
2014-2015	387.7	136.5	251.2
2015-2016	345.8	106.0	239.8

Table 3.3 Results of the analysis of similarity (ANOSIM) pairwise test between the three LSG disturbance categories (undisturbed, actively-disturbed, severely-disturbed) for 2015 ($R = 0.649$, $p = 0.001$, $r^2 = 0.62$) and 2016 ($R = 0.879$, $p = 0.001$, $r^2 = 0.77$) data. All P -values are statistically significant at $\alpha = 0.05$ (bold values represent statistical significance).

	<u>2015</u>		<u>2016</u>	
	<i>R</i> statistic	<i>P</i> -value	<i>R</i> statistic	<i>P</i> -value
Undisturbed vs. Actively disturbed	0.652	0.667	0.856	0.009
Actively disturbed vs. Severely disturbed	0.603	0.042	0.844	0.037
Undisturbed vs. Severely disturbed	0.691	0.013	0.937	0.001

Table 3.4 P-values from Kruskal-Wallis tests that compared values of limnological variables among lakes within the Lesser Snow Goose disturbance categories (undisturbed, actively disturbed, and severely disturbed). All *P*-values are statistically significant at alpha = 0.05 (bold values represent statistical significance).

Limnological Parameters	2015	2016
pH	0.001	0.001
TP	0.002	0.001
TKN	0.001	0.001
DIC	0.001	0.001
DOC	0.001	0.001
$\delta^{13}\text{C}_{\text{DIC}}$	0.004	0.001
$\delta^{13}\text{C}_{\text{PHYTOPOM}}$	0.015	0.001
$\Delta^{13}\text{C}_{\text{DIC-PHYTOPOM}}$	0.002	0.000

Table 3.5 P-values from post-hoc Dunn’s test to determine which specific lake categories (undisturbed, actively disturbed, severely disturbed) were significant from the others in 2015 and 2016. The three different comparison columns are: undisturbed vs. actively disturbed, actively disturbed vs. severely disturbed, and undisturbed vs. severely disturbed. *P*-values < 0.05 represent significant difference. Bold values represent statistically significant values.

Limnological Parameters	Undisturbed vs. Actively disturbed	Actively disturbed vs. Severely disturbed	Undisturbed vs. Severely disturbed
2015			
pH	1.000	0.016	0.010
TP	1.000	0.004	0.002
TKN	0.410	0.001	0.001
DIC	0.395	0.001	0.001
DOC	0.786	0.004	0.000
$\delta^{13}\text{C}_{\text{DIC}}$	1.000	0.008	0.004
$\delta^{13}\text{C}_{\text{PHYTOPOM}}$	0.153	0.293	0.027
$\Delta^{13}\text{C}_{\text{DIC-PHYTOPOM}}$	1.000	0.043	0.001
2016			
pH	1.000	0.016	0.010
TP	1.000	0.004	0.002
TKN	0.410	0.001	0.001
DIC	0.395	0.001	0.001
DOC	0.786	0.004	0.000
$\delta^{13}\text{C}_{\text{DIC}}$	1.000	0.008	0.004
$\delta^{13}\text{C}_{\text{PHYTOPOM}}$	0.153	0.293	0.027
$\Delta^{13}\text{C}_{\text{DIC-PHYTOPOM}}$	1.000	0.043	0.001

3.9 Chapter 3 Appendix

Table 3.A1 Key July 2015 field observations and conductivity values of Lesser Snow Goose (LSG) disturbance for the 45 sampling lakes within Wapusk National Park. Yellow represents lakes within the actively disturbed LSG-disturbance category, red represents lakes within the severely disturbed LSG-disturbance category, and green represents lakes that fall within the undisturbed LSG-disturbance category.

Lake	Conductivity ($\mu\text{S}/\text{cm}$)	Field Observations
WAP 42	240	Few feathers and feces
WAP 43	215	Feces
WAP 44	220	Few feathers and feces
WAP 45	200	Feces
WAP 46	274	Feces
WAP 47	298	Feces
WAP 48	809	Feces, tracks, geese present
WAP 49	108	Feces
WAP 50	971	Feces
WAP 51	926	Feces, tracks, geese present
WAP 52	3872	No geese present, lack of vegetation, exposed sediment
WAP 53	5714	No geese present, lack of vegetation, exposed sediment
WAP 54	5356	No geese present, lack of vegetation, exposed sediment
WAP 55	6948	No geese present, lack of vegetation, exposed sediment
WAP 56	7066	No geese present, lack of vegetation, exposed sediment
WAP 57	606	Feces, geese present
WAP 58	672	Feces
WAP 59	1207	Feathers, feces, tracks
WAP 60	450	Few feathers and feces
WAP 61	301	no LSG presence
WAP 62	324	no LSG presence
WAP 63	458	Feathers, feces, tracks
WAP 64	787	Feathers, feces, tracks, grubbing, geese present
WAP 65	452	Feathers, feces, tracks, geese present
WAP 66	187	Few feathers and feces
WAP 67	343	Few feathers and feces
WAP 68	164	no LSG presence
WAP 69	98	no LSG presence
WAP 70	913	no LSG presence
WAP 71	151	Few feathers and feces
WAP 72	1228	Feathers, feces, grubbing, geese present
WAP 73	247	Few feathers and feces

WAP 74	370	Few feathers and feces
WAP 75	979	no LSG presence
WAP 76A	332	Few feathers and feces
WAP 77	170	feathers
WAP 78	243	no LSG presence
WAP 79	94	Feathers and fresh feces present
WAP 80	160	Few feathers and feces
WAP 81	166	Feces
WAP 82	257	Few feathers and feces
WAP 83	334	Few feathers and feces
WAP 84	473	Few feathers and feces
WAP 85	111	Few feathers and feces
WAP 86	177	Feathers, feces, grubbing, geese present

Table 3.A2 Key July 2016 field observations and conductivity values of Lesser Snow Goose (LSG) disturbance for the 45 sampling lakes within Wapusk National Park. Yellow represents lakes within the actively disturbed LSG-disturbance category, red represents lakes within the severely disturbed LSG-disturbance category, and green represents lakes that fall within the undisturbed LSG-disturbance category.

Lake	Conductivity (µS/cm)	Field Observations
WAP 42	248	Few feathers and feces
WAP 43	258	Few feathers and feces
WAP 44	252	Few feathers and feces
WAP 45	254	Few feathers and feces
WAP 46	183	Few feathers and feces
WAP 47	145	Some feathers, feces, tracks
WAP 48	2872	Feces, tracks, geese present, grubbing
WAP 49	383	Few feathers and feces
WAP 50	2203	Feces, grubbing
WAP 51	2154	Feces, tracks, geese present, possible grubbing
WAP 52	6146	No geese present, lack of vegetation, exposed sediment
WAP 53	6958	No geese present, lack of vegetation, exposed sediment
WAP 54	7056	No geese present, lack of vegetation, exposed sediment
WAP 55	6433	No geese present, lack of vegetation, exposed sediment
WAP 56	7023	No geese present, lack of vegetation, exposed sediment
WAP 57	1193	Feathers, feces, geese present
WAP 58	1307	Few feathers
WAP 59	1275	Feathers, feces, tracks
WAP 60	480	Few feathers and feces
WAP 61	296	no LSG presence
WAP 62	361	no LSG presence
WAP 63	483	Feathers, feces, tracks
WAP 64	386	Few feathers, feces, grubbing, geese present
WAP 65	119	Feathers, feces, tracks, grubbing, geese present
WAP 66	189	Feathers, feces, tracks
WAP 67	440	Few feathers and feces
WAP 68	376	Few feathers and feces
WAP 69	195	no LSG presence
WAP 70	303	Few feathers and feces
WAP 71	121	Few feathers and feces
WAP 72	1727	Feathers, feces, grubbing, geese present

WAP 73	373	Few feathers and feces
WAP 74	256	Feces, tracks, and grubbing
WAP 75	410	Few feathers and feces
WAP 76B	1301	Few feathers and feces
WAP 77	261	Feces
WAP 78	371	Few feathers and feces
WAP 79	516	Few feathers and feces
WAP 80	329	Feces, tracks
WAP 81	306	Few feathers and feces
WAP 82	261	Few feathers and feces
WAP 83	282	Few feathers and feces
WAP 84	118	Few feathers and feces
WAP 85	128	Few feathers and feces
WAP 86	573	Few feathers and feces

Chapter 4: Translating science into a sustainable, long-term monitoring program

Canada is the second-largest polar nation in the world and recently, much attention has focused on social, economic, and governance development in the North, Arctic sovereignty, as well as concerns related to northern environmental changes in response to climate warming (Government of Canada, 2009; Bush and Lemmen, 2019). The Government of Canada has taken steps to ensure that northern ecosystems are protected for future Canadian generations through the creation of Canada's Northern Strategy (Government of Canada, 2009). This strategy emphasizes becoming a global leader in Arctic science and focuses on the importance of community-oriented and collaborative science and technology leadership and research in the North by incorporating the people and institutions that reside, utilize, and study the landscape year-round that we, as researchers, only typically visit for episodes of field work (Government of Canada, 2009). As southern scientists, we can recognize the significance of this strong governmental message on northern climate-related research and are typically motivated to answer the unending questions that arise throughout the scientific process. In recent years, a new research paradigm in northern Canada has emerged, where collaborative, interdisciplinary, and community-driven research reflects northern priorities and leads to action (Graham and Fortier, 2005; Wolfe et al., 2007a, 2011; Balasubramaniam, 2009; ISAC, 2012; Tondu et al., 2014; Adams et al., 2014).

Conducting northern, collaborative, and interdisciplinary research to address the priorities of communities and tackle the large environmental problems (e.g., climate warming, permafrost thaw, change occurring to freshwater resources) is often complex and challenging due to financial constraints, timeline limitations (e.g., short field seasons,

graduate student program lengths), and coordinating southern-based university research efforts with northern priorities. My research directly addresses two other challenges associated with the new northern research paradigm: ¹developing and maintaining partnerships and collaboration with local governmental agencies (Parks Canada) and community-based organizations and ²operationalizing agency-led monitoring in collaboration with university-based researchers.

My own field work and data collection led to the discovery of important changes to the lakes within Wapusk National Park as a result of multiple, complex stressors (including climate warming, changing precipitation patterns, waterfowl disturbance). For example, limnological trends indicative of chemically-enhanced CO₂ invasion, elevated catchment runoff of nutrients, carbon and ions, as well as enhanced aquatic productivity, increasingly influenced the nutrient and carbon balance of lakes along a Lesser Snow Goose disturbance gradient. These trends can be exacerbated if ice-free season duration, summer water temperatures, and lake water evaporation increase due to climate warming. I realized that strictly completing research science for the sake of improving our own scientific knowledge was not enough. It became a goal and passion to create long-lasting, collaborative relationships with local governmental (e.g., Parks Canada) and community-based (Churchill Northern Studies Centre) organizations and to translate our research methods and findings into an applicable product to be reproduced and shared with the local community if and/or when our research team was no longer involved.

Monitoring and anticipating lake hydrological and limnological change is challenging in the North due to its remoteness and the sensitivity of shallow northern lakes to multiple environmental stressors. Often, due to the lack of alignment and

effective communication of research priorities between researchers and northern agencies, the short duration of funding or continued funding, as well as the high turnover rates of staff and graduate students, the science and training necessary to create the foundations for agency-led monitoring is not always feasible. However, through an incredible amount of time and hard work, as well as the collaboration and commitment from myself, other graduate students and professors at Wilfrid Laurier University and University of Waterloo, and Parks Canada, a long-term lake monitoring program within Wapusk National Park, titled the Hydroecology Monitoring Program, was successfully established in 2015. This monitoring program has been developed in a format that fits into Parks Canada's mandate, can be utilized for their reporting requirements, and is designed to focus on two major threats to aquatic ecosystems: 1) Pond Water Dynamics/Lake Hydrology monitoring and 2) Goose Aquatic Impact monitoring.

Establishing these monitoring activities was an iterative process that began with reaching out and fostering a relationship with Parks Canada staff, instilling the significance of our research to Park's staff and the local community of Churchill, providing the necessary training and knowledge transfer, and providing ongoing assistance and guidance as the monitoring program transitioned from graduate student-led to Parks Canada-led. Along the way, I was able to generate several key contributions to transform our research science into action and application. These contributions fall under three main categories (operationalizing agency-led monitoring, communicating monitoring results with science practitioners, communicating research with the general public) and are outlined with examples below.

Operationalizing Agency-led Monitoring

During the summer of 2015, myself and a M.Sc. student from Wilfrid Laurier University (Stephanie Roy) spent a week working hands-on with Parks Canada staff to train them on lab and field protocols. This involved multiple lectures as well as hands-on training sessions both in the classroom and in the field, on how to utilize field equipment, how to collect samples, how to process samples, and how to store, package, and ship samples. The main purpose of this training was to give Parks Canada staff the knowledge and confidence to conduct the Hydroecology Monitoring Program sampling through an understanding of how to collect and interpret the generated data. Two important schematics were created to achieve this purpose (Figures 4.1, 4.2). With all this in mind, these training sessions allowed our field and research methods to be accessible and reproducible for new Parks staff (since there is a high turnover rate) and for other northern lake-rich national parks. Additionally, during the summer of 2015, I spent a tremendous amount of time developing Standard Operating Procedures (SOP) for the Hydroecology monitoring program to ensure that our research methods fit within Parks Canada guidelines and reporting requirements. Working closely with Park ecologist Chantal Ouimet, multiple SOP documents were generated and due to their collective length, only a short extract of these is included here (See Section 4.A). I played a large role in writing SOP 1, Pond Water Dynamic/Lake Hydrology; SOP 2-4, Goose Aquatic Impact SOP 2-4, SOP 5, and SOP 6 (Figure 4.3). The SOPs are now in the hands of Parks Canada to finalize.

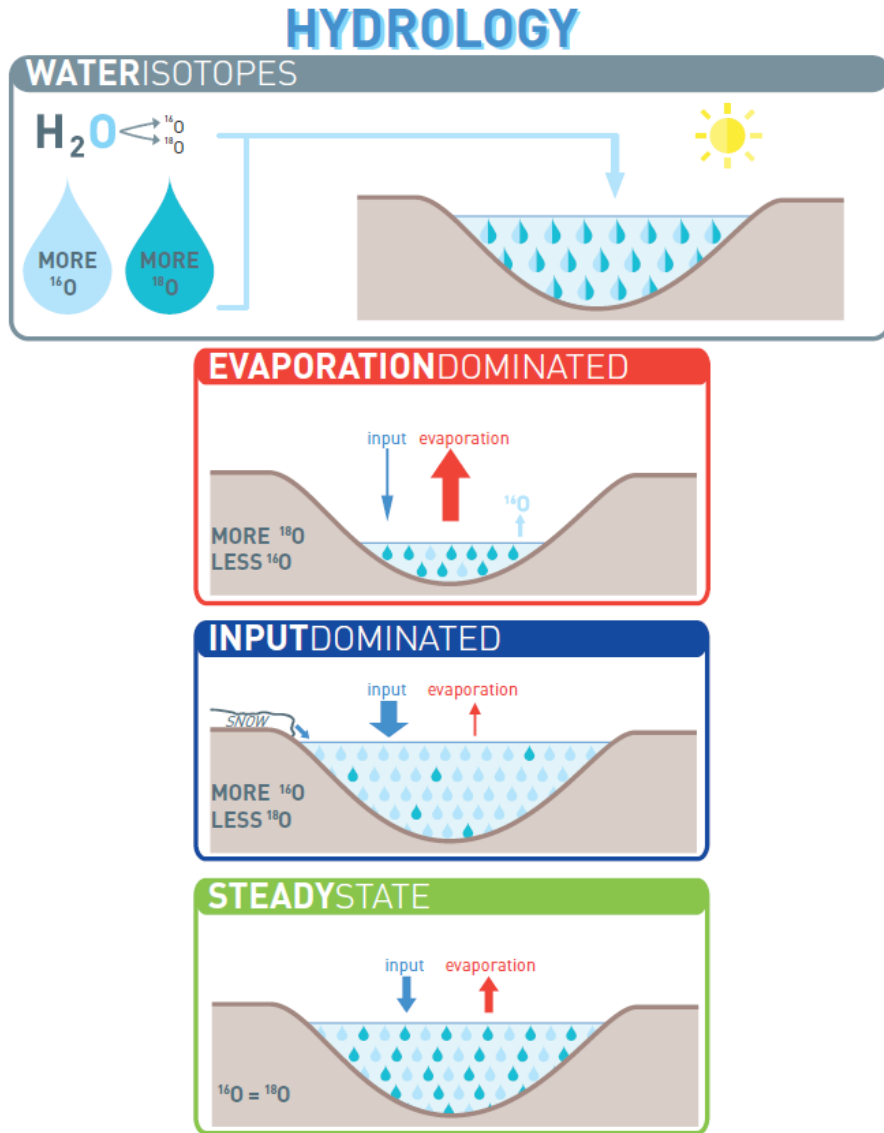


Figure 4.1 Schematic depicting hydrological processes that influence lake water isotope composition (designed in collaboration with University of Waterloo Ph.D. candidate, Pieter Aukes).

LESSER SNOW GEESE (LSG) MONITORING

LOW DISTURBANCE PONDS LSG DISTURBED PONDS

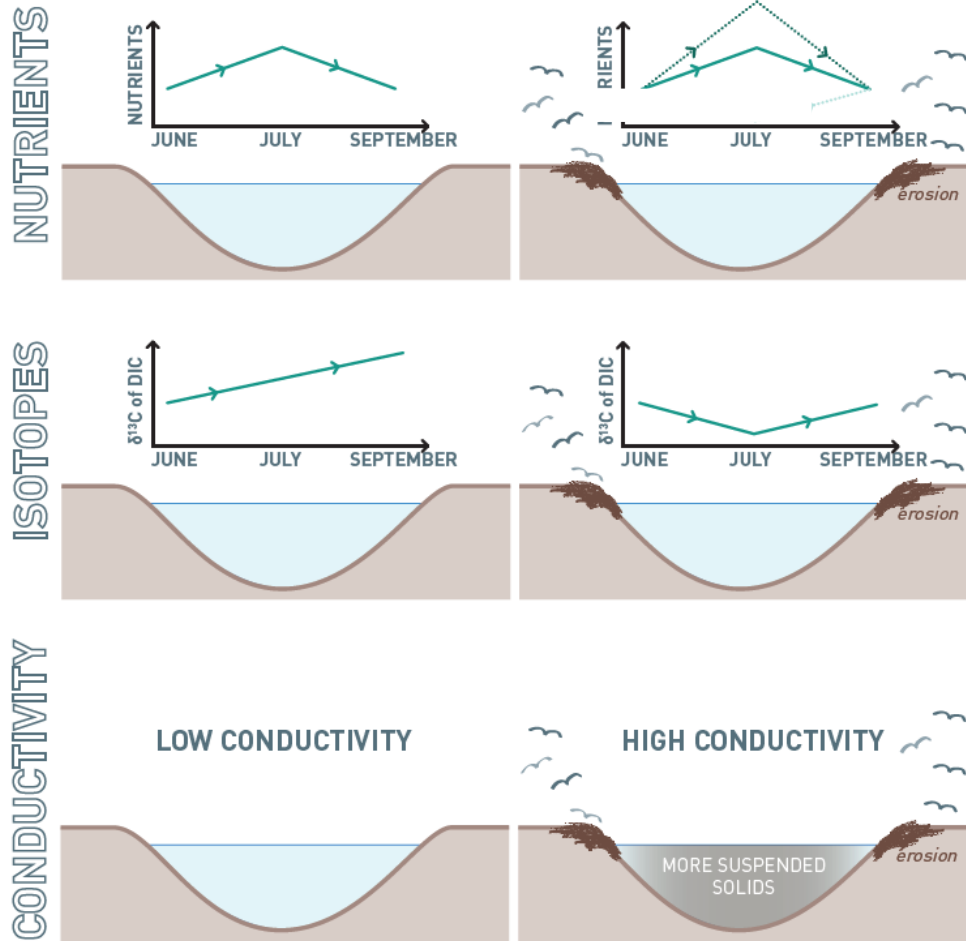


Figure 4.2 Schematic depicting the difference in nutrient (TKN, TP) concentrations, carbon isotope composition of dissolved inorganic carbon, and pond conductivity resulting from catchment erosion, in response to LSG disturbance (designed in collaboration with University of Waterloo Ph.D. candidate, Pieter Aukes).

Hydroecology Monitoring

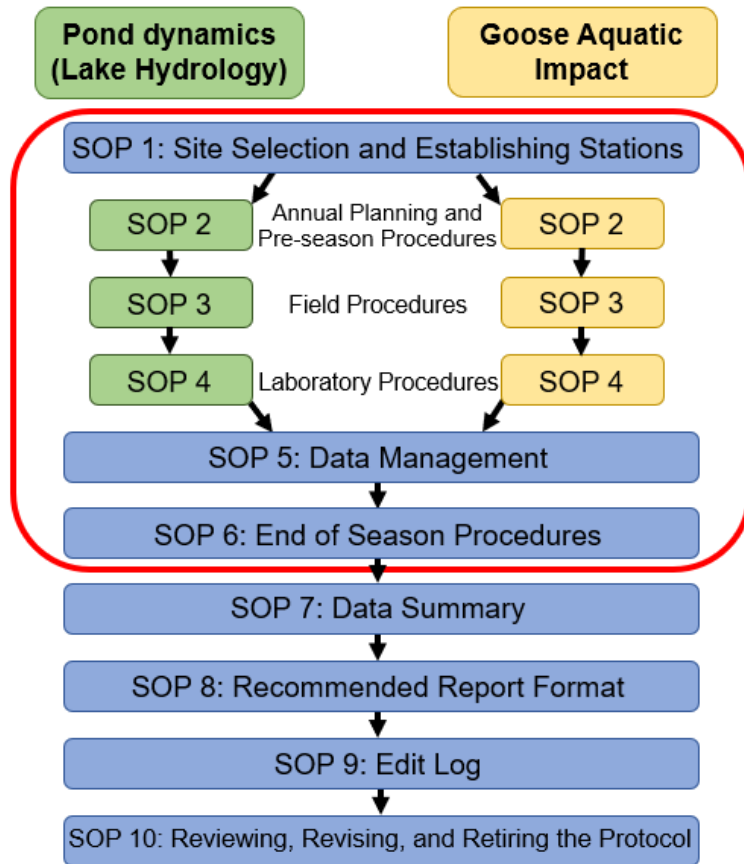


Figure 4.3 Schematic showing the organization of Wapusk National Park's, Hydroecology Monitoring Program Standard Operating Procedures (SOPs).



4.A. Sample of Generated SOPs for Parks Canada

Standard Operating Procedure # 3: Field and Laboratory Procedures

Draft – September 20, 2015

This SOP gives step-by-step instructions for conducting hydrological and limnological monitoring. This SOP describes:

1. The field and laboratory equipment required.
2. The timing and sequence of data collection in the field.
3. Detailed methods on pre-field preparation, safety, field protocols, lab protocols and post-field work tasks.
4. The procedure for filling in the field notes form that appears in Appendix 3-1.

3.1. Required Equipment and Forms

3.1.1. Field equipment

3.1.1.1. Hydrological monitoring field equipment

- 17 x 30mL high density polyethylene bottles (HDPB)
- YSI Multi Meter
- Black Sharpie markers
- Colourful electrical tape
- Waterproof notebook/data sheets
- Pens/pencils
- Ziploc bags for sample bottle storage (1 each for empty and full bottles)
- GPS with pond locations
- Booklet with map of ponds and photos for identification
- Camera
- Extra batteries

3.1.1.2. Limnological (Lesser Snow Goose) monitoring field equipment

- 35 x 5L carboys
- 35 x 2L bottles
- 35 x glass serum bottles
- 35 x glass serum stoppers
- 5 x needles
- 70 x 90mL plastic sample bottles (yellow lid)
- Milk jug for ease of pouring pond water into bottles
- Fishing rod
- 25 micron yellow phytoplankton tow net (to attach to fishing rod)
- Emergency fishing rod and net supplies

- YSI Multi Meter
- Black Sharpie markers
- Colourful electrical tape
- Waterproof notebook/data sheets
- Pens/pencils
- XXL zip lock bags for sample bottle storage and easy transport
- 1 x Rubbermaid bin to store collected glass sample bottles for protection in the helicopter
- GPS with ponds locations
- Booklet with map of ponds and photos for identification
- Camera
- Extra batteries

3.1.2. Lab equipment

3.1.2.1. Hydrological monitoring lab equipment

- No corresponding lab equipment

3.1.2.2. Limnological (Lesser Snow Goose) monitoring lab equipment

- 40 x crucibles
- Desiccator and desiccant
- Small whirlpak bags
- Oven for drying
- Filtering pump and units
- Graduated cylinders
- Pre-screen and funnel
- 35 x 125mL square glass bottles
- 35 x 1mL sulphuric acid (30% concentration) per pond
- 35 x 125mL round glass bottles
- 35 x GF/F filters
- 35 x Cellulose acetate filters
- 35 x 30mL high density polyethylene bottles (HDPB)
- Red pre-screen net
- 35 x Quartz filters
- 35 x 60mm Petri Dishes

3.1.3. Forms

The hydrological and limnological monitoring field notes form template (Appendix 3-1).

3.2. Timing and Sequence of Events

3.2.1. Monthly schedule of sampling periods

3.2.1.1. Hydrological monitoring

This sampling takes place three times a thaw season; typically, in June, July, and September. The purpose for sampling three times is to capture the pond water signature directly after the pond ice melts (June), during prime summer with peak evaporation (July), and before the pond freezes (September). The exact dates within June, July, and September are not critical as long as the ponds are sampled close to these indicators. Previous sampling over the past 6-7 years have occurred consistently around mid to late June, late July, and mid to late September. If field dates are much different than these, contact research partners (WLU) to discuss options.

3.2.1.2. Limnological (Lesser Snow Goose) monitoring

This sampling takes place once a thaw season at the same time as the July hydrological monitoring; typically, in late July.

3.2.2 Length of sampling

For each hydrological monitoring pond, sampling will take ~8 minutes. For each limnological (Lesser Snow Goose) monitoring pond, sampling will take ~15 minutes.

3.2.2.1. June sampling trip

In June, only the 16 hydrological ponds will be sampled. Ideally, all 16 of the ponds should be sampled on the same day. This decreases as much variability as possible within the dataset. If this is not possible, sampling over two consecutive days is acceptable as long as the weather between the two days is not drastically different. For example, sampling before and after a heavy rain event could skew the values considerably.

3.2.2.2. July sampling trip

In July, both the hydrological and limnological monitoring ponds will be sampled (46 ponds in total). For this sampling period, ponds will need to be sampled over 2-3 consecutive days (weather dependant). Sampling with similar weather over the multiple days is ideal, however, it is completely uncontrollable.

Additionally, hydrological ponds WAP 5, 7, 12, and 15 can be sampled following the limnological protocol for a more complete data set since they fall along the limnological sampling transect lines (pushing total number of sampled ponds for limnology/Lesser Snow Goose sampling to 34).

3.2.2.3. September sampling trip

In September, only the 16 hydrological ponds will be sampled. Ideally, all 16 of the ponds should be sampled on the same day. This decreases as much variability as possible within the dataset. If this is not possible, sampling over two consecutive days is acceptable as long as the weather between the two days is not drastically different. For example, sampling before and after a heavy rain event could skew the values considerably.

3.2.3. Tasks to complete during the winter months

Prepare Whatman quartz filters (CAT no. 1851-047) for Particulate Organic Matter (POM), 1 filter per sample as follows (done at CNSC):

- Quartz filters need to be pre-combusted or burnt to ensure all contaminants have been removed. Filters should only be handled carefully with tweezers.
- *Crucibles*
 - a. Clean 40 crucibles with deionized water and a brush
 - b. Dry in drying oven for 2 hours
 - c. Ash the crucibles in the furnace for 2 hours at 550°C
 - d. Remove crucibles from furnace and allow to cool in non-acid desiccator with desiccant
- *Filters*
 - a. Place 40 quartz filters into their own clean, dry large crucible
 - b. Combust (burn) the filters at 450°C for 4 hours in the furnace
 - c. Remove crucibles and filters from muffle furnace and allow to cool in non-acid desiccator
 - d. Label 40 small whirlpak bags (Quartz filter #____, date)
 - e. Place filters in a labelled small whirlpak bag

3.2.4. Month before tasks

- 1) Check in with Hudson Bay Helicopters regarding solidified sampling dates and helicopter model
- 2) Check in with LeeAnn Fishback at the Churchill Northern Studies Centre regarding fridge space for sample storage, lab bench space for processing samples, as well as deionized water and other miscellaneous lab supplies (i.e. sulphuric acid/fume hood use)
- 3) Prepare YSI Multi Meter:
 - a. *Plan A*: Ensure Parks Canada's YSI is properly calibrated and instrument is fully functional
 - b. *Plan B*: If Parks Canada's YSI is unable to be properly calibrated and/or is broken, contact an instrument rental provider and schedule an appropriate delivery date for YSI

3.2.5. Week before tasks

The field trip plan should be solidified with potential back up plans. Additionally, supplies for hydrological and limnological monitoring are stored in Storage Room M05 in the CNSC old building and must be transferred to the work space in the allotted CNSC laboratory before field and laboratory preparation can begin.

3.2.5.1. Trip Plan

Typically, sampling starts at the farthest south pond for both hydrological and limnological monitoring. Ponds would then be sampled working your way back to the CNSC. This plan may be changed depending on logistical and weather restraints.

3.2.5.2. Field preparation for hydrological monitoring (June, July, and September)

- 1) Label 17 x 30mL HDPB bottles using colourful electric tape. Label “WAP _____ and Month/year” (pond name will be filled when at the pond).
- 2) Place bottles into large Ziploc bag with a black sharpie marker. Label a second large Ziploc bag, “FULL Hydrological Monitoring Samples”, for filled water bottles in the field.
- 3) Prepare ‘emergency supply kit’ with spare batteries, pens/pencils, Sharpies, and tape.
- 4) Check YSI Multi Meter calibration and ensure battery is charged.
- 5) Ensure GPS has correct coordinates and batteries are fully charged.
- 6) Prepare field notes binder/clipboard Ensure there are enough waterproof hydrological and limnological monitoring field notes forms.

3.2.5.3. Field and Laboratory preparation for Limnological (Lesser Snow Goose) monitoring (July)

Field:

- 1) Label 31 x 5L carboys, 31 x 2L bottles, 31 x 90mL plastic sample bottles with yellow lid (2 per pond), and 31 x glass serum bottles, using colourful electric tape. Label “WAP _____ and Month/year” (fill in pond name once getting to pond).
 - Complete set of sample bottles required for one pond = 1 x 5L carboy, 1 x 2L bottle, 1 x glass serum bottle, and 2 x 90mL plastic sample bottles with yellow lid
- 2) Prepare ‘grab bags’ for sampling: place bottles for five ponds in each XXL Ziploc bag (one bag will have six because of extra bottle set).
- 3) Prepare ‘emergency supply kit’ with spare batteries, pens/pencils, Sharpies, tape, glass serum lids and needles, and extra fishing rod and net supplies.
- 4) Check YSI Multi Meter calibration and ensure battery is charged.
- 5) Ensure GPS has correct coordinates and batteries are fully charged.
- 6) Prepare field notes binder/clipboard. Ensure there are enough waterproof hydrological and limnological monitoring field notes forms.

Lab:

- 1) Prepare bottles for each pond for water filtration for water isotopes, nutrients, and all carbon parameters as follows:
 - Label 16 square glass bottles, 16 petri dishes, 16 30mL HDPB bottles with electrical tape stating WAP ‘name’ and date (month/year)
 - Label 16 round glass bottles for DIC/DOC using NLET labels. (Refer to labelling picture)

- 2) Prepare filtering pump and units by ensuring the pump hoses are attached and units have been washed with DI water.

3.2.6. Day before tasks

Gather all required supplies for the first helicopter day and place them in one spot, ready to be checked and grabbed the morning prior to sampling:

Table 3-1. Packing lists for helicopter sampling

Hydrological Monitoring	Limnological Monitoring
GPS	GPS
Pond picture booklet	Pond picture booklet
Camera	Camera
YSI Multi Meter	YSI Multi Meter
Field note binder/clipboard	Field note binder/clipboard
Sharpies	Sharpies
Ziploc bag with empty sample bottles	Grab bags of sample bottles
Ziploc bag for full sample bottles	Milk Jug
Emergency supply kit	Glass serum lids and needles
	Fishing rod and net
	Rubbermaid bin (glass sample storage)
	Emergency supply kit

3.2.7. Thirty minutes before departing for sampling

Double check that you have all the supplies needed for the days sampling. If you are missing anything, you are NOT able to return to the CNSC to grab anything!

3.2.7.1. Helicopter Day Checklist

- Items in packing lists (Section 3.2.6, Table 3-1)
- Trip plan confirmed with helicopter company
- Trip plan filed with resource conservation manager or public safety specialist

3.2.8. Upon return to CNSC – same day as sampling

3.2.8.1. Hydrological monitoring samples

Ziploc bag of 16 full hydrological samples should be placed in fridge directly after returning to the CNSC. There is no corresponding laboratory work.

3.2.8.2. Limnological monitoring samples

- 1) Place all water samples into the fridge directly after returning to the CNSC. They will be stored here until all the water filtering is finished within the two days after field work.
- 2) Particulate Organic Matter (POM) filtering **must be completed** on the **same day as sample collection** (See 3.4.2 for POM laboratory protocol). If this is not done, the **samples will be ruined**.

3.3. Hydrological and Limnological Monitoring Field Protocols

3.3.1. Hydrological monitoring field work protocol

- 1) In Helicopter
 - a. Identify pond using a combination of GPS point, map, and pond photo.
 - b. Prep 30 mL bottle in helicopter – write pond name on bottle and place it in an easily accessible location to grab when at the pond (i.e. pocket).
 - c. Take a photo of the pond from the helicopter.
 - d. Take photo of pond number before getting out of helicopter, this enables you to know that all of the following photos are from that pond.
- 2) On the ground at pond
 - a. Take photos of pond, take three shots from left to right, covering the whole pond area.
 - b. Take 30 mL bottle and rinse with pond water **three** times. Fill to very brim and tightly cap. Place in Ziploc bag for filled bottles.
 - c. Turn on YSI, submerge probe into water making sure that it is not touching sediment. Wait until numbers stabilize before recording.
 - d. Record values of temperature (°C), pH and conductivity ($\mu\text{S}/\text{cm}^2$) in waterproof field notes.
 - e. Fill out field notes (3.3.3.)

3.3.2. Limnological monitoring field work protocol

- 1) In Helicopter
 - a. Identify pond using a combination of GPS point, map, and pond photo.
 - b. Take a photo of the pond from the helicopter.
 - c. Take photo of pond number before getting out of helicopter, this enables you to know that all the following photos are from that pond.
- 2) On the ground at pond
 - a. Take photos of pond, take three shots from left to right, covering the whole pond area.
 - b. Label all bottles with pond number upon reaching pond, this includes: 5L carboy, 2L bottle, 2x90mL bottles and glass serum bottle.
 - c. Rinse 5L carboy with pond water three times. Fill to the brim using milk jug and tightly cap.
 - d. Rinse 2L bottle with pond water three times. Fill to the brim and cap tightly.
 - e. Rinse two 90mL sample bottles three times. Fill using yellow phytoplankton tow net clipped to the end of the fishing rod. Do this by gently swishing the fishing rod back and forth, keeping the tow net in the

- top 5-10cm of the water column. Fill two 90mL sample bottles with the water that filters through the tow net.
- f. Rinse glass serum bottle three times. Fill glass serum by completely submerging bottle until full of water. Once full, keep bottle submerged, place rubber stopper on top of bottle and expel any extra air by inserting needle into the middle of the rubber stopper. This must all be completed **underwater** to ensure no air bubbles are left in bottle. The rubber stopper lid is sensitive so be sure to safely store the bottles in the Rubbermaid bin for transport back to the CNSC.
 - f. Turn on YSI, submerge probe into water making sure that it is not touching sediment. Wait until numbers stabilize before recording.
 - g. Record values of temperature (°C), pH and conductivity ($\mu\text{S}/\text{cm}^2$) in waterproof field notes.
 - h. Fill out field notes (3.3.3.)

3.3.3. Field note data collection

Fill in the field note data collection sheet at each pond (Appendix 3-1)

- Lake ID: lake number (i.e. WAP 05)
- Date: record the month, day, and year (MM-DD-YYY)
- Time: record time of arrival at pond in 24 hour clock (hh:mm)
- Sampling Crew: identify who is collecting samples.
- Weather: note things like precipitation, wind strength and direction, cloud cover.
- Evidence of geese: note if there are geese present, if there are signs of grubbing, feces, feathers, tracks, etc.
- Water depth: record in meters (m); approximate depth at sampling point and the pond as a whole.
- Hydrology: indicate lake level compared to previous seasons/years (if possible) and give a pond sediment description (colour and texture).
- Water quality: record if colour of the pond water and whether the water is clear or murky. Indicate if the sediment has been stirred up (turbidity).
- Evidence of pond connectivity: indicate how wet the adjacent landscape is and whether or not ponds are connected to other ponds, streams, rivers, etc.
- Other: record the vegetation cover in and around pond (shrubs, trees, grasses, macrophytes, etc.). Note if there is any shoreline erosion or if there is any other wildlife present.
- YSI Multi Meter
 - Temperature: record in degrees Celsius (°C)
 - Conductivity: record in micro Siemens per centimeter ($\mu\text{S}/\text{cm}$)
 - pH: record unit-less value

3.4. Laboratory work Protocol

3.4.1. Hydrological monitoring laboratory protocol

There is no corresponding laboratory work for the hydrological monitoring.

3.4.2. Limnological laboratory protocol

3.4.2.1. *Same day as field sampling (Particulate Organic Matter filtering)*

- 1) Prepare a filtering unit with a pre-combusted quartz filter
 - a. Place circular filter holder firmly on the neck of the filtering unit.
 - b. Using tweezers, place the filter in the centre of the circular filter holder (do not touch the filter with your hands)
 - c. Place the filtering unit lid on carefully, firmly pushing down, and ensuring that you are screwing the lid on straight and tightly.
- 2) Remove the two 90mL plastic sample bottles (yellow lid) for a single pond and obtain the corresponding petri dish for the same pond.
- 3) Shake the 90mL plastic sample bottles to ensure a homogenous water sample.
- 4) Place the red pre-screen net over the prepared filtering unit in the sink, ensure that the pre-screen is indented into the filtering unit so water will pour IN to the unit and NOT over the edges and OUT of the unit...
- 5) Pour both 90mL plastic sample bottles through the pre-screen net, ensuring all water goes through.
- 6) Carefully transfer the filtering unit to the lab bench and attach to the pump. Turn the pump on and ensure that the air flow is correct.
- 7) Once all the water has filtered through, turn off the pump and carefully unscrew the lid.
- 8) Open the petri dish and using your tweezers (DO NOT TOUCH WITH YOUR HANDS), carefully transfer the filter into the petri dish.
- 9) Transfer the petri dish (still open with the lid underneath) into the oven at 60°C for at least 24 hours (it is okay if they stay in longer but it needs to be at least 24 hours).
- 10) Discard filtered water and rinse entire filtering unit with de-ionized water. Rinse red pre-screen net with tap water.
- 11) Repeat for all 16 ponds. (*It is possible to do 2 samples at once but **always** ensure you know which pond water sample is in which filtering unit!!!*)
- 12) Remove tape and clean/rinse the 90mL plastic sample bottles and lids with hot water.

3.4.2.2. *Within two days of field sampling (Processing of water isotope, nutrient, and Dissolved Inorganic Carbon parameters)*

- 1) Remove a 5L carboy from the fridge and obtain all the sample bottles for the same pond number.
- 2) Shake the carboy to ensure a homogenous water sample and rinse the graduated cylinders with pond water.
- 3) Fill one graduated cylinder with un-filtered and un-pre-screened pond water and fill the 30mL HDPB to the brim (water isotope sample). With this same water, fill the 125mL square glass bottle to just below the neck of the bottle and add 1mL 30% sulphuric acid (phosphorus and nitrogen sample). Ensure lids are screwed on tightly.
- 4) Pre-screen the pond water, by pouring pond water through funnel with the pre-screen mesh attached to the bottom (for Dissolved Inorganic Carbon Sample).
- 5) Prepare two filtering units, one unit with a GF/F filter (coarser filtering) and one unit with a cellulose acetate filter (finer filtering). Keep track of which unit has which filter!!!!

- 6) Pour ~300mL of pre-screened pond water into the filtration unit with the GF/F filter for the initial coarse filtration and turn on the pump (ensuring that the flow of air is correct).
- 7) When all of the water has filtered through (absolutely no water left on the filter), turn off the water pump, unscrew the filtering unit lid off of the GF/F filter, remove the circular filter holder with filter, and transfer the water into the top of the second filtering unit.
- 8) Turn on the pump (ensuring air flow is correct) and filter water through the cellulose acetate filter for a finer filtration.
- 9) Once all of the water has been filtered, turn off the water pump, unscrew the filtering unit lid off of the cellulose acetate filter, remove the circular filter holder with filter, and transfer the water to the 125mL round glass bottles (It is easiest to pour the water out of the small spout on the side of the filtering into the mouth of the 125mL round glass bottles). Fill bottle just above the neck but not all the way to the brim.
- 10) Transfer the 30mL HDPB, 125mL square glass bottle, and 125mL round glass bottle to the fridge.
- 11) Discard the GF/F and cellulose acetate filters as well as the excess water in the filtering units, graduate cylinder, and 5L carboy (ONLY DO THIS AFTER EVERYTHING HAS BEEN FILTERED AND PLACED INTO SAMPLE BOTTLES CORRECTLY!)
- 12) Rinse all parts of the filtering units (base, filter holder, and lid) thoroughly with de-ionized water.
- 13) Repeat these steps for all of the ponds.
- 14) When all samples have been filtered and placed into sample bottles, the 2L bottles can be dumped and cleaned/rinsed with hot water. Clean/rinse 5L carboys with hot water as well. Make sure to remove all labelling tape.

3.5. Post-collection Processing and Storage

3.5.1. Post-collection tasks and procedures

- 1) **Data Entry**: Transfer data from field note sheets to the excel file template provided by research partner (WLU). The excel file can be found at [archive data within a Parks Canada database]. Although all the data will be transcribed to a datasheet or a computer spreadsheet equivalent, original field notes should be preserved at least one year, and preferably indefinitely as part of the weather record.
- 2) **Ship samples**: All filtered samples (water and petri dishes) should be packaged and shipped to research partner at 75 University Ave. N., Wilfrid Laurier University, Department of Geography and Environmental Studies, Waterloo, Ontario, N2L 3C5 after **each** sampling trip.
 - a. Wrap electrical tape around the glass serum lids to ensure they stay on through transport
 - b. Wrap bottles with NLET labels with clear packaging tape to ensure label is secure.
 - c. Wrap all glass bottles in newspaper and place in a cooler

- d. Place all other samples (petri dishes and 30 mL HDPE bottles) on top
 - e. Ship cooler in a way where they can stay cold and arrive in Waterloo fast
 - f. Send an email to the research partners regarding the shipment and also attach the field notes file.
- 3) Inventory: Do a complete inventory of all the supplies and store in an excel spreadsheet for easy access to order for next season
 - 4) Storage: Package and store all of the supplies back into CNSC old building storage room M05 in an organized fashion. Ensure the lab bench is clean when finished.

3.6. Safety and Logistics

3.6.1. Trip Plan Logistics

A trip plan must be filed with the visitor safety and resource management specialist and/or the resource conservation manager. This includes location of sites, planned route, estimated time for each task and calling-in procedures. This should be saved in: G:\Resource Conservation Function\Visitor Safety\Check-In for Field Work.

3.6.1.1. Helicopter

Your exact trip plan should be confirmed with the helicopter company well in advance. Ensure your handheld GPS is fully charged and put on the compass screen for the helicopter pilot. Handheld GPS units should be programmed appropriately for the region. NAD 87 is the most accurate setting for Wapusk. Use UTM format for co-ordinates.

Use booklet of pond photos and aerial imagery in combination with the handheld GPS for accuracy and speed while navigating to ponds. Idle time while the helicopter is running results in considerable expense.

Be prepared to mark down waypoints and details in a waterproof field book and handheld GPS unit, if you spot a polar bear or other wildlife of interest. The rest of the information can be filled out on an observation form afterwards.

3.6.2. Check-in Procedures

Staff must check-in twice daily while in the field. Satellite phone is the primary means for field staff communicating with the Visitor Safety Coordinator, the Administration Office or Asset Management staff.

You can contact the Visitor Safety Coordinator or designate 24 hours a day when staff are in the field (204-675-0144), or during operational hours call the Administration Office (204-675-8863). The on-call phone is monitored 24 hours per day all year. You should call this number if you have questions related to the operation of equipment at the site. If the on-call phone (204-675-0082) cannot be reached, your manager should be phoned at his or her contact number.

Jasper Dispatch can be contacted 24 hours, 7 days / week, in the case of emergencies 877-852-3100 or 780-852-3100 when calling from a satellite phone. Jasper Dispatch has contact information for various PCA staff in Churchill.

3.6.3. Mode of Travel

3.6.3.1. Helicopter Safety

Prior to your arrival, a safety briefing will be given to passengers by the pilots. All rules must be obeyed, for your safety and the safety of others. Staff should familiarize themselves with safe practices of enplaning and deplaning a rotary wing aircraft. Safe work practices around helicopters including enplaning/deplaning and door-off operations with a helicopter are available in: G:\OSH\SWPs approved locally\SWPs approved by Marilyn.

The following hazards should be taken into consideration when dealing with helicopters:

- Injury due to inclement weather conditions;
- Injury resulting from inexperience or inadequate training
- Injury resulting from insufficient or inadequate equipment
- Injury due to wildlife encounters, particularly polar bears
- Injury due to slip, trip, fall, joint strains/sprains, muscle sprains, strains
- No briefing given, or is incomplete/not understood
- Injury due to slip, trip, fall, joint strains/sprains, muscle sprains, strains (path to helicopter is wet, icy, uneven terrain, fuel spills, debris, etc.)
- Cuts, contusions, abrasions
- Injury or death as a result of contact between person/equipment with main or tail rotor, exhaust exposure, or hit by other aircraft or vehicle.
- Hearing or eye Injuries
- Load too heavy, not balanced or secured (potential flight complications)
- Dangerous Goods on board (potential flight complications)
- Injury due to improper lifting, handling and transportation of equipment.
- Injury due to improper inspection and storage of equipment

The guidelines for flying over national parks is 2,000 AGL, to minimize the impact on wildlife and other park users. It is possible to fly lower than 2,000 for specific reasons (i.e. research, weather, length of travel). The pilot will ultimately make the call on the elevation in inclement weather and that will trump other factors.

Helicopter emergency kits are located in dry bags in the basement of the administration office. Staff should always take one when travelling by air. Helicopters have had to land in the past, due to mechanical difficulties or low cloud ceiling/poor visibility. The emergency kit should always be with staff and researchers if dropped off by the

helicopter. Weather conditions can change suddenly which can result in the helicopter being delayed or cancelled for pick-up, leaving researchers stranded.

3.6.3.2. Fuel considerations

There are currently 5 permanent and 1 temporary fuel caches in Wapusk and 1 at York Factory National Historic Site. There are multiple types of fuel that can be found at these sites: aviation fuel, jet A or B; diesel and natural gas. It is important to know which kind of fuel it is and who the drum belongs to. The helicopter may need to land to refuel depending on the distance travelled and weather conditions. Talk to Jill or the resource conservation manager about fuel availability and locations before allowing the pilot to refuel. It is important to keep track of how much fuel is used and from where, so that others do not become stranded due to miscommunication.

More information is available in: G:\Resource Conservation Function\Resource Management\Fuel Cache, Park Clean-up & Contaminated Sites\Fuel Cache.

3.6.3.3. Recommended emergency packing list

Wapusk is a northern and coastal wilderness park, which means weather conditions can vary in extremes in a matter of hours. It is important to be well-prepared for rapid changes in temperature, wind and rain. It is a good idea to consult with experienced staff members on what to pack during the summer field season. However, the following list provides some of the basic necessities:

- Helicopter emergency kit (includes first aid kit) for day trips
- Communication device and extra batteries (bring alternate if spending nights in the field)
- Firearm and ammunition (slugs)
- Water filter
- Bug spray and sunscreen
- Hat and sunglasses
- Rubber boots
- Good quality packable rain gear
- Extra clothing layers
- AA3 key – the Broad River shed is padlocked.
- Bug jacket
- 1L water bottle x2
- Water purification tablets

3.6.4. Health Risk Potential

This field work involves working in severely Lesser Snow Goose disturbed landscapes and ponds where there is an abundance of goose feces. The chance of contact is high while working in these areas. Additionally, one of the field protocols involves using a small needle to release excess air from a sample bottle.

In cold temperatures and water with numb hands, the potential to injure oneself with the needle is a possibility.

3.7. Appendices

Appendix 3-1: Hydrological and Limnological Monitoring Field Notes

Wapusk National Park Hydrological and Limnological Monitoring		
Lake ID: _____	Date: _____	Time: _____
Sampling Crew: _____		
Weather (precipitation, wind, cloud cover):		
Evidence of geese (are there geese present? signs of grubbing, feces, feathers, tracks, etc.):		
Water depth (m; at sampling point and whole pond depth approximation):		
Hydrology (lake level compared to other seasons/years, pond sediment description):		
Water clarity (clear, murky, is the sediment stirred up/turbid, lake colour):		
Evidence of pond connectivity (how wet is the adjacent landscape, are ponds connected):		
Other (vegetation cover in and around pond, any shoreline erosion? other wildlife?):		
YSI:		
Temp. (°C): _____		
Conductivity (µS/cm): _____		
pH: _____		

Communicating monitoring results with science practitioners

As part of the Hydroecology Monitoring project with Parks Canada, reports for each section (Pond Water Dynamics/Lake Hydrology and Goose Aquatic Impact) were generated annually starting in 2016 (see Section 4.B and 4.C for sample reports). These documents are a critical piece in the knowledge translation from scientific data to a concise report that can be used by Parks Canada's management staff to help protect and manage the park. These reports also serve as a model for reporting long-term monitoring data that can be adapted elsewhere.

As a final contribution of this work, all the data that we helped generate within the Hydroecology monitoring program (Pond Water Dynamics/Lake Hydrology and Aquatic Goose Impact), has become public domain through the Open Governmental Portal (Section 4. D, 1 and 2). This is an excellent scientific contribution since our research and the research that staff at Wapusk National Park will continue through the Hydroecology Monitoring program is transparent and accessible to the public.

4.B. 2018 Pond Water Dynamics/Lake Hydrology Report

2018 Wapusk National Park Lake Hydrology Report

Hilary White & Brent Wolfe

Department of Geography and Environmental Studies
Wilfrid Laurier University
January 14, 2019



Table of Contents

1.0 Executive Summary	137
2.0 Introduction	138
2.1 General Introduction	138
2.2 Tracking Lake Hydrology using Water Isotopes	139
3.0 2018 WNP Field Sampling	141
4.0 Water Isotope Results	142
4.1 Evaporation Pan Data	142
4.2 Precipitation Bucket Data	143
4.3 Seasonal Variability	144
4.4 Ecotype Variability	145
5.0 Contextualizing Water Isotope Results	146
5.1 Evaporation to Inflow Ratios as a Tool for Tracking Lake Hydrology	146
5.2 Alignment of Hydrological Threshold Analysis with Wapusk National Parks' Monitoring Protocol	149
5.3 Calculation of 'Lake Hydrology' Scores	150
A. Coastal	150
B. Wetland	151
5.4 Tracking Hydrological Health Over Time	152
A. Coastal	152
B. Wetland	153
6.0 Appendix	154
7.0 References	160

List of Figures

Figure 1: 'δ ¹⁸ O-δ ² H space' Explanation Schematic	140
Figure 2: Hydrological Processes Schematic	141
Figure 3: Site Map	142
Figure 4: Evaporation Pan Data	143
Figure 5: Precipitation Bucket Data	144
Figure 6: Seasonal Variability of Lake Hydrology	145
Figure 7: Ecotype Variability of Lake Hydrology	146
Figure 8: Coastal Hydrological Health Over Time	152
Figure 9: Wetland Hydrological Health Over Time	153
Figure A1: Three-year E/I Threshold Justification	157
Figure A2: WNP Meteorological Data from 2009-2018	159

List of Tables

Table 1: E/I Thresholds for Hydrological Assessment of WNP Lakes	147
Table 2: Hydrological Threshold Analysis for Coastal Fen Monitoring Lakes	148
Table 3: Hydrological Threshold Analysis for Interior Peat-Plateau Palsa Bog Lakes	148
Table 4: Hydrological Threshold Analysis for Boreal Spruce Forest Lakes	148
Table 5: 2016-2017 Meteorological Conditions within WNP	149
Table 6: E/I Thresholds for Hydrological Assessment of WNP Lakes	150
Table 7: Coastal Measure Condition for 2018 Field Season	150
Table 8: Wetland Measure Condition for 2018 Field Season	151
Table A1: Evaporation Pan Water Isotope Compositions	154
Table A2: Precipitation (rainfall) Bucket Water Isotope Compositions	155
Table A3: Lake Water Isotope Compositions and E/I Ratios	156
Table A4: 5-year threshold values based on 2010-2014 E/I ratios	158

1.0 Executive Summary

All sixteen 'Lake Hydrology' lakes across the three main ecotypes (boreal spruce forest, interior peat plateau-palsa bog, coastal fen) were successfully sampled for lake water isotopes ($\delta^{18}\text{O}$, $\delta^2\text{H}$) three times during the 2018 sampling period (spring/June, summer/July, fall/September). Additionally, the evaporation pan and precipitation bucket were successfully maintained and sampled for water isotopes by Parks Canada staff throughout the ice-free season.

The water isotope results from the evaporation pan, precipitation bucket, and each 'Lake Hydrology' lake was then evaluated to assess the hydrological conditions of the lakes with respect to ecotypes and seasons. Similar to previous years, the influence of both ecotype and seasonality were identified in water isotope results. Lakes begin the ice-free season influenced by inputs (e.g., snowmelt), become more influenced by evaporation during the summer, and are again influenced by inputs (e.g., rainfall) in the fall. Additionally, lakes within the boreal spruce forest ecotype are the most stable due to the higher amount of snow storage during the winter, which leads to higher amounts of snowmelt replenishing the lakes in the spring. Interior peat-plateau palsa bog and coastal fen lakes show a stronger influence of evaporation during the spring and summer seasons.

Evaporation to Inflow (E/I) ratios were then calculated to depict the relative influence of evaporation and inputs on each lake. Hydrological thresholds of E/I ratios were also established to provide a quantitative representation of lake hydrological health. Three states ('poor', 'fair', and 'good') have been used to define the hydrological thresholds within two of Wapusk National Park's ecological measures (coastal and wetland) to align with identifying status and trends for State of the Park reports. While E/I ratios of both coastal and wetland measure lakes were generally within the 'fair' to 'poor' categories from 2010 to 2013, lake E/I ratios have now consistently been within the 'good' to 'fair' categories since 2014. In 2018, fall precipitation (rainfall) had a large influence on these lakes, contributing to all sampling lakes ending the ice-free season within

the 'good' category. The long-term dataset that is now emerging as well as the shifting trends, demonstrate the value of continuing to monitor these lakes to track their hydrological trajectory.

2.0 Introduction

2.1 General Introduction

Wapusk National Park (WNP), northern Manitoba, contains thousands of shallow ponds and lakes (hereafter referred to as lakes) that provide important habitat for a variety of wildlife (Parks Canada, 2011). During the past ~50 years, this region has experienced some of the greatest warming in the circumpolar North and is considered one of the most sensitive regions in northern Canada to permafrost thaw (Smith and Burgess, 2004; Kaufman et al., 2009; Hochheim et al., 2010). Therefore, these freshwater resources are particularly sensitive to accelerating climate change which is causing pronounced variation in hydrological conditions (conditions of and relating to lake water) that have the potential to substantially alter aquatic ecosystems (Smol et al., 2005; Schindler and Smol, 2006; Prowse et al., 2006). Throughout the subarctic and arctic, declines in both the abundance and size of lakes due to warmer temperatures, longer ice-free seasons, and increased evaporation (Labrecque et al., 2009; Turner et al., 2010; Bouchard et al., 2013) have been observed as well as the increasing susceptibility of permafrost thaw (Marsh et al., 2009; Jones et al., 2011). Detecting and anticipating these hydrological responses to climate warming are challenging in northern landscapes due to the speed in which changes are occurring and the remoteness of the landscape that impedes conventional monitoring approaches. Within Wapusk National Park, in collaboration with Wilfrid Laurier University and University of Waterloo, water isotopes have been utilized as a practical and affordable monitoring tool to track hydrological conditions at the landscape scale since samples can be easily collected in the field, are broadly applicable, sensitive and diagnostic (Gibson and Edwards, 2002; Brock et al., 2007; Wolfe et al., 2007; Turner et al., 2010;

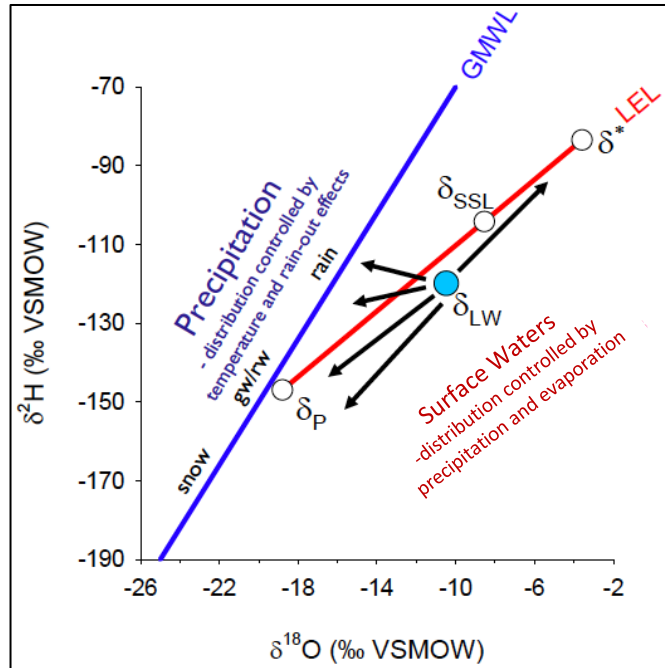
Tondu et al., 2013; Anderson et al., 2013; Brooks et al., 2014; Remmer et al., 2018).

2.2 Tracking Lake Hydrology using Water Isotopes

Previous research has successfully utilized water (chemical symbol: H₂O) isotopes to characterize lake hydrology (e.g., Tondu et al., 2013, MacDonald et al., 2017). An isotope is an element that contains the same number of protons, but different number of neutrons in its nucleus. Specifically, the water isotopes, ¹⁸O and ²H, are very useful since the oxygen and hydrogen isotope compositions of water vary in a systematic and predictable manner as water passes through the hydrological cycle (Clark and Fritz, 1997; Edwards et al. 2004). Water isotope compositions are expressed as variations in the relative abundance of rare, heavy (¹⁸O, ²H) isotope species of water with respect to the common, light (¹⁶O, ¹H) isotope species. These ratios are conventionally reported in delta (δ) notation as per mil (‰) values.

Lake water isotope results are reported with respect to the Global Meteoric Water Line (GMWL) and the Local Evaporation Line (LEL) (Figure 1). The GMWL is a linear representation of all global precipitation, where values higher up on the GMWL are typically rainfall and values lower down are typically snow. The LEL is based on local meteorological factors (i.e., temperature, relative humidity) and can be calculated from δ_P, δ_{SSL}, and δ* (read as 'delta P', 'delta steady-state limiting', and 'delta star', respectively). δ_P represents the mean annual isotope composition of precipitation, which can be determined from the Canadian Network for Isotopes in Precipitation (CNIP). δ_{SSL}, calculated using evaporation pan data, represents steady-state where inputs (precipitation) equal outputs (evaporation) and δ* is the isotopic representation of a last drop of water in a lake before it completely desiccates or dries up. δ* is calculated utilizing local atmospheric conditions including the isotope composition of atmospheric moisture, temperature, and relative humidity. Where the sampled lake water values (δ_{LW}) fall within this "δ¹⁸O-δ²H space" gives us information about how a lake is influenced by precipitation (inputs) and evaporation (outputs). For example, if the blue circle in Figure 1 were to be positioned closer to δ*, it is

isotopically “enriched” and is highly influenced by evaporation. Whereas, if the blue circle plotted closer to δ_P , that particular lake would be considered isotopically “depleted” and more influenced by rainfall or snowmelt. Figure 2 provides a schematic illustrating how changes in lake hydrology influence lake water isotope composition.



Terminology Legend

GMWL = Global Meteoric Water Line

LEL = Local Evaporation Line

$\delta^2\text{H}$ = isotope composition of hydrogen

$\delta^{18}\text{O}$ = isotope composition of oxygen

δ_P = Delta P = mean annual isotope composition of precipitation

δ_{LW} = Delta Lake Water = sampled lake water isotope value

δ_{SSL} = Delta Steady State Limiting = isotopic value of lake water where inputs equal outputs

δ^* = Delta Star = isotopic value of the last drop of water in a lake before it dries

Figure 1. Schematic illustrating the potential hydrological processes that influence the isotope composition of lake water (δ_{LW}) within “ $\delta^{18}\text{O}$ - $\delta^2\text{H}$ space”.

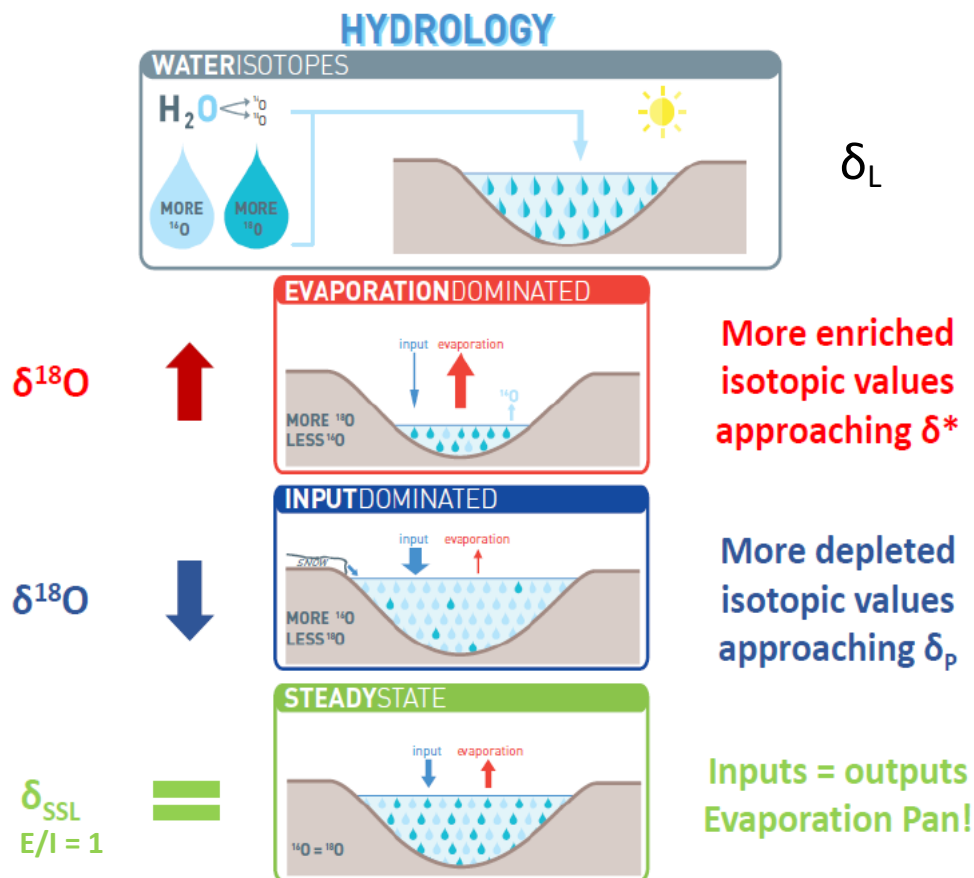


Figure 2. Schematic depicting hydrological processes that influence lake water isotope composition.

3.0 2018 WNP Field Sampling

Sixteen WNP monitoring lakes spanning the three main ecotypes (coastal fen, interior peat plateau-palsa bog, boreal spruce forest) were sampled for water isotope three times during the field season (spring, summer, fall) (Figure 3). A Class-A evaporation pan was also deployed and maintained by Parks Canada staff throughout the ice-free season to simulate the isotopic and hydrological behaviour of a steady-state terminal lake (i.e., closed-basin) where inflow is equal to evaporation (δ_{SSL}). Water within the evaporation pans was maintained at a constant volume on a weekly basis and water samples were collected weekly for isotopic analysis. Additionally, a precipitation bucket was maintained and sampled after significant rainfall events took place. All water samples were collected and stored in 30 ml bottles until analysis at the University of Waterloo

Environmental Isotope Laboratory (UW-EIL). Raw isotope data for lake and evaporation pan water samples can be found in the Appendix.

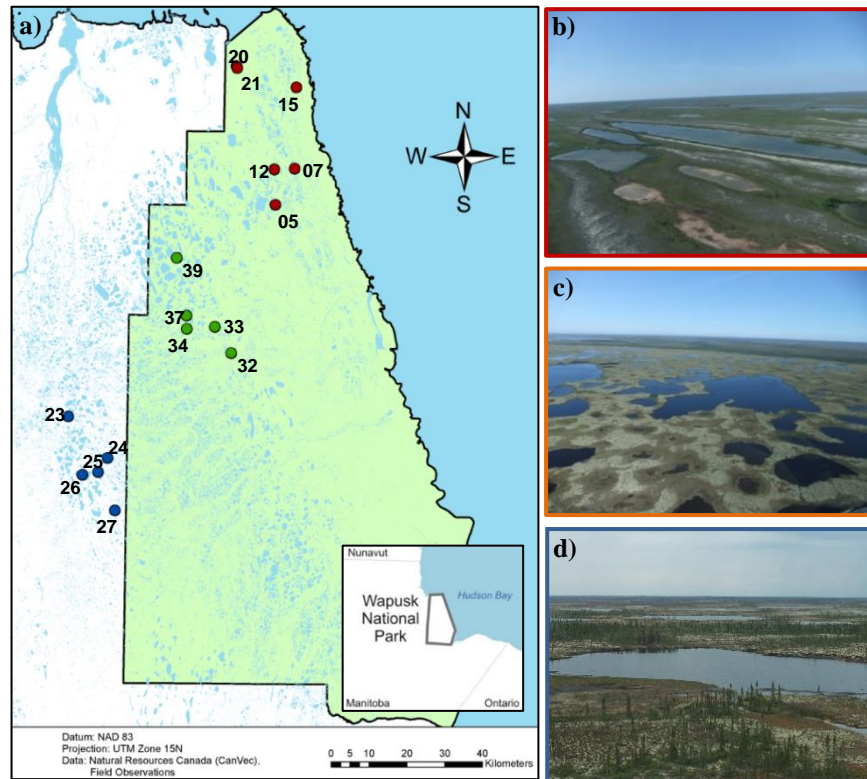


Figure 3. a) Map showing the location of 16 lakes selected for the WNP hydrological monitoring program. Red circles are lakes within the coastal fen ecotype, green circles are lakes within the interior peat plateau-palsa bog ecotype, and blue circles are lakes within the boreal spruce forest ecotype; b) WNP 5 within the coastal fen ecotype; c) WNP 33 within the interior peat plateau-palsa bog ecotype; d) WNP 26 within the boreal spruce forest ecotype.

4.0 Water Isotope Results

4.1 Evaporation Pan Data

As previously mentioned, an evaporation pan was maintained by Parks Canada staff throughout the ice-free season to simulate a steady-state terminal lake (Table A1 for raw data). The weekly sampling of evaporation pan water allows us to see when the pan reaches an isotopic ‘steady-state’ where inflow is equivalent to evaporation. We use these values (see Figure 4) to calculate δ_{SSL} , a critical component of the Local Evaporation Line.

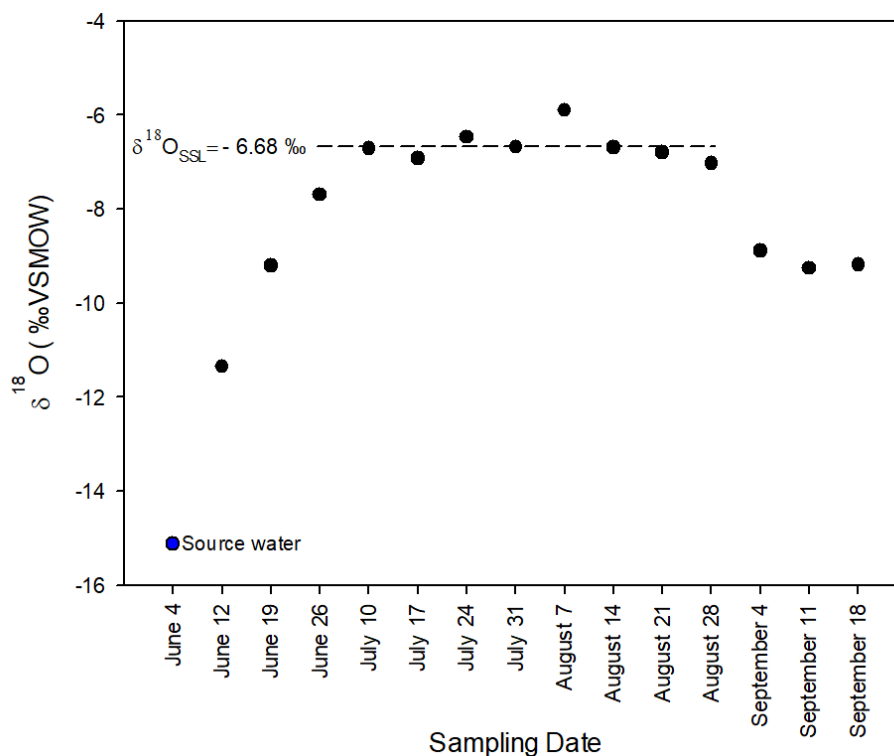


Figure 4. Isotope compositions ($\delta^{18}\text{O}$) of evaporation pan water samples during the 2018 ice-free season. Isotopic ‘steady-state’ was reached by July 10, 2018 and values from July 10 to August 28, 2018 were averaged to generate $\delta^{18}\text{O}_{\text{SSL}}$ values. The same approach was used to estimate $\delta^2\text{H}_{\text{SSL}}$.

4.2 Precipitation Bucket Data

Most precipitation bucket water isotope results fall close to the Global Meteoric Water Line (GMWL) (Figure 5; Table A2). This supports the coupled-isotope tracer method used to calculate E/I ratios (discussed in this report), which uses the GMWL to constrain δ_i (the isotope composition of lake-specific input water; Yi et al., 2008). Some rainfall events show evidence of evaporation, either during descent or prior to sampling (July 19, 24, August 4, 23; Figure 5).

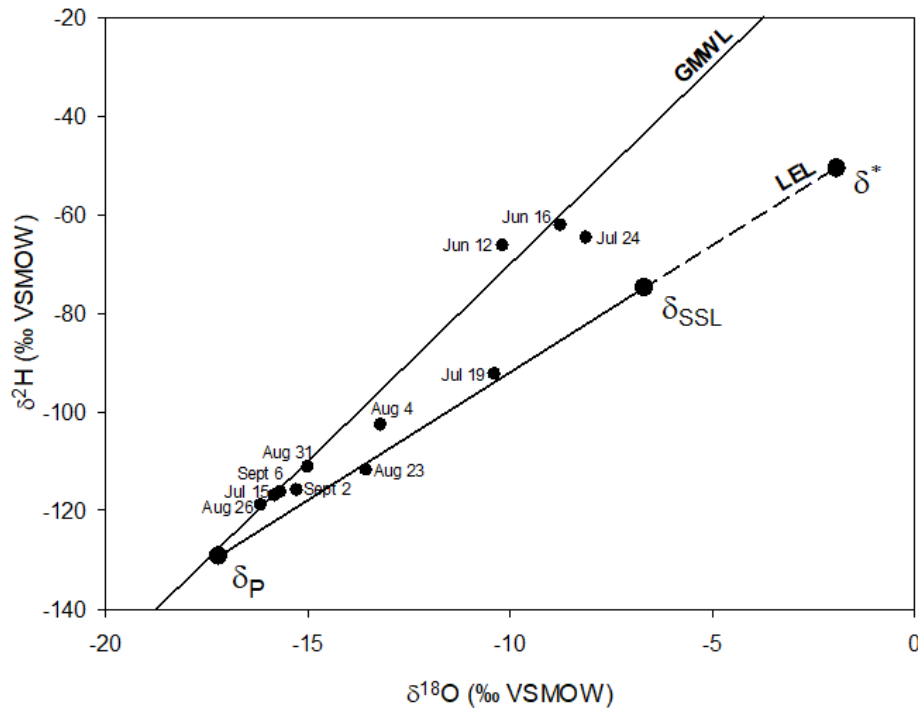


Figure 5. 2018 ice-free season isotope compositions of precipitation bucket samples plotted in “ $\delta^{18}\text{O}$ - $\delta^2\text{H}$ space.”

4.3 Seasonal Variability

Figure 6 contains all 2018 lake water isotope values plotted by season superimposed upon the GMWL and LEL (Table A3 for raw data). While there is large variability between lakes seasonally, there are a few general trends to report. Lakes generally begin the ice-free season more isotopically depleted (e.g., input dominated), plotting closer to δ_P , due to the influence of spring snowmelt. During the summer, the height of evaporative drawdown, isotopic compositions are more isotopically enriched (e.g., evaporation dominated) and plot closer to δ^* . Fall values are between spring and summer compositions due to the influence of late ice-free season rainfall.

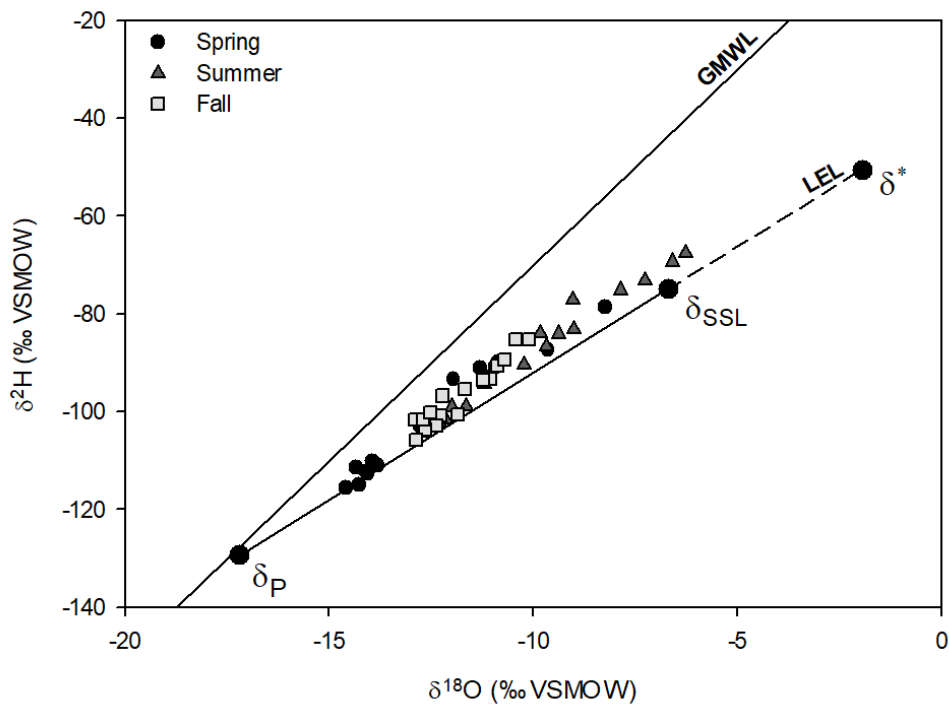


Figure 6. Isotope compositions of WNP ‘Lake Hydrology’ lakes during the 2018 ice-free season.

4.4 Ecotype Variability

Variability exists between ecotypes (coastal fen, interior peat-plateau, and boreal spruce forest) during all three of the sampling periods. Boreal spruce forest lakes are consistently more isotopically depleted and stable, due to the higher amount of snow storage during the winter, thus, higher amounts of snowmelt enter the lakes. Interior peat-plateau and coastal fen lakes are more isotopically-enriched, reflecting a stronger influence of evaporation. Additionally, interior peat plateau palsa bog and coastal fen lakes are on average, more shallow than boreal spruce lakes and thus are more sensitive to small climatic shifts (i.e., precipitation, temperature). However, in the fall, lakes from all three ecotypes group closer together due to late ice-free season precipitation.

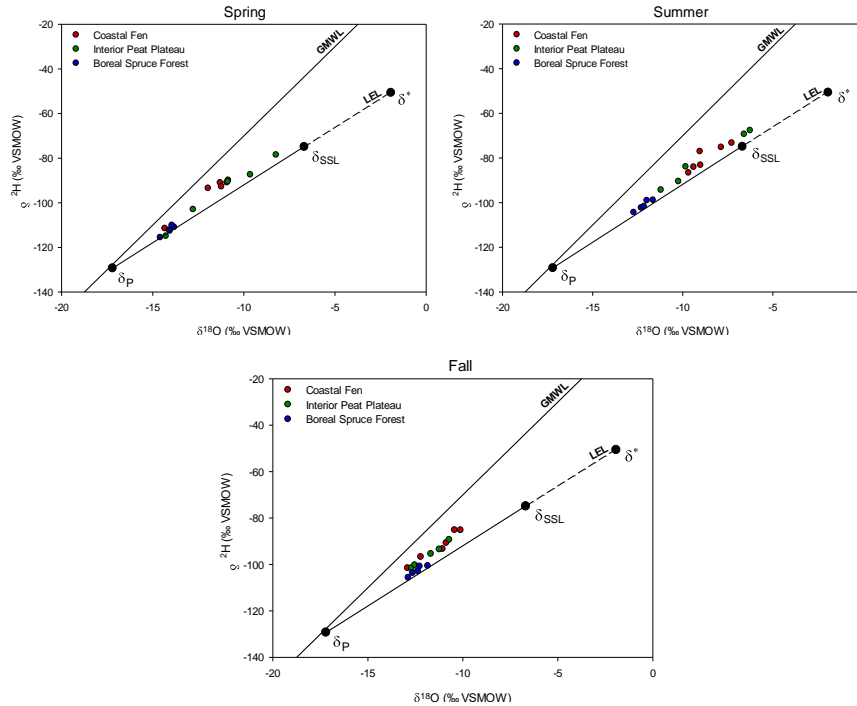


Figure 7. Isotope compositions of WNP ‘Lake Hydrology’ lakes separated by ecotype for each sampling season during the 2018 ice-free season.

5.0 Contextualizing Water Isotope Results

5.1 Evaporation to Inflow Ratios as a Tool for Tracking Lake Hydrology

Evaporation to inflow (E/I) ratios were calculated from lake water isotope compositions using an isotope-mass balance model (Yi et al., 2008; Turner et al., 2010; Table A3). This metric is a quantitative expression of the relative influence of lake-specific input water and evaporation; thus, they are excellent indicators of the hydrological health of each monitoring lake. An E/I value of 1 is equal to the terminal basin steady-state limiting composition (δ_{SSL}) where inflow is equal to evaporation. Therefore E/I ratios greater than 1 provide a clear indication for lakes that have a negative water balance and are experiencing net evaporative drawdown.

Interim hydrological thresholds of E/I ratios were established based on 2010-2012 data, to provide a quantitative representation of hydrological status (see Appendix for 3-year threshold justification; Figure A1, Table A4). Here, a hydrological threshold is defined as a critical value past which a water body faces an increasing risk of evaporative loss. Three states (‘poor’, ‘fair’, and ‘good’) have

been used to define the hydrological thresholds to align with identifying status and trends for Wapusk National Park’s State of the Park reports. “Fair” and “poor” thresholds are statistical representations of the 68th and 95th percentiles on the average, analogous to 1 and 2 standard deviations above the mean for normal data. “Good” thresholds are a description of central tendency, representing ~68% of the data. Separate thresholds are set for the coastal fen, interior peat-plateau, and boreal spruce forest ecotypes and are shown in Table 1. Assessments are based on the most recent year of field data (2018).

Table 1. E/I thresholds for hydrological assessment of WNP lakes.

Lake Category	Season	‘Good’	‘Fair’	‘Poor’
Coastal fen	Spring	< 0.09	0.09 – 0.16	> 0.16
	Summer	< 0.26	0.26 – 0.51	> 0.51
	Fall	< 0.10	0.10 – 0.16	> 0.16
Peat plateau-palsa bog	Spring	< 0.10	0.10 – 0.16	> 0.16
	Summer	< 0.23	0.23 – 0.49	> 0.49
	Fall	< 0.10	0.10 – 0.15	> 0.15
Boreal spruce forest	Spring	< 0.06	0.06 – 0.08	> 0.08
	Summer	< 0.09	0.09 – 0.13	> 0.13
	Fall	< 0.08	0.08 – 0.11	> 0.11

These thresholds were applied to 2018 E/I ratios for each of the three sampled ecotypes (coastal fen, interior peat-plateau palsa bog, boreal spruce forest; Tables 2-4). Overall measure condition is determined as follows:

- If E/I ratios per lake are beneath the green thresholds, the condition is **GOOD**
- If E/I ratios per lake are within the yellow thresholds, the condition is **FAIR**
- If E/I ratios per lake exceeds the red thresholds, the condition is **POOR**

Note that elevated E/I ratios and consequent water-level drawdown is considered to impair aquatic habitats with potential impacts on surrounding terrestrial ecosystems.

Table 2. Hydrological threshold analysis for coastal fen monitoring lakes.

Lake	Spring	Summer	Fall
WAP 05	0.08	0.20	0.09
WAP 07	0.06	0.13	0.09
WAP 12	0.08	0.17	0.05
WAP 15	0.04	0.10	0.07
WAP 20	0.04	0.14	0.09
WAP 21	0.08	0.16	0.05

Table 3. Hydrological threshold analysis for interior peat-plateau palsa bog lakes.

Lake	Spring	Summer	Fall
WAP 32	0.14	0.24	0.06
WAP 33	0.08	0.10	0.09
WAP 34	0.17	0.23	0.09
WAP 37	0.06	0.13	0.06
WAP 39	0.06	0.09	0.07

Table 4. Hydrological threshold analysis for boreal spruce forest lakes.

Lake	Spring	Summer	Fall
WAP 23	0.06	0.10	0.06
WAP 24	0.05	0.08	0.06
WAP 25	0.05	0.09	0.07
WAP 26	0.05	0.08	0.05
WAP 27	0.06	0.09	0.07

Coastal fen lakes are entirely within the ‘good’ category, implying that these lakes were not overly influenced by evaporation. Peat-plateau palsa bog and boreal spruce forest ecotypes had E/I values spanning ‘good’, ‘fair’, and ‘poor’ categories during the spring and summer seasons. However, there is a strong influence of fall precipitation since all of the lakes were in the ‘good’

category at the end of the ice-free season. While winter (October to April) precipitation during the 2017-2018 sampling year was 45.6 mm less than the 1971-2000 climate normals, the ice-free season (May to September) precipitation was similar to climate normals (Table 5). However, an above normal amount of precipitation fell during the month of August (90 mm), prior to the fall sampling period (Table 5). This explains the strong influence of rainfall on all sampling lakes by the end of the ice-free season. Average winter and ice-free season temperatures were comparable to climate normals (Table 5).

Table 5. 2017-2018 meteorological conditions within WNP compared to climate normal (Environment Canada, 2018). A sampling ‘year’ has been defined as October to September in order to capture full winter and summer records. See Appendix Figure A2 for a graphical representation of WNP meteorological conditions.

Month	Mean Air Temperature (°C)	1971-2000 Climate Normals Temperature (°C)	Total Precipitation (mm)	1971-2000 Climate Normals Precipitation (mm)
October	-1.1	-1.7	70.6	46.9
November	-14.9	-12.6	13.4	33.1
December	-23.1	-22.8	11.8	20
January	-25.0	-26.7	2.5	16.9
February	-26.9	-24.6	3.3	15.7
March	-16.1	-19.5	7.3	16.1
April	-10.2	-9.7	13.2	19
May	-1.9	-0.7	13.3	31.9
June	8.5	6.6	37.9	44.3
July	14.5	12	53.9	56
August	12.6	11.7	90	68.3
September	3.9	5.6	58	63.4

5.2 Alignment of Hydrological Threshold Analysis with Wapusk National Parks’ Monitoring Protocol

Two unique ‘measures’ are used for Wapusk National Park’s current long-term hydrological monitoring: coastal (equivalent to the coastal fen ecotype) and wetland (equivalent to the interior peat plateau-palsa bog ecotype). Therefore, for ease in reporting monitoring results, interim threshold values have been recalculated and averaged for the entire field season to create one set of thresholds for the two reported Parks Canada ‘measures’ (Table 6).

Table 6. E/I thresholds for hydrological assessment of coastal and wetland WNP lakes.

Lake Category/ Measure	'Good'	'Fair'	'Poor'
Coastal	< 0.15	0.15 – 0.28	> 0.28
Wetland	< 0.14	0.14 – 0.27	> 0.27

Overall measure condition is determined as follows (Tables 7 and 8):

- If E/I ratios per lake are beneath the green thresholds, the condition is **GOOD; designated as 2**
- If E/I ratios per lake are within the yellow thresholds, the condition is **FAIR; designated as 1**
- If E/I ratios per lake exceeds the red thresholds, the condition is **POOR; designated as 0**

Note that elevated E/I ratios and consequent water-level drawdown is considered to impair aquatic habitats with potential impacts on surrounding terrestrial ecosystems.

5.3 Calculation of 'Lake Hydrology' Scores

A. Coastal

Table 7. Coastal measure condition for 2018 field season.

Lake	E/I	Condition Score
WAP 05	0.12	2
WAP 07	0.09	2
WAP 12	0.10	2
WAP 15	0.10	2
WAP 20	0.09	2
WAP 21	0.10	2

Detailed calculations to quantify lake hydrological health:

Average score for the ‘Lake Hydrology’ measure: 2.0

$((6 \text{ sites} \times 2) + (0 \text{ sites} \times 1) + (0 \text{ sites} \times 0)) / 6 \text{ sites in total}$

Average score scaled 0-100: 100

(Measure average score $\times 50 = 2 \times 50$)

Scaled score: 100 → Good EI (green)

(0-33 = Red (Poor EI); 34-66 = Yellow (Fair EI); 67-100 = Green (Good EI))

In the Coastal Ecosystem EI indicator, lake hydrology displays no significant change based on calculated baseline thresholds and the 2018 field data. Therefore, the Coastal Ecosystem ‘Lake Hydrology’ score is considered to be good (green).

B. Wetland

Table 8. Wetland measure condition for 2018 field season.

Lake	E/I	Condition Score
WAP 32	0.15	1
WAP 33	0.09	2
WAP 34	0.16	1
WAP 37	0.08	2
WAP 39	0.07	2

Detailed calculations to quantify lake hydrological health:

Average score for the ‘Lake Hydrology’ measure: 1.6

$((3 \text{ sites} \times 2) + (2 \text{ sites} \times 1) + (0 \text{ sites} \times 0)) / 5 \text{ sites in total}$

Average score scaled 0-100:

(Measure average score $\times 50 = 1.6 \times 50$)

Scaled score: 80 → Good EI (green)

(0-33 = Red (Poor EI); 34-66 = Yellow (Fair EI); 67-100 = Green (Good EI))

In the Wetland Ecosystem EI indicator, lake hydrology displays no significant change based on calculated baseline thresholds and the 2018 field data. Therefore, the Wetland Ecosystem ‘Lake Hydrology’ score is considered to be good (green).

5.4 Tracking Hydrological Health Over Time

E/I ratios for each lake have been seasonally averaged to generate one E/I value per sampled year. This enables us to see how the hydrological health of a lake has changed over the entire sampling period.

A. Coastal

Over the 9 sampling years, similar trends stand out within the coastal lake measure. From 2010 to 2013, coastal lakes had generally higher E/I ratios with values ranging between the ‘fair’ and ‘poor’ categories. However, from 2014 to present most E/I ratios are within the ‘good’ category.

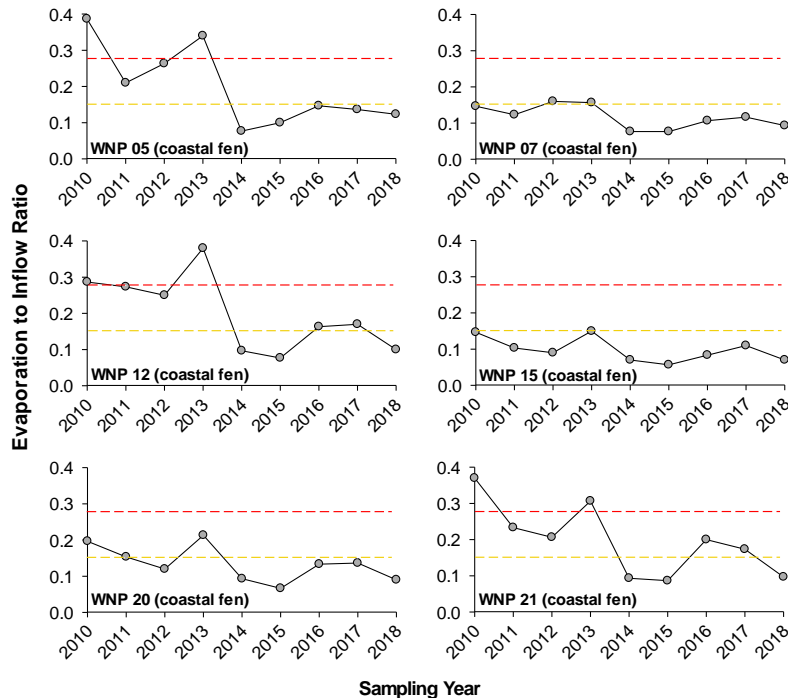


Figure 8. Averaged E/I ratios from 2010 to 2018 for lakes within the coastal measure. Dashed lines delineate thresholds; lake E/I values that fall below the yellow dashed line are categorized as ‘good’, lake E/I values between the yellow and red dashed lines are categorized as ‘fair’, and lake E/I values above the red dashed line are categorized as ‘poor’.

B. Wetland

WAP 32 and 34 have trends similar to the coastal measure lakes, with values falling within mainly 'fair' to 'poor' categories between 2010 and 2013 and values within the 'good' to 'fair' categories from 2014 to the present. WAP 33, 37, and 39 have very consistent E/I ratio values showing that these lakes have more resilience to annual variability in changing meteorological conditions.

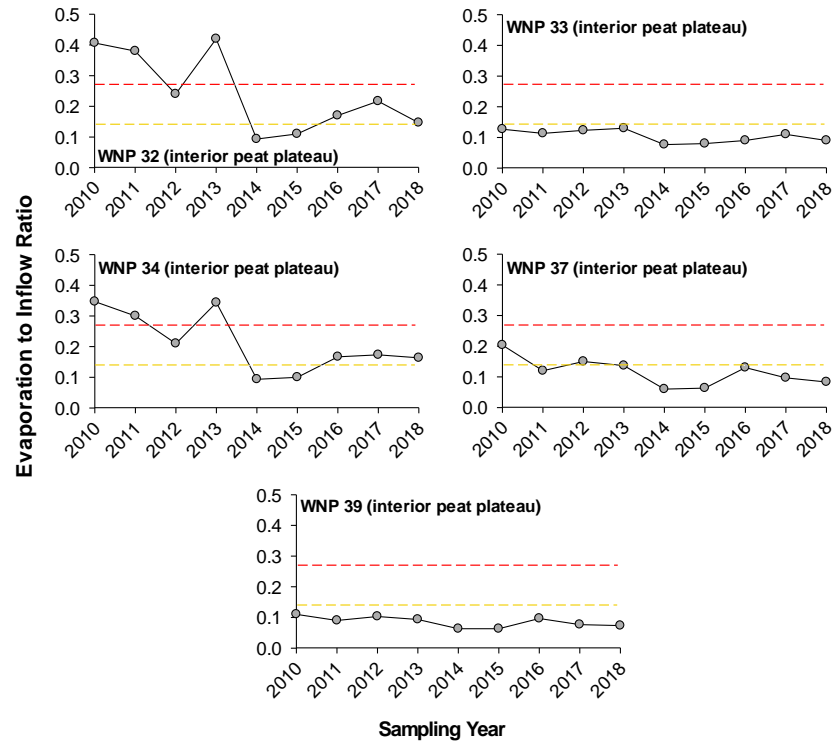


Figure 9. Averaged E/I ratios from 2010 to 2018 for lakes within the wetland measure. Dashed lines delineate thresholds; lake E/I values that fall below the yellow dashed line are categorized as 'good', lake E/I values between the yellow and red dashed lines are categorized as 'fair', and lake E/I values above the red dashed line are categorized as 'poor'.

6.0 Appendix

Evaporation Pan, Precipitation Bucket, and Lake Water Isotope Results

Table A1. Evaporation Pan Water Isotope Compositions from 2018 ice-free season. Blue shading represents interval used to determine δ_{SSL} (-6.68, -74.90 ‰).

Date Sampled	$\delta^{18}\text{O}$ (‰)	$\delta^2\text{H}$ (‰)
June 12, 2018	-11.35	-101.14
June 19, 2018	-9.21	-101.17
June 26, 2018	-7.69	-85.96
July 10, 2018	-6.71	-78.64
July 17, 2018	-6.92	-76.90
July 24, 2018	-6.47	-74.94
July 31, 2018	-5.90	-69.77
August 7, 2018	-6.91	-74.61
August 14, 2018	-6.69	-73.17
August 21, 2018	-6.80	-74.23
August 28, 2018	-7.03	-76.98
September 4, 2018	-8.89	-90.82
September 11, 2018	-9.26	-97.34
September 18, 2018	-9.18	-97.97
Averaged value for δ_{SSL}	-6.68	-74.90

Table A2. Precipitation (rainfall) Bucket Water Isotope Compositions from 2018 ice-free season.

Date Sampled	$\delta^{18}\text{O}$	$\delta^2\text{H}$
June 12, 2018	-10.18	-66.36
June 16, 2018	-8.75	-62.21
July 15, 2018	-15.81	-117.01
July 19, 2018	-10.38	-92.37
July 24, 2018	-8.11	-64.71
August 4, 2018	-13.20	-102.73
August 23, 2018	-13.56	-111.84
August 26, 2018	-16.16	-118.99
August 31, 2018	-15.00	-111.25
September 2, 2018	-15.27	-115.95
September 6, 2018	-15.67	-116.32

Table A3. 2018 Lake Water Isotope Compositions and E/I Ratios.

	Spring			Summer			Fall		
Lake	$\delta^{18}\text{O}$	$\delta^2\text{H}$	E/I	$\delta^{18}\text{O}$	$\delta^2\text{H}$	E/I	$\delta^{18}\text{O}$	$\delta^2\text{H}$	E/I
WAP 05	-10.86	-89.85	0.08	-7.27	-73.25	0.20	-10.88	-90.73	0.09
WAP 07	-11.30	-91.00	0.06	-9.39	-84.07	0.13	-10.11	-85.21	0.09
WAP 12	-11.23	-92.79	0.08	-7.86	-75.15	0.17	-12.21	-96.76	0.05
WAP 15	-11.96	-93.45	0.04	-9.04	-77.09	0.10	-10.43	-85.17	0.07
WAP 20	-14.34	-111.47	0.04	-9.67	-86.65	0.14	-11.07	-93.33	0.09
WAP 21	-10.93	-90.93	0.08	-9.01	-83.22	0.16	-12.90	-101.56	0.05
WAP 23	-13.82	-110.94	0.06	-11.65	-98.91	0.10	-11.84	-100.59	0.06
WAP 24	-13.95	-110.09	0.05	-11.99	-99.06	0.08	-12.27	-100.81	0.06
WAP 25	-14.10	-112.20	0.05	-12.31	-102.33	0.09	-12.36	-102.89	0.07
WAP 26	-14.59	-115.53	0.05	-12.72	-104.40	0.08	-12.64	-103.70	0.05
WAP 27	-14.06	-112.61	0.06	-12.15	-101.69	0.09	-12.87	-105.70	0.07
WAP 32	-9.64	-87.37	0.14	-6.26	-67.63	0.24	-12.70	-101.56	0.06
WAP 33	-10.88	-90.54	0.08	-9.83	-83.92	0.10	-10.71	-89.34	0.09
WAP 34	-8.23	-78.52	0.17	-6.59	-69.32	0.23	-11.23	-93.51	0.09
WAP 37	-14.28	-114.92	0.06	-10.23	-90.50	0.13	-12.53	-100.30	0.06
WAP 39	-12.78	-102.97	0.06	-11.21	-94.34	0.09	-11.68	-95.45	0.07

Three Year Hydrological Threshold Development

For this report, hydrological thresholds are based on E/I ratios from 2010-2012. In the past, a 5-year baseline (2010-2014) was used as an arbitrary choice that covered 5 years of data, half of the typical Parks Canada minimum 10-year baseline, with the idea that once 10 years of data had been collected a new baseline would be calculated. However, further statistical analysis (bootstrapping) concluded that generating thresholds only using the first three years of data is comparable to using the entire data set (Figure A1). The 5-year baseline (2010-2014) E/I threshold values (Table A1) are identical to the 3-year baseline (2010-2012) to two decimal points.

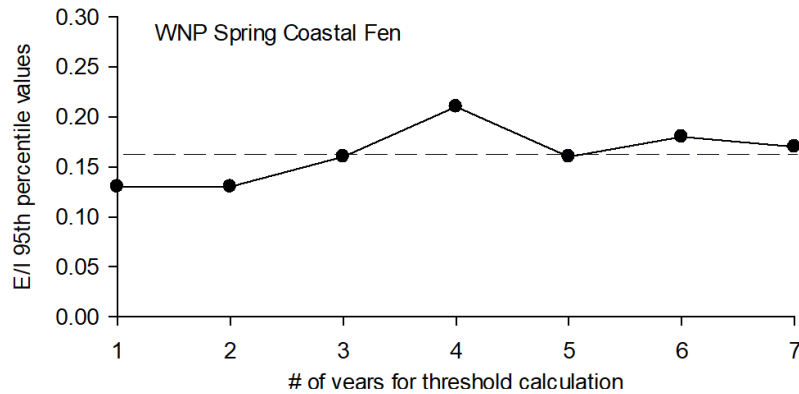


Figure A1. Example of 3-year threshold calculations used for this research as an accurate representation of WNP data. Threshold calculations based on 1 to 7 years of data for spring samples of coastal fen lakes in WNP. Dashed line represents the mean threshold value (mean E/I = 0.1628).

Table A4. 5-year threshold values based on 2010-2014 E/I ratios.

<u>Lake Category</u>	Season	Good	Fair (1σ)	Poor (2σ)
Coastal Fen	Spring	<0.09	0.09-0.16	>0.16
	Summer	<0.26	0.26-0.51	>0.51
	Fall	<0.10	0.10-0.16	>0.16
Interior Peat-Plateau	Spring	<0.10	0.10-0.16	>0.16
	Summer	<0.23	0.23-0.49	>0.49
	Fall	<0.10	0.10-0.15	>0.15
Boreal Spruce Forest	Spring	<0.06	0.06-0.08	>0.08
	Summer	<0.09	0.09-0.13	>0.13
	Fall	<0.08	0.08-0.11	>0.11

Compiled meteorological data from 2009 to 2018

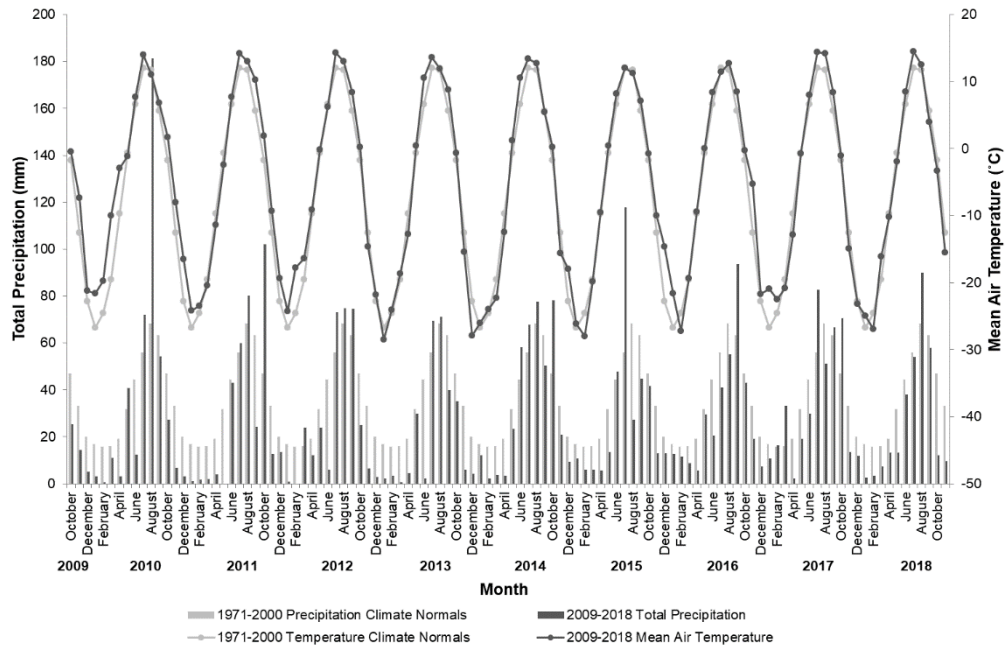


Figure A2. WNP meteorological data from 2009-2018 compared to climate normals.

7.0 References

Anderson, L., Birks, J., Rover, J., and Guldager, N. 2013. Controls on recent Alaskan lake changes identified from water isotopes and remote sensing. *Geophys. Res. Lett.* 40(13): 3413–3418. doi: 10.1002/grl.50672.

Bouchard, F., Turner, K.W., MacDonald, L.A., Deakin, C., White, H., Farquharson, N., Medeiros, A.S., Wolfe, B.B., Hall, R.I., Pienitz, R., and Edwards, T.W.D. 2013. Vulnerability of shallow subarctic lakes to evaporate and desiccate when snowmelt runoff is low. *Geophysical Research Letters*, 40: 6112-6117.

Brock, B.E., Wolfe, B.B., Edwards, T.W.D. 2007. Characterizing the hydrology of shallow floodplain lakes in the Slave River Delta, NWT, Canada, using water isotope tracers. *Arctic and Alpine Research*, 39: 388-401.

Brooks, J.R., Gibson, J.J., Birks, S.J., Weber, M.H., Rodecap, K.D., and Stoddard, J.L. 2014. Stable isotope estimates of evaporation: inflow and water residence time for lakes across the United States as a tool for national lake water quality assessments. *Limnol. Oceanogr.* 59(6): 2150–2165. doi: 10.4319/lo.2014.59.6.2150.

Clark, I. and Fritz, P. 1997. *Environmental Isotopes in Hydrogeology*. 1-77, Lewis Publishers. New York

Edwards, T.W.D., Wolfe, B.B., Gibson, J.J., and Hammarlund, D. 2004. Use of water isotope tracers in high latitude hydrology and paleohydrology. In *Long-Term Environmental Change in Arctic and Antarctic Lakes*, Pienitz R, Douglas MSV, and Smol, JP (eds). Springer: Dordrecht, The Netherlands; 187-207.

Environment Canada, 2017. National Climate Data and Information Archive. <http://climate.weatheroffice.gc.ca/Welcome_e.html>

Gibson, J.J. and Edwards, T.W.D. 2002. Regional water balance trends and evaporation-transpiration partitioning from a stable isotope survey of lakes in northern Canada. *Global Biogeochemical Cycles*, 16, 10-28.

Hochheim, K., Barber, D.G., and Lukovich, J.V. 2010. Changing sea ice conditions in Hudson Bay, 1980-2005. In Ferguson, S.H., Loseto, L.L., and Mallory, M.L. (eds.), *A Little Less Arctic: Top Predators in the World's Largest Inland Sea, Hudson Bay*. Dordrecht: Springer, 39-52.

- Jones, B. M., Grosse, G., Arp, C. D., Jones, M. C., Walter Anthony, K. M., and Romanovsky, V. E., 2011: Modern thermokarst lake dynamics in the continuous permafrost zone, northern Seward Peninsula, Alaska. *Journal of Geophysical Research*, 116: G00M03, <http://dx.doi.org/10.1029/2011JG001666>.
- Kaufman, D.S., Schneider, D.P., McKay, N.P., Ammann, C.M., Bradley, R.S., Briffa, K.R., Miller, G.H., Otto-Bliesner, B.L., Overpeck, J.T., Vinther, B.M. and Arctic Lakes 2k Project Members. 2009. Recent warming reverses long-term Arctic cooling. *Science*, 325: 1236-1239.
- Labrecque, S., Lacelle, D., Duguay, C., Lauriol, B., Hawkings, J. 2009. Contemporary (1951-2001) evolution of lakes in the Old Crow Basin, northern Yukon, Canada: Remote sensing, numerical modeling and stable isotope analysis. *Arctic*, 62, 225-238.
- MacDonald, L.A., Wolfe, B.B., Turner, K.W., Anderson, L., Arp, C.D., Birks, S.J., Bouchard, F., Edwards, T.W.D., Farquharson, N., Hall, R.I., McDonald, I., Narancic, B., Ouimet, C., Pienitz, R., Tondou, J., White, H. 2017. A synthesis of thermokarst lake water balance in high-latitude regions of North America from isotope tracers. *Arctic Science* 3: 118-149.
- Marsh, P., Russell, M., Pohl, S., Haywood, H., and Onclin, C., 2009: Changes in thaw lake drainage in the Western Canadian Arctic from 1950 to 2000. *Hydrological Processes*, 23(1): 145–158.
- Parks Canada Agency, 2011. State of the Park Report 2011: Wapusk National Park of Canada. Ottawa: Parks Canada Agency, 41 pp.
- Prowse, T.D., Wrona, F.J., Reist, J.D., Gibson, J.J., Hobbie, J.E., Lévesque, L.M.J., Vincent, W.F. 2006. Climate change effects on hydroecology of Arctic freshwater ecosystems. *Ambio*, 35: 347-358.
- Remmer, C.R., Klemm, W.H., Wolfe, B.B., and Hall, R.I. 2018. Inconsequential effects on flooding in 2014 on lakes in the Peace-Athabasca Delta (Canada) due to long term drying. *Limnology and Oceanography*, 63: 1502-1518.
- Schindler, D.W. and Smol, J.P. 2006. Cumulative effects of climate warming and other human activities on freshwaters of Arctic and subarctic North America. *Ambio*, 35, 160-168.
- Smith, S.L. and Burgess, M.M. 2004. Sensitivity of permafrost to climate warming in Canada. Geological Survey of Canada. Bulletin 579

Smol, J. P., A. P. Wolfe, H. J. B. Birks, M. S. V. Douglas, V. J. Jones, and A. Korhola, et al. 2005. Climate-driven regime shifts in the biological communities of arctic lakes. *Proc. Natl Acad. Sci.* 102:4397–4402.

Tondu JME, Turner KW, Wolfe BB, Hall RI, Edwards TWD, McDonald I. 2013. Using water isotope tracers to develop the hydrological component of a long-term aquatic ecosystem monitoring program for a northern lake-rich landscape. *Arct. Antarct. Alp. Res* 45(4): 594-614.

Turner, K.W., Wolfe, B.B., Edwards, T.W.D., 2010. Characterizing the role of hydrological processes on lake water balances in the Old Crow Flats, Yukon Territory, Canada, using water isotope tracers. *Journal of Hydrology*, 386: 103-117.

Wolfe, B.B., Karst-Riddoch, T.L., Hall, R.I., Edwards, T.W.D., English, M.C., Palmini, R., McGowan, S., and Vardy, S.R., 2007. Classification of hydrologic regimes of northern floodplain basins (Peace-Athabasca Delta, Canada) from analysis of stable isotopes ($d^{18}O$, d^2H) and water chemistry. *Hydrological Processes*. 21, 151–168.

Yi, Y., Brock, B.E., Falcone, M.D., Wolfe, B.B., Edwards, T.W.D. 2008. A coupled isotope tracer method to characterize input water to lakes. *Journal of Hydrology*, 350: 1-13.

4.C. 2017 Goose Aquatic Impact Report

2017 Wapusk National Park Goose Aquatic Impacts Report

Hilary White & Brent Wolfe

Department of Geography and Environmental Studies
Wilfrid Laurier University
April 24, 2018



Table of Contents

1.0 Introduction	166
2.0 2017 WNP Field Sampling	167
3.0 Goose Aquatic Impact Results	168
3.1 Assessing Catchment Erosion	168
3.11 LSG Aquatic Impact Measure Condition Assessment	169
3.2 Other Water Quality Indicators	172
3.21 Pond Water Nutrients and Productivity	172
3.22 Pond Water Carbon Behaviour and Productivity	175
4.0 Conclusions	176
5.0 Appendix	177
6.0 References	178

List of Figures

Figure 1: Examples of Lesser Snow Goose disturbance on the landscape	166
Figure 2: LSG Aquatic Impact Monitoring Field Sites	167
Figure 3: Schematic depicting pond conductivity variability in response to LSG disturbance	168
Figure 4: 2017 conductivity values	169
Figure 5: Box plots depicting data for 2017 limnological parameters	173
Figure 6: Schematic showing nutrient (TKN, TP) responses to LSG disturbance	174
Figure 7: 2017 TP and TKN values	174
Figure 8: Schematic showing carbon isotopic composition of dissolved organic carbon in response to LSG disturbance	175

List of Tables

Table 1: Condition thresholds for LSG Aquatic Impact measure	170
Table 2: July 2017 field observation, conductivity results, and condition designation	171
Table A1: Complete Goose Aquatic Impact data	177

1.0 Introduction

Wapusk National Park (WNP) contains over 10,000 shallow, mainly thermokarst lakes and ponds, hereafter referred to as ponds, which provide important habitat for wildlife (Parks Canada, 2011). During the past ~50 years, coastal regions of WNP have witnessed rapid increases (5-7% per year) in the population density and nesting area range of Lesser Snow Goose (LSG) (Batt et al., 1997; Jefferies et al., 2006). This has raised concerns and uncertainty regarding the degree of disturbance on the abundant shallow ponds and the adjacent vegetation and habitat (Handa et al., 2002; Jefferies and Rockwell, 2002; Jefferies et al., 2006; MacDonald et al., 2015). As the LSG population expands farther inland, their activities (i.e., grubbing, nesting, and defecating) have been identified within both the coastal fen and interior peat plateau-palsa bog ecotypes of WNP. Additionally, this region has experienced some of the greatest warming in the circumpolar North during the past ~50 years and is considered one of the most sensitive regions in northern Canada to permafrost thaw (Smith and Burgess, 2004; Kaufman et al., 2009; Hochheim et al., 2010). Therefore, the influence of LSG population growth has the potential to be exacerbated by increased evaporation due to longer ice-free seasons and alterations in seasonal precipitation. Parks Canada (2011) acknowledged that the combination of expanding LSG population and climate warming could, potentially, drastically alter the ecological integrity of ponds in WNP.

Ongoing studies have identified varying LSG disturbance levels in the Park, spanning from low disturbance, to active disturbance, to severe disturbance (White et al., unpublished; Figure 1). Additionally, a suite of limnological (*meaning of or related to inland waters*) variables (e.g., conductivity, carbon isotope composition of dissolved inorganic carbon, carbon and nitrogen isotope compositions of particulate organic matter) have been identified to be sensitive to catchment disturbance by LSG (MacDonald et al., 2014; 2015). These variables will be explained in Section 2.

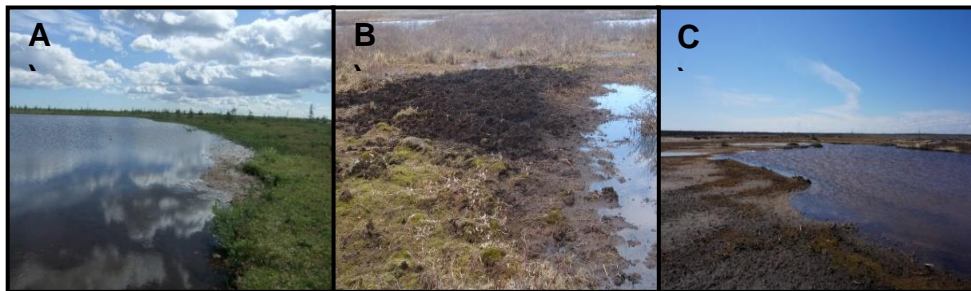


Figure 1 Examples of a **A)** low disturbance, **B)** active disturbance with grubbing, and **C)** severe disturbance showing an absence of catchment vegetation.

To address concerns regarding LSG disturbance to aquatic ecosystems of WNP, a monitoring program was established in 2016 with the following objective: ***to determine the effects of LSG disturbance on ponds by comparing limnological conditions among ponds of different disturbance levels over seasonal and yearly timescales.*** Results are separated into two sections: ¹assessing pond catchment erosion including the LSG Aquatic Impact Measure Condition Assessment, and ²the reporting of other pond water quality indicators including nutrient cycling, pond productivity, and pond carbon behaviour. These will be described in detail in section 3.0.

2.0 2017 WNP Field Sampling

During late July 2017, 30 ponds were sampled across the north-eastern portion of Wapusk National Park (Figure 2). These ponds were initially selected and sampled in July 2015 to cover a representative portion of WNP containing the different levels of goose disturbance (low, active, and severe; Figure 1). In situ measurements included conductivity and water temperature. Surface water samples were collected and analyzed for nutrients and the carbon isotope composition of dissolved inorganic carbon and particulate organic matter. Additionally, spatial analysis of datasets have been utilized to map gradients and to identify 'hotspots' of disturbance.

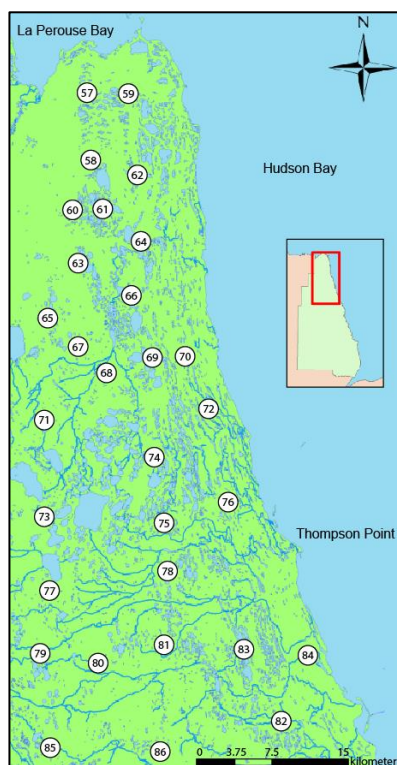


Figure 2 2017 LSG Aquatic Impact Monitoring Field Sites.

3.0 Goose Aquatic Impacts Results

3.1 Assessing Catchment Erosion

Conductivity is utilized in order to determine the extent and effects of catchment erosion on the ponds of WNP. Conductivity is water's ability to conduct electrical current and it represents the amount of dissolved substances in water (i.e., salts, chlorides, etc.). Conductivity can be influenced by ¹the surrounding geology and the composition of the underlying rocks, ²the climate (warmer temperatures and/or decreases in rainfall can lead to more evaporation and an increase in the conductivity of a particular water body), ³biological influences (i.e., LSG defecation and grubbing which decreases soil compaction by root removal), as well as ⁴proximity to a salt water body (i.e., Hudson Bay) and the potential input of sea spray. Within WNP, substantially higher values of conductivity may indicate proximity to the Hudson Bay (specifically coastal WNP) or increased erosional inputs from both LSG disturbance and climate warming (Figure 3).

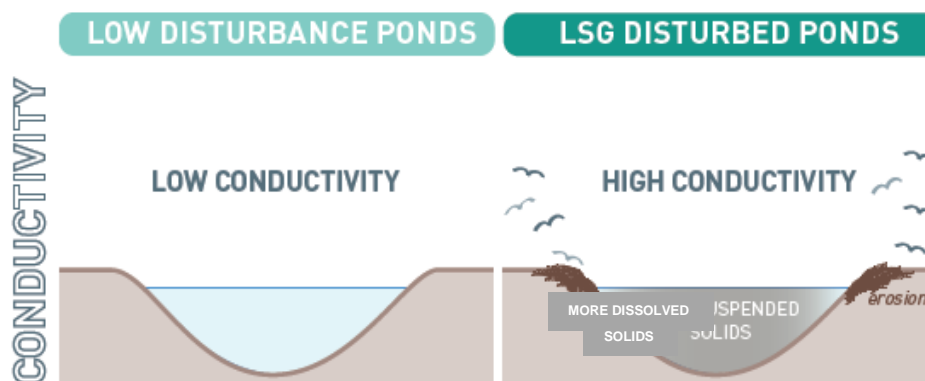


Figure 3 Schematic depicting the difference in pond conductivity resulting from catchment erosion.

Conductivity values have been spatially interpolated to identify potential hotspots in catchment erosion. Results in Figure 4 display values ranging from high (red) to low (blue). Two unique zones of higher conductivity values within the study area have been identified and are attributed to LSG disturbance. These “hotspots” are located within ¹the northern region by La Perouse Bay and ²along the eastern coast near Thompson Point. These two areas represent locations of the most extreme effects of LSG on catchment erosion. The La Perouse Bay area represents the LSG's initial nesting location in the area and the region along

the coast north of Thompson Point represents the LSG short-stop location in 2001. These high conductivity levels are unlikely related to sea spray from Hudson Bay, since higher conductivity values would be expected all along the coast.

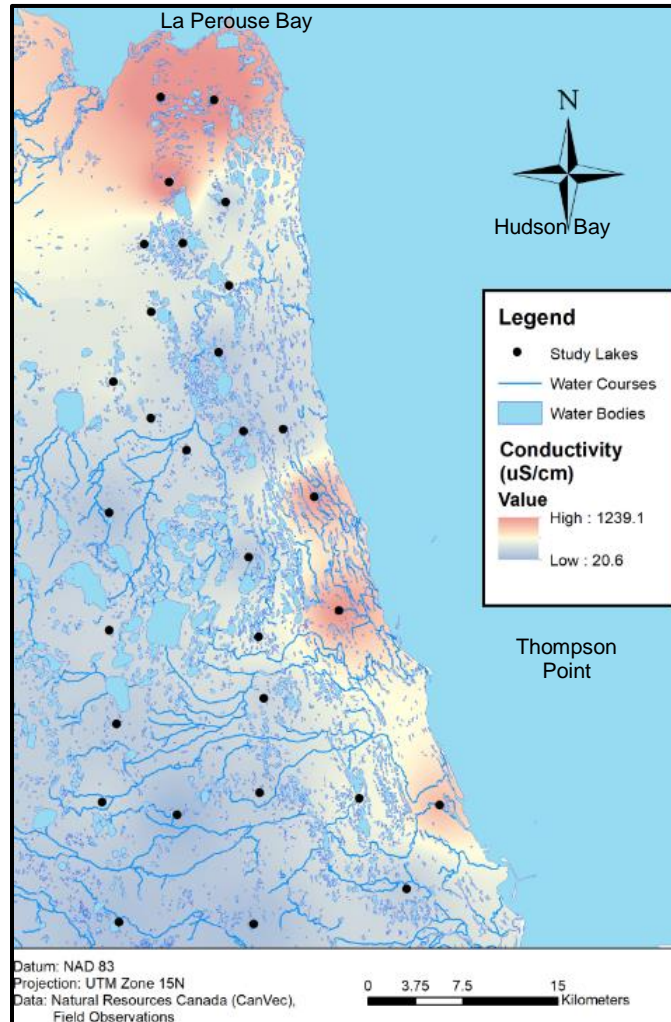


Figure 4 2017 conductivity values.

3.11 LSG Aquatic Impact Measure Condition Assessment

The preliminary assessment for the impact of LSG populations on WNP coastal ponds is based on two variables: visual LSG disturbance in pond catchments and pond water conductivity. Separate thresholds are set for each variable, resulting in two thresholds. Interim condition thresholds are shown in Table 1.

Table 1 Condition thresholds for LSG Aquatic Impact Measure.

Variables	Good	Fair	Poor
Visual LSG disturbance	2	1	0
Conductivity ($\mu\text{S/cm}$)	<500	500-3000	>3000

Visual LSG disturbance thresholds have been determined based on 2015 and 2016 field notes using a 0-2 scale. Ponds with a value of 2 represent ponds with no obvious LSG disturbance in the catchment (i.e., little to no goose presence, feces). Ponds with a value of 1 represent ponds with some LSG disturbance in the catchment (i.e., goose presence, some feces, little to no grubbing). Ponds with a value of 0 represent ponds with large amounts of LSG disturbance in the catchment (i.e., substantial goose presence, abundant goose feces, obvious grubbing).

Conductivity thresholds were determined using three years of field data (2014-2016) from 15 ponds spanning a gradient of LSG disturbance (undisturbed, actively disturbed, severely disturbed) within the coastal region of the Park. Three statistically distinct groups were established within the conductivity data using breakpoint analysis.

Preliminary baseline condition thresholds will be updated once more years of data have been collected. While these thresholds have been developed using only 3 years of data, the results of the assessment support the presence of a definitive gradient of LSG disturbance in WNP ponds. Assessments are applied to 30 ponds sampled in July 2017 (Table 2).

Overall pond condition is determined as follows:

- If both variables per pond are beneath the green thresholds, the condition is **GOOD; designated as 2**.
- If both variables per pond are within the yellow thresholds, the condition is **FAIR; designated as 1**.
- If both variables per pond exceed the red thresholds, the condition is **POOR; designated as 0**.
- If different thresholds are determined for an individual pond, the condition is designated as the **worse** condition.

Note that elevated conductivity values indicate increased erosional inputs from LSG disturbance, which can impair aquatic ecosystems.

Table 2 July 2017 field observation, conductivity results and condition designation

Pond	Visual LSG Disturbance	Conductivity (µS/cm)	Condition
WAP 57	1	1163	1
WAP 58	0	1202	0
WAP 59	0	1239	0
WAP 60	2	406	2
WAP 61	2	235	2
WAP 62	2	260	2
WAP 63	2	408	2
WAP 64	2	433	2
WAP 65	1	427	1
WAP 66	2	146	2
WAP 67	2	306	2
WAP 68	2	274	2
WAP 69	2	136	2
WAP 70	2	234	2
WAP 71	2	123	2
WAP 72	0	1002	0
WAP 73	2	273	2
WAP 74	2	172	2
WAP 75	2	463	2
WAP 76	0	1044	0
WAP 77	2	175	2
WAP 78	2	251	2
WAP 79	2	260	2
WAP 80	2	21	2
WAP 81	2	188	2
WAP 82	2	201	2
WAP 83	1	481	1
WAP 84	0	840	0
WAP 85	2	87	2
WAP 86	2	73	2

The 2017 LSG aquatic impact measure condition assessment categorized WAP 57, 65 and 83 in **FAIR** condition, WAP 58, 59, 72, 76 and 84 in **POOR** condition, and the remaining WAP ponds (WAP 60-64, 66-71, 73-75, 77-82, and 85-86) in **GOOD** condition.

3.2 Other Pond Water Quality Indicators

All limnological parameters have been separated by the three LSG aquatic impact measure conditions (good, fair, poor) and displayed using boxplots (Figure 5). Limnological parameters show differences associated with pond condition, as defined by Table 2 and except for TKN, there is a significant difference between ponds within the 'good' and 'poor' conditions for rest of the limnological parameters (p -values = < 0.05 ; Figure 5). Conductivity values range between 21 and 1239 $\mu\text{S}/\text{cm}$ with lower conductivity values corresponding to 'good' pond condition and higher conductivity values corresponding to 'fair' and 'poor' pond conditions (Figure 5a).

3.2.1 Pond Water Nutrients and Productivity

Nutrients are essential for the functioning of aquatic ecosystems, similar to humans. We focus on two specific nutrient cycles within the aquatic ecosystems of WNP: nitrogen and phosphorus. Nitrogen and phosphorus are nutrients essential for plant and algal growth and can be tracked by measuring Total Kjeldahl Nitrogen (TKN) and Total Phosphorus (TP). Typically, nutrient levels increase during mid-July, corresponding to the height of pond productivity. However, previous work in Wapusk National Park has found a variety of responses to nutrient levels due to LSG disturbance. During mid-summer (July), higher and lower nutrient values as compared to low disturbance ponds were observed (MacDonald et al., 2014, 2015; Figure 6). Additionally, pH can be used as an indicator of pond productivity and degree of inputs from the catchment. MacDonald et al. (2014, 2015) found that elevated pH values indicate increased productivity due to active LSG disturbance.

Due to financial constraints for a long-term monitoring program within WNP, all 30 ponds cannot be sampled three times during the ice-free season. By sampling in July only, we still capture a snapshot of nutrient variability. TP and pH values within the 'poor' pond condition are significantly higher than the ponds within 'good' and 'fair' conditions (Figure 5b and c). TKN, however, shows no significant difference between all three aquatic impact measure conditions potentially due to rapid consumption by aquatic productivity (Figure 5d). Elevated TP and pH values could be an indication of increased productivity due to LSG disturbance. It should also be noted that several ponds within the 'good' condition show elevated pH, TP, and TKN values, within the range of the 'poor' condition (Figure 5b, d, and d). This could be a first indication of LSG disturbance within those ponds; continued monitoring of these ponds will be able to substantiate or refute this hypothesis.

To visually see variability, TP and TKN nutrient values have been plotted spatially with data ranging from high (red) to low (blue) values (Figure 7). Three

areas of high nutrient levels or “hotspots” can be identified; ¹the northern region by La Perouse Bay, ²along the eastern coast near Thompson Point, and ³the southern inland portion of the sampling area. The La Perouse Bay region has sustained the longest and most intense impact from LSG presence and the coastal region near Thompson Point was the location of a LSG short-stop in 2001. Both areas have been identified as regions of extensive LSG nesting and disturbance. Therefore, there is a correlation between LSG disturbance and high nutrient levels where higher/longer influence from the LSG can be characterized by higher nutrient levels in 2016. The third location of higher nutrient levels, in the southern inland portion of the sampling area associated with ponds that fall within the ‘good’ condition, may have higher nutrients due to the early evidence of LSG disturbance.

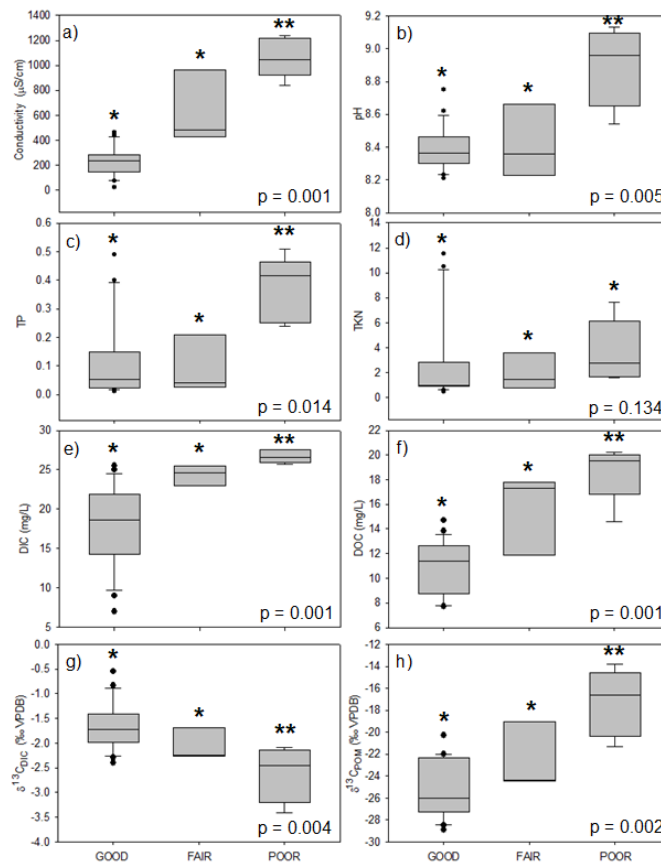


Figure 5 Box plots depicting data for 2017 limnological parameters; a) conductivity, b) pH, c) total phosphorus (TP), d) total nitrogen (TKN), e) dissolved inorganic carbon (DIC), f) dissolved organic carbon (DOC), g) carbon isotope composition of dissolved inorganic carbon ($\delta^{13}\text{C}_{\text{DIC}}$), and h) carbon isotope composition of particulate organic matter ($\delta^{13}\text{C}_{\text{POM}}$). Each plot contains data from all three aquatic impact measure conditions; GOOD (n=22), FAIR (n=3), and POOR (n=5). The boxes identify the 25th percentile, median value, and 75th percentiles, the whisker bars represent the 10th and 90th percentiles, the solid black circles represent outliers. Asterisks (*) represent groups that are significantly different from one another.

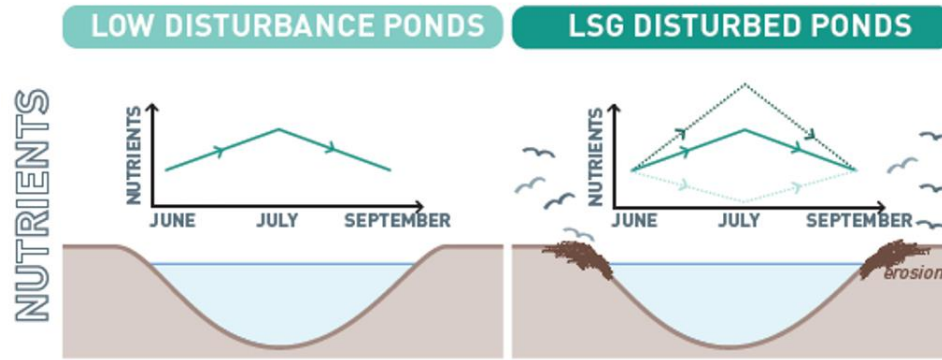


Figure 6 Schematic showing the difference in nutrient (TKN, TP) responses to LSG disturbance.

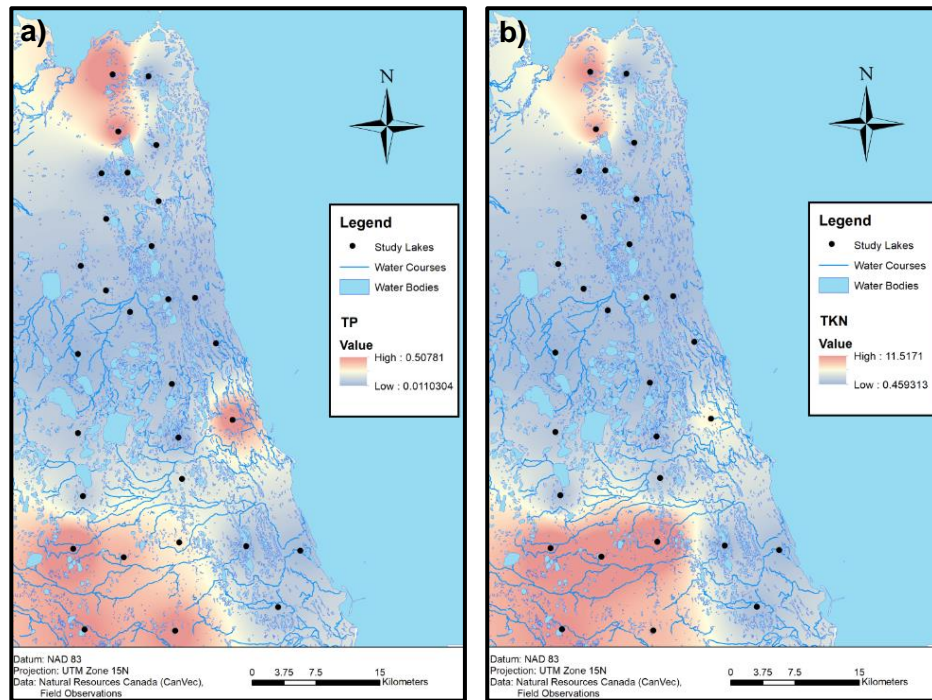


Figure 7 a) 2017 TP values. b) 2017 TKN values.

3.22 Pond Water Carbon Behaviour and Productivity

Carbon is a nutrient that is necessary for plant and algal growth within an aquatic ecosystem and can be influenced by a variety of processes such as catchment erosion and runoff as well as productivity (referring to the rate of generation of biomass in an ecosystem). We can track carbon as it is cycled through the aquatic system by examining the dissolved inorganic carbon (DIC) concentration, the dissolved organic carbon (DOC) concentration as well as the carbon isotope composition of DIC and particulate organic carbon (POM). DIC refers to the sum of dissolved inorganic carbon species (i.e., carbon dioxide, carbonic acid, bicarbonate, carbonate), DOC refers to the dissolved organic matter within the water column, and POM refers to the plant or animal material suspended in the water column.

Research on the effects of waterfowl populations in Arctic ponds by Côté et al. (2010) found no significant difference in DIC and DOC concentrations in lakes with or without geese. However, MacDonald et al. (2014, 2015) found elevated DOC levels in a lake with active LSG disturbance. DIC levels were comparable between lakes with or without LSG disturbance. Additionally, previous work in Wapusk National Park has found that the carbon isotope composition of DIC within LSG disturbed ponds has a different seasonal pattern than low disturbance ponds (MacDonald et al., 2014, 2015; Figure 8). At ponds with low LSG disturbance, the carbon isotope composition of DIC and POM increases during the ice-free season due to an increase in aquatic primary productivity through photosynthesis. This likely reflects an increase in primary productivity under conditions where carbon supply is exceeded by carbon demand. However, at ponds with LSG disturbance, the carbon isotope composition of DIC typically shows a sharp decline in mid-summer (Figure 8) and the carbon isotope composition of POM rises more sharply, thus implying a different behaviour of the dissolved inorganic carbon within a goose disturbed pond and a higher demand for carbon in the mid-summer.

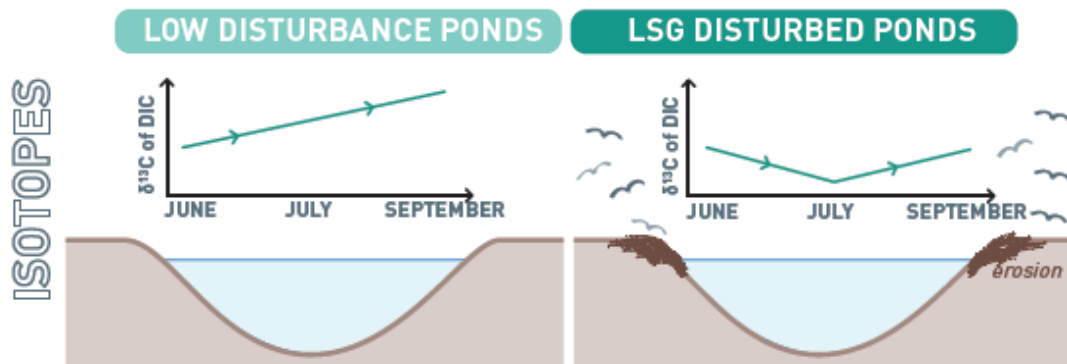


Figure 8 Schematic depicting the difference in the carbon isotope composition of dissolved inorganic carbon in response to LSG disturbance.

Similar to pH and nutrient values, DIC and DOC concentrations of ponds within the 'poor' pond condition are significantly higher than the values within the 'good' and 'fair' conditions (Figure 5e and f). These elevated concentrations of DIC and DOC could reflect a greater supply of carbon from the LSG disturbed catchments. Additionally, in alignment with MacDonald et al. (2014, 2015), the carbon isotope composition of DIC progressively decreases as pond condition decreases (Figure 5g). Correspondingly, the carbon isotope composition of POM values increase with decreasing pond condition likely reflecting the increased demand on carbon in ponds most disturbed by LSG (Figure 5h).

4.0 Conclusions

This is only the second year of the Goose Aquatic Impact monitoring program and identifying the best data to collect and depict is a work in progress. It is important to note that the different variables measured (i.e., conductivity, pH, TP, TKN, DIC, DOC, carbon isotope composition of DIC and POM) combined, provide a comprehensive picture of the effects of LSG disturbance on the aquatic ecosystems in WNP (Figure 5). By using all of these limnological parameters, three areas of disturbance have been identified (¹the northern region by La Perouse Bay, ²along the eastern coast near Thompson Point, and ³the southern inland portion of the sampling area) and continued monitoring is necessary to understand how these areas continue to evolve in response to LSG disturbance. For more in depth results on samples collected in 2015 and 2016 refer to the Ph.D. thesis of H. White (Wilfrid Laurier University) and the corresponding publication (White et al., in preparation).

5.0 Appendix

Table A1 2017 Goose Aquatic Impact data

Pond	pH	TP	TKN	DIC (mg/L)	DOC (mg/L)	$\delta^{13}\text{C}_{\text{DIC}}$ (‰)	$\delta^{13}\text{C}_{\text{POM}}$ (‰)
WAP 57	8.23	0.21	8.60	17.50	7.80	-2.25	-19.08
WAP 58	8.54	0.42	7.64	21.50	9.50	-3.41	-13.77
WAP 59	9.13	0.51	0.71	21.60	9.10	-2.09	-21.32
WAP 60	8.48	0.02	0.91	28.50	11.70	-1.60	-21.99
WAP 61	8.44	0.02	0.95	23.30	10.20	-1.70	-23.79
WAP 62	8.54	0.04	0.94	29.60	11.10	-1.45	-22.22
WAP 63	8.37	0.08	1.40	28.70	12.30	-1.72	-22.32
WAP 64	8.31	0.11	0.97	18.50	9.00	-2.63	-23.44
WAP 65	8.36	0.04	1.43	27.00	14.30	-2.27	-24.33
WAP 66	8.35	0.04	0.68	14.60	8.10	-3.97	-22.28
WAP 67	8.27	0.06	1.13	25.00	13.00	-1.79	-27.94
WAP 68	8.36	0.03	0.91	22.00	13.80	-2.40	-26.82
WAP 69	8.37	0.01	0.77	17.10	8.00	-2.30	-22.03
WAP 70	8.37	0.02	0.60	25.50	7.70	-1.27	-20.30
WAP 71	8.75	0.01	0.46	15.00	7.80	-1.01	-23.66
WAP 72	9.06	0.03	1.57	25.70	14.60	-2.31	-19.45
WAP 73	8.54	0.05	1.36	28.60	16.50	-1.85	-28.41
WAP 74	8.62	0.04	0.67	21.80	7.80	-2.09	-26.06
WAP 75	8.45	0.02	1.19	20.90	12.70	-2.57	-23.90
WAP 76	8.46	0.42	4.66	26.60	9.90	-	-15.45
WAP 77	8.36	0.06	0.98	13.90	12.30	-1.94	-27.92
WAP 78	8.46	0.12	1.48	20.50	17.70	-2.20	-26.62
WAP 79	8.27	0.49	9.66	11.50	20.70	-2.01	-28.48
WAP 80	8.21	0.32	10.49	14.30	19.30	-1.88	-28.90
WAP 81	8.25	0.22	11.52	14.20	20.40	-1.03	-25.91
WAP 82	8.36	0.05	0.91	18.70	12.20	-1.72	-26.45
WAP 83	8.66	0.03	0.77	17.60	11.90	-1.69	-24.45
WAP 84	8.76	0.24	0.78	22.10	10.20	-2.60	-16.61
WAP 85	8.31	0.38	8.26	9.00	12.60	-0.55	-27.09
WAP 86	8.23	0.40	6.77	7.00	12.70	-0.84	-26.78


6.0 References

- Batt, B.D.J., editor. 1997. Arctic ecosystems in peril: report of the Arctic Goose Habitat Working Group. Arctic Goose Joint Venture Special Publication. US Fish and Wildlife Service, Washington, D.C. and Canadian Wildlife Service, Ottawa, Ontario. 120pp.
- Côté G., Pienitz, R., Velle, G., and Wang, X. 2010. Impact of geese on the limnology of lakes and ponds from Bylot Island (Nunavut, Canada). *International Review of Hydrobiology*, 95:2:105-129.
- Handa, I.T., Harmsen, R., and Jefferies R.L. 2002. Patterns of vegetation change and the recovery potential of degraded areas in a coastal marsh system of the Hudson Bay lowlands. *Journal of Ecology*, 90:1:86-99.
- Hochheim, K., Barber, D.G., and Lukovich, J.V. 2010. Changing sea ice conditions in Hudson Bay, 1980-2005. In Ferguson, S.H., Loseto, L.L., and Mallory, M.L. (eds.), *A Little Less Arctic: Top Predators in the World's Largest Inland Sea, Hudson Bay. Dordrecht: Springer*, 39-52.
- Jefferies, R.L., Jano, A.P., and Abraham, K.F. 2006. A biotic agent promotes large-scale catastrophic change in the coastal marshes of Hudson Bay. *Journal of Ecology*, 94:1:234-242.
- Jefferies, R.L. and Rockwell, R.F. 2002. Foraging geese, vegetation loss and soil degradation in an Arctic salt marsh. *Applied Vegetation Science*, 5:1:7-16.
- Kaufman, D.S., Schneider, D.P., McKay, N.P., Ammann, C.M., Bradley, R.S., Briffa, K.R., Miller, G.H., Otto-Bliesner, B.L., Overpeck, J.T., Vinther, B.M. and Arctic Lakes 2k Project Members. 2009. Recent warming reverses long-term Arctic cooling. *Science*, 325: 1236-1239.
- MacDonald, L.A., Farquharson, N., Hall, R.I., Wolfe, B.B., Macrae, M.L., and Sweetman, J.N. 2014. Avian-driven Modification of Seasonal Carbon Cycling at a Tundra Pond in the Hudson Bay Lowlands (Northern Manitoba, Canada). *Arctic, Antarctic, and Alpine Research*, 46:1:206-217.
- MacDonald, L.A., Farquharson, N., Merritt, G., Fooks, S., Medeiros, A.S., Hall, R.I., Wolfe, B.B., Macrae, M.L., Sweetman, J.N. 2015. Limnological regime shifts caused by climate warming and Lesser Snow Goose population expansion in the western Hudson Bay Lowlands (Manitoba, Canada). *Ecology and Evolution*, 5:4:921-939.
- Smith, S.L. and Burgess, M.M. 2004. Sensitivity of permafrost to climate warming in Canada. Geological Survey of Canada. *Bulletin 579*.
- Parks Canada Agency, 2011. State of the Park Report 2011: Wapusk National Park of Canada. Ottawa: Parks Canada Agency, 41 pp.
- White et al. Use of limnological techniques to assess the effects of Lesser Snow Geese disturbance on ponds in Wapusk National Park, northern Manitoba, in preparation.

4.D. Open Access Data

https://open.canada.ca/data/en/dataset?q=Wapusk&portal_type=dataset&sort=

1. Pond Water Dynamics/Lake Hydrology Public Data



Government of Canada
Gouvernement du Canada

Jobs ▾
Immigration ▾
Travel ▾
Business ▾
Benefits ▾
Health ▾
Taxes ▾
More services ▾

[Home](#) → [Open Government](#) → Lake Hydrology - Wapusk ...

Lake Hydrology - Wapusk National Park

Wapusk National Park protects a vast landscape of coastal salt marshes, countless lakes and ponds, and a diversity of boreal-tundra interface habitats, and serves as staging areas for migrating birds, and habitat for a diversity of wildlife. Shallow lakes and ponds are created in part by thermokarst processes resulting from the melting of ground ice in areas underlain by permafrost. In northern areas, climate change brings fluctuations in temperature, permafrost and snow fall and cover which affect lake dynamics, water composition and water levels, and the plants and animals dependent on them. Lake hydrology is assessed based on hydroecological methods developed during the International Polar Year in Vuntut National Park, and initiated in Wapusk in 2010 by the Hydroecological Team, a multidisciplinary research group from Wilfrid Laurier University and University of Waterloo led by Dr. Brent Wolfe. Lake water from forest, wetlands and coastal ecosystem habitats is monitored using the composition of naturally occurring isotopic tracers to assess the evaporation to input ratio (E/I ratio). The E/I ratio, for which high values indicate lake drying, is used as a coarse assessment of climate change for ecological integrity monitoring for state-of-the-park reporting. We are currently publishing part 1 of the data; a more complete dataset will be posted at a later date. This provides collaborators the opportunity to publish papers and finalise theses.

Publisher - Current Organization Name: Parks Canada

Contributor: Hilary White (PhD candidate at Wilfrid Laurier University), Dr. Brent Wolfe (Wilfrid Laurier University)

Licence: [Open Government Licence - Canada](#)

Have your say

★★★★★

[Rate this dataset](#)

[Comment\(s\)](#)

Additional Information

Creator: Chantal Ouimet

Contact Email: chantal.ouimet@pc.gc.ca

Keywords:

- Thermokarst processes
- water samples
- stable isotope
- hydrology
- Wapusk National Park
- climate change
- Evaporation/Inpu ratio
- E/I ratio
- wetlands
- peatlands
- coastal ecosystem
- forest
- ecological integrity monitoring
- goose impact


Subject:

- Nature and Environment

Resources

Resource Name ↑↓	Resource Type ↑↓	Format ↑↓	Language ↑↓	Links
Lake Hydrology - Wapusk National Park	Dataset	CSV	English French	Access
Lake Hydrology - Wapusk National Park - Data Dictionary	Terminology	CSV	English French	Access

2. Goose Aquatic Assessment Public Data



Government of Canada
Gouvernement du Canada

Jobs ▾
Immigration ▾
Travel ▾
Business ▾
Benefits ▾
Health ▾
Taxes ▾
More services ▾

[Home](#) → [Open Government](#) → [Goose Aquatic Assessment](#) - ...

Goose Aquatic Assessment - Wapusk National Park

Wapusk National Park (WNP), protects a vast landscape of coastal salt marshes, countless ponds, and a diversity of boreal-tundra interface habitats, and serves as staging areas for migrating birds, including the Lesser Snow Goose (LSGO). Over the last few decades LSGO populations have increased exponentially due to multiple factors the LSGO is now considered hyper-abundant. Grazing LSGO create large disturbed and barren areas altering vegetation, soil, and ponds, and affecting the ecological integrity of the parks terrestrial and aquatic ecosystems. To assess goose impacts and their spatial expansion, thirty (30) ponds were selected to form a coarse grid covering the area north of the Broad River and east of Nestor Two camp. Water composition, including conductivity, is monitoring in July annually. As geese feed, they remove vegetation; and their droppings add nutrient and organic matter in and around ponds. Increased water nutrients and sediment results in increased conductivity, a sign of increased goose presence and impacts. The field crew also records evidence of geese at each pond and pond water is sampled for laboratory analyses of naturally occurring isotopic tracers to assess the water Evaporation to Input (shortened to E/I ratio), and measure nutrients and organic matter dynamic. Water samples are sent for laboratory analysis to our monitoring partners, the Hydroecology Team led by Dr. Brent Wolfe (Wilfrid Laurier University). We are currently publishing part 1 of the data; a more complete dataset will be posted at a later date.

Publisher - Current Organization Name: Parks Canada

Contributor: Hilary White (PhD candidate at Wilfrid Laurier University), Dr. Brent Wolfe (Wilfrid Laurier University)

Licence: [Open Government Licence - Canada](#)

Have your say

★ ★ ★ ★ ★

[Rate this dataset](#)

[Comment\(s\)](#)

Additional Information

Creator: Chantal Ouimet

Contact Email:
chantal.ouimet@pc.gc.ca

Keywords:

Water samples
stable isotope
hydroecology
Wapusk National Park
climate change
goose populations
conductivity
wetland
coastal
forest
water chemistry and nutrients
pond
lake
ecological integrity monitoring
hydrology
Lesser snow goose impact
Evaporation/Input ratio
E/I ratio

Resources

Resource Name ↑↓	Resource Type ↑↓	Format ↑↓	Language ↑↓	Links
Goose Aquatic Assessment - Wapusk National Park	Dataset	CSV	English French	Access
Goose Aquatic Assessment - Wapusk National Park - Data Dictionary	Terminology	CSV	English French	Access

Communicating research with the general public

I believe that one of the most important responsibilities we have as scientists, is to educate and communicate our knowledge with people outside of the scientific community. This kind of communication has been a high priority for me during my Ph.D. and began with reaching out to Parks Canada staff to write an article for Wapusk News, the yearly publication for all-things related to Wapusk National Park (Section 4.E). This article was meant to convey our research findings in an easy to understand format to Parks staff, Churchill residents, and the thousands of tourists that travel through Churchill every year. I also gave several public presentations to the Churchill community and visitors at the Parks Canada Office and the Churchill Northern Studies Centre, all with the goal of being transparent and open about the research that we were conducting. Additionally, I contributed content for the recently launched ‘Expedition Churchill’, an interactive platform on the Churchill region and all the incredible research that is taking place there (<http://umanitoba.ca/research/expeditionchurchill/> , which you can get on your phone as an app).

White, H. 2014. Climate change and the lakes of Wapusk National Park. Wapusk News: The Voice of Wapusk National Park, 7, 15.



Hilary White

PhD candidate
Department of Geography and
Environmental Studies
Wilfrid Laurier University

Wapusk National Park, a representative portion of the Hudson Bay Lowlands, has an abundance of shallow lakes. This freshwater landscape is a highly productive northern oasis and provides habitat for a variety of wildlife. However, the very existence of these lakes may become increasingly vulnerable to the effects of climate change.

Since 2010, researchers at Wilfrid Laurier University and University of Waterloo have been conducting a number of studies to determine how the lakes have changed in response to recent warming and what is in store for the future. With the help and guidance of staff from Wapusk National Park, our research group has collected water and sediment samples from approximately 40 lakes that are located from the boreal forest to the coastal tundra regions in the park. A key focus of our research has been to examine both present and past hydrological conditions of the lakes.

Issue 7 – 2014

To learn how current climate conditions influence the lakes, we use water isotope tracers (^{18}O , ^2H) to track the varying influence of snowmelt, rainfall and evaporation. Our results show that there are strong relations among the hydrology of the lakes, meteorological conditions and catchment characteristics. For example, regions of the park with sparse vegetation and flat terrain are most susceptible to lake-level decline following springs of low snowmelt runoff. Notably, several lakes underwent partial or complete “desiccation” or drying during the summers of 2010, 2012 and 2013.

Understanding how lakes have changed over longer periods of time is also important and therefore we use “paleolimnology,” the study of sediments that accumulate at the bottom of lakes. We collected several sediment cores in summer 2013 from lakes that we had observed to desiccate. Analyses of these cores will be used to determine if lake desiccation is a recent outcome of climate change or if this has occurred in the past. Initial findings from one lake show that recently observed drying has not previously occurred over the past 200 years.

Above: PhD students Lauren MacDonald and Hilary White collecting sediment cores from a desiccated lake in Wapusk National Park (July 2013).
Below: A landscape shot of Wapusk National Park with evidence of widespread lake desiccation (July 2013).

Looking towards the future, we are collaborating with staff from Wapusk National Park to establish a lake monitoring program using the techniques we have developed. This information will help to track the ongoing and increasingly dynamic effects of climate change on lakes in the park. □



Chapter 5: Conclusions and Recommendations

Freshwater ecosystems are abundant features across northern landscapes and provide the necessary resources and habitat for a variety of wildlife as well as supporting the traditional lifestyles of Indigenous cultures (Rouse et al., 1997; Prowse et al. 2006; Schindler and Smol, 2006). However, a more complete understanding of both the observed and predicted effects of multiple environmental stressors is necessary in light of increasing change and disturbance. These freshwater environments are particularly sensitive to climate change, but remain amongst the least studied and poorly understood ecosystems, especially how they respond to the effects of multiple, compounding environmental stressors (e.g., Rouse et al., 1997; ACIA, 2004; Abraham et al., 2005a; Prowse et al., 2006; Schindler and Smol, 2006; IPCC, 2014; Luoto et al., 2014). This thesis has provided a new understanding of the effects of climate change and waterfowl disturbance on freshwater ecosystems within two subarctic national parks (Vuntut National Park, Wapusk National Park). This information is crucial to determine the relative roles of multiple environmental stressors on the hydrology, limnology and carbon behaviour of subarctic lakes, to develop sustainable long-term monitoring programs, and to translate scientific research into action and application. Below is a synthesis of the key contributions that address the objectives of this thesis.

5.1 Synthesis of Key Contributions

Development of novel hydrological thresholds using water isotopes to monitor the Ecological Integrity of northern shallow lakes

Rapid climate-induced shifts in northern freshwater ecosystems are of increasing concern, leading to the necessity to better understand and monitor the impacts of such change (Smith et al., 2005; Smol et al., 2005; Prowse et al., 2006; Riordan et al., 2006; Schindler and Smol, 2006; Labreque et al., 2009; Carroll et al., 2011). Parks Canada has identified that the hydrological condition of freshwater lakes within VNP and WNP are a critical ‘Ecological Integrity Measure’ and must be monitored. To address this, my research focuses on monitoring individual northern lake-rich landscapes to identify changes in the local hydrology over time in response to varying meteorological conditions by utilizing thresholds. Since hydrology (‘snowmelt-dominated’ vs. ‘rainfall-dominated’ or coastal fen vs. interior peat plateau vs. boreal spruce forest) and seasonality (spring vs. summer vs. fall) influence lakes in a variety of ways, this study provides an alternative to the static E/I threshold of > 0.5 used in previous studies and defines thresholds specific to lake categories and seasons. While this approach may not always signal aquatic ecosystem impairment, it has the advantage of providing a more sensitive, quantitative means to assess and detect hydrological change.

Integration of novel thresholds to assess the hydrological ‘Ecological Integrity Measure’ condition within two subarctic Canadian national parks

An important contribution of this work is the alignment of hydrological thresholds with Parks Canada’s usage of thresholds as 1) a tool to evaluate ‘Ecological Integrity’

and 2) to establish the ‘condition’ of an individual ecosystem. These hydrological thresholds allow for the translation of scientific research into metrics that serve Parks Canada and their reporting requirements. The lake status designations of ‘good’, ‘fair’, and ‘poor’ were generated for each lake category and season to represent easily quantifiable Ecological Integrity conditions. Variability in the condition (‘good’, ‘fair’, ‘poor’) of VNP monitoring lakes exists between lake category (‘rainfall-dominated’, ‘snowmelt-dominated’, intermediate) as well as by season (spring, fall) from 2007 to 2015. However, rainfall-dominated lakes show the most variability in lake condition, spanning from lakes that fall entirely within the ‘good’ condition to lakes that are almost entirely in ‘fair’ to ‘poor’ conditions. In WNP, variability in lake condition exists between lake category (coastal fen, boreal spruce forest, interior peat plateau) and season (spring, summer, fall) from 2010 to 2013. However, during the spring and summer of 2014 and the entire ice-free season of 2015, all lakes improved to ‘fair’ or ‘good’ conditions, reflecting an increase in the precipitation/evaporation ratio. There was a large amount of rainfall during the month of July prior to and during sampling in 2014. This rainfall likely caused the homogenization of lake hydrological conditions. Although there were no large rain events prior to the other sampling periods in 2014 and 2015, precipitation/evaporation ratios were evidently sufficient for lakes to maintain ‘good’ or ‘fair’ status. Most interior peat plateau lakes fall within ‘good’ and ‘fair’ conditions and many boreal spruce forest lakes fall within ‘good’ and ‘fair’ conditions due to the stronger snow trapping ability of the forest, indicating more resistance to evaporative drawdown compared to lakes in other ecotypes. However, low snow during 2009-2010, 2010-2011, and 2012-2013 seasons led several boreal spruce forest lakes to approach or

cross the 'poor' threshold, despite snow-trapping effects of their forested catchments, implying that these lakes may become more vulnerable to evaporation under a climate change scenario of low snowfall. While their E/I ratios remain low relative to the other lake categories, boreal spruce forest lakes may become more vulnerable to evaporation under a climate change scenario of low snowfall. Parks Canada can now incorporate these Ecological Integrity conditions into their 'State of the Park' report to quantify the fluctuations in the hydrological status of lakes in response to climate change.

Variation of limnological conditions and carbon behaviour in relation to LSG disturbance

Previous research found that carbon isotope measurements (e.g., $\delta^{13}\text{C}_{\text{DIC}}$) were more informative regarding LSG-disturbance than standard water chemistry measurements (e.g., pH, TP, TKN) and captured marked differences in carbon behaviour between undisturbed lakes and one LSG-disturbed lake (MacDonald et al., 2014). However, the one LSG-disturbed lake chosen by MacDonald et al. (2014) may not be representative of all LSG-disturbed lakes and likely did not capture the full spectrum of limnological differences caused by LSG disturbance. Findings reported here identified that limnological trends caused by chemically-enhanced CO_2 invasion, elevated catchment runoff of nutrients, carbon and ions, as well as enhanced aquatic productivity, increasingly influenced the nutrient and carbon balance of lakes along a LSG disturbance gradient (undisturbed, actively disturbed, severely disturbed).

Spatial patterns of Lesser Snow Geese (LSG) disturbance

A key contribution is the generation of a map (Chapter 3, Figure 3.9) that synthesizes the effects of all limnological and carbon isotope variables (specific conductivity, TP, TKN, $\delta^{13}\text{C}_{\text{DIC}}$, $\delta^{13}\text{C}_{\text{PHYTOPOM}}$) that are deemed sensitive to LSG disturbance. From this map, old, current, and emerging areas of LSG disturbance (La Perouse Bay, north/northwest of Thompson Point, and inland area in the southern portion of study area, respectively) are identified. Although, previous studies (MacDonald et al., 2014) found that specific conductivity and carbon isotope measurements (e.g., $\delta^{13}\text{C}_{\text{DIC}}$) were more informative than standard water chemistry measurements (e.g., pH, TP, TKN), this spatial analysis determined that specific conductivity, carbon isotope measurements, and standard water chemistry variables are all useful for identifying levels of LSG disturbance across the WNP landscape.

Transforming research science into action and application

A new research paradigm in northern Canada has developed, where collaborative, interdisciplinary, and community-driven research reflects northern priorities and leads to action and application (Graham and Fortier, 2005; Wolfe et al., 2007a, 2011; Balasubramaniam, 2009; ISAC, 2012; Tondu et al., 2014; Adams et al., 2014). I believe that the most important contribution of this research has been the transformation of our research science into an applicable, long-term, and sustainable monitoring program for Wapusk National Park, in partnership with Parks Canada. Conducting northern, collaborative, and interdisciplinary research to address large environmental problems (e.g., climate warming, permafrost thaw, change occurring to freshwater resources) is

often complex and challenging, but through a tremendous amount of effort and collaboration, the Hydroecology Monitoring Program was successfully established and maintained. This monitoring program has been developed in a format that aligns with Parks Canada's mandate and can be utilized for their reporting requirements.

5.2 Final Comments and Recommendations

All of these contributions could not have been possible without the commitment and collaboration of both university and Parks Canada partners. It has been a challenging and iterative process, but also an incredibly rewarding experience creating the now sustainable and long-term Hydroecology Monitoring Program. As previously mentioned, this monitoring program has two main components: 1) Pond Water Dynamics/Lake Hydrology monitoring which is associated with Chapter 2 and 2) Goose Aquatic Impact monitoring which is associated with Chapter 3. Specific recommendations for the continuation of these two monitoring program components have been laid out in their individual chapters and a summary of key recommendations are provided below.

Pond Water Dynamics/Lake Hydrology monitoring

Three main recommendations have been established to maintain the longevity of the Pond Water Dynamics/Lake Hydrology program.

1) If financially feasible, water isotope sampling should be completed every spring and fall with summer sampling added every three years to capture a broad spectrum of hydrological conditions. By not including the summer sampling period, the maximum influence of evaporation on the lakes may not be captured. However, with the

difficulties in securing reliable funding sources every year in mind, spring and fall sampling may be deemed sufficient since only one lake water isotope value (δ_L) from this research fell outside the range captured by the spring and fall seasons.

2) An evaporation pan should be maintained every ice-free season by Parks Canada staff. The evaporation pan simulates the isotopic and hydrological behaviour of a steady-state terminal lake where inflow is equivalent to evaporation (δ_{SSL}). This value is an important component of the Local Evaporation Line and helps to constrain δ_{AS} (the isotopic composition of the ice-free season atmospheric moisture) which is an important component for calculating E/I ratios, the basis of our lake thresholds.

3) The partnership between Parks Canada staff and researchers needs to remain strong and long-term. Funding needs to be secured, field collection and processing needs to be carried out efficiently and accurately, data collection and the corresponding isotope framework calculations need to be completed, and E/I values plotted within the Ecological Integrity thresholds is necessary. Additionally, a yearly report and a complete data file should be created by both researchers and Parks Canada staff and made public to ensure the science is understandably portrayed and can inform policy and land-management decisions.

Goose Aquatic Impact monitoring

Three major recommendations have been established to ensure that the Goose Aquatic Impact monitoring program is successful and sustainable.

1) Collecting one lake-water sample for water chemistry as well as carbon isotope compositions of DIC and phytoplankton at peak primary productivity (e.g., mid-summer)

is sufficient to delineate a range of conditions and influence of LSG disturbance on WNP lakes. Although sampling multiple times during the ice-free season would be ideal for tracking seasonal variability, it is not always sustainable and feasible (e.g., financial, time, available personnel constraints).

2) This study substantiates the utility of a suite of limnological variables sensitive to catchment disturbance by LSG including pH, specific conductivity, total phosphorus (TP), total Kjeldahl nitrogen (TKN), and carbon isotope measures ($\delta^{13}\text{C}_{\text{Dissolved Inorganic Carbon (DIC)}}$, $\delta^{13}\text{C}_{\text{Phytoplanktonic Particulate Organic Matter (PHYTOPOM)}}$, and $\Delta^{13}\text{C}_{\text{DIC-PHYTOPOM}}$). One option is to obtain specific conductivity and field observations from all 45 lakes annually since they are simple and cost-effective measures and then sample the full suite of water chemistry and carbon isotope variables from all lakes every other or every three years depending on funding. Incorporation of yearly water isotope measurements is recommended given the potential confounding effects of rainfall on detecting limnological consequences of LSG disturbance, as occurred in 2015.

3) Repeated sampling over several years of the same lakes will provide the basis for examining LSG disturbance trends over time and the potential to identify new areas of disturbance, areas of increasing disturbance, or perhaps even the first signs of post-disturbance recovery, especially since LSG populations may be stabilizing. Therefore, the generation of synthesis maps after each sampling can be used as a management tool to help identify trends in the area and degree of LSG disturbance within WNP over time.

References

- Abnizova, A., Siemens, J., Langer, M., Boike, J. 2012. Small ponds with major impact: The relevance of ponds and lakes in permafrost landscapes to carbon dioxide emissions. *Global Biogeochemical Cycles*, 26: GB2041.
- Abraham, K.F., Jefferies, R.L., and Rockwell, R.F. 2005a. Goose-induced changes in vegetation and land cover between 1976 and 1997 in an Arctic coastal marsh. *Arctic, Antarctic and Alpine Research*, 37: 260-275.
- Abraham, K.F., Jefferies, R.L., Alisauskas, R.T. 2005b. The dynamics of landscape change and snow geese in mid-continent North America. *Global Change Biology*, 11: 841-855.
- ACIA. 2004. Arctic Climate Impact Assessment. Cambridge University Press, Cambridge, pp. 1042.
- Adams, M.S., Carpenter, J., Housty, J.A., Neasloss, D., Paquet, P.C., Service, C., Walkus, J., and Darimont, C.T. 2014. Toward increased engagement between academic and indigenous community partners in ecological research. *Ecology and Society*, 19(3): 5.
- Alisauskas, R.T., Rockwell, R.F., Duofor, K.W., Cooch, E.G., Zimmerman, G., Drake, K.L., Leafloor, J.O., Moser, T.J., and Reed, E.T. 2011. Harvest, survival, and abundance of midcontinent lesser snow geese relative to population reduction efforts. *Wildlife Monographs*, 179(1): 1-42.
- Anderson, L., Birks, J., Rover, J., and Guldager, N. 2013. Controls on recent Alaskan lake changes identified from water isotopes and remote sensing. *Geophysical Research Letters*, 40(13): 3413–3418.
- Anselin, L. 1995. Local indicators of spatial association – LISA. *Geographical Analysis*, 27(2): 93-115.
- Antoniades, D., Douglas, M.S.V., and Smol, J.P. 2005. Quantitative estimates of recent environmental changes in the Canadian High Arctic inferred from diatoms in lake and pond sediments. *Journal of Paleolimnology*, 33: 349-360.
- Avis, C.A., Weaver, A.J., and Meissner, K.J. 2011. Reduction in areal extent of high-latitude wetlands in response to permafrost thaw. *Nature Geoscience* 4: 444-448.
- Balasubramaniam, A.M. 2009. Community-based research, youth outdoor education and other highlights of a northern research internship experience in Old Crow, Yukon Territory. *Meridian*, Spring/Summer, 14-18.
- Bade, D.L., Carpenter, S.R., Cole, J.J., Hanson, P.C., and Hesslein, R.H. 2004. Controls of $\delta^{13}\text{C}$ -DIC in lakes: Geochemistry, lake metabolism, and morphometry. *Limnology and Oceanography*, 49: 1160-1172.

- Bade, D.L. and Cole, J.J. 2006. Impact of chemically enhanced diffusion on dissolved inorganic carbon stable isotopes in a fertilized lake. *Journal of Geophysical Research*, 11: C01014.
- Baldwin, F., Naylor, L., Leafloor, J., Dooley, J. and members of the Mississippi Flyway Council Technical Section-Arctic Goose Committee. 2018. Management plan for midcontinent lesser snow geese in the Mississippi Flyway. *Mississippi Flyway Council*.
- Batt, B.D.J. 1997. Arctic ecosystems in peril: report of the Arctic Goose Habitat Working Group. *Arctic Goose Joint Venture Special Publication*. U.S. Fish and Wildlife Service, Washington D.C. and Canadian Wildlife Service, Ottawa, Ontario. 120pp.
- Bouchard, F., Turner, K.W., MacDonald, L.A., Deakin, C., White, H., Farquharson, N., Medeiros, A.S., Wolfe, B.B., Hall, R.I., Pienitz, R., and Edwards, T.W.D. 2013. Vulnerability of shallow subarctic lakes to evaporate and desiccate when snowmelt runoff is low. *Geophysical Research Letters*, 40: 6112-6117.
- Boyd, H., Smith, G.E.J., and Cooch, F.G. 1982. The lesser snow geese of the eastern Canadian arctic: their status during 1964-1979 and their management from 1981 to 1990. *Canadian Wildlife Service Occasional Papers*, 46.
- Brisk, D.D., Fuhlendorf, S.D., and Smeins, F.E. 2005. State-and-transition models, thresholds, and rangeland health: A synthesis of ecological concepts and perspectives. *Rangeland Ecological Management*, 58(1): 1-10.
- Brock, B.E., Wolfe, B.B., Edwards, T.W.D. 2007. Characterizing the hydrology of shallow floodplain lakes in the Slave River Delta, NWT, Canada, using water isotope tracers. *Arctic and Alpine Research*, 39: 388-401.
- Brock, B.E., Martin, M.E., Mongeon, C.L., Sokal, M.A., Wesche, S.D., Armitage, D., Wolfe, B.B., Hall, R.I., Edwards, T.W.D. 2010. Flood frequency variability during the past 80 years in the Slave River Delta, NWT, as determined from multi-proxy paleolimnological analysis. *Canadian Water Resources Journal*, 35: 281–300.
- Brooks, J.R., Gibson, J.J., Birks, S.J., Weber, M.H., Rodecap, K.D., and Stoddard, J.L. 2014. Stable isotope estimates of evaporation: inflow and water residence time for lakes across the United States as a tool for national lake water quality assessments. *Limnology and Oceanography*, 59(6): 2150–2165.
- Bush, E. and Lemmen, D.S., editors. 2019. Canada's Changing Climate Report. *Government of Canada*, Ottawa, Ontario. 444 pp.
- Capon, S.J., Lynch, A.J.J., Bond, N., Chessman, B.C., Davis, J., Finlayson, M., Gell, P.A., Hohnberg, D., Humphrey C., Kingsford, R.T., Thomson, J.R., Ward, K., and MacNally R. 2015. Regime shifts, thresholds, and multiple stable states in freshwater

ecosystems; a critical appraisal of the evidence. *Science of the Total Environment*, 534: 122-130.

Carroll, M.L., Townshend, J.R.G., DiMiceli, C.M., Loboda, T., and Sohlberg, R.A. 2011. Shrinking lakes of the Arctic: Spatial relationships and trajectory of change, *Geophysical Research Letters*, 38: L20406.

Clark, I. and Fritz, P. 1997. *Environmental Isotopes in Hydrogeology*. 1-77, Lewis Publishers. New York.

Coplen, T.B. 1996. New guidelines for reporting hydrogen, carbon, and oxygen isotope-ratio data. *Geochimica et Cosmochimica Acta*, 60: 3359-3360.

Côté, G., Pienitz, R., Velle, G., and Wang, X. 2010. Impact of geese on the limnology of lakes and ponds from Bylot Island (Nunavut, Canada). *International Review of Hydrobiology*, 95: 105-129.

Craig H. 1961. Isotopic variations in meteoric waters. *Science*, 133: 1702–1703.

Craig, H. and Gordon, L.I. 1965. Deuterium and oxygen 18 variations in the ocean and marine atmosphere. In Tongiorgi, E. (ed.), *Stable Isotopes in Oceanographic Studies and Paleotemperatures*. Pisa, Italy: Laboratorio di Geologia Nucleare.

Derksen, C. and Brown, R. 2012. Spring snow cover extent reductions in the 2008-2012 period exceeding climate model projections. *Geophysical Research Letters*, 39: L19504.

Dredge, L.A. and Nixon, F.M. 1992. Glacial and environmental geology of northern Manitoba. *Geological Survey of Canada Memoirs*, 432.

Duguay, C.R. and Lafleur, P.M. 2003. Determining depth and ice thickness of shallow sub-Arctic lakes using space-borne optical and SAR data. *International Journal of Remote Sensing*, 24: 475-489.

Dyke, L.D. and Sladen, W.E. 2010. Permafrost and peatland evolution in the northern Hudson Bay Lowland. *Manitoba, Arctic*, 63: 429-441.

Edwards, T.W.D., Wolfe, B.B., Gibson, J.J., and Hammarlund, D. 2004. Use of water isotope tracers in high latitude hydrology and paleohydrology. In *Long-Term Environmental Change in Arctic and Antarctic Lakes*, Pienitz R, Douglas MSV, and Smol, JP (eds). Springer: Dordrecht, The Netherlands, 187-207.

Environment Canada. 1994. Manual of Analytical Methods: Major Ions and Nutrients, Volume 1. *National Laboratory for Environmental Testing*. Canadian Centre for Inland Waters, Burlington, ON.

- Environment Canada. 2019. National Climate Data and Information Archive, <http://climate.weather.gc.ca/>.
- ESRI. 2017. ArcGIS Desktop: Release 10.5.1. *Environmental Systems Research Institute*, Redlands, CA.
- Farquharson, N. 2013. Characterizing the roles of hydrological processes, climate change and Lesser Snow Geese on ponds in Wapusk National Park using isotopic methods. *Unpublished MSc Thesis*. Wilfrid Laurier University, Waterloo, Ontario.
- Fry B. 2006. *Stable Isotope Ecology*. Springer, New York.
- Gagnon, A. and Gough, W. 2005a. Climate change scenarios for the Hudson Bay Region: An intermodel comparison. *Climate Change*, 69: 269-297.
- Gagnon, A. And Gough, W. 2005b. Trends in the dates of ice freeze-up and breakup over Hudson Bay, Canada. *Arctic* 58: 370-382.
- Gibson J.J., Edwards, T.W.D., and Prowse, T.D. 1999. Pan-derived isotopic composition of atmospheric water vapour and its variability in northern Canada. *Journal of Hydrology*, 217: 55–74.
- Gibson, J.J. and Edwards, T.W.D. 2002. Regional water balance trends and evaporation-transpiration partitioning from a stable isotope survey of lakes in northern Canada. *Global Biogeochemical Cycles*, 16: 10-28.
- Gibson, J.J., Birks, S.J., and Yi, Y. 2016. Stable isotope mass balance of lakes: A contemporary perspective. *Quaternary Science Reviews*, 131: 316-328.
- Gilvear, D.J., and Bradley, C. 2000. Hydrological monitoring and surveillance for wetland conservation and management; a UK perspective. *Physics and Chemistry of the Earth (B)*, 25: 571–588.
- Gonfiantini, R. 1986. Environmental isotopes in lake studies. In: Fritz, P., Fontes, J.-C. (Eds.), *Handbook of Environmental Isotope Geochemistry, The Terrestrial Environment*, vol. 2, Elsevier, New York, pp. 113-168.
- Government of Canada. 2009. Canada's northern strategy: Our north, our heritage, our future. Published under the authority of the Minister of Indian Affairs and Northern Development and Federal Interlocutor for Métis and Non-Status Indians, Ottawa, Ontario. 48 pp.
- Graham, J. and Fortier, E. 2005. From opportunity to action: A progress report on Canada's renewal of northern research. Report submitted by the Institute on Governance to the Planning Committee for the Dialogue on Northern Research. Ottawa: NSERC. 78 pp.

Gregory-Eaves, I., Finney, B.P., Douglas, M.S.V., and Smol, J.P. 2004. Inferring sockeye salmon (*Oncorhynchus nerka*) population dynamics and water quality changes in a stained nursery lake over the past similar to 500 years. *Canadian Journal of Fisheries and Aquatic Sciences*, 61: 1235-1246.

Griffis, T.J., Rouse, W.R., and Waddington, J.R. 2000. Interannual variability of net ecosystem CO₂ exchange at a subarctic fen. *Global Biogeochemical Cycles*, 14: 1109-1121.

Groffman, P.M., Baron, J.S., Blett, T., Gold, A., Goodman, I., Gunderson, L.H., Levinson, B.M., Palmer, M.A., Paerl, H.W., Peterson, G.D., LeRoy Poff, N., Rejeski, D.W., Reynolds, J.F., Turner, M.G., Weathers, K.C., and Wiens, J. 2006. Ecological thresholds: The key to successful environmental management or an important concept with no practical application?. *Ecosystems*, 9: 1-13.

Handa, I.T., Harmsen, R., Jefferies, R.L. 2002. Patterns of vegetation change and the recovery potential of degraded areas in a coastal marsh system of the Hudson Bay Lowlands. *Journal of Ecology*, 90: 86-99.

Harris, S.A., French, H.M., Heginbottom, J.A., Johnston, G.H., Ladanyi, B., Segó, D.C., Everdingen, R.O. 1988. Glossary of Permafrost and Related Ground-Ice Terms, National Research Council of Canada, Technical Memorandum No. 142: 156.

Hik, D.S., Jefferies, R.L., and Sinclair, A.R.E. 1992. Foraging by geese, isostatic uplift and asymmetry in the development of salt-marsh plant communities. *Journal of Ecology*, 80(3): 395-406.

Herczeg, A.L. and Fairbanks, R.G. 1987. Anomalous carbon isotope fractionation between atmospheric CO₂ and dissolved inorganic carbon induced by intense photosynthesis. *Geochimica et Cosmochimica Acta*, 51: 895-899.

Hochheim, K., Barber, D.G., and Lukovich, J.V. 2010. Changing sea ice conditions in Hudson Bay, 1980-2005. In Ferguson, S.H., Loseto, L.L., and Mallory, M.L. (eds.), *A Little Less Arctic: Top Predators in the World's Largest Inland Sea, Hudson Bay*. Dordrecht: Springer, pp. 39-52.

Horita, J. and Wesolowski, D. 1994. Liquid-vapour fractionation of oxygen and hydrogen isotopes of water from the freezing to the critical temperature. *Geochimica et Cosmochimica Acta*, 58: 3425-3497.

Hughes, O. L. 1972: Surficial geology of northern Yukon Territory and northwestern District of Mackenzie Northwest Territories. *Geological Survey of Canada*, Paper 69-36: 1-11.

IPCC. 2014. Climate Change 2014: The synthesis report (SYR) of the IPCC fifth assessment report (AR5). Cambridge University Press, Cambridge, U.K.

ISAC. 2012. Responding to arctic environmental change: Translating our growing understanding into a research agenda for action. Published for An International Study of Arctic Change Workshop: Queen's University, Kingston, Ontario. 36 pp.

Jefferies, R.L. and Rockwell, R.F. 2002. Foraging geese, vegetation loss and soil degradation in an Arctic salt marsh. *Applied Vegetation Science*, 5: 7-16.

Jefferies, R.L., Rockwell, R.F., and Abraham, K.F. 2003. The embarrassment of riches: agricultural food subsidies, high goose numbers, and loss of Arctic wetlands – a continuing saga. *Environmental Reviews*, 11: 193-232.

Jefferies, R.L., Jano, A.P., and Abraham, K.F. 2006. A biotic agent promotes large-scale catastrophic change in the coastal marshes of Hudson Bay. *Journal of Ecology*, 94: 234-242.

Jones, B.M., Grosse, G., Arp, C.D., Jones, M.C., Walter Anthony, K.M., and Romanovsky, V.E. 2011. Modern thermokarst lake dynamics in the continuous permafrost zone, northern Seward Peninsula, Alaska. *Journal of Geophysical Research*, 116: G00M03.

Karlsson, J. M., Bring, A., Peterson, G. D., Gordon, L. J., and Destouni, G. 2011. Opportunities and limitations to detect climate-related regime shifts in inland Arctic ecosystems through eco-hydrological monitoring. *Environmental Research Letters*, 6(1): 014015.

Kaufman, D.S., Schneider, D.P., McKay, N.P., Ammann, C.M., Bradley, R.S., Briffa, K.R., Miller, G.H., Otto-Bliesner, B.L., Overpeck, J.T., Vinther, B.M., and Arctic Lakes 2k Project Members. 2009. Recent warming reverses long-term Arctic cooling. *Science*, 325: 1236-1239.

Keeley, J.E. and Sandquist, D.R. 1992. Carbon: Freshwater plants. *Plant, Cell and Environment*, 15: 1021-1035.

Klinger, L.F. and Short, S.K. 1996. Succession in the Hudson Bay Lowland, northern Ontario, Canada. *Arctic and Alpine Research*, 28:172-183.

Koons, D.N., Rockwell, R.F., and Aubry, L.M. 2014. Effects of exploitation on an overabundant species: the lesser snow goose predicament. *Journal of Animal Ecology*, 83: 365-374.

Labrecque, S., Lacelle, D., Duguay, C., Lauriol, B., Hawkings, J. 2009. Contemporary (1951-2001) evolution of lakes in the Old Crow Basin, northern Yukon, Canada: Remote sensing, numerical modeling and stable isotope analysis. *Arctic*, 62: 225-238.

- Lambert, A., Courtier, N., Sasagawa, G.S., Klopping, F., Winester, D., James, T.S., Liard, J.O. 2001. New constraints on Laurentide postglacial rebound from absolute gravity measurements. *Geophysical Research Letters*, 28: 2109-2112.
- Lantz, T.C. and Turner, K.W. 2015. Changes in lake area in response to thermokarst processes and climate in Old Crow Flats, Yukon. *Journal of Geophysical Research*, 120: 513-524.
- Lauriol, B., Duguay, C. R., and Riel, A. 2002. Response of the Porcupine and Old Crow Rivers in northern Yukon, Canada, to Holocene climatic change. *The Holocene*, 12: 27-34.
- Lemmen, D.S., Warren, F.J., Lacroix, J., Bush, E. (eds.). 2008. *From Impacts to Adaptation: Canada in a Changing Climate 2007*. P 448. Government of Canada, Ottawa, Ontario.
- Lim, D.S.S., Douglas, M.S.V., and Smol, J.P. 2005. Limnology of 46 lakes and ponds on Banks Island, N.W.T., Canadian Arctic Archipelago. *Hydrobiologia*, 545: 11-32.
- Lorrain, A., Savoye, N., Chauvaud, L., Paulet, Y.-M., and Nault, N. 2003. Decarbonation and preservation method for the analysis of organic C and N contents and stable isotope ratios of low-carbonated suspended particulate material. *Analytica Chimica Acta*, 491: 125-133.
- Luoto, T.P., Oksman, M., and Ojala, A.E.K. 2014. Climate change and bird impact as drivers of High Arctic pond deterioration. *Polar Biology*, 38: 357-368.
- MacDonald, L.A., Farquharson, N., Hall, R.I., Wolfe, B.B., Macrae, M.L., and Sweetman, J.N. 2014. Avian-driven Modification of Seasonal Carbon Cycling at a Tundra Pond in the Hudson Bay Lowlands (Northern Manitoba, Canada). *Arctic, Antarctic, and Alpine Research*, 46(1): 206-217.
- MacDonald, L.A., Farquharson, N., Merritt, G., Fooks, S., Medeiros, A.S., Hall, R.I., Wolfe, B.B., Macrae, M.L., and Sweetman, J.N. 2015. Limnological regime shifts caused by climate warming and Lesser Snow Goose population expansion in the western Hudson Bay Lowlands (Manitoba, Canada). *Ecology and Evolution*, 5(4): 921-939.
- MacDonald, L.A., Wolfe, B.B., Turner, K.W., Anderson, L., Arp, C.D., Birks, S.J., Bouchard, F., Edwards, T.W.D., Farquharson, N., Hall, R.I., McDonald, I., Narancic, B., Ouimet, C., Pienitz, R., Tondou, J., White, H. 2017. A synthesis of thermokarst lake water balance in high-latitude regions of North America from isotope tracers. *Arctic Science*, 3(2): 118-149.
- Macrae, M.L., Brown, L.C., Duguay, C.R., Parrott, J.A., and Petrone, R.M. 2014. Observed and projected climate change in the Churchill region of the Hudson Bay

- Lowlands and implications for pond sustainability. *Arctic, Antarctic, and Alpine Research*, 46(1): 272-285.
- Mamet, S.D. and Kershaw, G.P. 2012. Subarctic and alpine tree line dynamics during the last 400 years in north-western and central Canada. *Journal of Biogeography*, 39(5): 855-868.
- Marsh, P., Russell, M., Pohl, S., Haywood, H., and Onclin, C., 2009. Changes in thaw lake drainage in the Western Canadian Arctic from 1950 to 2000. *Hydrological Processes*, 23(1): 145–158.
- Michelutti, N., Keatley, B.E., Brimble, Y., Blais, J.M., Liu, H., Douglas, M.S.V., Mallory, M., Macdonald, R.W., and Smol, J.P. 2009. Seabird-driven shifts in arctic pond ecosystems. *Proceedings of the Royal Society: Biological Sciences*, 276: 591-596.
- Michelutti, N., Brash, J., Thienpont, J., Blais, J.M., Kimpe, L., Mallory, M.L., Douglas, M.S.V., and Smol, J.P. 2010. Trophic position influences the efficacy of seabirds as contaminant biovectors. *Proceedings of the National Academy of Science*, 107: 10543-10548.
- Oksanen, J., Blanchet, F.G., Friendly, M., Kindt, R., Legendre, P., McGlenn, D., Minchin, P.R., O'Hara, R.B., Simpson, G.L., Solymos, P., Stevens, M.H.H., Szoecs, E., and Wagner, H. 2019. Package 'vegan' – Community Ecology Package. R Statistical Environment, Vienna, Austria.
- Parks Canada. 2000. Background information to the Wapusk Ecological Integrity Statement. 102 pp.
- Parks Canada. 2009. State of the park report, Vuntut National Park. Ottawa: Parks Canada Agency, 58 pp.
- Parks Canada. 2011. State of the park report, Wapusk National Park of Canada. Ottawa: Parks Canada Agency, 41 pp.
- Parks Canada Agency. 2011. Consolidated guidelines for ecological integrity monitoring in Canada's national parks. Ottawa: Parks Canada Agency, 115 pp.
- Payette, S. 2004. Accelerated thawing of subarctic peatland permafrost over the last 50 years. *Geophysical Research Letters*, 31: L18208.
- Peterson, S.L., Rockwell, R.F., Witte, C.R., and Koons, D.N. 2013. The legacy of destructive snow goose foraging on supratidal marsh habitat in the Hudson Bay Lowlands. *Arctic, Antarctic, and Alpine Research*, 45(4): 575-583.

- Plug L.J., Walls C., Scott B.M. 2008. Tundra lake changes from 1978 to 2001 on the Tuktoyaktuk Peninsula, western Canadian Arctic. *Geophysical Research Letters*, 35: L03502.
- Prowse, T.D., Wrona, F.J., Reist, J.D., Gibson, J.J., Hobbie, J.E., Lévesque, L.M.J., Vincent, W.F. 2006. Climate change effects on hydroecology of Arctic freshwater ecosystems. *Ambio*, 35: 347-358.
- Quay, P.D., Emerson, S.R., Quay, B.M., and Devol, A.H. 1986. The carbon cycle for Lake Washington – A stable isotope study. *Limnology and Oceanography*, 31: 596-611.
- R Core Team (2015). R: A language and environment for statistical computing. R Foundation for Statistical Computing, Vienna, Austria.
- R Core Team (2015). R: A language and environment for statistical computing. R Foundation for Statistical Computing, Vienna, Austria.
- Rau, G. 1978. Carbon-13 depletion in a subalpine lake: carbon flow implications. *Science*, 201: 901-902.
- Remmer, C.R., Klemm, W.H., Wolfe, B.B., and Hall, R.I. 2018. Inconsequential effects of flooding in 2014 on lakes in the Peace-Athabasca Delta (Canada) due to long-term drying. *Limnology and Oceanography*, 63: 1502-1518.
- Revenge, C., Campbell, I., Abell, R., de Villiers, P., and Bryer, M. 2005. Prospects for monitoring freshwater ecosystems towards the 2010 targets. *Philosophical Transactions: Biological Sciences*, 360: 397-413.
- Riordan, B., Verbyla, D., and McGuire, A.D. 2006. Shrinking ponds in subarctic Alaska based on 1950-2002 remotely sensed images. *Journal of Geophysical Research*, 111: G04002.
- Rockwell, R.F., Abraham, K.F., Witte, C.R., Matulonis, P., Usai, M., Larsen, D., Cooke, F., Pollak, D., and Jefferies, R.L. 2009. The birds of Wapusk National Park. *Parks Canada*, Ottawa.
- Rouse, W.R. 1991. Impacts of Hudson Bay on the terrestrial climate of the Hudson Bay Lowlands. *Arctic and Alpine Research*, 23: 24-30.
- Rouse, W.R., Douglas, M.V., Hecky, R.E., Hershey, A.E., Kling, G.W., Lesack, L., Marsh, P., McDonald, M., Nicholson, B.J., Roulet, N.T., Smol., J.P. 1997. Effects of climate change on the freshwaters of Arctic and Subarctic North America. *Hydrological Processes*, 11: 873-902.
- Roy-Leveillee, P., and Burn, C. R. 2011. Permafrost conditions near shorelines of oriented lakes in Old Crow Flats, Yukon Territory. Calgary: Canadian Geotechnical

Society, 63rd Canadian Geotechnical Conference and 6th Canadian Permafrost Conference, pp. 1509-1516.

Rowland, J.C., Jones, C.E., Altmann, G., Bryan, R., Crosby, B.T., Geernaert, G.L., Hinzman, L.D., Kane, D.L., Lawrence, D.M., Mancino, A., Marsh, P., McNamara, J.P., Romanovsky, V.E., Toniolo, H., Travis, B.J., Trochim, E., and Wilson, C.J. 2010. Arctic landscapes in transition: responses to thawing permafrost. *EOS, Transactions, American Geophysical Union*, 91: 229-236.

Rozanski, K., Araguas-Araguas, L., and Gonfiantini, R. 1993. Isotopic patterns in modern global precipitation. In: Swart, P.K., Lohmann, K.C., McKenzie, J., Savin, S. (Eds.), *Climate Change in Continental Isotopic Records*. American Geophysical Union Geophysical Monograph 78, pp. 1-36.

Rühland, K., Priesnitz, A., and Smol, J.P. 2003. Paleolimnological evidence from diatoms for recent environmental changes in 50 lakes across Canadian arctic treeline. *Arctic, Antarctic and Alpine Research*, 35: 110–123.

Rühland, K. and Smol, J.P. 2005. Diatom shifts as evidence for recent subarctic warming in a remote tundra lake, NWT, Canada. *Palaeogeography, Palaeoclimatology, Palaeoecology*, 226: 1-16.

Rühland, K.M., Paterson, A.M., Keller, W., Michelutti, N., and Smol, J.P. 2013. Global warming triggers the loss of a key Arctic refugium. *Proceedings of the Royal Society: Biological Sciences*, 280: 1772.

Sauchyn, D. and Kulshreshtha, S. 2008. Prairies. In *From impacts to adaptation: Canada in a changing climate 2007*. Government of Canada, Ottawa.

Schindler, D.W. and Smol, J.P. 2006. Cumulative effects of climate warming and other human activities on freshwaters of Arctic and subarctic North America. *Ambio*, 35: 160-168.

Smith, S.L. and Burgess, M.M. 2004. Sensitivity of permafrost to climate warming in Canada. Geological Survey of Canada. *Bulletin 579*.

Smith, L.C., Sheng, Y., MacDonald, G.M., and Hinzman, L.D. 2005. Disappearing Arctic lakes. *Science*, 308: 1429.

Smol, J.P., Wolfe, A.P., Birks, H.J.B., Douglas, M.S.V., Jones, V.J., Korhola, A., Pienitz, R., Rühland, K., Sorvari, S., Antoniades, D., Brooks, S.J., Fallu, M.-A., Hughes, M., Keatley, B.E., Laing, T.E., Michelutti, N., Nazarova, L., Nymen, M., Paterson, A.M., Perren, B., Quinlan, R., Rautio, M., Saulnier-Talbot, E., Siitonen, S., Solovieva, N., and Weckström, J. 2005. Climate-driven regime shifts in the biological communities of arctic lakes. *Proceedings of the National Academy of Sciences*, 102: 4397–4402.

- Smol, J.P. and Douglas, M.S.V. 2007. From controversy to consensus: making the case for recent climate change in the Arctic using lake sediments. *Frontiers in Ecology and Environment*, 5: 466-474.
- Sun, L.G., Emslie, S.D., Huang, T., Blais, J.M., Xie, Z.Q., Liu, X.D., Yin, X.B., Wang, Y.H., Huang, W., Hodgson, D.A., and Smol, J.P. 2013. Vertebrate records in polar sediments: Biological responses to past climate change and human activities. *Earth Science Reviews*, 126: 147-155.
- Takahashi, K., Yoshioka, T., Wada, E., and Sakamoto, M. 1990. Temporal variations in carbon isotope ratio of phytoplankton in a eutrophic lake. *Journal of Plankton Research*, 12: 799-808.
- Tape, K., Sturm, M., and Racine, C. 2006. The evidence for shrub expansion in Northern Alaska and the Pan-Arctic. *Global Change Biology*, 12: 686–702.
- Thorntwaite, C. 1948. An approach toward a rational classification of climate. *The Geographical Review*, 38: 1-94.
- Tondu, J.M.E., Turner, K.W., Wolfe, B.B., Hall, R.I., Edwards, T.W.D., McDonald, I. 2013. Using water isotope tracers to develop the hydrological component of a long-term aquatic ecosystem monitoring program for a northern lake-rich landscape. *Arctic, Antarctic and Alpine Research*, 45(4): 594-614.
- Tondu, J.M.E., Balasubramaniam, A.M., Chavarie, L., Gantner, N., Knopp, J.A., Provencher, J.F., Wong, P.B.Y., and Simmons, D. 2014. Working with northern communities to build collaborative research partnerships: perspectives from early career researchers. *Arctic*, 67(3): 419-429.
- Tondu, J.M.E., Turner, K.W., Wiklund, J.A., Wolfe, B.B., Hall, R.I., and McDonald, I. 2017. Limnological evolution of Zelma Lake, a recently drained thermokarst lake in Old Crow Flats (Yukon, Canada). *Arctic Science*, 3(2): 220-236.
- Turner, K.W., Wolfe, B.B., and Edwards, T.W.D. 2010. Characterizing the role of hydrological processes on lake water balances in the Old Crow Flats, Yukon Territory, Canada, using water isotope tracers. *Journal of Hydrology*, 386: 103-117.
- Turner, K.W., Wolfe, B.W., Edwards, T.W.D., Lantz, T.C., Hall, R.I., and Larocque, G. 2014. Controls on water balance of shallow thermokarst lakes and their relations with catchment characteristics: a multi-year, landscape-scale assessment based on water isotope tracers and remote sensing in Old Crow Flats, Yukon (Canada). *Global Change Biology*, 20(5): 1585-1603.
- van der Molen, M.K., van Huissteden, J., Parmentier, J.W., Petrescu, M.R., Dolman, J., Maximov, T.C., Kononov, A.V., Karsanaev, S.V., and Suzdalov, D.A. 2007. The

growing season greenhouse gas balance of a continental tundra site in the Indigirka lowlands, NE Siberia. *Biogeosciences*, 4: 985-1003.

Van Geest, G.J., Hessen, D.O., Spierenburg, P., Dahl-Hansen, G.A.P., Christensen, G., Faerovig, P.J., Brehm, M., Loonen, M.J.J.E., and Van Donk, E. 2007. Goose-mediated nutrient enrichment and planktonic grazer control in Arctic freshwater ponds. *Oecologia*, 153: 653-662.

Wachniew, P. and Rózański, K. 1997. Carbon budget of a mid-latitude, groundwater-controlled lake: Isotopic evidence for the importance of dissolved inorganic carbon recycling. *Geochimica et Cosmochimica Acta*, 61: 2453-2465.

Wanninkhof, R. 1985. Kinetic fractionation of the carbon isotopes ^{13}C and ^{12}C during transfer of CO_2 from air to seawater. *Tellus B: Chemical and Physical Meteorology*, 37B: 128-135.

Wanninkhof, R. and Knox, M. 1996. Chemical enhancement of CO_2 exchange in natural waters. *Limnology and Oceanography*, 41(4): 689-397.

White, H. 2014. Climate change and the lakes of Wapusk National Park. *Wapusk News: The Voice of Wapusk National Park*, 7: 15.

Wolfe, B.B., Edwards, T.W.D., Elgood, R.J., and Beuning, K.R.M. 2001. Carbon and oxygen isotope analysis of lake sediment cellulose: methods and applications. *In: Tracking Environmental Change Using Lake Sediments: Physical and Chemical Techniques, Developments in Paleoenvironmental Research, Vol 2* (eds Last WM, Smol JP). Kluwer Academic Publishers: Dordrecht; pp. 373-400.

Wolfe, B.B., Armitage, D., Wesche, S., Brock, B.E., Sokal, M.A., Clogg-Wright, K.P., Mongeon, C.L., Adam, M.E., Hall, R.I., and Edwards, T.W.D. 2007a. From isotopes to TK interviews: Towards interdisciplinary research in Fort Resolution and the Slave River Delta, Northwest Territories. *Arctic*, 60(1): 75-87.

Wolfe, B.B., Karst-Riddoch, T.L., Hall, R.I., Edwards, T.W.D., English, M.C., Palmieri, R., McGowan, S., and Vardy, S.R. 2007b. Classification of hydrologic regimes of northern floodplain basins (Peace-Athabasca Delta, Canada) from analysis of stable isotopes ($\delta^{18}\text{O}$, $\delta^2\text{H}$) and water chemistry. *Hydrological Processes*. 21: 151-168.

Wolfe, B.B. and Turner, K.W. 2008. Near-record precipitation causes rapid drainage of Zelma Lake, Old Crow Flats, Northern Yukon Territory. *Meridian*, Spring Edition, pp. 7-12.

Wolfe, B.B., Light, E.M., Macrae, M.L., Hall, R.I., Eichel, K., Jasechko, S., White, J., Fishback, L., Edwards, T.W.D. 2011a. Divergent hydrological responses to 20th century climate change in shallow tundra ponds, western Hudson Bay Lowlands. *Geophysical Research Letters*, 38: 1-6.

Wolfe, B.B., Humphries, M.M., Pisaric, M.F.J., Balasubramaniam, A.M., Burns, C.R., Chan, L., Cooley, D., Froese, D.G., Graupe, S., Hall, R.I., Lantz, T., Porter, T.J., Roy-Léveillé, P., Turner, K.W., Wesche, S.D., and Williams, M. 2011b. Environmental change and traditional use of the Old Crow Flats in northern Canada: an IPY opportunity to meet the challenges of the new northern research paradigm. *Arctic*, 64: 127–135.

Yi, Y., Brock, B.E., Falcone, M.D., Wolfe, B.B., and Edwards, T.W.D. 2008. A coupled isotope tracer method to characterize input water to lakes. *Journal of Hydrology*, 350: 1-13.

Yoshikawa K, and Hinzman L.D. 2003. Shrinking thermokarst ponds and groundwater dynamics in discontinuous permafrost near Council, Alaska. *Permafrost and Periglacial Processes*, 14: 151-160.

Yukon Ecoregions Working Group. 2004. Old Crow Flats. In Smith, C. A. S., Meikle, J. C., and Roots, C. F. (eds.), *Ecoregions of the Yukon Territory: Biophysical Properties of Yukon Landscapes*. Summerland, British Columbia: Agriculture and Agri-Foods Canada, pp.m 115-123.

Zazula, G. D., Duk-Rodkin, A., Schweger, C. E., and Morlan, R. E. 2004. Late Pleistocene chronology of Glacial Lake Old Crow and the north-west margin of the Laurentide Ice Sheet. In Ehlers, J., and Gibbard, P. L. (eds.), *Quaternary Glaciations—Extent and Chronology, Part II*, Amsterdam: Elsevier, pp. 347-342.

Appendix A

Bouchard et al., 2013

GEOPHYSICAL RESEARCH LETTERS, VOL. 40, 6112–6117, doi:10.1002/2013GL058635, 2013

Vulnerability of shallow subarctic lakes to evaporate and desiccate when snowmelt runoff is low

F. Bouchard,^{1,2} K. W. Turner,^{2,3} L. A. MacDonald,⁴ C. Deakin,² H. White,² N. Farquharson,² A. S. Medeiros,² B. B. Wolfe,² R. I. Hall,⁴ R. Picnitz,¹ and T. W. D. Edwards⁵

Received 11 November 2013; accepted 12 November 2013; published 8 December 2013.

[1] Snowmelt is a crucial source of water for many shallow subarctic lakes, but climate models predict that snowfall will decrease in some regions, with profound ecological consequences. Here we use lake water isotope data across gradients of terrestrial vegetation cover (open tundra to closed forest) and topographic relief to identify lakes that are vulnerable to desiccation under conditions of low snowmelt runoff in two subarctic landscapes—Old Crow Flats, Yukon, and Hudson Bay Lowlands, Manitoba (Canada). Lakes located in low-relief, open tundra catchments in both landscapes displayed a systematic, positive offset between directly measured lake water $\delta^{18}\text{O}$ over multiple sampling campaigns and lake water $\delta^{18}\text{O}$ inferred from cellulose in recently deposited surface sediments. We attribute this offset to a strong evaporative ^{18}O -enrichment response to lower-than-average snowmelt runoff in recent years. Notably, some lakes underwent near-complete desiccation during midsummer 2010 following a winter of very low snowfall. Based on the paleolimnological record of one such lake, the extremely dry conditions in 2010 may be unprecedented in the past ~200 years. Findings fuel concerns that a decrease in snowmelt runoff will lead to widespread desiccation of shallow lakes in these landscapes. **Citation:** Bouchard, F., et al. (2013), Vulnerability of shallow subarctic lakes to evaporate and desiccate when snowmelt runoff is low, *Geophys. Res. Lett.*, 40, 6112–6117, doi:10.1002/2013GL058635.

1. Introduction

[2] Northern lake-rich landscapes are vital for wildlife, carbon exchange with the atmosphere, and natural resources utilized by local indigenous communities. Shallow ponds and lakes (typically $\leq 1\text{m}$ depth) are the dominant basin type in

these regions. Numerous studies have examined recent changes in the distribution and surface area of these water bodies; some have reported lake expansion (e.g., in the case of thermokarst lakes), while others have documented water level decline [Smith et al., 2005; Carroll et al., 2011]. An especially acute concern is that longer ice-free seasons and increasing importance of open water evaporation will lead to desiccation of shallow lakes, as observed in Canada's High Arctic [Smol and Douglas, 2007]. In these landscapes, snowmelt is important for replenishing shallow lakes and is likely to become even more crucial as evaporative drawdown intensifies with continued warming [Schindler and Smol, 2006].

[3] Old Crow Flats (OCF), Yukon, and northwestern Hudson Bay Lowlands (HBL), Manitoba, are two of Canada's largest lake-rich subarctic landscapes. Total surface water areas (including several thousand ponds and lakes; hereafter referred to as "lakes") comprise a significant portion of these landscapes, and both regions have undergone recent warming. In OCF, dendroclimatological records indicate anomalously warm conditions during the twentieth century in the context of the past 300 years [Porter and Pisarcic, 2011]. Paleolimnological data from the southern HBL indicate that lakes began to respond to climate warming in the 1990s [Rühland et al., 2013]. Prior studies of lakes in these landscapes have identified several potential future hydrological consequences in response to continued warming, which will depend upon changes in catchment vegetation, hydrological connectivity, permafrost conditions, seasonal distribution of precipitation, and other factors [Turner et al., 2010; 2013; Wolfe et al., 2011].

[4] Here we explore the sensitivity of shallow lakes in OCF and HBL to one hydrological outcome: evaporative lake level drawdown following winters of low snow accumulation. We compare multiple measurements of lake water oxygen isotope composition ($\delta^{18}\text{O}_{\text{lw}}$) with that inferred from the cellulose fraction ($\delta^{18}\text{O}_{\text{mf-lw}}$) of surface sediments of 70 lakes spanning a broad gradient of vegetation cover. Winters of very low snow accumulation occurred immediately prior to several of the ice-free seasons when we conducted water isotope sampling, whereas the 5 year intervals prior to the water sampling were characterized by snowfall similar to (HBL) or greater than (OCF) the 1971–2000 climate normals. This provided a unique opportunity to identify the characteristics of shallow lakes in these subarctic landscapes that are most vulnerable to desiccation under conditions of low snowmelt runoff.

2. Study Areas

[5] Located in the continuous permafrost zone at the northern boreal tree line ~25 km north of the town of Old Crow, OCF encompasses ~2700 shallow lakes, mostly of thermokarst

Additional supporting information may be found in the online version of this article.

¹Centre d'études nordiques and Département de Géographie, Université Laval, Québec, Québec, Canada.

²Department of Geography and Environmental Studies, Wilfrid Laurier University, Waterloo, Ontario, Canada.

³Department of Geography, Brock University, St. Catharines, Ontario, Canada.

⁴Department of Biology, University of Waterloo, Waterloo, Ontario, Canada.

⁵Department of Earth and Environmental Sciences, University of Waterloo, Waterloo, Ontario, Canada.

Corresponding author: F. Bouchard, Centre d'études nordiques, Université Laval, 2405 rue de la Terrasse, Québec, QC G1V 0A6, Canada. (frederic.bouchard@cen.ulaval.ca)

©2013. American Geophysical Union. All Rights Reserved.
0094-8276/13/10.1002/2013GL058635

6112

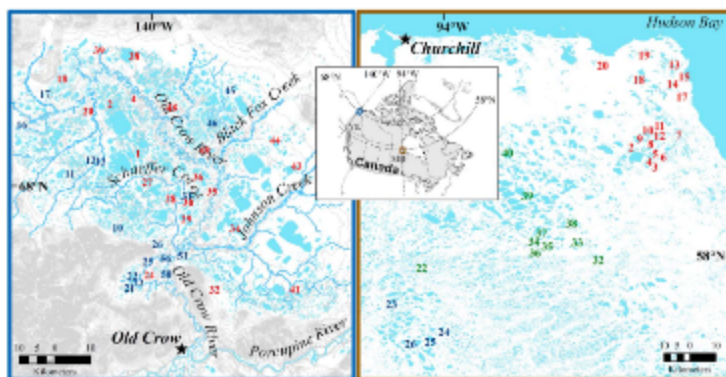


Figure 1. Location of the study areas: (a) Old Crow Flats (OCF), Yukon, (b) northwestern Hudson Bay Lowlands (HBL), Manitoba. The sampled shallow lakes are identified by numbers, color coded based on their classification (i.e., OCF: snowmelt-dominated and rainfall-dominated lakes are labeled in blue and red, respectively; HBL: BSF, IPP, and CF lakes are labeled in blue, green, and red, respectively).

origin (Figure 1). This ~5600 km² wetland complex, recognized by the Ramsar Convention for its ecological and cultural importance, provides habitat for abundant wildlife and supports the traditional lifestyle of the Vuntut Gwitchin First Nation. OCF is the former lakeland of Glacial Lake Old Crow [Zazula et al., 2004]. The permafrost and fine-grained glaciolacustrine sediments inhibit infiltration of surface water. Thus, lake water level fluctuations are mainly reflective of hydrological processes operating at or near the surface. Lakes have been classified mainly as snowmelt- or rainfall-dominated, reflecting their predominant source waters, and are associated with forest or tundra vegetation in their catchments, respectively [Turner et al., 2010, 2013].

[6] HBL is a low-relief landscape that spans continuous and discontinuous permafrost and traverses the northern boreal tree line. HBL developed following the end of the Wisconsinian glaciation and the retreat of the Laurentide Ice Sheet and is underlain by impermeable silts and clays deposited by the Tyrrell Sea [Dredge and Nixon, 1992]. Consequently, water pools on the surface creating thousands of lakes; many of which are formed by thermokarst processes. Near the Hudson Bay coast, isostatic rebound has produced a series of raised beaches, and the topographic depressions between them are also often occupied by lakes. Three major ecological zones can be identified in Wapusk National Park in northwestern HBL: coastal fen (CF) dominated by tundra vegetation, interior peat plateaus/palsa bog (IPP) that contains small shrubs, and boreal spruce forest (BSF) (Figure 1) [Parks Canada, 2013].

3. Methods

[7] Lake water and surface sediment samples were retrieved from 38 snowmelt- ($n=17$) and rainfall-dominated ($n=21$) lakes in OCF (as defined by Turner et al. [2010]) and from 32 lakes spanning the three major ecozones in Wapusk National Park, HBL (CF: $n=18$; IPP: $n=10$; BSF: $n=4$; Figure 1). Water samples were collected in 30 ml high-density polyethylene bottles at ~10 cm depth three times (June, July, and September) during the ice-free season in OCF (2007–2008) and HBL (2010–2012). Surface sediments (upper 1–2 cm) were collected in September 2008 in OCF and

September 2012 in HBL using a coring tube (38mm internal diameter). Cellulose was isolated from the sediments following several steps designed to remove noncellulose organic and inorganic fractions [Wolfe et al., 2001, 2007]. Water and surface sediment cellulose oxygen isotope compositions were determined at the University of Waterloo-Environmental Isotope Laboratory (UW-EIL) using conventional techniques [Epstein and Mayeda, 1953; Wolfe et al., 2007]. Results are expressed as δ values, representing deviations (‰) from Vienna Standard Mean Ocean Water (VSMOW) such that $\delta_{\text{sample}} = [(R_{\text{sample}}/R_{\text{VSMOW}}) - 1] \times 10^3$, where R is the ¹⁸O/¹⁶O ratio in sample and VSMOW. The δ values are normalized to -55.5‰ for Standard Light Antarctic Precipitation [Coplen, 1996]. Surface sediment $\delta^{18}\text{O}_{\text{inf-lw}}$ was calculated using a cellulose-water fractionation factor of 1.028 [DeNiro and Epstein, 1981; Wolfe et al., 2001].

4. Results

[8] Comparison of $\delta^{18}\text{O}_{\text{inf-lw}}$ with $\delta^{18}\text{O}_{\text{lw}}$ showed good agreement for several lakes in OCF (Figure 2a). These results were obtained mainly for the snowmelt-dominated lakes, whereas rainfall-dominated lakes on average possessed $\delta^{18}\text{O}_{\text{inf-lw}}$ values ~7‰ lower than $\delta^{18}\text{O}_{\text{lw}}$. Closer inspection of the relation between $\delta^{18}\text{O}_{\text{inf-lw}}$ and $\delta^{18}\text{O}_{\text{lw}}$ revealed that $\delta^{18}\text{O}_{\text{inf-lw}}$ best aligned with early ice-free season (mean June) $\delta^{18}\text{O}_{\text{lw}}$ for the snowmelt-dominated lakes (Figure 2b). In contrast, all but one of the rainfall-dominated lakes plotted systematically above the 1:1 line. Time series plots of $\delta^{18}\text{O}_{\text{lw}}$ for selected lakes of the snowmelt- (OCF13) and rainfall-dominated (OCF24) categories further demonstrate good agreement between $\delta^{18}\text{O}_{\text{inf-lw}}$ and early ice-free season $\delta^{18}\text{O}_{\text{lw}}$ for OCF13. Yet a much lower $\delta^{18}\text{O}_{\text{inf-lw}}$ was obtained from OCF24 compared to all $\delta^{18}\text{O}_{\text{lw}}$ values (Figure 2c).

[9] Similar patterns were evident when comparing $\delta^{18}\text{O}_{\text{inf-lw}}$ with $\delta^{18}\text{O}_{\text{lw}}$ for lakes in HBL (Figures 2d–2f). For lakes in the BSF and most lakes in the IPP, $\delta^{18}\text{O}_{\text{inf-lw}}$ was in good agreement with $\delta^{18}\text{O}_{\text{lw}}$ (Figure 2d). In contrast, eight of the 18 lakes in the CF had $\delta^{18}\text{O}_{\text{inf-lw}}$ that averaged ~6.5‰ lower than $\delta^{18}\text{O}_{\text{lw}}$. Similar to the OCF lakes, $\delta^{18}\text{O}_{\text{inf-lw}}$ agreed best with

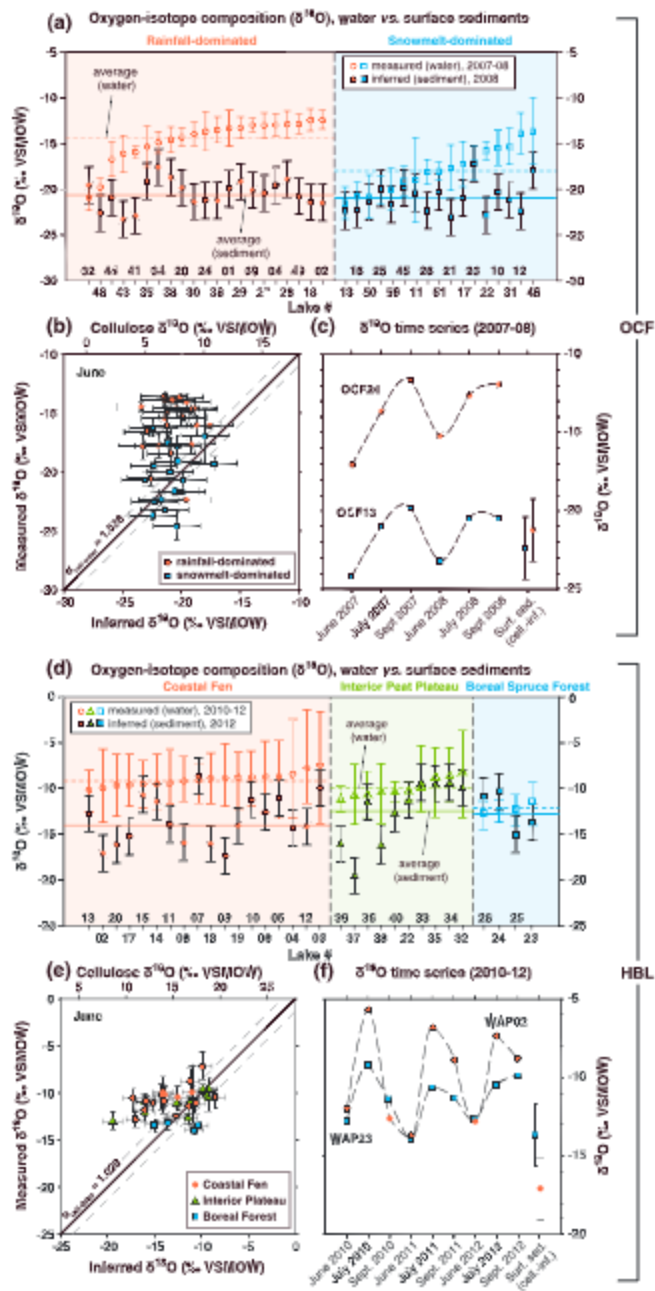


Figure 2

Table 1. Winter (October to April) Precipitation (mm) for Old Crow (Yukon; Station 2100800) and Churchill (Manitoba; Average of Stations 5060600, 5060606, and 5060608)^a

Period	Old Crow	Churchill
2001–2002	99.7 ^b	
2002–2003	99.3 ^b	
2003–2004	135.3 ^b	
2004–2005	151.2 ^b	185.6 ^b
2005–2006	>61.9 ^c	165.2 ^b
2006–2007	148.0 ^d	180.2 ^b
2007–2008	35.0 ^d	151.9 ^b
2008–2009		133.5 ^b
2009–2010		62.9 ^d
2010–2011		46.0 ^d
2011–2012		164.9 ^d
Climate normal, 1971–2000	104.3	167.7
Average, years prior to water sampling	121.4	163.3
Average, years of water sampling	91.5	91.3

^aEnvironment Canada [2013].^bYears prior to water sampling.^cIncomplete record (not included in average calculation).^dYears of water sampling.

early ice-free season (mean June) $\delta^{18}\text{O}_{\text{lw}}$ (Figures 2c and 2f). For the lakes that did not display agreement between $\delta^{18}\text{O}_{\text{mf-lw}}$ and $\delta^{18}\text{O}_{\text{lw}}$ (mainly in the CF), results were positioned systematically above the 1:1 line (Figure 2c) and $\delta^{18}\text{O}_{\text{mf-lw}}$ was lower than the seasonal range of $\delta^{18}\text{O}_{\text{lw}}$ (Figure 2f).

5. Discussion and Conclusions

[10] Agreement between $\delta^{18}\text{O}_{\text{mf-lw}}$ and mean June $\delta^{18}\text{O}_{\text{lw}}$ for most of the snowmelt-dominated lakes in OCF, as well as all BSF and most IPP lakes in HBL, can be explained by high aquatic production during the early part of the ice-free season. At this time, lake waters are supplied by isotopically depleted snowmelt runoff that is rich in dissolved nutrients from interactions with soil and plant organic matter. In OCF, snowmelt-dominated lakes have higher concentrations of nutrients including dissolved phosphorus, silica, and organic carbon compared to rainfall-dominated lakes [Balasubramanian, 2012]. Furthermore, incorporation of isotopic signatures from the early ice-free season by aquatic cellulose has been identified in paired analyses of seasonal $\delta^{18}\text{O}_{\text{lw}}$ and surface sediment $\delta^{18}\text{O}_{\text{mf-lw}}$ from other shallow boreal lakes [e.g., Wolfe et al., 2012].

[11] We considered several hypotheses to explain the positive offset in $\delta^{18}\text{O}_{\text{lw}}$ relative to $\delta^{18}\text{O}_{\text{mf-lw}}$ that is evident for most of the rainfall-dominated lakes in OCF and some of the CF and IPP ecozone lakes of HBL. Potential incorporation of nonaquatic cellulose from terrestrial sources always poses concern when using sediment cellulose as a lake water oxygen isotope archive [Sauer et al., 2001], yet this would not yield a positive offset, since terrestrial cellulose should be more enriched under the same climatic conditions

[Edwards and McAndrews, 1989]. Organic carbon and nitrogen elemental and isotope data for the surface sediments of these lakes (see Table S1 in the supporting information) also supports a fully aquatic origin for sedimentary organic matter, and hence the validity of the inferred positive $\delta^{18}\text{O}_{\text{lw}} - \delta^{18}\text{O}_{\text{mf-lw}}$ offset. On the other hand, meteorological records reveal that three of our water-sampling campaigns were performed following winters of substantially lower snowfall (i.e., winter 2007–2008 for OCF and 2009–2010, 2010–2011 for HBL) compared to climate normals (Table 1). Furthermore, average snowfall was 25% and 44% less during the water-sampling years in Old Crow and Churchill, respectively, compared to the average of the 5 years immediately prior. Although we recognize that precipitation can be spatially heterogeneous, a meteorological station deployed in central OCF during our water-sampling years showed good agreement with the Environment Canada meteorological station records from the hamlet of Old Crow [Turner et al., 2013]. Thus, less snow generated less snowmelt runoff to several lakes during the water-sampling years, which resulted in more pronounced isotopic enrichment by evaporation compared to the time intervals captured by the surface sediments (which span ~5–10 years based on paleolimnological studies) [e.g., Wolfe et al., 2011; MacDonald et al., 2012]. Turner et al. [2013] identified strong evaporative isotopic enrichment in OCF lake waters during 2008, following a winter of low snow accumulation. Our results suggest that a similar evaporative response explains the positive offset in $\delta^{18}\text{O}_{\text{lw}}$ relative to $\delta^{18}\text{O}_{\text{mf-lw}}$, albeit over longer time scales. These hydrologically sensitive or “flashy” lakes are mostly situated in catchments characterized by low-relief terrain and sparse tundra vegetation where snow cover is vigorously redistributed by wind.

[12] Shallow subarctic lakes that undergo pronounced evaporation when snowmelt runoff is low may desiccate. In fact, this was observed in midsummer 2010 in HBL (Figure 3a), which may reflect an extreme hydrological consequence of recent climate warming in this region—warming that has led to shifts in algal communities in deeper lakes in the southern HBL [Rühland et al., 2013]. Additional paleolimnological data suggest that shallow subarctic lakes in northwestern HBL, like their high-arctic counterparts, may indeed be approaching the “final ecological threshold” [cf. Smol and Douglas, 2007]. Lake water $\delta^{18}\text{O}$ reconstructed from cellulose $\delta^{18}\text{O}$ measurements along a 24.5 cm long sediment core retrieved from CF lake WAP12, which almost completely desiccated during midsummer 2010, indicate remarkably stable hydrological conditions over most of the past ~200 years (Figure 3b). Although desiccation horizons in lacustrine strata can be difficult to identify, the WAP12 record appears to contain no evidence of comparably dry intervals in the past.

[13] Low snowmelt runoff and lake desiccation during midsummer 2010 may be a sign of things to come for the HBL and other regions with shallow lakes in catchments having low-relief and sparse tundra vegetation. Based on

Figure 2. Comparison of measured lake water oxygen isotope composition ($\delta^{18}\text{O}_{\text{lw}}$) with surface sediment cellulose-inferred lake water oxygen isotope composition ($\delta^{18}\text{O}_{\text{mf-lw}}$) for (a–c) Old Crow Flats (OCF) and (d–f) northwestern Hudson Bay Lowlands (HBL) lakes: $\delta^{18}\text{O}_{\text{lw}}$ range versus $\delta^{18}\text{O}_{\text{mf-lw}}$ (Figures 2a and 2d), mean and range for June $\delta^{18}\text{O}_{\text{lw}}$ versus $\delta^{18}\text{O}_{\text{mf-lw}}$ (Figures 2b and 2e), time series of $\delta^{18}\text{O}_{\text{lw}}$ for lakes OCF13 (snowmelt dominated) and OCF24 (rainfall dominated), WAP02 (coastal fen) and WAP23 (boreal spruce forest), and $\delta^{18}\text{O}_{\text{mf-lw}}$ (Figures 2c and 2f). Lake categories and ecological zones as defined by Turner et al. [2010] and Parks Canada [2013], respectively. Error bars for $\delta^{18}\text{O}_{\text{mf-lw}}$ represent estimated uncertainties of +2.0‰.

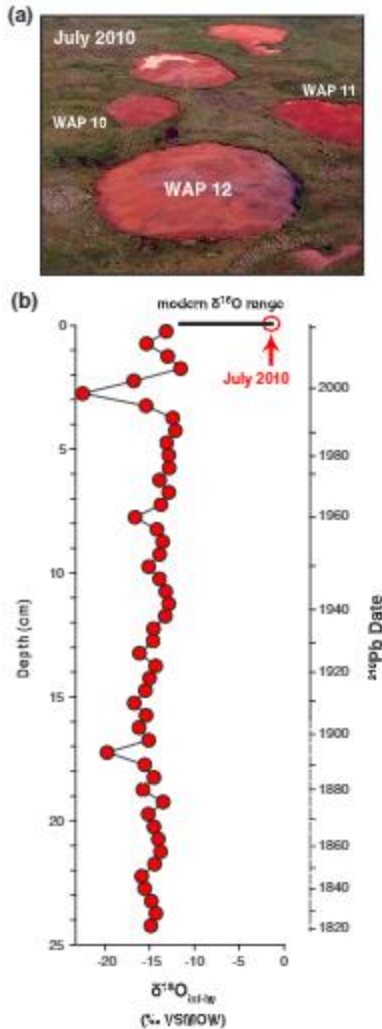


Figure 3. (a) Near-complete desiccation of WAP12 (and other nearby lakes) during midsummer of 2010. Note that despite lower snowfall in 2010–2011, substantial late summer rainfall in 2010 prevented desiccation of WAP12 in 2011. (b) cellulose-inferred lake water oxygen isotope composition ($\delta^{18}\text{O}_{\text{meq-1w}}$) record from lake WAP12 (coastal fen ecozone). The depth-age model was determined using ^{210}Pb (see supporting information).

satellite data spanning the past 4 decades, *Derksen and Brown* [2012] reported marked reductions in spring (April to June) snow cover extent over the Northern Hemisphere and indicated that the rate of snow cover loss from 1979 to 2011 (−17.8% per decade) was almost double the rate of September sea ice loss during the same period (−10.8% per decade). Moreover, the lowest spring snow cover extent for

both North America and Eurasia has occurred during the 2008–2012 period; the year 2010 set a record low for North America. Trends toward declining snow cover are expected to continue [*Derksen and Brown*, 2012], although significant spatial and seasonal differences are projected to occur [*Arctic Monitoring and Assessment Programme*, 2011; *Krasting et al.*, 2013].

[14] For regions that experience a decline in snow cover extent and reduction in snowmelt runoff with continued warming, our isotope data coupled with field observations from two of Canada's largest lake-rich subarctic landscapes indicate that shallow lakes located in low-relief, open tundra terrain are particularly susceptible to desiccation by evaporation. Such hydrological changes will have profound effects on wildlife habitat, carbon cycling, and other aquatic ecosystem services [e.g., *van der Molen et al.*, 2007; *Abnizova et al.*, 2012].

[15] **Acknowledgments.** This research was supported by the Natural Sciences and Engineering Research Council (NSERC) of Canada, the Government of Canada International Polar Year Program, the Northern Scientific Training Program of Aboriginal Affairs and Northern Development Canada, the Polar Continental Shelf Program, and the Churchill Northern Studies Centre. A. M. Balasubramanian contributed to fieldwork. We thank the staff of the UW-EIL for isotope analyses and two anonymous reviewers and the Editor for their helpful comments. This article is a contribution to the NSERC Discovery Frontiers project ADAPT (Arctic Development and Adaptation to Permafrost in Transition).

[16] The Editor thanks two anonymous reviewers for their assistance in evaluating this manuscript.

References

- Abnizova, A., J. Siemens, M. Langer, and J. Boike (2012), Small ponds with major impact: The relevance of ponds and lakes in permafrost landscapes to carbon dioxide emissions, *Global Biogeochem. Cycles*, *26*, GB2041, doi:10.1029/2011gb004237.
- Arctic Monitoring and Assessment Programme (2011), *Snow, Water, Ice and Permafrost in the Arctic (SWIPA): Climate Change and the Cryosphere*, pp. 538, Arctic Monitoring and Assessment Programme (AMAP), Oslo.
- Balasubramanian, A. M. (2012), Characterizing hydro-limnological relationships in the shallow thermokarst lakes of the Old Crow Flats Yukon Territory, *Arctic*, *65*, 500–503.
- Carroll, M. L., J. R. G. Townshend, C. M. DiMiceli, T. Loboda, and R. A. Sohlberg (2011), Shrinking lakes of the Arctic: Spatial relationships and trajectory of change, *Geophys. Res. Lett.*, *38*, L20406, doi:10.1029/2011gl049427.
- Coplen, T. B. (1996), New guidelines for reporting stable hydrogen, carbon, and oxygen isotope-ratio data, *Geochim. Cosmochim. Acta*, *60*, 3359–3360.
- DeNiro, M. J., and S. Epstein (1981), Isotopic composition of cellulose from aquatic organisms, *Geochim. Cosmochim. Acta*, *45*, 1885–1894.
- Derksen, C., and R. Brown (2012), Spring snow cover extent reductions in the 2008–2012 period exceeding climate model projections, *Geophys. Res. Lett.*, *39*, L19504, doi:10.1029/2012gl053387.
- Dredge, L. A., and F. M. Nixon (1992), Glacial and environmental geology of northeastern Manitoba, 80 pp., Geological Survey of Canada, Memoir 432.
- Edwards, T. W. D., and J. H. McAndrews (1989), Paleohydrology of a Canadian Shield lake inferred from ^{18}O in sediment cellulose, *Can. J. Earth Sci.*, *26*, 1850–1859.
- Environment Canada (2013), Climate Data Online, http://climate.weatheroffice.gc.ca/climateData/canada_e.html (last accessed: 2013-06-01).
- Epstein, S., and T. Mayeda (1953), Variation of O^{18} content of waters from natural sources, *Geochim. Cosmochim. Acta*, *4*, 213–224.
- Krasting, J. P., A. J. Broccoli, K. Dixon, and J. Lanzante (2013), Future changes in northern hemisphere snowfall, *J. Clim.*, doi:10.1175/JCLI-D-12-00832.1.
- MacDonald, L. A., K. W. Turner, A. M. Balasubramanian, B. B. Wolfe, R. I. Hall, and J. N. Sweetman (2012), Tracking hydrological responses of a thermokarst lake in the Old Crow Flats (Yukon Territory, Canada) to recent climate variability using aerial photographs and paleolimnological methods, *Hydro. Process.*, *26*, 117–129, doi:10.1002/hyp.8116.
- Parks Canada (2013), Wapusk National Park of Canada, <http://www.pc.gc.ca/pn-tp/mb/wapusk/index.aspx> (last accessed: 2013-06-01).
- Porter, T. J., and M. F. J. Pisarcic (2011), Temperature growth divergence in white spruce forests of Old Crow Flats, Yukon Territory, and adjacent

- regions of northwestern North America, *Global Change Biol.*, *17*, 3418–3430, doi:10.1111/j.1365-2486.2011.02507.x.
- Rübländ, K. M., A. M. Paterson, W. Keller, N. Michelutti, and J. P. Smol (2013), Global warming triggers the loss of a key Arctic refugium, *Proc. R. Soc. B.*, *280*, 20131887, doi:10.1098/rspb.2013.1887.
- Sauer, P. E., G. H. Miller, and J. T. Overpeck (2001), Oxygen isotope ratios of organic matter in arctic lakes as a paleoclimate proxy: Field and laboratory investigations, *J. Paleolimnol.*, *25*, 43–64.
- Schindler, D. W., and J. P. Smol (2006), Cumulative effects of climate warming and other human activities on freshwaters of Arctic and subarctic North America, *AMBIO*, *35*, 160–168, doi:10.1579/0044-7447(2006)35[160:ceocwa]2.0.co;2.
- Smith, L. C., Y. Sheng, G. M. MacDonald, and L. D. Hinzman (2005), Disappearing Arctic lakes, *Science*, *308*, 1429, doi:10.1126/science.1108142.
- Smol, J. P., and M. S. V. Douglas (2007), Crossing the final ecological threshold in high Arctic ponds, *Proc. Natl. Acad. Sci. U.S.A.*, *104*, 12,395–12,397, doi:10.1073/pnas.0702777104.
- Turner, K. W., B. B. Wolfe, and T. W. D. Edwards (2010), Characterizing the role of hydrological processes on lake water balances in the Old Crow Flats, Yukon Territory, Canada, using water isotope tracers, *J. Hydrol.*, *386*, 103–117, doi:10.1016/j.jhydrol.2010.03.012.
- Turner, K. W., B. B. Wolfe, T. W. D. Edwards, T. C. Lantz, R. I. Hall, and G. Larocque (2013), Controls on water balance of shallow thermokarst lakes and their relations with catchment characteristics: A multi-year, landscape-scale assessment based on water isotope tracers and remote sensing in Old Crow Flats, Yukon (Canada), *Global Change Biol.*, doi:10.1111/gcb.12465, in press.
- van der Molen, M. K., J. van Huissteden, F. J. W. Parmentier, A. M. R. Petrescu, A. J. Dolman, T. C. Maximov, A. V. Kononov, S. V. Karsanaev, and D. A. Suzdalov (2007), The growing season greenhouse gas balance of a continental tundra site in the Indigirka lowlands, NE Siberia, *Biogeochemistry*, *4*, 985–1003.
- Wolfe, B. B., T. W. D. Edwards, R. J. Elgood, and K. R. M. Beuning (2001), Carbon and oxygen isotope analysis of lake sediment cellulose: Methods and applications, in *Tracking Environmental Change Using Lake Sediments. Volume 2: Physical and Geochemical Methods*, edited by W. M. Last and J. P. Smol, pp. 373–400, Kluwer, Dordrecht, The Netherlands.
- Wolfe, B. B., M. D. Falcone, K. P. Clogg-Wright, C. L. Mongeon, Y. Yi, B. E. Brock, N. A. St. Amour, W. A. Mark, and T. W. D. Edwards (2007), Progress in isotope paleohydrology using lake sediment cellulose, *J. Paleolimnol.*, *37*, 221–231, doi:10.1007/s10933-006-9015-8.
- Wolfe, B. B., E. M. Light, M. I. Macrae, R. I. Hall, K. Eichel, S. Jasechko, J. White, L. Fishback, and T. W. D. Edwards (2011), Divergent hydrological responses to 20th century climate change in shallow tundra ponds, western Hudson Bay Lowlands, *Geophys. Res. Lett.*, *38*, L23402, doi:10.1029/2011gl049766.
- Wolfe, B. B., R. I. Hall, T. W. D. Edwards, and J. W. Johnston (2012), Developing temporal hydroecological perspectives to inform stewardship of a northern floodplain landscape subject to multiple stressors: Paleolimnological investigations of the Peace-Athabasca Delta, *Environ. Rev.*, *20*, 191–210, doi:10.1139/a2012-008.
- Zazula, G. D., A. Duk-Rodkin, C. E. Schweger, and R. E. Morlan (2004), Late Pleistocene chronology of glacial Lake Old Crow and the northwest margin of the Laurentide ice sheet, in *Quaternary Glaciations—Extent and Chronology. Part II: North America*, edited by J. Ehlers and P. L. Gibbard, pp. 347–362, Elsevier, Amsterdam, The Netherlands.

**JOHN WILEY AND SONS LICENSE
TERMS AND CONDITIONS**

Apr 04, 2019

This Agreement between Wilfrid Laurier University -- Hilary White ("You") and John Wiley and Sons ("John Wiley and Sons") consists of your license details and the terms and conditions provided by John Wiley and Sons and Copyright Clearance Center.

License Number	4557741103894
License date	Mar 28, 2019
Licensed Content Publisher	John Wiley and Sons
Licensed Content Publication	Geophysical Research Letters
Licensed Content Title	Vulnerability of shallow subarctic lakes to evaporate and desiccate when snowmelt runoff is low
Licensed Content Author	F. Bouchard, K. W. Turner, L. A. MacDonald, et al
Licensed Content Date	Dec 8, 2013
Licensed Content Volume	40
Licensed Content Issue	23
Licensed Content Pages	6
Type of use	Dissertation/Thesis
Requestor type	Author of this Wiley article
Format	Electronic
Portion	Full article
Will you be translating?	No
Title of your thesis / dissertation	Development and application of hydrological and limnological monitoring in pond-rich landscapes of Canada's subarctic National Parks
Expected completion date	May 2019
Expected size (number of pages)	200
Requestor Location	Wilfrid Laurier University 75 University Ave W Department of Geography Arts Building Waterloo, ON N2L 3C5 Canada Attn: Hilary White
Publisher Tax ID	EU826007151
Total	0.00 CAD



A synthesis of thermokarst lake water balance in high-latitude regions of North America from isotope tracers¹

Lauren A. MacDonald, Brent B. Wolfe, Kevin W. Turner, Lesleigh Anderson, Christopher D. Arp, S. Jean Birks, Frédéric Bouchard, Thomas W.D. Edwards, Nicole Farquharson, Roland I. Hall, Ian McDonald, Biljana Narancic, Chantal Ouimet, Reinhard Pienitz, Jana Tondou, and Hilary White

Abstract: Numerous studies utilizing remote sensing imagery and other methods have documented that thermokarst lakes are undergoing varied hydrological transitions in response to recent climate changes, from surface area expansion to drainage and evaporative desiccation. Here, we provide a synthesis of hydrological conditions for 376 lakes of mainly thermokarst origin across high-latitude North America. We assemble surface water isotope compositions measured during the past decade at five lake-rich landscapes including Arctic Coastal Plain (Alaska), Yukon Flats (Alaska), Old Crow Flats (Yukon), northwestern Hudson Bay Lowlands (Manitoba), and Nunavik (Quebec). These landscapes represent the broad range of thermokarst environments by spanning gradients in meteorological, permafrost, and vegetation conditions. An isotope framework was established based on flux-weighted long-term averages of meteorological conditions for each lake to quantify water balance metrics. The isotope composition of source water and evaporation-to-inflow ratio for each lake were determined, and the results demonstrated a substantial array of regional and subregional diversity of lake hydrological conditions. Controls on lake water balance and how these vary among the five landscapes and with differing environmental drivers are assessed. Findings reveal that lakes in the Hudson Bay Lowlands are most vulnerable to evaporative desiccation, whereas those in Nunavik are most resilient. However, we also identify the complexity in predicting hydrological responses of these thermokarst landscapes to future climate change.

Key words: thermokarst lakes, high-latitude regions, water isotope tracers, hydrology, permafrost, climate change.

Received 14 June 2016. Accepted 3 November 2016.

L.A. MacDonald, B.B. Wolfe, N. Farquharson, and H. White. Department of Geography and Environmental Studies, Wilfrid Laurier University, 75 University Avenue West, Waterloo, ON N2L 3C5, Canada.

K.W. Turner. Department of Geography, Brock University, St. Catharines, ON L2S 3A1, Canada.

L. Anderson. Geosciences and Environmental Change Science Center, US Geological Survey, Denver, CO 80225, USA.

C.D. Arp. Water and Environmental Research Centre, University of Alaska Fairbanks, Fairbanks, AK 99775, USA.

S.J. Birks. InnoTech Alberta, Calgary, AB T2L 2A6, Canada; Department of Geography, University of Victoria, Victoria, BC V8W 3R4, Canada.

F. Bouchard, B. Narancic, and R. Pienitz. Département de Géographie, Université Laval, QC G1V 0A6, Canada.

T.W.D. Edwards. Department of Earth and Environmental Sciences, University of Waterloo, Waterloo, ON N2L 3G1, Canada.

R.I. Hall and J. Tondou. Department of Biology, University of Waterloo, Waterloo, ON N2L 3G1, Canada.

I. McDonald. Yukon Field Unit, Parks Canada, Whitehorse, YT Y1A 2B5, Canada.

C. Ouimet. Parks Canada Agency, Churchill, MB R0B 0E0, Canada.

Corresponding author: Lauren A. MacDonald (email: L7macdong@uwaterloo.ca).

¹This article is part of a Special issue entitled "Arctic permafrost systems".

Brent B. Wolfe currently serves as an Associate Editor; peer review and editorial decisions regarding this manuscript were handled by Warwick Vincent.

This article is open access. This work is licensed under a Creative Commons Attribution 4.0 International License (CC BY 4.0). http://creativecommons.org/licenses/by/4.0/deed.en_GB.

Résumé : De nombreuses études utilisant des images de télédétection et d'autres méthodes ont porté à notre connaissance que les lacs thermokarstiques subissent des transitions hydrologiques diverses en réponse aux changements climatiques récents, soit de l'expansion de leur superficie au drainage et à la dessiccation par l'évaporation. Ici, nous fournissons une synthèse des conditions hydrologiques de 376 lacs d'origine principalement thermokarstique, et ce, à travers les hautes latitudes en Amérique du Nord. Nous assemblons des compositions isotopiques d'eau de surface mesurées au cours de la dernière décennie et provenant de cinq régions abondantes en lacs y compris la plaine côtière de l'Arctique (Alaska), la plaine du Yukon (Alaska), la plaine Old Crow (Yukon), les basses terres de la baie d'Hudson du nord-ouest (Manitoba) et le Nunavik (Québec). Ces régions représentent la vaste gamme d'environnements thermokarstiques couvrant des gradients de conditions météorologiques, de pergélisol et de végétation. Un cadre d'isotopes a été établi en fonction des moyennes à long terme pondérées par le flux des conditions météorologiques pour chaque lac afin de quantifier les paramètres du bilan hydraulique. On a déterminé la composition des isotopes d'eau de source et le rapport entre l'évaporation et le débit entrant pour chaque lac et les résultats ont indiqué que les conditions hydrologiques des lacs s'étalent sur une gamme substantielle de diversité régionale et sous régionale. On évalue les contrôles en matière du bilan hydraulique des lacs et comment ceux-ci varient entre les cinq régions et selon les différents facteurs environnementaux. Les résultats révèlent que les lacs des basses terres de la baie d'Hudson sont les plus vulnérables à la dessiccation par évaporation, tandis que ceux dans le Nunavik sont les plus résistants. Cependant, nous définissons aussi la complexité quant à la prédiction des réponses hydrologiques de ces régions thermokarstiques à la suite de changement climatique futur.

Mots-clés : lacs thermokarstiques, régions de hautes latitudes, traceur d'isotope d'eau, hydrologie, pergélisol, changement climatique.

Introduction

Thermokarst lakes and ponds (hereafter referred to collectively as lakes) are plentiful across permafrost terrain, occupying 15–50% of the landscape in northwestern Canada, Siberia, and Alaska (e.g., Mackay 1988; Rampton 1988; Frohn et al. 2005; Grosse et al. 2005; Plug et al. 2008). Thermokarst lakes form as ice-rich permafrost thaws and surface water accumulates where subsidence occurs. These shallow waterbodies (generally <10 m deep and frequently <2 m) are a key component of northern hydrological and biogeochemical cycles, provide habitat and resources for wildlife and waterfowl populations, and support the traditional lifestyle of many indigenous communities. During the past few decades, increasing air temperatures and changes in precipitation patterns have been observed throughout much of the Arctic (e.g., ACIA 2004; IPCC 2013). Understanding the effects of climate change on thermokarst lake water balance is particularly important, as the greatest effects on aquatic ecosystems will occur indirectly via alteration of hydrological processes and their cascading influences on limnology, biogeochemistry, and aquatic ecology rather than from simply air temperature rise (Rouse et al. 1997; Prowse et al. 2006; Schindler and Smol 2006; Tranvik et al. 2009). Indeed, numerous studies have sought to document the hydrological status of thermokarst lakes. Many of these studies indicate that thermokarst lake hydrology is changing rapidly (e.g., Smith et al. 2005; Carroll et al. 2011), but along varying trajectories including surface area expansion, rapid drainage, and evaporative desiccation (e.g., Yoshikawa and Hinzman 2003; Riordan et al. 2006; Labrecque et al. 2009; Rowland et al. 2010; Bouchard et al. 2013).

Understanding the myriad of potential responses of thermokarst lake hydrology to ongoing climate change requires knowledge of their water balances ($\Delta S/\Delta T$, i.e., change in storage (S) over time (T)), which can be generally characterized as follows (Turner et al. 2010):

$$(1) \quad \Delta S/\Delta T = P_S + P_R + I_{OW} + I_S - E - O_{GW} - O_S$$

Positive contributors to thermokarst lake water balance include snowmelt (P_S), rainfall (P_R), subsurface inflow (I_{CW}), and surface channelized inflow (I_S), whereas lake water loss may occur via evaporation (E), subsurface outflow (O_{CW}), and surface outflow (O_S) — the latter potentially occurring catastrophically. Relative roles of hydrological processes that control thermokarst lake water balances may be influenced by a variety of drivers, including meteorological and permafrost (continuous, discontinuous, and sporadic) conditions as primary drivers (e.g., Riordan et al. 2006; Plug et al. 2008; Labrecque et al. 2009). Changes in temperature can alter rates of evaporation (E), while changes in precipitation regimes can lead to direct fluctuations in snowmelt (P_S) and rainfall (P_R) input, surface channelized inflow (I_S), and surface outflow (O_S). Consequently, high rates of evaporation with low snowmelt or rainfall supply can cause lakes to desiccate, while low rates of evaporation and abundant supply from precipitation may result in attaining maximum basin capacity, which can lead to shoreline erosion and lake expansion or even rapid lateral lake drainage (e.g., Riordan et al. 2006; Hinkel et al. 2007; Plug et al. 2008; Marsh et al. 2009; Turner et al. 2010; Jones et al. 2011; MacDonald et al. 2012; Bouchard et al. 2013). A warming climate also causes increased permafrost degradation, which can influence thermokarst lake hydrological status (e.g., Yoshikawa and Hinzman 2003; Smith et al. 2005). For many thermokarst lakes, continuous permafrost impedes subsurface inflow (I_{CW}) and outflow (O_{CW}) from contributing significantly to lake water balance. However, as permafrost degrades, subsurface flow pathways can develop, which can lead to vertical lake drainage (e.g., Yoshikawa and Hinzman 2003; Jepsen et al. 2013). Additionally, landscape characteristics, such as catchment vegetation, strongly influence thermokarst lake water balance (Bouchard et al. 2013; Turner et al. 2014). For example, densely forested areas entrap snow, which results in enhanced snowmelt runoff to lakes during spring (P_S) compared to runoff generated in more sparsely vegetated areas.

Deciphering the relative influence of hydrological processes represented in eq. 1 is challenging, especially for lake-rich permafrost landscapes where there may be substantial spatial heterogeneity among lakes and their catchments. Due to logistical constraints of field work in remote locations, it is often impractical to perform direct conventional measurements of hydrological processes on a spatially extensive set of lakes that is required to capture the potential diversity of prevailing conditions. Alternatively, and especially for multiple lake studies across landscapes, measurement of water isotope composition ($\delta^2\text{H}$ and $\delta^{18}\text{O}$) and application of isotope mass-balance models can be used to provide information of hydrological interest, as has recently been demonstrated for the continental United States (Brooks et al. 2014). For remote locations in particular, analysis of lake water isotope compositions is an excellent alternative to more instrument-intensive hydrological approaches. Surface water samples can easily and quickly be obtained during fieldwork, and their isotope compositions are sensitive to hydrological processes that influence lake water balances because systematic and well-understood isotopic fractionation of water occurs as it passes through the hydrological cycle (Edwards et al. 2004; Darling et al. 2006). Thus, the isotope composition of water provides quantitative information on lake water balance conditions, including the relative contributions of input waters (e.g., snowmelt, rain, and permafrost thaw waters as “ δ_i values”) and the relative importance of evaporation (frequently expressed as an evaporation-to-inflow ratio (E/I)). Water isotope analysis has been applied in several northern and remote landscapes on thermokarst as well as other shallow lake systems, yielding novel insight into the diversity and importance of hydrological processes on lake water balances spanning multiple environmental gradients

(e.g., Gibson and Edwards 2002; Brock et al. 2007; Yi et al. 2008; Turner et al. 2010, 2014; Anderson et al. 2013; Tondu et al. 2013; Arp et al. 2015).

As an outcome of the Natural Sciences and Engineering Research Council of Canada Discovery Frontiers ADAPT (Arctic Development and Adaptation to Permafrost in Transition) project (Vincent et al. 2013), we provide a synthesis and snapshot of water balance conditions for 376 lakes in high-latitude North America that mainly formed by thermokarst processes. Specifically, we assemble surface water isotope compositions measured during summers of the past decade from mainly thermokarst lakes across five expansive lake-rich permafrost landscapes. From west to east, these include Arctic Coastal Plain (Alaska) (Arp et al. 2015), Yukon Flats (Alaska) (Anderson et al. 2013), Old Crow Flats (Yukon) (Turner et al. 2010, 2014; Tondu et al. 2013), western Hudson Bay Lowlands (Manitoba) (Bouchard et al. 2013), and Nunavik (Quebec) (Narancic et al. 2017). We use isotope–mass balance modeling to determine lake input–water isotope compositions and E/I ratios and explore their relations among landscapes and with environmental drivers. Results provide a unique opportunity to rank hydrological vulnerability of these lake-rich permafrost landscapes and to predict hydrological responses to various climate change scenarios. While most of these data have been previously published as part of individual landscape hydrological studies, to our knowledge, the present analysis is the first, broad spatial synthesis of lake water balance status across lake-rich permafrost landscapes of North America.

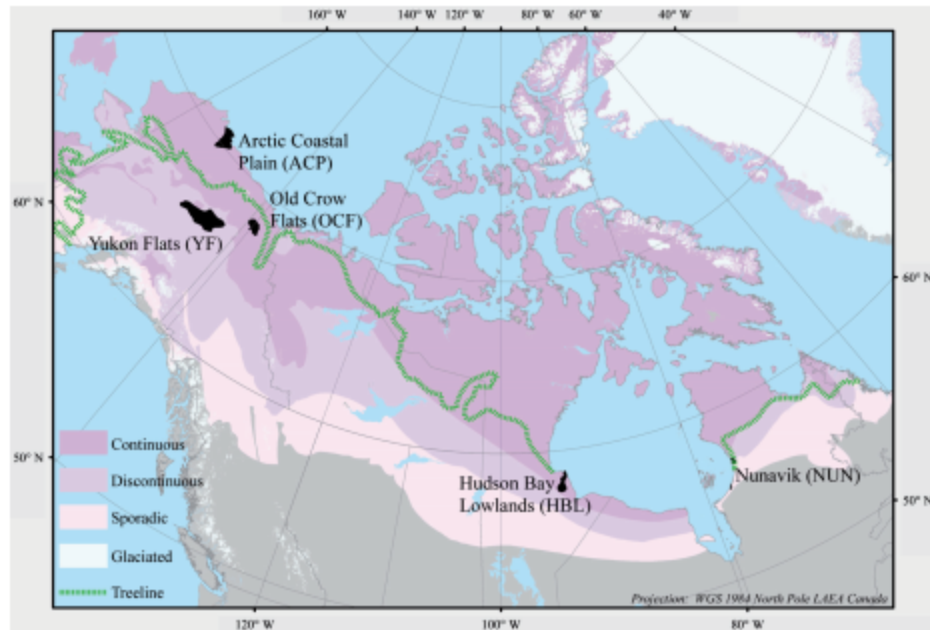
Methods

Study areas

The five study regions (Fig. 1) selected for this synthesis collectively span broad gradients in permafrost, catchment vegetation, and meteorological conditions and contain abundant thermokarst lakes that have been previously sampled and analyzed for water isotope composition. The Arctic Coastal Plain (ACP) north of the Brooks Range in Alaska including lands between Barrow and Prudhoe Bay contains abundant shallow lakes mainly of thermokarst origin, is underlain by continuous permafrost, and contains tundra vegetation (Arp and Jones 2009). The Yukon Flats (YF) spans ~118 000 km² and is set along the Yukon River floodplain and its terraces south of the Brooks Range in Alaska. This lowland interior landscape is located within the zone of discontinuous permafrost and contains over 40 000 lakes of thermokarst, fluvial, and eolian origin (Williams 1962; Arp and Jones 2009). Catchment vegetation includes grassy meadows and muskeg to spruce and birch forests (Anderson et al. 2013). Old Crow Flats (OCF) spans 5600 km² and is situated ~55 km north of the village of Old Crow in northern Yukon Territory. This low-relief landscape is located within an area of continuous permafrost and contains over 2700 shallow primarily thermokarst lakes (Lauriol et al. 2002; Turner et al. 2014). Vegetation in OCF is variable and captures a gradient from spruce forest to tall shrubs to tundra vegetation (Turner et al. 2014). The western Hudson Bay Lowlands (HBL) spans 475 000 km² and contains over 10 000 shallow mainly thermokarst lakes. The HBL is underlain by discontinuous permafrost in the southwest and continuous permafrost in the northeast. Vegetation ranges from boreal spruce forest in the southwest to arctic tundra in the northeast (Rouse 1991; Duguay and Lafleur 2003). Nunavik (NUN), located north of the 55° parallel along the eastern coast of Hudson Bay in northern Quebec, contains abundant thermokarst lakes. Permafrost ranges from sporadic in the south to discontinuous in the north (Allard and Séguin 1987; Brown et al. 2002). Vegetation is mainly spruce–lichen forest in the south and shrub tundra in the north.

Lakes included in this study are considered mainly thermokarst in origin. However, they include a small number of lakes of fluvial and eolian origin in YF, oxbow lakes in OCF, and

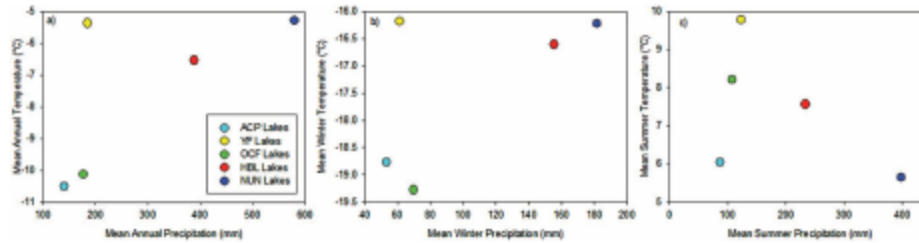
Fig. 1. Location of study regions and their relations with permafrost category. Permafrost spatial data are from Brown et al. (2002).



lakes located in topographic depressions between former beach ridges in HBL. These are included in this synthesis because they constitute a portion of the shallow aquatic ecosystems in these landscapes and for simplicity, we refer to “thermokarst lakes” as all encompassing. Thermokarst lakes from which isotope data have been obtained tend to be shallow and range in surface area (ACP: 0.6–16.2 m, 0.04–9.8 km²; YF: 1–30 m, 0.017–5 km² (Anderson et al. 2013); OCF: 0.47–4.15 m, 2×10^{-3} – 13.181 km² (Turner et al. 2010); HBL: $\sim < 0.5$ m, $< 7 \times 10^{-4}$ – 7.6 km² (Bouchard et al. 2013); NUN: 1–5 m, $\sim 1.3 \times 10^{-6}$ to 2.1×10^{-3} km² (Bouchard et al. 2014; Narancic et al. 2017)).

A common gridded climate database was used to compile regional meteorological records for comparative purposes, to provide necessary parameters for water isotope mass balance modeling, and to gain insight of meteorological influence on lake water balances. The New et al. (2002) gridded climate database was selected due to the availability of lake-specific meteorological data and the ease of use of the database for a large data set, even though it predates our sampling intervals. Mean annual, summer, and winter temperatures and precipitation vary substantially among the five landscapes, based on mean monthly values for 1961–1990 (Fig. 2). Mean annual temperature ranges from -10.5 °C (ACP) to -5.3 °C (NUN) and annual precipitation ranges from 141 mm (ACP) to 580 mm (NUN) (Fig. 2a). ACP and OCF have lower mean annual temperature and precipitation than the other landscapes. YF has relatively low mean annual precipitation but high mean annual temperature, while HBL and NUN have relatively high mean annual temperature and precipitation. Similar patterns exist for mean winter temperature and winter precipitation, with mean winter temperature ranging from -19.2 °C (OCF) to -16.2 °C (NUN) and winter precipitation ranging from 53 mm (ACP) to 182 mm (NUN) (Fig. 2b). Mean summer temperature ranges from 5.6 °C (NUN) to 9.8 °C (YF) and summer precipitation ranges from 88 mm (ACP) to 399 mm (NUN) (Fig. 2c). Compared to mean annual and winter meteorological data, similar patterns

Fig. 2. Average landscape values for (a) mean annual temperature and mean annual precipitation, (b) mean winter temperature and mean winter precipitation, and (c) mean summer temperature and mean summer precipitation extracted from the New et al. (2002) climate database. Winter and summer intervals were defined by mean monthly temperatures below and above 0 °C, respectively.



for ACP, YF, and OCF are evident for summer temperature and summer precipitation. However, HBL has a more midrange mean summer temperature and NUN has the lowest mean summer temperature.

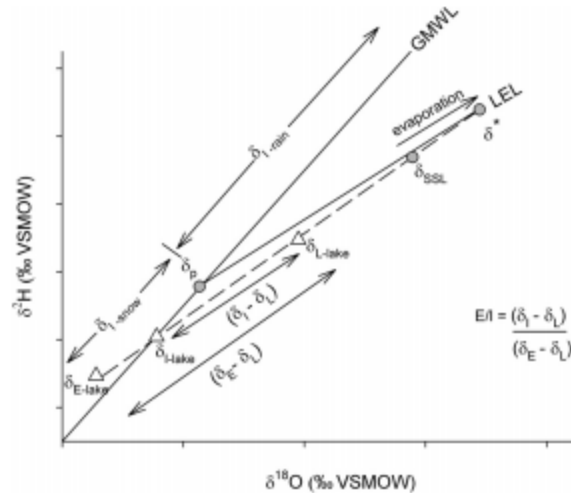
Isotope hydrology

We assembled water isotope compositions ($\delta^2\text{H}$ and $\delta^{18}\text{O}$) for 376 lakes sampled during the past decade in the five study regions. Forty-four lakes were sampled during August 2015 in ACP, 149 lakes were sampled once during the summer between 2007 and 2011 in YF (Anderson et al. 2013), 53 lakes were sampled each summer from 2007 to 2009 and four additional lakes were sampled in 2007 and 2009 in OCF (Turner et al. 2010, 2014), 40 lakes were sampled in the summer of 2010 in HBL and 37 lakes were sampled in the summers of 2011–2012 (Bouchard et al. 2013), and 86 lakes were sampled from one to four times during summers 2011–2014 in NUN (Narancic et al. 2017). Samples were collected at 10–15 cm water depth in either 30 mL high density polyethylene bottles or 20 mL scintillation vials with plastic cone-shaped caps. Samples were transported back to the field base and then shipped to the Alaska Stable Isotope Facility at the University of Alaska Fairbanks (ACP), University of Arizona Environmental Isotope Laboratory (YF), or the University of Waterloo Environmental Isotope Laboratory (OCF, HBL, and NUN) for determination of hydrogen and oxygen isotope compositions using standard mass spectrometric techniques (Epstein and Mayeda 1953; Morrison et al. 2001), with the exception of NUN samples collected in 2014, which were analyzed using Off-Axis Integrated Cavity Output Spectroscopy. Isotope composition results are reported in δ notation, which represents deviations in per mil from Vienna Standard Mean Ocean Water (VSMOW) and are normalized to -428‰ and -55.5‰ for $\delta^2\text{H}$ and $\delta^{18}\text{O}$, respectively, for Standard Light Antarctic Precipitation (Coplen 1996). We restricted our analysis to July and August sample collection time periods to reduce seasonal effects caused by the influence of snowmelt while also capturing the expected midsummer peak in evaporation. For lakes that were sampled more than once per summer (July and August), or over multiple summers, we used the average value in our analyses.

Isotope framework development

Raw water isotope compositions were initially assessed in conventional $\delta^{18}\text{O}$ – $\delta^2\text{H}$ space, superimposed upon an “isotope framework” consisting of the Global Meteoric Water Line (GMWL) and the Local Evaporation Line (LEL) predicted for each landscape (Fig. 3). The GMWL, described by $\delta^2\text{H} = 8\delta^{18}\text{O} + 10$ (Craig 1961), reflects the isotopic distribution of global precipitation. The position of amount-weighted precipitation along the GMWL is mainly dependent on the distillation history of atmospheric moisture contributing to precipitation

Fig. 3. Schematic $\delta^{18}\text{O}$ - $\delta^2\text{H}$ diagram illustrating an approach for the interpretation of lake water isotope data within a region. Key features include the Global Meteoric Water Line (GMWL), the landscape-predicted Local Evaporation Line (LEL), average annual isotope composition of precipitation (δ_p), the terminal basin steady-state isotope composition (δ_{SSL}), the limiting non-steady-state isotope composition (δ^*), lake water isotope composition (δ_L), input water isotope composition (δ_i), and the isotope composition of evaporated vapour from the lake (δ_E).



and commonly leads to snow plotting along an isotopically depleted portion of the GMWL relative to rain (Fig. 3). Surface water isotope compositions, including lakes, typically plot along a LEL, which generally has a slope of 4–6 (Fig. 3). The LEL for a given landscape, as applied in this context, defines the expected isotopic evolution of a surface waterbody undergoing evaporation, fed by waters representing the average annual isotope composition of precipitation (δ_p) for that region. Displacement of water compositions along the LEL from δ_p reflects evaporative loss, while deviation from the LEL is often indicative of mixing with source waters such as snowmelt or rainfall, which tend to plot along the GMWL (Fig. 3). Key reference points along the LEL include the terminal (i.e., closed-drainage) basin steady-state isotope composition (δ_{SSL}), which represents the special case of a waterbody at hydrologic and isotopic steady-state in which evaporation exactly equals inflow and the limiting non-steady-state isotope composition (δ^*), which indicates the maximum potential transient isotopic enrichment of a waterbody as it approaches complete desiccation (Fig. 3).

For each landscape, the LEL was predicted using the linear resistance model of Craig and Gordon (1965) following similar approaches presented in Brock et al. (2007) and Wolfe et al. (2011). Hereafter, we refer to this as the “landscape-predicted LEL.” Predicting the LEL, rather than the more commonly used empirical technique of applying linear regression through measured lake water isotope compositions, allows lake water isotope compositions to be interpreted independently based on their position along (degree of evaporation) and about (i.e., above/below; relative influence of different input waters such as snowmelt and rainfall) the LEL (e.g., see Tondou et al. 2013; Turner et al. 2014).

The following equations were used to develop the landscape-predicted LELs and are expressed in decimal notation. The equilibrium liquid–vapour fractionation factors (α^*)

for oxygen and hydrogen are dependent on temperature and have been determined empirically by Horita and Wesolowski (1994), where

$$(2) \quad 1000 \ln \alpha^* = -7.685 + 6.7123(10^3/T) - 1.6664(10^6/T^2) + 0.35041(10^9/T^3)$$

for $\delta^{18}\text{O}$ and

$$(3) \quad 1000 \ln \alpha^* = 1158.8(T^3/10^9) - 1620.1(T^2/10^6) + 794.84(T/10^3) - 161.04 + 2.9992(10^9/10^3)$$

for $\delta^2\text{H}$, where T represents the interface temperature in K. ϵ^* is the temperature-dependent equilibrium separation between liquid and vapour water given by

$$(4) \quad \epsilon^* = \alpha^* - 1$$

and kinetic separation (ϵ_K) is expressed by

$$(5) \quad \epsilon_K = C_K(1 - h)$$

where constant enrichment values (C_K) for oxygen and hydrogen are 0.0142 and 0.0125, respectively, and h is relative humidity (Gonfiantini 1986). δ_{AS} is the isotope composition of ambient open-water season atmospheric moisture, often assumed to be in isotopic equilibrium with evaporation-flux-weighted local open-water season precipitation (δ_{PS}) (Gibson et al. 2008) such that

$$(6) \quad \delta_{AS} = (\delta_{PS} - \epsilon^*)/\alpha^*$$

The limiting isotopic enrichment of a waterbody approaching desiccation (δ^*) has been defined by Gonfiantini (1986) and can be determined from

$$(7) \quad \delta^* = (h\delta_{AS} + \epsilon_K + \epsilon^*/\alpha^*)/(h - \epsilon_K - \epsilon^*/\alpha^*)$$

δ_{SSL} represents the isotope composition of a terminal basin in which evaporation is exactly compensated by inflow, as defined by Gonfiantini (1986)

$$(8) \quad \delta_{SSL} = \alpha^* \delta_i(1 - h - \epsilon_K) + \alpha^* h \delta_{AS} + \alpha^* \epsilon_K + \epsilon^*$$

where the isotope composition of inflow, δ_i , is assumed to be equal to δ_p . The landscape-predicted LEL was determined by linear regression through δ_p and δ^* .

Water-balance metrics

The water balance metrics, δ_l and E/I ratios, were determined for each of the 376 lakes using the Yi et al. (2008) coupled-isotope tracer approach, which assumes conservation of mass and isotope composition during evaporation. According to mass conservation, the isotope composition of evaporated vapour from a lake (δ_E) will lie on the extension of the lake-specific LEL to the left of the GMWL (Fig. 3) and was determined from the formulation provided by Gonfiantini (1986), where δ_l is the measured lake water isotope composition:

$$(9) \quad \delta_E = ((\delta_l - \epsilon^*)/\alpha^* - h\delta_{AS} - \epsilon_K)/(1 - h - \epsilon_K)$$

Values for δ_l were derived from calculating lake-specific evaporation lines and their intersection with the GMWL, which reasonably assumes that input waters are nonevaporated and plot on the GMWL and that all lake-specific evaporation lines converge at δ^* (Yi et al. 2008) (Fig. 3). The relative contributions of rainfall and snowmelt were then assessed by evaluating the position of δ_l compared to the landscape value of δ_p along the GMWL. For example, δ_l values that were more isotopically enriched than δ_p were categorized as *rainfall-dominated* lakes and δ_l values that were more isotopically depleted than δ_p were categorized as *snowmelt-dominated* lakes. For some YF lakes, very low δ_l values are interpreted as lakes fed primarily by permafrost thaw waters (see below and Anderson et al. 2013).

E/I ratios, which provide a snapshot of water balance through the mass-balance relation of evaporation to inflow, were calculated from Gibson and Edwards (2002):

$$(10) \quad E/I = (\delta_i - \delta_L)/(\delta_E - \delta_L)$$

An E/I ratio of 0.5 represents lakes where 50% of the inflow has evaporated, and we use this threshold to define *evaporation-dominated* lakes (after Tondu et al. 2013). As applied here, E/I ratios estimate net evaporative loss in midsummer and can indicate whether lake water volumes are increasing ($E/I \ll 1$) or decreasing ($E/I > 1$) where no drainage outlet exists. This approach assumes a well-mixed lake at isotopic steady-state; thus, values greater than 1 are inconsistent with the assumptions in the model but are used comparatively to identify lakes strongly influenced by evaporation.

Model input climate parameters, T and h , for calculation of the landscape-predicted LELs and lake water balance metrics were derived from the New et al. (2002) gridded climate database, which provided output for individual lake coordinates. This approach was used in the isotope mass-balance modeling of the individual lakes to account for spatial gradients in meteorological conditions within and among landscapes. Monthly T and h averages for the open-water season were flux-weighted according to potential evaporation using Thornthwaite (1948) for each landscape and for each of the 376 lakes. Values for δ_p (to anchor the landscape-predicted LEL) and δ_{ps} (used to determine δ_{As} ; eq. 6 for both the landscape-predicted LEL and each individual lake to account for spatial variations) were extracted from “The online isotopes in precipitation calculator” (waterisotopes.org; Bowen 2016). This database uses global precipitation oxygen and hydrogen isotope data to calculate average monthly and annual δ_p values for any given location and elevation (Bowen et al. 2005). Sampling year(s) meteorological conditions (temperature, relative humidity, and precipitation) for a representative location from each landscape were extracted from the NCEP North American Regional Reanalysis (NARR 2015) monthly composites and compared with the 1961–1990 landscape averages from the New et al. (2002) gridded database to assess the representativeness of meteorological conditions during the specific sampling years.

The influence of catchment vegetation on the water-balance metrics was assessed after land cover for each lake was broadly classified as *tundra dominant* or *forest dominant*. Tundra-dominant vegetation included catchments with high proportions of dwarf shrubs and areas of sparse vegetation, while forest-dominant vegetation included lake catchments with high proportions of deciduous and coniferous woodland or forest and tall shrub vegetation. Vegetation classes for ACP and YF were determined using the USGS National Land Cover Database of Alaska. For OCF, vegetation classes were simplified based on analysis of a Landsat 5 TM mosaic (Turner et al. 2014). Vegetation type for HBL and NUN was identified based on visual observations during field work.

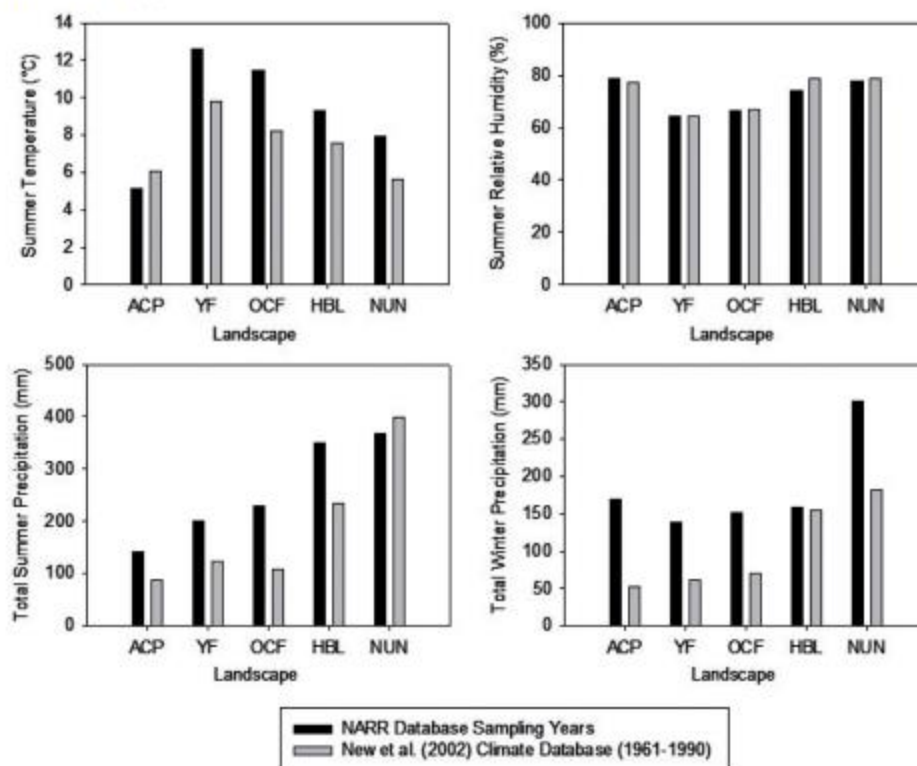
Nonparametric Kruskal–Wallis statistical tests were conducted to assess whether E/I distributions differed among lakes in different permafrost zones (continuous, discontinuous, and sporadic) and between vegetation categories (forest dominant versus tundra dominant) and whether $\delta^{18}\text{O}_i$ values differed among lakes in the different vegetation categories. When Kruskal–Wallis tests involving the permafrost zones produced a significant result ($P \leq 0.05$), pairwise comparisons were conducted using Dunnett’s post hoc tests. All statistical tests were performed using the software SPSS version 20. E/I values for lakes that were evaporating under strongly non-steady-state conditions ($E/I > 1$) were set to 1.5 for boxplot analyses and the statistical tests.

Results

Meteorological conditions during sampling years

Comparison of specific sampling year meteorological conditions (NARR) with the 1961–1990 average values (New et al. 2002) for each landscape reveals some similarities

Fig. 4. Comparison of average sampling year (solid bars, NARR 2015) and 1961–1990 average (grey bars, New et al. 2002) values for summer temperature, summer relative humidity, summer precipitation, and winter precipitation for the five landscapes.



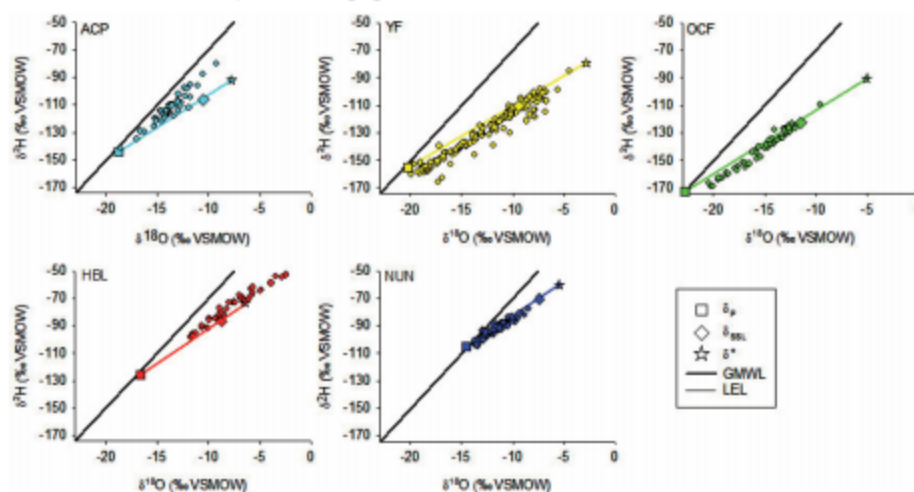
and differences (Fig. 4). Summer temperatures were higher (1.8–3.3 °C) during sampling years for YF, OCF, HBL, and NUN landscapes than the 1961–1990 average. At ACP, the summer temperatures were lower (0.9 °C) than the 1961–1990 average. Humidity values for the sampling years were similar to the 1961–1990 averages at all five landscapes. Precipitation shows the greatest difference between the values for the sampling years versus the 1961–1990 average. During the sampling years, ACP, YF, and OCF had consistently higher summer (54–121 mm) and winter precipitation (78–115 mm) than the 1961–1990 average, while HBL had higher summer precipitation (115 mm) during sampling years when compared to the 1961–1990 averages. In contrast, NUN had lower summer precipitation (32 mm) and higher winter precipitation (119 mm) during sampling years when compared to the 1961–1990 averages.

Isotope hydrology

Lake water isotope compositions (δ_L)

Lake water isotope compositions (δ_L) from all of the assembled data range from -20.5‰ to -2.4‰ and from -168.7‰ to -53.0‰ for $\delta^{18}\text{O}$ and $\delta^2\text{H}$, respectively (Appendix; Fig. 5). The wide range of δ_L values reflects the diverse lake hydrological conditions at the time of sampling in these high-latitude regions. YF has the greatest range of δ_L values, indicating substantial within-landscape variability, while NUN has the smallest range, signifying that lakes possess a narrower range of hydrological conditions in this landscape.

Fig. 5. Water isotope compositions (δ_L) from 376 lakes superimposed onto the landscape-specific isotope frameworks. The data defining the landscape-predicted LELs are shown in Table 1.



For each of the five landscapes, δ_L values form a linear trend that typically plot along a similar trajectory as the landscape-predicted LELs, supporting the contention that the frameworks are reasonable approximations of isotopic evaporative trajectories (Fig. 5). Indeed, the landscape-predicted LELs are in close agreement with the empirically defined LELs, except for ACP (Table 1). For ACP, δ_L values plot along a trajectory with a somewhat steeper slope than the landscape-predicted LEL, likely due to high rainfall immediately prior to sampling (Fig. 4). The LELs and δ_L values for OCF and YF, and HBL and NUN, are positioned in similar $\delta^{18}\text{O}$ – $\delta^2\text{H}$ space, likely reflecting similar latitudes and the associated well-known effect on isotope composition of precipitation (Rozanski et al. 1993). ACP, the most northerly landscape, does not follow this pattern, perhaps due to its closer proximity to the Arctic coast and associated reduced continental influence on precipitation isotope composition. δ_L values from NUN are evenly distributed about the LEL, while δ_L values from HBL and ACP typically plot above their respective LELs, suggesting a stronger influence of rainfall compared to snowmelt on lake water balance. Conversely, δ_L values from YF and OCF generally plot below their respective LELs, reflecting a stronger influence of snowmelt compared to rainfall on water balances. Additionally, a small group of lakes ($n = 15$) from YF have δ_L values that plot on a particularly low trajectory (i.e., parallel to, but offset below, the landscape-predicted LEL), which Anderson et al. (2013) suggested reflect more dominant input by isotopically depleted water from permafrost thaw in this region (elaborated on in the next section). δ_L values from HBL are positioned farthest away from the GMWL on the LEL, with many lakes plotting beyond δ_{SSL} and some approaching and surpassing the landscape-predicted δ^* , indicating strong non-steady-state evaporative isotopic enrichment at the time of sampling. In contrast, δ_L values from NUN are positioned closest to the GMWL on the LEL, indicating that lakes in this landscape are least influenced by evaporation.

Source water identification (δ_1)

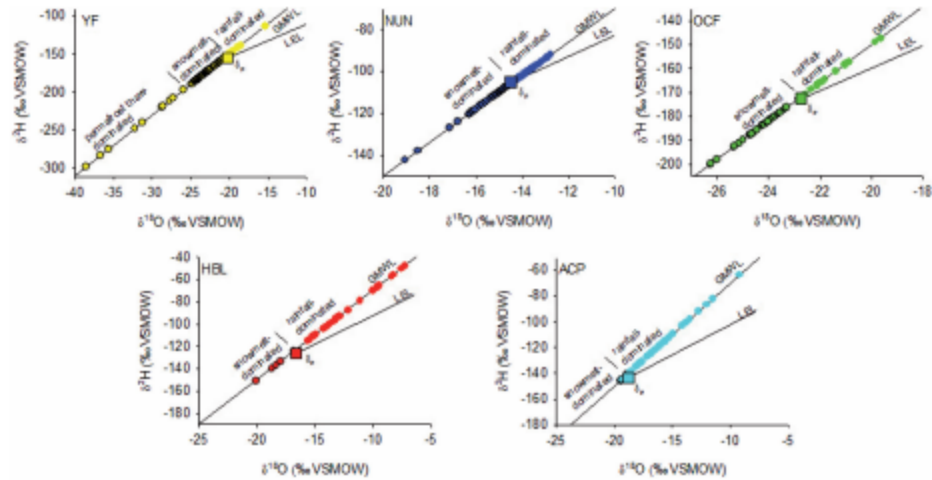
The isotope composition of lake-specific input water (δ_1) was calculated for each lake in the five landscapes to evaluate the relative roles of different source waters on lake hydrological conditions (Fig. 6). Lake-specific $\delta^{18}\text{O}_1$ values range from -38.6‰ to -7.2‰ and lake-specific $\delta^2\text{H}_1$ values range from -298.4‰ to -47.7‰ . The large range in δ_1 values illustrates

Table 1. Parameters used to construct the landscape-specific isotopic frameworks.

Parameter	ACP	YF	OCF	HBL	NUN	Equation(s)	Source
h (%)	76	63	65	78	79		New et al. (2002)
T (K)	2807	284.2	283.3	283.7	281.2		New et al. (2002)
α^* (^{18}O , ^2H)	1.0110, 1.1005	1.0106, 1.0955	1.0107, 1.0968	1.0107, 1.0962	1.0109, 1.0997	2, 3	Horita and Wesolowski (1994)
ϵ^* (^{18}O , ^2H) (‰)	11.0, 300.5	106, 95.5	107, 96.8	107, 96.2	109, 99.7	4	Gonflanti (1986)
ϵ_k (^{18}O , ^2H) (‰)	3.5, 3.1	5.3, 4.6	5.0, 4.4	3.1, 2.8	3.0, 2.6	5	Gonflanti (1986)
δ_{ss} (^{18}O , ^2H) (‰)	-26.6, -205	-27.8, -213	-29.1, -221	-23.9, 181	-22.9, -171	6	Gibson and Edwards (2002)
δ^* (^{18}O , ^2H) (‰)	-7.8, -92	-2.8, -79	-5.0, -90	-6.4, -74	-5.4, -60	7	Crig and Gordon (1965)
δ_{SL} (^{18}O , ^2H) (‰)	-10.5, -106	-9.4, -110	-11.5, -123	-8.7, -87	-7.4, -71	8	Gibson and Edwards (2002)
δ_p (^{18}O , ^2H) (‰)	-18.8, -144	-20.2, -155	-22.7, -173	-16.6, -126	-14.5, -105		Bowen (2016)
δ_{ps} (^{18}O , ^2H) (‰)	-15.9, -126	-17.5, -138	-18.7, -146	-13.5, -103	-12.2, -89		Bowen (2016)
L-P LEL	4.67 $\delta^{18}\text{O}$ -55.9	4.37 $\delta^{18}\text{O}$ -66.8	4.63 $\delta^{18}\text{O}$ -67.2	5.10 $\delta^{18}\text{O}$ -41.0	4.98 $\delta^{18}\text{O}$ -33.0		
L-E LEL	6.40 $\delta^{18}\text{O}$ -24.9	4.64 $\delta^{18}\text{O}$ -70.1	5.41 $\delta^{18}\text{O}$ -59.4	4.91 $\delta^{18}\text{O}$ -38.3	4.28 $\delta^{18}\text{O}$ -42.6		

Note: h , humidity; T , temperature; α^* , equilibrium liquid-vapour fractionation factor; ϵ^* , temperature-dependent equilibrium separation between liquid and vapour water; ϵ_k , kinetic separation; δ_{ss} , isotopic composition of ambient open-water season atmospheric moisture; δ^* , limiting non-steady-state isotope composition; δ_{ps} , terminal basin steady-state isotope composition; δ_{p} , average annual isotope composition of precipitation; δ_{ps} , average open-water sea son isotope composition of precipitation; L-P LEL, landscape-predicted Local Evaporation Line; L-E LEL, empirically defined Landscape Local Evaporation Line. ACP, Arctic Coastal Plain, Alaska; YF, Yukon Flats; OCF, Old Crow Flats; HBL, Hudson Bay Lowlands; NUN, Nunavut.

Fig. 6. Isotope compositions of lake-specific input water (δ_i) for each of the five landscapes. Classification of snowmelt-dominated lakes ($\delta_i \leq \delta_p$), rainfall-dominated lakes ($\delta_i > \delta_p$), and permafrost thaw-dominated lakes ($\delta_i \ll \delta_p$) are represented by the diagonal lines. Note the different axis scales.



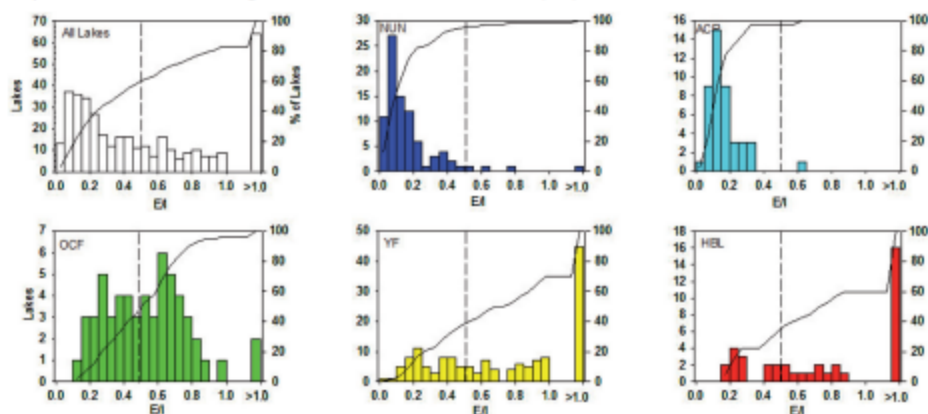
the high variability in the average proportion of source water type (i.e., rain and snowmelt) to all lakes within and among the landscapes. YF lakes possess the largest range of δ_i values, indicating substantial within-landscape variability in the proportions of source water types, while lakes in NUN have the smallest range of δ_i values, signifying less variability in proportions of source water type. Lakes with the lowest δ_i values are found in YF, while lakes in HBL have the highest δ_i values.

For each landscape, δ_i values were compared with the mean annual isotope composition of precipitation value (δ_p) to classify lakes as snowmelt ($\delta_i \leq \delta_p$) versus rainfall ($\delta_i > \delta_p$) dominated (Fig. 6). YF and OCF have the highest proportions of snowmelt-dominated lakes, 89% and 72%, respectively, indicating the strong influence of snowmelt on lake water balances in these landscapes, even during midsummer sampling. Of note, there was a small group of lakes in YF with particularly low δ_i values, likely due to input from snowmelt and permafrost thaw (Anderson et al. 2013). YF is underlain by discontinuous permafrost, and the observed values were within the range of values for permafrost thaw waters in this area (Meyer et al. 2010; Lachniet et al. 2012; Anderson et al. 2013). Slightly more than half of the lakes (52%) in NUN are snowmelt dominated, indicating a more even distribution of snowmelt versus rainfall source waters throughout the landscape. Some rainfall-dominated lakes in NUN may also be fed by permafrost thaw waters (Narancic et al. 2017). Rainfall-dominated lakes are the overwhelming majority in HBL (80%) and ACP (91%), reflecting the strong influence of rainfall on lake water balances in these landscapes at the time of sampling.

Evaporation-to-inflow (E/I) estimates

Evaporation-to-inflow ratios (E/I) were calculated for each lake in the five different landscapes to evaluate the relative importance of vapour loss on lake hydrological conditions (Fig. 7). The 376 lakes span a wide spectrum of E/I values, from close to 0 to much greater than 1, illustrating a range of water balances from those dominated by input waters to those dominated by evaporation. Overall, 219 lakes (58%) have $E/I < 0.5$, while 157 lakes (42%) have $E/I > 0.5$ (i.e., >50% evaporative water loss), which we consider as evaporation dominated. Calculated E/I distributions vary among landscapes (Fig. 7). For NUN and ACP, the vast

Fig. 7. Cumulative proportions (lines, right y-axis) and frequency (bars, left y-axis) distributions of E/I values for thermokarst lakes from the five landscapes. The vertical broken line represents $E/I = 0.5$. Water balance of lakes with $E/I > 0.5$ is considered evaporation dominated. Note the varying vertical scales.



majority of lakes (95% and 98%, respectively) have $E/I < 0.5$. Lakes in OCF have a relatively even distribution with $E/I < 0.5$ in 46% of lakes. In contrast, a majority of lakes in YF and HBL have $E/I > 0.5$ (63% and 68%, respectively), and these two regions have the largest proportion of lakes with $E/I > 1$ (30% and 40%, respectively). In HBL and YF, $E/I > 1$ is consistent with field observations of lakes throughout the landscape having undergone desiccation by midsummer (Anderson et al. 2013; Bouchard et al. 2013).

Discussion

Thermokarst lakes have been undergoing hydrological transitions in response to recent climate change (e.g., Yoshikawa and Hinzman 2003; Smith et al. 2005; Riordan et al. 2006; Labrecque et al. 2009; Rowland et al. 2010; Carroll et al. 2011; Bouchard et al. 2013). Our analysis of water isotope compositions and calculations of δ_1 and E/I ratios for 376 lakes at five lake-rich permafrost landscapes (ACP, YF, OCF, HBL, and NUN) in arctic and subarctic North America indicate that the importance of input types (rainfall, snowmelt, and permafrost) and evaporation are highly variable. Results show that striking similarities and differences in thermokarst lake hydrology exist among landscapes. Large gradients in δ_1 occur within and among landscapes and identify that lakes in HBL and ACP are mainly rainfall dominated, whereas lakes in OCF and YF are mainly snowfall dominated. Lakes in NUN have roughly equal proportions of rainfall- and snowfall-dominated lakes. Snowfall-dominated lakes from YF also likely include lakes with substantial contributions from permafrost thaw water (and possibly also in NUN, although these are isotopically indistinguishable from rainfall-dominated lakes; Narancic et al. 2017). E/I values span from almost 0 to much greater than 1. Most lakes in ACP and NUN have $E/I < 0.5$, while the majority of lakes in YF and HBL are evaporation dominated despite higher-than-normal (1961–1990) precipitation during sampling years. These findings underscore the strong hydrological gradients that exist across thermokarst lakes from high-latitude regions. In the discussion below, we first acknowledge assumptions and uncertainties in the isotope modeling approach. Then, relations of δ_1 and E/I ratios with climate and catchment characteristics among the five landscapes are explored, which provide the basis for anticipating how thermokarst lake hydrology in these northern regions may change in the future.

Assumptions and uncertainties

The nature of this broad continental-scale meta-analysis necessarily assumes that lakes sampled are representative of their landscapes and required decisions to ensure a consistent modeling approach given availability of existing data. Water balance metrics derived in this study were calculated from a single lake water isotope measurement or an average of July and August lake water isotope measurements over multiple years and thus they represent a snapshot of conditions. Also, the specific sampling years varied among the five landscapes. Although comparing water isotope data from different years for the five landscapes may result in some inherent variability, it is unlikely that the interannual variability for a single lake would exert a strong influence on comparisons within and among the five landscapes given the large range of lake water isotope compositions and E/I and δ_l values across the landscapes. We explored this for landscapes where multiple years of summer water isotope measurements were available (OCF, HBL, and NUN), and indeed, spatial variability far exceeded annual summer variability of individual lakes. For OCF, the range in $\delta^{18}\text{O}$ and $\delta^2\text{H}$ values for all lakes was 11.9‰ (minimum = -21.0‰, maximum = -9.1‰) and 64.6‰ (minimum = -172.3‰, maximum = -107.7‰), respectively. In contrast with the large spatial variability, the greatest range for an individual lake in OCF over the 3 year sampling period was 2.3‰ and 11.9‰ for $\delta^{18}\text{O}$ and $\delta^2\text{H}$, respectively. For HBL, the range in $\delta^{18}\text{O}$ and $\delta^2\text{H}$ values for all lakes was 10.6‰ (minimum = -12.0‰, maximum = -1.4‰) and 51.5‰ (minimum = -100.3‰, maximum = -48.8‰), respectively, whereas the greatest range for an individual lake in HBL over the 3 year sampling period was much lower (4.7‰ and 20.5‰ for $\delta^{18}\text{O}$ and $\delta^2\text{H}$, respectively). Similarly for NUN, the range in $\delta^{18}\text{O}$ and $\delta^2\text{H}$ values for all lakes was 6.6‰ (minimum = -14.4‰, maximum = -7.8‰) and 35.2‰ (minimum = -107.7, maximum = -72.5), respectively, while the greatest range for an individual lake over multiple years was much lower (2.8‰ and 19.8‰ for $\delta^{18}\text{O}$ and $\delta^2\text{H}$, respectively).

The availability and quality of climate records also varied among the five landscapes, and we used a common gridded climate database to extract meteorological conditions. These data were used to calculate water balance metrics for each individual lake, which allowed for a consistent approach to modeling of all lakes. However, this also added some uncertainty to the model output given that the gridded data set estimates a 30-year average (1961–1990), which was used to represent meteorological conditions during the recent years of actual water sampling. Fortunately, the gridded 30-year averages for humidity were well aligned with sample year humidity, which is a parameter that the isotope-mass balance model is sensitive to. Yet, precipitation during the sampling years was generally higher than the 1961–1990 averages (Fig. 4). Relatively wet conditions may have led to an underestimation of some of the E/I values relative to expected long-term averages, particularly for ACP. Additionally, summer temperature was warmer during the sampling years than the 1961–1990 estimates, with the exception of ACP. Different data sources were used to demarcate catchment vegetation among landscapes (field observations, remote sensing, aerial photographs), which also result in some further uncertainty to comparisons we make below.

Our attempt to develop a consistent modeling approach that could be applied to all lakes and landscapes results in some differences in values presented in this paper compared to the previous landscape-specific studies. For example, estimates of δ_p produced using water-isotopes.org (Bowen 2016) were lower than local precipitation isotope data utilized by Narancic et al. (2017), which placed some lakes in different classifications (snowmelt- versus rainfall-dominated categories). However, both approaches robustly identify that lakes in NUN experience a low degree of evaporation. Assumptions and limitations of data availability were unavoidable, but they are more likely to influence individual lake behaviour than the

large-scale spatial patterns within and among landscapes (the primary aim of this paper), which clearly emerged.

Drivers of hydrological conditions

Meteorological conditions exert a strong influence on water balance of thermokarst lakes (e.g., Riordan et al. 2006; Plug et al. 2008; Labrecque et al. 2009). For temperature and precipitation, mean annual, mean winter, and mean summer values vary greatly among the five landscapes (Fig. 2). Previous water isotope studies of lakes in northern Canada and the continental United States (Gibson and Edwards 2002; Brooks et al. 2014) found that colder regions typically have lower E/I values compared to warmer regions. This is likely in response to more rapid evaporation at higher temperature and perhaps differences in the length of the open-water season. Variation in ice-out timing within a region due to lake morphometry and among years and regions due to spring temperatures can also strongly affect evaporation season duration (Arp et al. 2015). Based on differences in mean summer temperature of the five landscapes in this study, one might anticipate the lowest E/I values at ACP and NUN and the highest values at OCF and YF. Indeed, lakes in ACP and NUN have the lowest E/I values and YF has some of the highest E/I values, but lakes in OCF have more moderate E/I values (Fig. 7). However, HBL has a much higher percentage (40%) of lakes with $E/I > 1$ compared to OCF (4%) and YF (30%).

The amount of snowmelt and rainfall input to lakes (direct to the lake surface and via runoff) affects the water balance of thermokarst lakes through the degree of water replenishment that offsets evaporative losses (Schindler and Smol 2006; Bouchard et al. 2013). It may be anticipated that YF has the greatest proportion of lakes with $E/I > 1$, owing to higher temperatures and relatively low mean annual winter and summer precipitation available to offset evaporation. In contrast, NUN was expected to have the lowest E/I values because it has the lowest mean summer temperature and highest mean winter and summer precipitation. In general, the results are consistent with these expectations; 30% of lakes in YF have E/I values > 1 and 95% of lakes in NUN have E/I values < 0.5 . However, HBL, with moderate temperature and precipitation, has the overall greatest proportion of lakes with $E/I > 1$ (40%). Thus, although HBL has the second highest mean annual summer and winter precipitation relative to the other landscapes, precipitation inputs do not offset midsummer evaporative losses for many lakes compared to the other landscapes, evidently even during years of apparent high summer precipitation. Bouchard et al. (2013) came to a similar conclusion that many lakes in HBL do not receive adequate precipitation, particularly snowmelt runoff, to offset midsummer evaporation leading to lake level decline. Snowmelt bypass, which occurs when snowmelt passes through a lake basin while the water mass is still frozen as ice, has been observed in some arctic lakes (e.g., Bergmann and Welch 1985) and may also serve to enhance E/I ratios in the absence of diluting effects of rainfall (Edwards and McAndrews 1989).

Source waters to lakes in both HBL and ACP were dominated by rainfall at the time of sampling (Fig. 6), but there is a large difference in amount of mean summer precipitation (Fig. 2). Similarly, lakes in OCF, YF, and NUN have snowmelt-dominated source waters, but again, these landscapes differ strongly in their mean winter precipitation. Thus, factors other than seasonal precipitation amounts must play a role in the relative importance of rainfall versus snowmelt inputs to thermokarst lakes in these landscapes. Interestingly, Fig. 2 shows that YF has relatively high temperature and low precipitation compared to the pattern observed for the other landscapes. YF is also the only landscape with lakes with input isotope compositions distinctly characteristic of water from permafrost thaw (Anderson et al. 2013). Higher temperatures since the early 1980s may be promoting more intense permafrost thaw in YF (Anderson et al. 2013). Overall, the data suggest that climate

normals are not the best predictor of hydrological classification of thermokarst lakes when used alone.

Permafrost conditions, which are influenced by climate, affect surface area of thermokarst lakes throughout the Arctic and Subarctic. For example, studies have shown that lake surface area is decreasing in regions of discontinuous permafrost (Yoshikawa and Hinzman 2003; Smith et al. 2005) but expanding in areas of continuous permafrost (Smith et al. 2005). Decreasing lake surface area has largely been attributed to drainage, but increased evaporation in response to climate warming may also play a role (Riordan et al. 2006). The five landscapes in this study span permafrost classifications from sporadic to continuous as well as from water balances indicative of increasing or stable lake water volume ($E/I < 0.5$) to water balances indicative of decreasing lake water volume due to evaporation ($E/I > 1$). E/I values for lakes from the three permafrost categories are highly variable (Table 2; Fig. 8). Lakes in terrain with sporadic permafrost (NUN) have the lowest E/I values, whereas lakes in terrain with discontinuous permafrost (YF, HBL, and NUN) have the highest E/I values. However, lakes from regions classified as having continuous (ACP, OCF, and HBL) and discontinuous (YF, HBL, and NUN) permafrost do have a wide and comparable range of E/I values spanning from close to 0 to greater than 1. Thus, relations among permafrost zones, lake surface area, and lake water balance are not straightforward.

Lake surface area and depth, as imparted by permafrost or other factors, can influence lake water balance. For example, in ACP, Arp et al. (2015) identified that lakes tend to experience longer ice-free seasons if they are shallow enough to have bedfast ice. In YF, Anderson et al. (2013) proposed that lakes with high E/I values are more likely to be relatively shallow. Although specific lake depth measurements were not available for the entire data set in this study, lakes in HBL were by far the shallowest of the five landscapes and, analogous to observations of Anderson et al. (2013) for YF, had the highest E/I ratios.

Of the permafrost categories, lakes located in the discontinuous permafrost zone, where average temperatures are warmer, have the highest proportion classified as evaporation dominated ($E/I > 0.5$) and 25% had $E/I > 1$. This suggests that evaporation in response to climate warming is likely playing an important role in the observed decline of surface area of thermokarst lakes in discontinuous permafrost zones and that lake drainage (lateral or internal) is likely not the sole cause. The dominance of low E/I values (<0.5) in lakes located within the region of sporadic permafrost may be due to ground thaw, which allows increased lateral hydrological connectivity to offset effects of evaporation. Permafrost thaw and the subsequent increased lateral hydrologic connectivity have been shown to maintain positive lake water balances (low E/I values) in Churchill, Manitoba (Wolfe et al. 2011). Overall, E/I results suggest that large-scale predictions of changes in lake area based strictly on permafrost zonation throughout the Arctic and Subarctic likely would not account for the apparent spatial heterogeneity in thermokarst lake hydrological conditions. Additionally, our analysis suggests that lake drainage is not the only cause of lake level decline for thermokarst lakes in discontinuous permafrost zones and that increased evaporation associated with air temperature increase is likely playing an important role in observed water level changes.

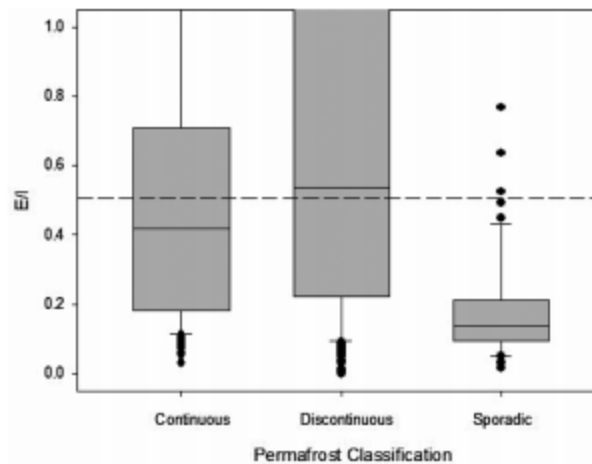
Studies from northern regions have suggested that lakes in low-relief, tundra landscapes are more vulnerable to evaporative losses and desiccation than lakes in forested landscapes (e.g., Brock et al. 2009; Turner et al. 2010, 2014; Bouchard et al. 2013). In forested landscapes, taller and denser vegetation entraps greater amounts of wind-redistributed snow than areas of sparse tundra vegetation (Pomeroy et al. 1997; Liston and Sturm 1998; McFadden et al. 2001; Sturm et al. 2001; Brock et al. 2009). In spring, snowmelt runoff to lakes helps to offset evaporative losses throughout the summer. Based on these observations, it could be reasoned that in this study, lakes located in forest-dominant catchments should have lower

Table 2. Results of Kruskal–Wallis tests, which compare evaporation-to-inflow ratios (E/I) or oxygen isotope composition of lake-specific input water ($\delta^{18}O_1$) values for the different permafrost zones (continuous, discontinuous, and sporadic) and vegetation categories (forest versus tundra dominant).

	χ^2	P	df
Permafrost E/I	60.754	6.417×10^{-14}	2
Vegetation E/I			
YF	0.702	0.402	1
OCF	3.429	0.064	1
HBL	11.599	0.001	1
NUN	4.811	0.028	1
Vegetation $\delta^{18}O_1$			
YF	3.915	0.048	1
OCF	7.021	0.008	1
HBL	5.951	0.015	1
NUN	4.111	0.043	1

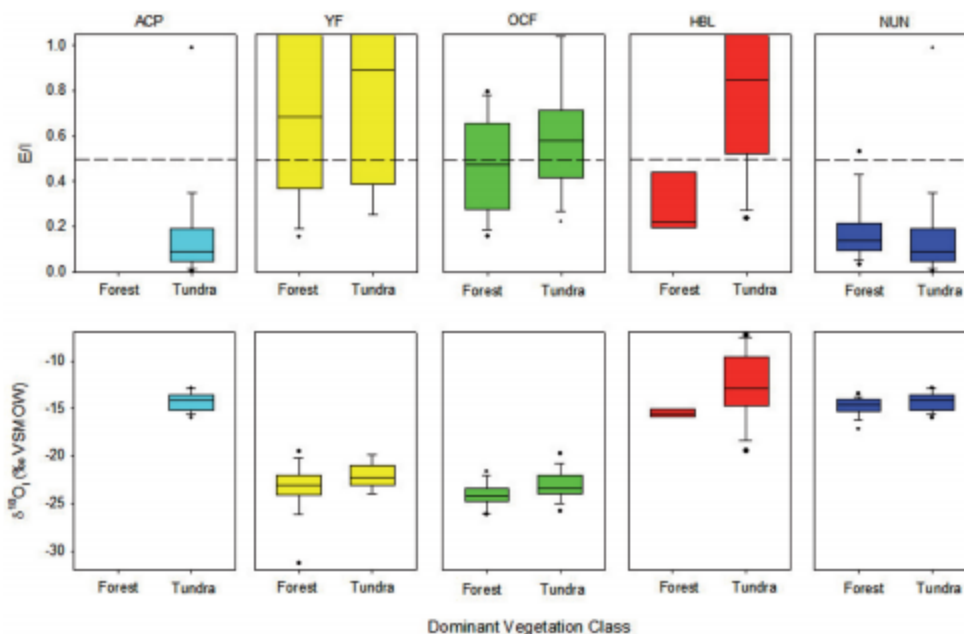
Note: YF, Yukon Flats; OCF, Old Crow Flats; HBL, Hudson Bay Lowlands; NUN, Nunavik.

Fig. 8. Boxplots comparing evaporation-to-inflow ratios (E/I) for all 376 lakes among permafrost types. The broken line represents $E/I = 0.5$, the threshold for evaporation-dominated lakes.



E/I and $\delta^{18}O_1$ values than lakes located in tundra-dominant catchments among the five landscapes. Results show that lakes from HBL display the clearest separation of E/I values between the two catchment vegetation classes with tundra-dominant catchments having higher E/I values followed by OCF, while lakes from YF have more similar ranges of observed E/I values for both vegetation classes (Table 2; Fig. 9). Additionally, more lakes in OCF, HBL, and YF have $E/I > 1$ in tundra-dominant landscapes compared to lakes situated in forest-dominant catchments. In fact, YF is the only landscape that has forest-dominant lake catchments with $E/I > 1$. In contrast, lakes from NUN do not follow this pattern (Fig. 9). Within this landscape, E/I values span similar albeit low ranges for lakes from both vegetation classes, but E/I ratios are significantly higher in lakes with forest-dominant catchments compared to lakes with tundra-dominant catchments (Table 2; Fig. 9). For ACP, all E/I values are relatively low despite that all lakes are situated in tundra-dominant catchments. Results also show that lakes with tundra-dominant catchments in YF, OCF, HBL, and NUN all had higher median $\delta^{18}O_1$ values compared to lakes in these landscapes situated in

Fig. 9. Boxplots comparing evaporation-to-inflow ratios (E/I , top) and oxygen isotope composition of lake-specific input water ($\delta^{18}\text{O}_i$, bottom) for thermokarst lakes at each of the five landscapes between the two vegetation classes (forest versus tundra). The broken line in the upper panel represents $E/I = 0.5$, the threshold for evaporation-dominated lakes.



forest-dominant catchments (Table 2; Fig. 9). Thus, tundra-dominant catchments appear to favour greater relative input of rainfall than snowmelt source waters to lakes. Overall, the data suggest that while vegetation appears to influence the composition of thermokarst lake input waters in YF, OCF, HBL, and NUN, the role of vegetation in vapour loss appears to be more important in HBL and OCF, and to a lesser degree in YF, than in NUN.

Interactions among meteorological conditions and catchment characteristics, such as vegetation and permafrost classifications, likely play key roles in promoting the similarities and diversity of hydrological conditions observed among the five landscapes. For example, variability in year-to-year meteorological conditions likely has the ability to mask the expected lake responses to other drivers such as vegetation and permafrost characteristics. ACP lakes all had E/I values that were relatively low despite all lakes being situated in catchments dominated by tundra vegetation. These values may have been lower than expected due to relatively high rainfall prior to sampling compared to long-term averages (Fig. 4). We speculate that in years of more typical precipitation in ACP, catchment vegetation may play a larger role in thermokarst lake hydrology and E/I values may be higher and perhaps more comparable to the tundra landscapes observed in HBL, OCF, and YF. Conversely, catchment vegetation may also mediate changes in meteorological conditions. For example, thermokarst lakes in HBL and ACP are mainly rainfall dominated but are also coastal landscapes with the majority of lakes located within open tundra. The coastal tundra settings may promote more wind redistribution of snowfall in these landscapes compared to the more inland snowmelt-dominated landscapes of YF and OCF, perhaps causing the lakes in these tundra landscapes to be more susceptible to hydrological changes in response to yearly fluctuations in rainfall. We further contend that because permafrost and overlying vegetation are influenced by climate conditions, precisely identifying

discrete roles of permafrost and vegetation is difficult. For instance, within a landscape, water balance differences may be due to the climatic conditions that result in vegetation differences rather than caused solely by vegetation. Recognition of the complex interactions and relative importance among different drivers of thermokarst lake hydrology throughout high-latitude regions is required to anticipate future hydrological trajectories (Turner et al. 2014).

Future hydrological trajectories

During the next century, northern regions are expected to experience continued rise of air temperature, longer duration of the ice-free season, and changes in the amount and timing of precipitation (Kattsov et al. 2005; Prowse et al. 2006; AMAP 2011). Increased temperatures and longer ice-free seasons will promote greater vapour loss from lakes during summer (Schindler and Smol 2006; Arp et al. 2015), leading to increased E/I values. If increases in precipitation do not occur at a similar rate, this could cause widespread desiccation of thermokarst lakes (Bouchard et al. 2013), which has also been observed in shallow non-thermokarst lakes in Canada's High Arctic (Smol and Douglas 2007). Spring snow cover has declined over many areas of northern North America and this pattern is expected to continue, although with substantial spatial and temporal variability (AMAP 2011; Dersken and Brown 2012; Krasting et al. 2013), which may result in a reduction of runoff available for offsetting vapour loss. Thermokarst lakes in HBL have already begun to desiccate during the ice-free season, and analysis of a sediment core from one desiccated lake in HBL indicates that this recent drying trend is unprecedented in the context of the past 200 years (Bouchard et al. 2013). YF, OCF, and perhaps ACP may also evolve towards this scenario under conditions of continued climate warming. Based on the E/I results of this study, field observations, and the degree to which hydrological conditions in each landscape appear to be influenced by meteorological conditions as outlined above, we suggest that HBL is the most vulnerable of the five landscapes to widespread lake desiccation in the future followed by YF, OCF, and ACP, while NUN is likely the least vulnerable. Interestingly, the landscapes at the two ends of this lake hydrological spectrum lie on opposite sides of Hudson Bay, and this may be related to the more maritime conditions in NUN on the eastern shore (Fig. 2; Narancic et al. 2017).

Increases in shrub growth in response to longer ice-free seasons and warmer temperatures have been observed along tundra-taiga transition zones (Myers-Smith et al. 2011; Lantz et al. 2013). Increased shrub growth may result in an increase in the number of lakes having snowmelt-dominated input waters and, conversely, a decrease in the proportion of rainfall-dominated lakes. This increase may result in greater water replenishment for some lakes in HBL, OCF, YF, and possibly ACP, where tundra-dominated landscapes typically have higher E/I values. However, the ratio of catchment area to lake size of individual lakes will determine whether sufficient snowmelt runoff can be generated to offset evaporative losses. Furthermore, with more vegetation productivity, increases in terrestrial evapotranspiration may dampen this response.

Greater permafrost thaw throughout high-latitude regions of North America (Osterkamp and Romanovsky 1999; Burn and Kokelj 2009) may result in lake-level declines via increases in vertical lake drainage (e.g., Yoshikawa and Hinzman 2003), or it may result in increased lateral hydrological connectivity, which may offset water losses due to evaporation and vertical drainage, ultimately causing a net increase in lake surface area (Avis et al. 2011; Wolfe et al. 2011). However, previous studies showed that lakes in YF with hydrological connections to the drainage network tend to experience greater fluctuations in intra- and interannual water balances (Chen et al. 2012, 2013). A subset of thermokarst lakes in YF show evidence of source waters derived from permafrost thaw, suggesting that this landscape may be

particularly sensitive to further changes in permafrost. E/I values of lakes in the sporadic permafrost zone of NUN may also be illustrating the effects of increased hydrological connectivity offsetting vapour loss. As the continuous permafrost warms in ACP, HBL, and OCF, these lakes may also become increasingly influenced by permafrost thaw waters. Overall, thermokarst lakes throughout permafrost regions of North America are unlikely to follow a uniform hydrological trajectory in response to amplified climate change. Rather, the hydrology of thermokarst lakes is likely to display dynamic and individualistic responses depending on their unique set of landscape and climate conditions and drivers.

Conclusions

We compiled water isotope data obtained during the past decade from 376 lakes of mainly thermokarst origin situated in arctic and subarctic permafrost landscapes across North America (Arctic Coastal Plain (Alaska), Yukon Flats (Alaska), Old Crow Flats (Yukon), north-western Hudson Bay Lowlands (Manitoba), and Nunavik (Quebec)). Our results, as well as those derived from calculation of isotope-based water-balance metrics (including source water isotope compositions and evaporation-to-inflow ratios), demonstrate a substantial array of regional and subregional diversity of lake hydrological conditions characterized by varying influence of snowmelt, rainfall, permafrost thaw waters, and evaporation. Thermokarst lake hydrology is driven by complex interactions among prevailing temperature and precipitation, catchment vegetation, and permafrost status. Some regional patterns emerged, such as the strong role of open-water evaporation on thermokarst lakes of the Hudson Bay Lowlands and Yukon Flats in particular, yet these hydrological drivers are all “moving targets” with ongoing climate change. Thus, they are likely to have pronounced influence on future thermokarst lake hydrological trajectories at a wide range of spatial and temporal scales, challenging our ability to anticipate their consequences for water resources, aquatic ecosystems, and biogeochemical cycling.

Acknowledgements

We would like to thank the many funding agencies and organizations that support our research as well as the many assistants in the field. This is a contribution to the NSERC Discovery Frontiers program, Arctic Development and Adaptation to Permafrost in Transition (ADAPT). Any use of trade, firm, or product names is for descriptive purposes only and does not imply endorsement by the US Government.

References

- ACIA. 2004. Arctic climate impact assessment. Cambridge University Press, Cambridge, UK.
- Allard, M., and Séguin, M.K. 1987. Le pergélisol au Québec nordique: bilan et perspectives. *Géograph. Phys. Quarter.* **41**(1): 141–152. doi: 10.7202/032671ar.
- Anderson, L., Birks, J., Rover, J., and Guldager, N. 2013. Controls on recent Alaskan lake changes identified from water isotopes and remote sensing. *Geophys. Res. Lett.* **40**(13): 3413–3418. doi: 10.1002/grl.50672.
- Arctic Monitoring and Assessment Programme (AMAP). 2011. Snow, water, ice and permafrost in the Arctic (SWIPA): climate change and the cryosphere. Arctic Monitoring and Assessment Programme, Oslo, Norway.
- Arp, C.D., and Jones, B.M. 2009. Geography of Alaska Lake Districts: identification, description, and analysis of lake-rich regions of a diverse and dynamic state. Scientific Investigations Report. US Geological Survey. doi: 10.1002/2015WR017362.
- Arp, C.D., Jones, B.M., Liljedahl, A.K., Hinkel, K.M., and Welker, J.A. 2015. Depth, ice thickness, and ice-out timing cause divergent hydrologic responses among Arctic lakes. *Water Resour. Res.* **51**(12): 9379–9401.
- Avis, C.A., Weaver, A.J., and Meissner, K.J. 2011. Reduction in areal extent of high-latitude wetlands in response to permafrost thaw. *Nat. Geosci.* **4**(7): 444–448. doi: 10.1038/ngeo1160.
- Bergmann, M.A., and Welch, W.E. 1985. Spring meltwater mixing in small arctic lakes. *Can. J. Fish. Aquat. Sci.* **42**(11): 1789–1798. doi: 10.1139/f85-224.
- Bouchard, F., Turner, K.W., MacDonald, L.A., Deakin, C., White, H., Farquharson, N., et al. 2013. Vulnerability of shallow subarctic lakes to evaporate and desiccate when snowmelt runoff is low. *Geophys. Res. Lett.* **40**(23): 6112–6117. doi: 10.1002/2013GL058635.

- Bouchard, F., Francus, P., Pienitz, R., Laurion, I., and Feyte, S. 2014. Subarctic thermokarst ponds: investigating recent landscape evolution and sediment dynamics in thawed permafrost of northern Québec (Canada). *Arct. Antarct. Alp. Res.* **46**(1): 251–271. doi: 10.1657/1938-4246-46.1.251.
- Bowen, G.J. 2016. The online isotopes in precipitation calculator, version 2.2. <http://www.waterisotopes.org>.
- Bowen, G.J., Wassenaar, L.I., and Hobson, K.A. 2005. Global application of stable hydrogen and oxygen isotopes to wildlife forensics. *Oecologia*. **143**(3): 337–348. doi: 10.1007/s00442-004-1813-y.
- Brock, B.E., Wolfe, B.B., and Edwards, T.W.D. 2007. Characterizing the hydrology of shallow floodplain lakes in the Slave River Delta, NWT, Canada, using water isotope tracers. *Arct. Antarct. Alp. Res.* **39**(3): 388–401. doi: 10.1657/1523-0430(06-026)[BROCK]2.0.CO;2.
- Brock, B.E., Yi, Y., Clogg-Wright, K.P., Edwards, T.W.D., and Wolfe, B.B. 2009. Multi-year landscape-scale assessment of lakewater balances in the Slave River Delta, NWT, using water isotope tracers. *J. Hydrol.* **379**(1–2): 81–91. doi: 10.1016/j.jhydrol.2009.09.046.
- Brooks, J.R., Gibson, J.J., Birks, S.J., Weber, M.H., Rodecap, K.D., and Stoddard, J.L. 2014. Stable isotope estimates of evaporation: inflow and water residence time for lakes across the United States as a tool for national lake water quality assessments. *Limnol. Oceanogr.* **59**(6): 2150–2165. doi: 10.4319/lo.2014.59.6.2150.
- Brown, J., Ferrians, O., Heginbottom, J.A., and Melnikov, E.S. 2002. Circum-arctic map of permafrost and ground-ice conditions, version 2. NSIDC: National Snow and Ice Data Center/World Data Center for Glaciology, Boulder, CO. <http://nsidc.org/data/ggd318> [accessed May 24, 2016].
- Burn, C.R., and Kokelj, S.V. 2009. The environment and permafrost of the Mackenzie Delta area. *Permafrost Periglacial Process.* **20**(2): 83–105. doi: 10.1002/ppp.655.
- Carroll, M.L., Townshend, J.R.G., DiMiceli, C.M., Loboda, T., and Sohlberg, R.A. 2011. Shrinking lakes of the Arctic: spatial relationships and trajectory of change. *Geophys. Res. Lett.* **38**(20): L20406, doi: 10.1029/2011GL049427.
- Chen, M., Rowland, J.C., Wilson, C.J., Altmann, G.L., and Brumby, S.P. 2012. Temporal and spatial pattern of thermokarst lake area changes at Yukon Flats, Alaska. *Hydrol. Process.* **28**(3): 837–852. doi: 10.1002/hyp.9642.
- Chen, M., Rowland, J.C., Wilson, C.J., Altmann, G.L., and Brumby, S.P. 2013. The importance of natural variability in lake areas on the detection of permafrost degradation: a case study in the Yukon Flats, Alaska. *Permafrost Periglacial Process.* **24**(3): 224–240. doi: 10.1002/ppp.1783.
- Coplen, T.B. 1996. New guidelines for reporting stable hydrogen, carbon and oxygen isotope ratio data. *Geochim. Cosmochim. Acta.* **60**(17): 3359–3360. doi: 10.1016/0016-7037(96)00263-3.
- Craig, H. 1961. Isotopic variations in meteoric waters. *Science.* **133**(3465): 1702–1703. doi: 10.1126/science.133.3465.1702.
- Craig, H., and Gordon, L.I. 1965. Deuterium and oxygen 18 variations in the ocean and the marine atmosphere. In *Stable isotopes in oceanographic studies and paleotemperatures*. Edited by E. Tongiorgi. Laboratorio Di Geologia Nucleare, Pisa, Italy, pp. 9–130.
- Darling, G., Bath, A., Gibson, J.J., and Rozanski, K. 2006. Isotopes in water. In *Isotopes in palaeoenvironmental research*. Edited by M.J. Leng. Springer, Netherlands, pp. 1–66.
- Dersken, C., and Brown, R. 2012. Spring snow cover extent reductions in the 2008–2012 period exceeding climate model projections. *Geophys. Res. Lett.* **39**(19): L19504.
- Duguay, C.R., and Lafleur, P.M. 2003. Determining depth and ice thickness of shallow sub-Arctic lakes using space-borne optical and SAR data. *Int. J. Rem. Sens.* **24**(3): 475–489. doi: 10.1080/01431160304992.
- Edwards, T.W.D., and McAndrews, J.H. 1989. Paleohydrology of a Canadian Shield lake inferred from ^{18}O in sediment cellulose. *Can. J. Earth Sci.* **26**(9): 1850–1859. doi: 10.1139/e89-158.
- Edwards, T.W.D., Wolfe, B.B., Gibson, J.J., and Hammarlund, D. 2004. Use of water isotope tracers in high latitude hydrology and paleohydrology. In *Long-term environmental change in Arctic and Antarctic lakes*. Edited by R. Pienitz, M.S.V. Douglas, and J.P. Smol. Springer, Dordrecht, pp. 187–207.
- Epstein, S., and Mayeda, T. 1953. Variation of ^{18}O content of waters from natural sources. *Geochim. Cosmochim. Acta.* **4**(5): 213–224. doi: 10.1016/0016-7037(53)90051-9.
- Frohn, R.C., Hinkel, K.M., and Eisner, W.R. 2005. Satellite remote sensing classification of thaw lakes and drained thaw lake basins on the North Slope of Alaska. *Rem. Sens. Environ.* **97**(1): 116–126. doi: 10.1016/j.rse.2005.04.022.
- Gibson, J.J., and Edwards, T.W.D. 2002. Regional water balance trends and evaporation–transpiration partitioning from a stable isotope survey of lakes in northern Canada. *Glob. Biogeochem. Cycles.* **16**(2): 10–14.
- Gibson, J.J., Birks, S.J., and Edwards, T.W.D. 2008. Global prediction of δ_{A} and $\delta^2\text{H}-\delta^{18}\text{O}$ evaporation slopes for lakes and soil water accounting for seasonality. *Glob. Biogeochem. Cycles.* **22**(2): GB2031. doi: 10.1029/2007GB002997.
- Gonfiantini, R. 1986. Environmental isotopes in lake studies. In *Handbook of environmental isotope geochemistry*. Edited by P. Fritz and J.C. Fontes. Elsevier, New York, pp. 113–168.
- Grosse, G., Schirmer, L., Kunitsky, V.V., and Hubberten, H.-W. 2005. The use of CORONA images in remote sensing of periglacial geomorphology: an illustration from the NE Siberian coast. *Permafrost Periglacial Process.* **16**(2): 163–172. doi: 10.1002/ppp.509.
- Hinkel, K.M., Jones, B.M., Eisner, W.R., Cuomo, C.J., Beck, R.A., and Frohn, R. 2007. Methods to assess natural and anthropogenic thaw lake drainage on the western Arctic coastal plain of northern Alaska. *J. Geophys. Res.* **112** (F2): F02S16. doi: 10.1029/2006JF000584.
- Horita, J., and Wesolowski, D.J. 1994. Liquid–vapor fractionation of oxygen and hydrogen isotopes of water from the freezing to the critical temperature. *Geochim. Cosmochim. Acta.* **58**(16): 3425–3437. doi: 10.1016/0016-7037(94)90096-5.
- IPCC. 2013. Climate change 2013: the physical science basis. Working Group I contribution to the fifth assessment report of the Intergovernmental Panel on Climate Change. In *IPCC fifth assessment report*. Edited by T.F. Stocker,

- D. Qin, G.-K. Plattner, M.M.B. Tignor, S.K. Allen, J. Boschung, A. Nauels, Y. Xia, V. Bex, and P.M. Midgley. Cambridge University Press, Cambridge, UK.
- Jepsen, S.M., Voss, C.I., Walvoord, M.A., Minsley, B.J., and Rover, J. 2013. Linkages between lake shrinkage/expansion and sublacustrine permafrost distribution determined from remote sensing of interior Alaska, USA. *Geophys. Res. Lett.* **40**(5): 882–887. doi: 10.1002/grl.50187.
- Jones, B.M., Grosse, G., Arp, C.D., Jones, M.C., Walter Anthony, K.M., and Romanovsky, V.E. 2011. Modern thermokarst lake dynamics in the continuous permafrost zone, northern Seward Peninsula, Alaska. *J. Geophys. Res.* **116**(G2): G00M03. doi: 10.1029/2011JG001666.
- Kattsov, V.M., Källén, E., Cattle, H., Christensen, J., Drange, H., Hanssen-Bauer, I., Jóhannessen, T., Karol, I., Räisänen, J., et al. 2005. Future climate change: modeling and scenarios for the Arctic. In *Arctic climate impact assessment*. Edited by C. Symon, L. Arris, and B. Heal. Cambridge University Press, Cambridge, UK, pp. 99–150.
- Krasting, J.P., Broccoli, A.J., Dixon, K.W., and Lanzante, J.R. 2013. Future changes in northern hemisphere snowfall. *J. Clim.* **26**(20): 7813–7828. doi: 10.1175/JCLI-D-12-00832.1.
- Labrecque, S., Lacelle, D., Duguay, C., Lauriol, B., and Hawkings, J. 2009. Contemporary (1951–2001) evolution of lakes in the Old Crow Basin, northern Yukon, Canada: remote sensing, numerical modeling and stable isotope analysis. *Arctic*. **62**(2): 225–238. doi: 10.14430/arctic134.
- Lachniet, M.S., Lawson, D.E., and Sloat, A.R. 2012. Revised ¹⁴C dating of ice wedge growth in interior Alaska (USA) to MIS 2 reveals cold paleoclimate and carbon recycling in ancient permafrost terrain. *Quat. Res.* **78**(2): 217–225. doi: 10.1016/j.yqres.2012.05.007.
- Lantz, T.C., Marsh, P., and Kokelj, S.V. 2013. Recent shrub proliferation in the Mackenzie Delta uplands and microclimatic implications. *Ecosystems*. **16**(1): 47–59. doi: 10.1007/s10021-012-9595-2.
- Lauriol, B., Duguay, C.R., and Riel, A. 2002. Response of the Porcupine and Old Crow rivers in northern Yukon, Canada, to Holocene climatic change. *Holocene*. **12**(1): 27–34. doi: 10.1191/0959683602h1517rp.
- Liston, G.E., and Sturm, M. 1998. A snow-transport model for complex terrain. *J. Glaciol.* **44**(148): 498–516.
- MacDonald, L.A., Turner, K.W., Balasubramaniam, A.M., Wolfe, B.B., Hall, R.I., and Sweetman, J.N. 2012. Tracking hydrological responses of a thermokarst lake in the Old Crow Flats (Yukon Territory, Canada) to recent climate variability using aerial photographs and paleolimnological methods. *Hydrol. Process.* **26**(1): 117–129. doi: 10.1002/hyp.8116.
- Mackay, J.R. 1988. Catastrophic lake drainage, Tuktoyaktuk Peninsula area, District of Mackenzie. In *Current research, part D, geological survey of Canada, paper 88-1D*. pp. 83–90.
- Marsh, P., Russell, M., Pohl, S., Haywood, H., and Onclin, C. 2009. Changes in thaw lake drainage in the Western Canadian Arctic from 1950 to 2000. *Hydrol. Process.* **23**(1): 145–158. doi: 10.1002/hyp.7179.
- McFadden, J.P., Liston, G.E., Sturm, M., Pielke, R.A., and Chapin, F.S. 2001. Interactions of shrubs and snow in arctic tundra: measurements and models. In *Soil-vegetation-atmosphere transfer schemes and large-scale hydrological models*. Edited by A.J. Dolman, A.J. Hall, M.L. Kavvas, T. Oki, and J.W. Pomeroy. International Association of Hydrological Sciences, Wallingford, UK. pp. 317–325.
- Meyer, H., Schirmer, L., Yoshikawa, K., Opel, T., Wetterich, S., Hubberten, H.-W., and Brown, J. 2010. Permafrost evidence for severe winter cooling during the Younger Dryas in northern Alaska. *Geophys. Res. Lett.* **37**(3): L03501. doi: 10.1029/2009GL041013.
- Morrison, J., Brockwell, T., Merren, T., Fourel, F., and Phillips, A.M. 2001. On-line high-precision stable hydrogen isotopic analyses on nanolitre water samples. *Anal. Chem.* **73**(15): 3570–3575. doi: 10.1021/ac001447t.
- Myers-Smith, I.H., Forbes, B.C., Wilking, M., Hallinger, M., Lantz, T., Blok, D., et al. 2011. Shrub expansion in tundra ecosystems: dynamics, impacts and research priorities. *Environ. Res. Lett.* **6**(4): 045509. doi: 10.1088/1748-9326/6/4/045509.
- Narancic, B., Wolfe, B.B., Pienitz, R., Meyer, H., and Lamhonwah, D. 2017. Landscape-gradient assessment of thermokarst lake hydrology using water isotope tracers. *J. Hydrol.* **545**: 327–338. doi: 10.1016/j.jhydrol.2016.11.028.
- NARR. 2015. NCEP North American Regional Reanalysis. <http://www.esrl.noaa.gov/psd/data/gridded/data.narr.html> [accessed winter 2016].
- New, M., Lister, D., Hulme, M., and Makin, I. 2002. A high-resolution data set of surface climate over global land areas. *Clim. Res.* **21**(1): 1–25. <http://wcatlas.iwmi.org/Default.asp> [accessed fall 2015].
- Osterkamp, T.E., and Romanovsky, V.E. 1999. Evidence for warming and thawing of discontinuous permafrost in Alaska. *Permafrost Periglacial Process.* **10**(1): 17–37. doi: 10.1002/(SICI)1099-1530(199901)10:1<17::AID-PPP303>3.0.CO;2-4.
- Plug, L.J., Walls, C., and Scott, B.M. 2008. Tundra lake changes from 1978 to 2001 on the Tuktoyaktuk Peninsula, western Canadian Arctic. *Geophys. Res. Lett.* **35**(3): L03502. doi: 10.1029/2007GL032303.
- Pomeroy, J.W., Marsh, P., and Gray, D.M. 1997. Application of a distributed blowing snow model to the Arctic. *Hydrol. Process.* **11**(11): 1451–1464. doi: 10.1002/(SICI)1099-1085(199709)11:11<1451::AID-HYP449>3.0.CO;2-Q.
- Prowse, T.D., Wrona, F.J., Reist, J.D., Gibson, J.J., Hobbie, J.E., Lévesque, L.M., and Vincent, W.F. 2006. Climate change effects on hydroecology of Arctic freshwater ecosystems. *Ambio*. **35**(7): 347–358. doi: 10.1579/0044-7447(2006)35[347:CCEOHO]2.0.CO;2.
- Rampton, V. 1988. Quaternary geology of the Tuktoyaktuk Coastlands, Northwest Territories. Geological Survey of Canada Memoir No. 423.
- Riordan, B., Verbyla, D., and McGuire, A.D. 2006. Shrinking ponds in subarctic Alaska based on 1950–2002 remotely sensed images. *J. Geophys. Res.* **111**(G4): G04002. doi: 10.1029/2005JG000150.
- Rouse, W.R. 1991. Impacts of Hudson Bay on the terrestrial climate of the Hudson Bay Lowlands. *Arct. Alp. Res.* **23**(1): 24–30. doi: 10.2307/1551433.

- Rouse, W.R., Douglas, M.S.V., Hecky, R.E., Hershey, A.E., Kling, G.W., Lesack, L., et al. 1997. Effects of climate change on the freshwaters of Arctic and subarctic North America. *Hydrol. Process.* **11**(8): 873–902. doi: 10.1002/(SICI)1099-1085(19970630)11:8<873::AID-HYP510>3.0.CO;2-6.
- Rowland, J.C., Jones, C.E., Altmann, G., Bryan, R., Crosby, B.T., Geernaert, G.L., et al. 2010. Arctic landscapes in transition: responses to thawing permafrost. *EOS Trans. Am. Geophys. Union.* **91**(26): 229–236. doi: 10.1029/2010EO260001.
- Rozanski, K., Araguás-Araguás, L., and Gonfiantini, R. 1993. Isotopic patterns in modern global precipitation. In *Climate change in continental isotopic records*. Edited by P.K. Swart, J.A. McKenzie, K.C. Lohmann, and S. Savin. Geophys. Monogr. 78, American Geophysical Union, Washington, DC. pp. 1–36.
- Schindler, D.W., and Smol, J.P. 2006. Cumulative effects of climate warming and other human activities on freshwaters of Arctic and subarctic North America. *Ambio.* **35**(4): 160–168. doi: 10.1579/0044-7447(2006)35[160:CEOCWA]2.0.CO;2.
- Smith, L.C., Sheng, Y., MacDonald, G.M., and Hinzman, L.D. 2005. Disappearing arctic lakes. *Science.* **308**(5727): 1429. doi: 10.1126/science.1108142.
- Smol, J.P., and Douglas, M.S.V. 2007. Crossing the final ecological threshold in high Arctic ponds. *Proc. Natl Acad. Sci. U.S.A.* **104**(30): 12395–12397. doi: 10.1073/pnas.0702777104.
- Sturm, M., McFadden, J.P., Liston, G.E., Chapin, F.S., Racine, C.H., and Holmgren, J. 2001. Snow–shrub interactions in Arctic tundra: a hypothesis with climatic implications. *J. Clim.* **14**(3): 336–344. doi: 10.1175/1520-0442(2001)014<0336:SSIIAT>2.0.CO;2.
- Thornthwaite, C. 1948. An approach toward a rational classification of climate. *Geogr. Rev.* **38**(1): 55–94. doi: 10.2307/210739.
- Tondu, J.M.E., Turner, K.W., Wolfe, B.B., Hall, R.I., Edwards, T.W.D., and McDonald, I. 2013. Using water isotope tracers to develop the hydrological component of a long-term aquatic ecosystem monitoring program for a northern lake-rich landscape. *Arct. Antarct. Alp. Res.* **45**(4): 594–614. doi: 10.1657/1938-4246-45.4.594.
- Tranvik, L.J., Downing, J.A., Cotner, J.B., Loiselle, S.A., Striegler, R.G., Ballatore, T.J., et al. 2009. Lakes and reservoirs as regulators of carbon cycling and climate. *Limnol. Oceanogr.* **54**(6): 2298–2314. doi: 10.4319/lo.2009.54.6_part_2.2298.
- Turner, K.W., Wolfe, B.B., and Edwards, T.W.D. 2010. Characterizing the role of hydrological processes on lake water balances in the Old Crow Flats, Yukon Territory, Canada, using water isotope tracers. *J. Hydrol.* **386**(1–4): 103–117. doi: 10.1016/j.jhydrol.2010.03.012.
- Turner, K.W., Wolfe, B.W., Edwards, T.W.D., Lantz, T.C., Hall, R.I., and Larocque, G. 2014. Controls on water balance of shallow thermokarst lakes and their relations with catchment characteristics: a multi-year, landscape-scale assessment based on water isotope tracers and remote sensing in Old Crow Flats, Yukon (Canada). *Glob. Change Biol.* **20**(5): 1585–1603. doi: 10.1111/gcb.12465.
- Vincent, W.F., Lemay, M., Allard, M., and Wolfe, B.B. 2013. Adapting to permafrost change: a science framework. Brief report. *EOS.* **94**(42): 373–375. doi: 10.1002/2013EO420002.
- Williams, J.R. 1962. Geologic reconnaissance of the Yukon Flats district, Alaska. *U.S. Geol. Surv. Bull.* **1111-H**: H289–H331.
- Wolfe, B.B., Light, E.M., Macrae, M.L., Hall, R.I., Eichel, K., Jasechko, S., et al. 2011. Divergent hydrological responses to 20th century climate change in shallow tundra ponds, western Hudson Bay Lowlands. *Geophys. Res. Lett.* **38**(23): 123402. doi: 10.1029/2011GL049766.
- Yi, Y., Brock, B.E., Falcone, M.D., Wolfe, B.B., and Edwards, T.W.D. 2008. A coupled isotope tracer method to characterize input water to lakes. *J. Hydrol.* **350**(1–2): 1–13. doi: 10.1016/j.jhydrol.2007.11.008.
- Yoshikawa, K.S., and Hinzman, L.D. 2003. Shrinking thermokarst ponds and groundwater dynamics in discontinuous permafrost near Council, Alaska. *Permafrost Periglacial Process.* **14**(2): 151–160. doi: 10.1002/ppp.451.

Appendix

Table A1. Average summer water isotope compositions, coordinates, and vegetation and permafrost categories for each of the 376 lakes.

Lake	δ_L (^{18}O)	δ_L (^2H)	Latitude ($^\circ$ N)	Longitude ($^\circ$ W)	Vegetation	Permafrost
ACP1	-9.26	-80.20	70.752	-153.869	Tundra	Continuous
ACP2	-12.34	-97.92	70.766	-153.562	Tundra	Continuous
ACP3	-10.55	-87.84	70.789	-153.470	Tundra	Continuous
ACP4	-14.72	-114.15	70.790	-154.450	Tundra	Continuous
ACP5	-11.74	-95.53	70.793	-154.517	Tundra	Continuous
ACP6	-12.95	-102.04	70.706	-153.924	Tundra	Continuous
ACP7	-12.07	-98.70	70.361	-151.683	Tundra	Continuous
ACP8	-15.25	-119.47	70.367	-151.398	Tundra	Continuous
ACP9	-16.26	-129.62	70.321	-151.532	Tundra	Continuous
ACP10	-14.55	-116.74	70.308	-151.435	Tundra	Continuous
ACP11	-16.65	-129.27	70.299	-151.464	Tundra	Continuous
ACP12	-13.90	-110.61	70.265	-151.394	Tundra	Continuous
ACP13	-12.65	-110.53	70.270	-151.356	Tundra	Continuous
ACP14	-13.66	-109.73	70.246	-153.287	Tundra	Continuous
ACP15	-11.06	-96.07	70.248	-151.484	Tundra	Continuous
ACP16	-12.64	-108.11	70.253	-151.342	Tundra	Continuous
ACP17	-14.60	-114.59	70.229	-153.312	Tundra	Continuous
ACP18	-13.03	-114.18	70.218	-153.179	Tundra	Continuous
ACP19	-13.86	-115.03	70.230	-153.090	Tundra	Continuous
ACP20	-12.98	-106.65	70.231	-151.367	Tundra	Continuous
ACP21	-13.55	-110.14	70.208	-151.169	Tundra	Continuous
ACP22	-13.95	-114.54	70.198	-153.315	Tundra	Continuous
ACP23	-12.29	-103.76	70.214	-153.313	Tundra	Continuous
ACP24	-12.72	-110.64	70.213	-153.082	Tundra	Continuous
ACP25	-13.18	-109.87	70.204	-152.566	Tundra	Continuous
ACP26	-13.21	-110.17	70.179	-153.294	Tundra	Continuous
ACP27	-12.99	-108.00	70.187	-151.571	Tundra	Continuous
ACP28	-14.66	-121.73	70.146	-151.761	Tundra	Continuous
ACP29	-14.12	-118.35	70.129	-151.804	Tundra	Continuous
ACP30	-14.01	-114.25	70.097	-152.880	Tundra	Continuous
ACP31	-13.41	-118.04	70.068	-152.962	Tundra	Continuous
ACP32	-14.24	-118.47	70.035	-153.288	Tundra	Continuous
ACP33	-15.12	-120.13	70.035	-153.227	Tundra	Continuous
ACP34	-14.23	-114.72	70.035	-153.039	Tundra	Continuous
ACP35	-17.01	-135.16	70.018	-153.188	Tundra	Continuous
ACP36	-18.54	-142.04	70.012	-153.153	Tundra	Continuous
ACP37	-14.30	-119.44	70.012	-153.094	Tundra	Continuous
ACP38	-13.56	-110.80	70.000	-152.028	Tundra	Continuous
ACP39	-14.99	-121.29	69.997	-153.069	Tundra	Continuous
ACP40	-11.77	-104.34	70.000	-153.037	Tundra	Continuous
ACP41	-15.13	-122.04	69.979	-153.074	Tundra	Continuous
ACP42	-14.14	-114.37	69.969	-152.946	Tundra	Continuous
ACP43	-11.93	-112.28	69.992	-152.952	Tundra	Continuous
ACP44	-15.37	-125.56	69.659	-153.051	Tundra	Continuous
YF1	-7.90	-100.73	66.450	-145.546	Forest	Discontinuous
YF2	-4.46	-84.94	66.450	-145.563	Forest	Discontinuous
YF3	-13.04	-129.30	66.385	-146.360	Forest	Discontinuous
YF4	-12.89	-125.86	66.034	-147.544	Forest	Discontinuous

Table A1 (continued).

Lake	δ_L (^{18}O)	δ_L (^2H)	Latitude ($^\circ$ N)	Longitude ($^\circ$ W)	Vegetation	Permafrost
YF5	-9.04	-106.11	66.294	-148.114	Forest	Discontinuous
YF6	-8.97	-106.40	66.088	-146.733	Forest	Discontinuous
YF7	-9.49	-109.35	66.240	-146.394	Forest	Discontinuous
YF8	-10.02	-112.15	66.083	-146.316	Forest	Discontinuous
YF9	-11.68	-120.00	66.175	-146.144	Forest	Discontinuous
YF10	-14.77	-136.61	66.186	-147.493	Forest	Discontinuous
YF11	-16.49	-144.37	65.929	-146.596	Forest	Discontinuous
YF12	-10.50	-116.86	66.129	-146.660	Forest	Discontinuous
YF13	-18.00	-155.82	66.282	-149.321	Forest	Discontinuous
YF14	-9.98	-111.39	66.259	-148.935	Forest	Discontinuous
YF15	-15.14	-141.79	66.337	-148.984	Forest	Discontinuous
YF16	-15.22	-142.46	66.240	-148.825	Forest	Discontinuous
YF17	-17.59	-150.50	66.229	-146.943	Forest	Discontinuous
YF18	-9.91	-116.08	66.223	-146.688	Forest	Discontinuous
YF19	-13.58	-135.62	66.217	-146.417	Forest	Discontinuous
YF20	-10.54	-118.78	66.217	-146.385	Forest	Discontinuous
YF21	-8.77	-112.11	66.258	-146.331	Forest	Discontinuous
YF22	-10.52	-116.84	66.320	-146.320	Forest	Discontinuous
YF23	-12.00	-127.86	66.299	-146.187	Forest	Discontinuous
YF24	-18.29	-158.00	66.106	-148.220	Forest	Discontinuous
YF25	-9.17	-109.27	66.171	-147.975	Forest	Discontinuous
YF26	-18.21	-156.04	66.208	-147.669	Forest	Discontinuous
YF27	-11.20	-121.94	66.067	-149.327	Forest	Discontinuous
YF28	-14.50	-139.92	66.117	-149.069	Forest	Discontinuous
YF29	-7.76	-104.12	66.200	-148.682	Forest	Discontinuous
YF30	-9.13	-111.44	66.459	-147.903	Forest	Discontinuous
YF31	-8.40	-105.14	66.389	-147.573	Forest	Discontinuous
YF32	-7.37	-103.30	66.430	-147.412	Forest	Discontinuous
YF33	-17.43	-152.56	66.055	-146.384	Forest	Discontinuous
YF34	-14.16	-137.52	66.061	-145.782	Forest	Discontinuous
YF35	-13.72	-136.30	66.187	-145.668	Forest	Discontinuous
YF36	-18.51	-158.26	66.207	-145.658	Forest	Discontinuous
YF37	-18.70	-158.91	66.277	-145.708	Forest	Discontinuous
YF38	-14.53	-139.24	66.110	-145.561	Forest	Discontinuous
YF39	-11.48	-122.97	66.368	-145.562	Forest	Discontinuous
YF40	-18.85	-153.56	66.185	-145.444	Forest	Discontinuous
YF41	-15.41	-143.52	66.010	-146.444	Forest	Discontinuous
YF42	-18.63	-156.95	65.999	-146.468	Forest	Discontinuous
YF43	-10.44	-117.81	66.281	-148.593	Forest	Discontinuous
YF44	-12.87	-130.87	66.327	-148.595	Forest	Discontinuous
YF45	-9.70	-115.61	66.275	-148.221	Forest	Discontinuous
YF46	-10.03	-115.81	66.307	-148.102	Forest	Discontinuous
YF47	-10.30	-118.18	66.314	-148.106	Forest	Discontinuous
YF48	-10.18	-115.71	66.280	-148.120	Forest	Discontinuous
YF49	-11.30	-120.90	66.123	-148.153	Forest	Discontinuous
YF50	-18.80	-156.90	66.131	-149.159	Forest	Discontinuous
YF51	-16.90	-162.50	65.971	-149.450	Forest	Discontinuous
YF52	-11.60	-128.70	66.167	-149.159	Forest	Discontinuous
YF53	-17.30	-165.70	66.260	-148.878	Forest	Discontinuous
YF54	-7.40	-105.50	66.179	-148.989	Forest	Discontinuous
YF55	-10.40	-110.00	66.106	-147.554	Forest	Discontinuous

Table A1 (continued).

Lake	δ_L (^{18}O)	δ_L (^2H)	Latitude ($^{\circ}$ N)	Longitude ($^{\circ}$ W)	Vegetation	Permafrost
YF56	-13.20	-125.00	66.110	-147.753	Forest	Discontinuous
YF57	-11.90	-139.00	66.150	-147.731	Forest	Discontinuous
YF58	-9.20	-105.00	66.181	-148.010	Forest	Discontinuous
YF59	-16.10	-153.00	66.110	-148.313	Forest	Discontinuous
YF60	-16.70	-149.00	66.993	-146.169	Forest	Discontinuous
YF61	-10.30	-119.00	66.983	-146.041	Forest	Discontinuous
YF62	-10.70	-117.00	66.928	-146.125	Forest	Discontinuous
YF63	-19.10	-160.00	66.783	-145.799	Forest	Discontinuous
YF64	-10.40	-113.00	66.909	-145.113	Forest	Discontinuous
YF65	-10.50	-115.00	66.897	-145.170	Forest	Discontinuous
YF66	-7.20	-99.00	66.856	-145.170	Forest	Discontinuous
YF67	-7.30	-98.00	66.775	-145.258	Forest	Discontinuous
YF68	-12.90	-127.00	66.751	-145.458	Forest	Discontinuous
YF69	-12.10	-124.00	66.707	-145.530	Forest	Discontinuous
YF70	-16.70	-145.00	66.154	-144.118	Forest	Discontinuous
YF71	-14.50	-137.00	66.752	-143.502	Forest	Discontinuous
YF72	-10.50	-116.00	66.716	-143.673	Forest	Discontinuous
YF73	-18.90	-157.00	66.444	-144.384	Forest	Discontinuous
YF74	-10.80	-119.00	66.418	-145.368	Forest	Discontinuous
YF75	-7.80	-113.60	66.101	-146.007	Forest	Discontinuous
YF76	-7.90	-113.60	66.625	-146.234	Forest	Discontinuous
YF77	-7.80	-118.40	66.269	-145.902	Forest	Discontinuous
YF78	-6.80	-114.60	66.867	-143.837	Forest	Discontinuous
YF79	-8.00	-117.60	66.871	-143.829	Forest	Discontinuous
YF80	-10.30	-129.90	66.995	-143.749	Forest	Discontinuous
YF81	-13.70	-146.30	66.977	-143.327	Forest	Discontinuous
YF82	-8.30	-116.70	66.796	-143.538	Forest	Discontinuous
YF83	-8.60	-121.30	66.657	-143.839	Forest	Discontinuous
YF84	-8.44	-104.57	66.401	-146.384	Forest	Discontinuous
YF85	-13.78	-130.33	66.087	-146.729	Forest	Discontinuous
YF86	-6.95	-98.55	66.440	-145.477	Forest	Discontinuous
YF87	-6.74	-100.34	66.437	-145.479	Forest	Discontinuous
YF88	-5.61	-98.87	66.431	-145.536	Forest	Discontinuous
YF89	-15.87	-145.37	66.391	-148.325	Forest	Discontinuous
YF90	-8.48	-110.57	66.386	-148.344	Forest	Discontinuous
YF91	-15.87	-146.01	66.385	-148.328	Forest	Discontinuous
YF92	-17.16	-149.19	66.386	-148.321	Forest	Discontinuous
YF93	-7.66	-107.94	66.387	-148.304	Forest	Discontinuous
YF94	-8.05	-106.63	66.386	-148.290	Forest	Discontinuous
YF95	-15.51	-144.20	66.383	-148.317	Forest	Discontinuous
YF96	-10.91	-126.72	66.384	-148.350	Forest	Discontinuous
YF97	-6.93	-106.47	66.383	-148.355	Forest	Discontinuous
YF98	-12.11	-125.30	66.376	-148.348	Forest	Discontinuous
YF99	-10.17	-115.23	66.371	-148.312	Forest	Discontinuous
YF100	-11.68	-124.20	66.373	-148.350	Forest	Discontinuous
YF101	-12.03	-126.97	66.367	-148.324	Forest	Discontinuous
YF102	-6.68	-106.88	66.388	-148.298	Forest	Discontinuous
YF103	-9.15	-106.96	66.120	-148.048	Forest	Discontinuous
YF104	-12.98	-131.12	66.106	-148.076	Forest	Discontinuous
YF105	-19.29	-158.25	66.109	-148.089	Forest	Discontinuous
YF106	-19.91	-160.80	66.111	-148.050	Forest	Discontinuous

Table A1 (continued).

Lake	δ_L (^{18}O)	δ_L (^2H)	Latitude ($^{\circ}$ N)	Longitude ($^{\circ}$ W)	Vegetation	Permafrost
YF107	-16.01	-143.73	66.109	-148.056	Forest	Discontinuous
YF108	-18.68	-155.32	66.106	-148.089	Forest	Discontinuous
YF109	-12.31	-131.50	66.105	-148.071	Forest	Discontinuous
YF110	-18.20	-154.12	66.105	-148.056	Forest	Discontinuous
YF111	-17.05	-149.82	66.101	-148.097	Forest	Discontinuous
YF112	-18.53	-154.64	66.102	-148.093	Forest	Discontinuous
YF113	-13.04	-132.20	66.102	-148.079	Forest	Discontinuous
YF114	-17.59	-150.68	66.100	-148.100	Forest	Discontinuous
YF115	-13.61	-131.44	66.091	-148.077	Forest	Discontinuous
YF116	-19.32	-158.10	66.098	-148.097	Forest	Discontinuous
YF117	-17.72	-151.41	66.100	-148.090	Forest	Discontinuous
YF118	-17.95	-151.18	66.097	-148.087	Forest	Discontinuous
YF119	-17.33	-150.48	66.093	-148.057	Forest	Discontinuous
YF120	-11.03	-119.80	66.119	-148.063	Forest	Discontinuous
YF121	-11.06	-120.61	66.030	-144.742	Forest	Discontinuous
YF122	-15.21	-141.09	66.029	-144.737	Forest	Discontinuous
YF123	-16.08	-143.84	66.026	-144.727	Forest	Discontinuous
YF124	-19.66	-152.93	66.015	-144.728	Forest	Discontinuous
YF125	-11.84	-124.03	66.017	-144.780	Forest	Discontinuous
YF126	-13.85	-133.63	66.015	-144.769	Forest	Discontinuous
YF127	-12.13	-124.71	66.013	-144.773	Forest	Discontinuous
YF128	-13.64	-132.99	66.012	-144.781	Forest	Discontinuous
YF129	-9.16	-112.63	66.010	-144.783	Forest	Discontinuous
YF130	-15.09	-138.96	66.010	-144.759	Forest	Discontinuous
YF131	-16.66	-144.47	66.014	-144.739	Forest	Discontinuous
YF132	-11.05	-121.14	66.006	-144.769	Forest	Discontinuous
YF133	-15.38	-141.68	66.008	-144.743	Forest	Discontinuous
YF134	-16.78	-147.14	66.008	-144.739	Forest	Discontinuous
YF135	-19.03	-151.79	66.007	-144.735	Forest	Discontinuous
YF136	-15.33	-140.60	66.011	-144.748	Tundra	Discontinuous
YF137	-7.23	-102.70	66.359	-144.268	Tundra	Discontinuous
YF138	-8.86	-108.58	66.364	-144.253	Tundra	Discontinuous
YF139	-13.94	-131.38	66.361	-144.265	Tundra	Discontinuous
YF140	-17.14	-139.55	66.366	-144.233	Tundra	Discontinuous
YF141	-13.09	-129.97	66.359	-144.237	Tundra	Discontinuous
YF142	-7.06	-101.11	66.362	-144.225	Tundra	Discontinuous
YF143	-11.29	-122.05	66.355	-144.232	Tundra	Discontinuous
YF144	-15.52	-142.31	66.358	-144.250	Tundra	Discontinuous
YF145	-14.83	-136.58	66.359	-144.241	Tundra	Discontinuous
YF146	-8.68	-106.50	66.400	-146.371	Tundra	Discontinuous
YF147	-11.73	-126.31	66.397	-146.409	Tundra	Discontinuous
YF148	-10.13	-117.17	66.396	-146.355	Tundra	Discontinuous
YF149	-8.33	-103.76	66.386	-146.367	Tundra	Discontinuous
OCF1	-12.80	-129.03	68.077	-140.110	Forest	Continuous
OCF2	-12.31	-123.44	68.202	-140.296	Tundra	Continuous
OCF3	-16.85	-153.07	68.214	-140.097	Tundra	Continuous
OCF4	-12.67	-128.04	68.215	-140.134	Tundra	Continuous
OCF5	-12.90	-130.77	68.207	-139.884	Forest	Continuous
OCF6	-9.55	-109.56	67.919	-139.991	Tundra	Continuous
OCF7	-17.08	-151.61	67.921	-140.150	Forest	Continuous
OCF8	-14.16	-137.22	67.907	-140.124	Forest	Continuous

Table A1 (continued).

Lake	δ_L (^{18}O)	δ_L (^2H)	Latitude ($^\circ$ N)	Longitude ($^\circ$ W)	Vegetation	Permafrost
OCF9	-14.34	-137.44	67.906	-140.205	Forest	Continuous
OCF10	-14.70	-140.38	67.891	-140.235	Forest	Continuous
OCF11	-16.92	-155.19	68.028	-140.570	Forest	Continuous
OCF12	-12.60	-130.32	68.061	-140.411	Tundra	Continuous
OCF13	-20.21	-168.70	68.059	-140.364	Forest	Continuous
OCF14	-12.80	-129.64	67.977	-140.234	Forest	Continuous
OCF15	-13.51	-133.98	68.107	-140.674	Tundra	Continuous
OCF16	-19.58	-164.33	68.152	-140.893	Tundra	Continuous
OCF17	-15.37	-147.36	68.229	-140.735	Tundra	Continuous
OCF18	-11.79	-124.93	68.267	-140.619	Tundra	Continuous
OCF19	-12.04	-126.71	68.283	-140.522	Tundra	Continuous
OCF20	-14.17	-138.55	68.185	-140.444	Forest	Continuous
OCF21	-16.92	-152.17	67.739	-140.180	Forest	Continuous
OCF22	-15.76	-148.79	67.764	-140.152	Forest	Continuous
OCF23	-16.44	-152.50	67.765	-140.154	Forest	Continuous
OCF24	-13.44	-133.86	67.771	-140.049	Tundra	Continuous
OCF25	-19.18	-162.83	67.806	-140.055	Forest	Continuous
OCF26	-17.63	-154.29	67.848	-139.992	Forest	Continuous
OCF27	-12.81	-127.87	68.004	-140.052	Forest	Continuous
OCF28	-12.77	-126.14	67.962	-139.898	Forest	Continuous
OCF29	-13.13	-126.92	67.911	-139.794	Tundra	Continuous
OCF30	-14.01	-135.94	67.958	-139.781	Tundra	Continuous
OCF31	-15.00	-141.60	67.961	-139.787	Tundra	Continuous
OCF32	-20.46	-166.84	67.731	-139.615	Forest	Continuous
OCF33	-14.30	-135.53	67.810	-139.461	Tundra	Continuous
OCF34	-14.30	-134.33	67.884	-139.472	Tundra	Continuous
OCF35	-14.48	-137.73	67.979	-139.620	Tundra	Continuous
OCF36	-12.98	-128.15	68.015	-139.712	Tundra	Continuous
OCF37	-12.69	-126.97	68.044	-139.806	Forest	Continuous
OCF38	-14.58	-135.37	68.322	-140.129	Tundra	Continuous
OCF39	-12.64	-124.70	68.337	-140.367	Tundra	Continuous
OCF40	-15.69	-141.70	67.710	-139.432	Forest	Continuous
OCF41	-15.77	-144.69	67.726	-139.083	Tundra	Continuous
OCF42	-14.08	-127.90	67.865	-139.206	Tundra	Continuous
OCF43	-15.53	-140.36	68.036	-139.047	Tundra	Continuous
OCF44	-16.15	-144.14	68.103	-139.185	Tundra	Continuous
OCF45	-18.62	-160.83	68.231	-139.483	Tundra	Continuous
OCF46	-12.49	-128.87	68.150	-139.606	Tundra	Continuous
OCF47	-13.23	-134.00	68.205	-139.808	Forest	Continuous
OCF48	-18.76	-158.88	68.192	-139.879	Forest	Continuous
OCF49	-12.58	-126.60	68.082	-139.662	Tundra	Continuous
OCF50	-19.48	-163.04	67.772	-139.919	Forest	Continuous
OCF51	-17.86	-156.10	67.829	-139.823	Forest	Continuous
OCF52	-17.72	-157.39	67.843	-139.808	Forest	Continuous
OCF53	-13.75	-135.25	67.848	-139.777	Forest	Continuous
OCF54	-18.56	-159.53	67.931	-139.671	Tundra	Continuous
OCF55	-20.05	-168.60	67.843	-139.758	Forest	Continuous
OCF56	-18.55	-159.93	67.812	-139.937	Forest	Continuous
OCF57	-14.88	-139.46	68.208	-139.807	Forest	Continuous
HBL1	-10.67	-91.20	58.394	-93.382	Tundra	Continuous
HBL2	-6.63	-73.46	58.385	-93.345	Tundra	Continuous

Table A1 (continued).

Lake	δ_L (^{18}O)	δ_L (^2H)	Latitude ($^\circ$ N)	Longitude ($^\circ$ W)	Vegetation	Permafrost
HBL3	-2.85	-55.15	58.343	-93.271	Tundra	Continuous
HBL4	-4.83	-63.97	58.341	-93.268	Tundra	Continuous
HBL5	-5.75	-68.19	58.342	-93.265	Tundra	Continuous
HBL6	-5.70	-66.41	58.351	-93.232	Tundra	Continuous
HBL7	-7.60	-72.99	58.427	-93.178	Tundra	Continuous
HBL8	-7.46	-73.42	58.406	-93.264	Tundra	Continuous
HBL9	-6.65	-69.59	58.414	-93.307	Tundra	Continuous
HBL10	-5.86	-63.15	58.425	-93.268	Tundra	Continuous
HBL11	-5.66	-62.22	58.425	-93.266	Tundra	Continuous
HBL12	-3.89	-59.10	58.426	-93.269	Tundra	Continuous
HBL13	-8.91	-77.42	58.660	-93.194	Tundra	Continuous
HBL14	-7.47	-73.07	58.621	-93.174	Tundra	Continuous
HBL15	-8.02	-73.32	58.620	-93.171	Tundra	Continuous
HBL16	-9.32	-84.81	58.541	-93.161	Tundra	Continuous
HBL17	-7.51	-72.45	58.561	-93.167	Tundra	Continuous
HBL18	-6.90	-70.03	58.622	-93.318	Tundra	Continuous
HBL19	-6.95	-67.95	58.707	-93.299	Tundra	Continuous
HBL20	-7.41	-73.21	58.670	-93.444	Tundra	Continuous
HBL21	-5.86	-68.52	58.665	-93.441	Tundra	Continuous
HBL22	-9.94	-84.83	57.963	-94.077	Tundra	Discontinuous
HBL23	-10.12	-91.34	57.835	-94.183	Forest	Discontinuous
HBL24	-11.52	-95.78	57.739	-94.005	Forest	Discontinuous
HBL25	-11.29	-95.31	57.705	-94.046	Forest	Discontinuous
HBL26	-11.75	-98.23	57.698	-94.115	Forest	Discontinuous
HBL27	-11.52	-97.31	57.614	-93.970	Forest	Discontinuous
HBL28	-10.03	-92.44	57.661	-93.924	Forest	Discontinuous
HBL29	-8.59	-83.16	57.673	-93.432	Tundra	Continuous
HBL30	-3.45	-54.37	57.712	-93.383	Tundra	Continuous
HBL31	-2.40	-53.04	57.737	-93.377	Tundra	Continuous
HBL32	-4.93	-64.66	57.990	-93.459	Tundra	Continuous
HBL33	-8.25	-78.05	58.052	-93.533	Tundra	Continuous
HBL34	-6.43	-71.65	58.046	-93.659	Tundra	Continuous
HBL35	-6.07	-70.97	58.045	-93.659	Tundra	Continuous
HBL36	-8.93	-82.02	58.046	-93.660	Tundra	Continuous
HBL37	-8.53	-81.98	58.078	-93.661	Tundra	Continuous
HBL38	-8.69	-80.82	58.119	-93.554	Tundra	Continuous
HBL39	-10.67	-89.71	58.215	-93.708	Tundra	Continuous
HBL40	-9.91	-86.15	58.365	-93.777	Tundra	Continuous
NUN1	-12.18	-95.12	55.220	-77.707	Forest	Sporadic
NUN2	-12.81	-97.50	55.220	-77.707	Forest	Sporadic
NUN3	-12.46	-98.40	55.227	-77.696	Forest	Sporadic
NUN4	-12.38	-96.27	55.227	-77.698	Forest	Sporadic
NUN5	-12.13	-94.57	55.226	-77.698	Forest	Sporadic
NUN6	-12.09	-93.48	55.227	-77.698	Forest	Sporadic
NUN7	-13.22	-99.10	55.227	-77.698	Forest	Sporadic
NUN8	-11.97	-93.55	55.227	-77.696	Forest	Sporadic
NUN9	-12.42	-97.43	55.223	-77.706	Forest	Sporadic
NUN10	-11.86	-96.64	55.223	-77.706	Forest	Sporadic
NUN11	-12.46	-97.55	55.223	-77.706	Forest	Sporadic
NUN12	-12.25	-94.16	55.227	-77.697	Forest	Sporadic
NUN13	-12.75	-95.10	55.227	-77.697	Forest	Sporadic

Table A1 (continued).

Lake	δ_L (^{18}O)	δ_L (^2H)	Latitude ($^{\circ}$ N)	Longitude ($^{\circ}$ W)	Vegetation	Permafrost
NUN14	-11.67	-90.93	55.227	-77.696	Forest	Sporadic
NUN15	-12.72	-93.49	55.227	-77.698	Forest	Sporadic
NUN16	-11.93	-93.14	55.226	-77.698	Forest	Sporadic
NUN17	-12.59	-95.46	55.227	-77.698	Forest	Sporadic
NUN18	-12.81	-95.75	55.227	-77.698	Forest	Sporadic
NUN19	-12.73	-96.65	55.227	-77.696	Forest	Sporadic
NUN20	-10.40	-83.96	55.222	-77.706	Forest	Sporadic
NUN21	-11.01	-87.90	55.222	-77.706	Forest	Sporadic
NUN22	-11.55	-88.73	55.222	-77.706	Forest	Sporadic
NUN23	-11.61	-92.29	55.331	-77.503	Forest	Sporadic
NUN24	-11.32	-91.57	55.497	-77.503	Forest	Sporadic
NUN25	-11.82	-95.10	55.331	-77.503	Forest	Sporadic
NUN26	-10.23	-87.77	55.332	-77.503	Forest	Sporadic
NUN27	-11.98	-94.43	55.332	-77.502	Forest	Sporadic
NUN28	-8.47	-77.76	55.332	-77.502	Forest	Sporadic
NUN29	-10.53	-87.83	55.332	-77.501	Forest	Sporadic
NUN30	-11.54	-92.67	55.332	-77.502	Forest	Sporadic
NUN31	-8.83	-82.03	55.333	-77.500	Forest	Sporadic
NUN32	-9.70	-85.52	55.330	-77.503	Forest	Sporadic
NUN33	-11.57	-90.98	55.330	-77.504	Forest	Sporadic
NUN34	-11.09	-88.58	55.330	-77.504	Forest	Sporadic
NUN35	-9.45	-84.41	55.330	-77.503	Forest	Sporadic
NUN36	-9.76	-87.49	55.330	-77.502	Forest	Sporadic
NUN37	-10.97	-87.66	55.330	-77.503	Forest	Sporadic
NUN38	-10.92	-89.17	55.330	-77.503	Forest	Sporadic
NUN39	-9.09	-80.61	55.330	-77.505	Forest	Sporadic
NUN40	-10.73	-88.97	55.330	-77.504	Forest	Sporadic
NUN41	-10.93	-91.55	55.332	-77.502	Forest	Sporadic
NUN42	-11.50	-91.85	55.332	-77.503	Forest	Sporadic
NUN43	-11.58	-90.90	55.333	-77.502	Forest	Sporadic
NUN44	-9.82	-85.07	55.333	-77.502	Forest	Sporadic
NUN45	-11.42	-93.62	55.333	-77.502	Forest	Sporadic
NUN46	-11.15	-89.27	55.332	-77.502	Forest	Sporadic
NUN47	-11.46	-92.98	55.332	-77.503	Forest	Sporadic
NUN48	-11.55	-92.55	55.332	-77.503	Forest	Sporadic
NUN49	-10.66	-88.06	55.333	-77.501	Forest	Sporadic
NUN50	-10.03	-85.60	55.332	-77.500	Forest	Sporadic
NUN51	-11.06	-90.50	55.332	-77.501	Forest	Sporadic
NUN52	-10.06	-87.05	55.332	-77.502	Forest	Sporadic
NUN53	-11.96	-93.49	55.331	-77.502	Forest	Sporadic
NUN54	-11.07	-89.56	55.333	-77.503	Forest	Sporadic
NUN55	-11.86	-91.94	55.334	-77.502	Forest	Sporadic
NUN56	-11.84	-93.29	55.333	-77.502	Forest	Sporadic
NUN57	-9.30	-81.19	55.333	-77.500	Forest	Sporadic
NUN58	-10.82	-87.85	56.611	-76.215	Forest	Sporadic
NUN59	-12.26	-94.81	56.611	-76.216	Tundra	Discontinuous
NUN60	-13.30	-101.65	56.610	-76.215	Tundra	Discontinuous
NUN61	-12.94	-100.90	56.611	-76.214	Tundra	Discontinuous
NUN62	-13.36	-99.85	56.608	-76.217	Tundra	Discontinuous
NUN63	-11.39	-90.56	56.609	-76.217	Tundra	Discontinuous
NUN64	-11.11	-92.70	56.610	-76.214	Tundra	Discontinuous

Table A1 (concluded).

Lake	δ_L (^{18}O)	δ_L (^2H)	Latitude ($^{\circ}$ N)	Longitude ($^{\circ}$ W)	Vegetation	Permafrost
NUN65	-13.65	-104.51	56.610	-76.212	Tundra	Discontinuous
NUN66	-13.42	-104.72	56.609	-76.213	Tundra	Discontinuous
NUN67	-13.50	-104.09	56.610	-76.213	Tundra	Discontinuous
NUN68	-10.99	-92.09	56.609	-76.217	Tundra	Discontinuous
NUN69	-10.47	-90.24	56.609	-76.218	Tundra	Discontinuous
NUN70	-10.90	-88.95	56.608	-76.218	Tundra	Discontinuous
NUN71	-11.24	-91.90	56.608	-76.217	Tundra	Discontinuous
NUN72	-12.86	-100.82	56.608	-76.216	Tundra	Discontinuous
NUN73	-12.25	-95.42	56.609	-76.217	Tundra	Discontinuous
NUN74	-9.86	-84.74	56.611	-76.214	Tundra	Discontinuous
NUN75	-12.89	-93.14	56.924	-76.378	Tundra	Discontinuous
NUN76	-13.01	-93.81	56.924	-76.379	Tundra	Discontinuous
NUN77	-11.66	-90.62	56.923	-76.380	Tundra	Discontinuous
NUN78	-13.44	-100.80	56.923	-76.380	Tundra	Discontinuous
NUN79	-10.03	-83.45	56.924	-76.378	Tundra	Discontinuous
NUN80	-12.38	-94.39	56.923	-76.380	Tundra	Discontinuous
NUN81	-13.69	-100.87	56.924	-76.380	Tundra	Discontinuous
NUN82	-12.28	-94.46	56.924	-76.377	Tundra	Discontinuous
NUN83	-12.83	-93.40	56.924	-76.378	Tundra	Discontinuous
NUN84	-11.98	-89.36	56.923	-76.379	Tundra	Discontinuous
NUN85	-10.84	-87.35	56.924	-76.380	Tundra	Discontinuous
NUN86	-12.63	-94.84	56.924	-76.377	Tundra	Discontinuous

Note: ACP, Arctic Coastal Plain, Alaska; YF, Yukon Flats; OCF, Old Crow Flats; HBL, Hudson Bay Lowlands; NUN, Nunavik.

License – Open access

[Home](#) > [Journals](#) > [Arctic Science](#) > [Open Access Journals Licenses and Fees](#)



Licenses and fees

User license

Material published in Arctic Science is governed by the Creative Commons Attribution License CC BY. This has two major benefits:

- The CC BY license conforms with the licensing requirements of all major funding agencies
- Authors retain copyright

Under the CC BY license, users are permitted to share (copy and redistribute the material in any medium or format) or adapt (remix, transform, and build upon) the material for commercial or non-commercial purposes, so long as appropriate credit is given to the authors and the source of the work.

The license also ensures that the published material can be included in any scientific archive.

Note: By submitting to Arctic Science, you are agreeing to license your article under the CC BY License.

Appendix C

Hadley et al., 2019

J Paleolimnol (2019) 61:313–328
https://doi.org/10.1007/s10933-018-0061-9



ORIGINAL PAPER

Biological and geochemical changes in shallow lakes of the Hudson Bay Lowlands: a response to recent warming

Kristopher R. Hadley · Andrew M. Paterson · Kathleen M. Rühland · Hilary White · Brent B. Wolfe · Wendel Keller · John P. Smol

Received: 6 October 2016 / Accepted: 16 November 2018 / Published online: 24 January 2019
© Springer Nature B.V. 2019

Abstract The Hudson Bay Lowlands (HBL) region of the far north of Ontario (Canada) is expected to undergo considerable physical, chemical and biological change as a result of ongoing climatic change. Previous research in the region has shown marked limnological changes during the past ~ 20 years in relatively deep lakes that have been attributed to increased air temperatures and changes in sea ice phenology in Hudson Bay since the mid-1990s. Here, we present diatom assemblage, primary production and geochemical data from lake sediments documenting recent limnological change in two shallow sub-arctic lakes in the Sutton River region of the HBL.

Both lakes recorded increased whole-lake production and diatom diversity changes that are consistent with a longer ice-free period and growing season. Changes in diatom composition at Wolfgang Lake were characterized by a response amongst benthic/periphytic taxa whereas a modest increase in planktonic diatoms was observed at Sam Lake. Geochemical changes ($\delta^{15}\text{N}$, C/N and %N) were temporally coherent with diatom assemblage changes, but showed different responses in the two study lakes. Thus, although the biological and geochemical changes were consistent with recent warming, differences in the nature and timing of these shifts illustrate the heterogeneous nature of shallow lakes, and suggest that local (catchment-specific) factors are important determinants of the trajectory of limnological change in these sensitive systems.

K. R. Hadley (✉) · A. M. Paterson
Dorset Environmental Science Centre, Ontario Ministry of the Environment and Climate Change, Dorset, ON P0A1E0, Canada
e-mail: kris.hadley@gmail.com

K. R. Hadley · K. M. Rühland · J. P. Smol
Paleoecological Environmental Assessment and Research Laboratory (PEARL), Department of Biology, Queen's University, Kingston, ON K7L3N6, Canada

H. White · B. B. Wolfe
Department of Geography and Environmental Studies, Wilfrid Laurier University, Waterloo, ON N2L3C5, Canada

W. Keller
Cooperative Freshwater Ecology Unit, Vale Living with Lakes Centre, Laurentian University, Sudbury, ON P3E2C6, Canada

Keywords Diatoms · Climate change · Stable isotopes · Chlorophyll *a* · Paleolimnology · Lake sediments

Introduction

As a result of the moderating role of Hudson Bay sea ice on the regional climate, the northern Hudson Bay Lowlands (HBL) registered minimal warming throughout the mid- to late-twentieth century (Chapman and Walsh 1993; Gough et al. 2004). However, since the mid-1990s, the Hudson Bay region has

experienced marked warming, associated with decreased sea ice cover and changes in sea ice phenology (Hochheim and Barber 2010, 2014). The effects of warming during the past two decades are well documented in the Hudson Bay marine ecosystem, with changes to the productivity of the marine food web (Hoover 2010), declines in polar bear body condition, reproduction, survival, and abundance in several sub-populations (Obbard et al. 2006; Regehr et al. 2007), and marked changes to sea bird populations and their prey (Mallory et al. 2010; Gaston et al. 2012). There is also concern that warming may alter carbon dynamics in the region's extensive peatlands, with possible global consequences (Tarnocai 2006; Dunn and Freeman 2011; McLaughlin and Webster 2014).

Climate change may also alter fundamental water column properties and nutrient dynamics in lakes in several ways, with implications for biota. Increases in surface water temperatures (O'Reilly et al. 2015), longer and warmer ice-free seasons (O'Beirne et al. 2017), and increased thermal stability in stratified lakes (Stainsby et al. 2011; Hadley et al. 2014) have been linked to long-term changes in phytoplankton communities and sedimentary diatom assemblages in temperate, sub-arctic, and Arctic lakes (Sorvari et al. 2002; Smol et al. 2005; Rühland et al. 2008; Weckström et al. 2016; Bramburger et al. 2017; Reavie et al. 2017; Roberts et al. 2017). Increases in aquatic production, as inferred from sedimentary chlorophyll *a*, have also been observed with recent warming (Michelutti and Smol 2016), even in lakes with stable or declining nutrient concentrations (Paterson et al. 2017). In part, this may be attributed to a longer growing season that allows more time for the development of algal populations (Nelligan et al. 2016).

Limnological changes with 1990s warming have been documented in relatively deep lakes in the northern HBL. In a detailed analysis of diatom assemblages from four deep lakes within the HBL (all lakes > 10 metres maximum depth), diatom species assemblage changes were recorded in the mid-1990s, including an increase in species richness, and significant increases in the relative abundances of planktonic taxa that were coherent with increases in mean annual and seasonal air temperatures (Rühland et al. 2013). Similarly, in a comparison of diatom assemblages between recent and pre-industrial sediments in the HBL (i.e., using a "top-bottom"

paleolimnological approach), Rühland et al. (2014) reported higher diatom diversity in modern sediments, which they attributed to a longer ice-free period (and thus longer growing season), and the development of new aquatic habitats.

In general, less is known about long-term biological trajectories in shallow lakes in the northern HBL, despite their importance and prevalence in the region. However, recent research suggests that these shallow water bodies may be quite sensitive to 20th century climate change. In the Churchill region of northwestern HBL, for example, changes to hydrological connectivity and enhanced evaporation with warming have been linked to periods of hydrological instability in shallow freshwater tundra ponds. In some cases, declining snowmelt runoff has led to pond desiccation (Bouchard et al. 2013). It is apparent that biological (Shinneman et al. 2016) and hydrological (Wolfe et al. 2011) responses to warming can be quite variable in shallow lakes, as these responses are moderated by catchment-scale differences in landscape variables and vegetation. Moreover, shallow lakes may also show a heightened sensitivity and more pronounced biological response to warming, relative to deeper water bodies, because of their higher surface to volume ratios and lower water volumes (Roberts et al. 2015; Hargan et al. 2016; Smol 2016).

Here, we present diatom assemblage data and reconstructions of past primary production from lake sediment cores from two shallow lakes in the Sutton River region of the HBL. In light of evidence for recent changes in air temperature, and observed biological changes in nearby deeper lakes, our primary objective was to determine how the algal communities of shallow lakes in the HBL may have responded to a warming climate. In addition, we present detailed geochemical data ($\delta^{15}\text{N}$, C/N and %N) from the same sediment cores to explore the possible influence of the long-range deposition of atmospheric nitrogen as an alternative, synergistic, or confounding explanation for the recent algal changes. These data were then compared to results from four nearby relatively deep lakes (Rühland et al. 2013), as well as 13 lakes from a regional "top-bottom" paleolimnological survey (Rühland et al. 2014). We argue that increased nitrogen deposition is not responsible for these assemblage changes and that the paleolimnological data are consistent with recent climate warming in this region. However, we also note that the biological and

geochemical responses varied between the study lakes, suggesting that trajectories of change are moderated by local and catchment-scale factors.

Study lakes

Sam and Wolfgang (unofficial names) lakes are relatively small (32 and 157 ha, respectively), shallow (Z_{max} = 1.7 and 1.2 m, respectively) waterbodies located in the Sutton River region of the HBL, located 53 and 43 km south of the Hudson Bay coast (Fig. 1).

The northern HBL is considered to be sub-arctic, with regional climate strongly influenced by circulation patterns and ice dynamics within Hudson Bay (Martini 2006). For most of recorded history, air temperatures in this region have remained relatively stable, suggesting a lack of twentieth century warming. This is supported by paleoecological studies from the Hudson and James Bay region that show minimal biological changes over the past two centuries (Laing et al. 2002; Paterson et al. 2003) to millennia (Ponader et al. 2002; Fallu et al. 2005). However, beginning in the mid-

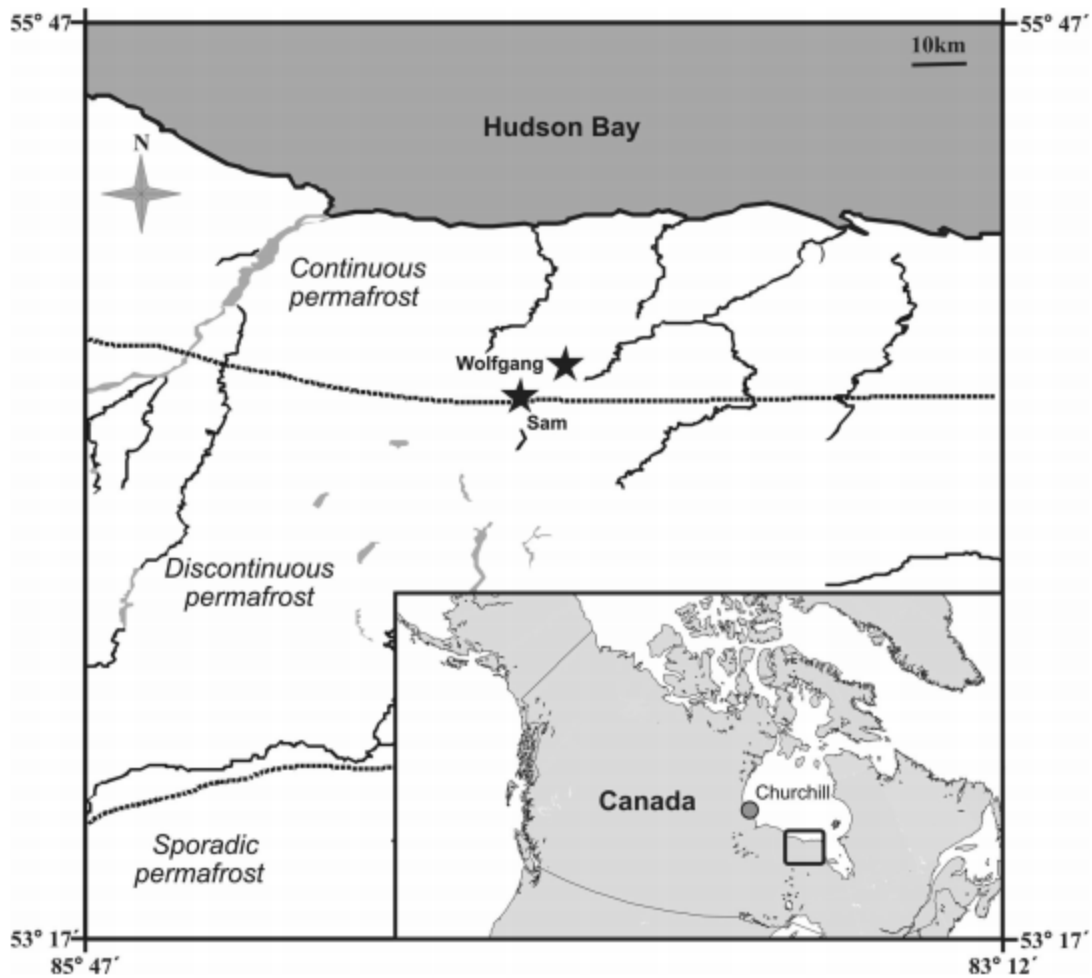


Fig. 1 Regional map showing the location of the lakes surveyed in the Sutton River region of the Hudson Bay Lowlands, and the location of the climate station at Churchill, MB, Canada (inset map). Sam and Wolfgang lakes (unofficial

names) are highlighted (stars). The approximate location (determined using GIS) of the boundaries between continuous, discontinuous, and sporadic permafrost are also indicated (dashed lines)

1990s, mean annual air temperature increases of 0.5–1.0 °C per decade were documented at Churchill, Manitoba, and at other HBL stations (e.g., Winisk/Peawanuck climate station) with shorter monitoring records. These changes in regional air temperature have resulted in altered sea ice dynamics, including delayed freeze-up (1.6–2.4 weeks) and earlier spring break-up (1.5–2.5 weeks) (Hochheim and Barber 2014).

The study lakes are alkaline and oligo-mesotrophic, with water chemistry influenced by the underlying limestone bedrock, calcareous till, the proximity of the sites to Hudson Bay, and the degree of permafrost development (Table 1; Paterson et al. 2014). Sam Lake is located very close to the continuous-discontinuous permafrost boundary, recognizing that the precise position of this boundary is based on very few sampling points.

Materials and methods

Field sampling

Water chemistry data for Sam and Wolfgang lakes were collected once per year in August, 2010 and 2011. At the coring location, a composite bottle was lowered and raised through the water column, from the surface to the Secchi disk depth (Ingram et al. 2013). Samples for water chemistry were analyzed at the Ontario Ministry of the Environment and Climate Change (OMOECC) Dorset Environmental Science Centre using standard OMOECC protocols (Ontario Ministry of the Environment 1983). A more detailed description of the limnological sampling and analyses is presented by Paterson et al. (2014).

Sediment cores were collected in August, 2011 from the deepest basin of each lake using a 7.6-cm internal-diameter Glew (1989) gravity corer, and

sectioned at 0.5-cm intervals on site using a Glew (1988) vertical extruder, following standard paleolimnological protocols. Core lengths for Wolfgang and Sam lakes were 26.5 and 48.5 cm, respectively. The sediment samples were stored in Whirlpak® bags and refrigerated in the dark until analysis.

Laboratory analyses

²¹⁰Pb dating

Sediment cores were dated using gamma spectroscopy to detect radio isotope activities of ²¹⁰Pb, ¹³⁷Cs and ²¹⁴Bi, following Schelske et al. (1994). The Constant Rate of Supply model (CRS, Appleby 2001) was applied to determine sediment age based on unsupported ²¹⁰Pb concentrations. Approximately 0.3–0.7 g of freeze-dried sediment was prepared for age determinations. Sediment was placed into plastic test tubes and sealed with 2-Ton Epoxy® to ensure equilibrium between ²²⁶Ra and ²¹⁴Bi prior to gamma counting. Activities were collected for 13 samples per core, and ²¹⁰Pb dates were estimated for the past ~ 100–150 years.

Diatoms

Sediment preparation for diatom analysis followed standard paleolimnological procedures (Battarbee et al. 2001). Briefly, 0.2–0.3 g of wet sediment was digested in a 50:50 molar mixture of concentrated nitric and sulphuric acid, and rinsed repeatedly with deionized water until a neutral pH was achieved. Diatom slurries were then dried onto coverslips and permanently mounted on microscope slides using Naphrax® mounting medium. Diatom microfossils were counted at 1000 × under oil immersion, using a Nikon Eclipse 80i microscope with differential interference contrast optics. A minimum of 400 diatom

Table 1 Selected limnological data for Sam and Wolfgang lakes, presented as 2-year means (2010–2011)

Lake name	Decimal Degree		Distance to sea (km)	Lake depth (m)	Area (ha)	pH	Conductivity (µS/cm)	SiO ₃ (mg/L)	TP (µg/L)	TIN (µg/L)	DOC (µg/L)
	Lat (N)	Long (W)									
Sam	54.76	– 84.60	53	1.7	32	8.1	160.5	0.5	8.0	21.0	6.7
Wolfgang	54.85	– 84.47	43	1.2	157	7.9	146.0	0.8	15.2	32.0	9.1

valves were counted for each sample and diatoms were identified using Krammer and Lange-Bertalot (1986–1991) and Antoniadou et al. (2008).

*Spectrally inferred chlorophyll *a**

To track temporal changes in whole-lake production of these lakes, we used spectral analysis to infer trends in sedimentary chlorophyll *a* concentration (Michelutti et al. 2010). Briefly, this analysis infers chlorophyll *a* based on a unique trough found in the 650–700 nm range of the spectral profile of the sediments. The area of this trough has been correlated to the concentration of chlorophyll *a* and its major derivatives in the sediment, providing a rapid, non-destructive method for estimating primary production. Following the development of this technique, research has demonstrated the applicability of the method in both temperate and Arctic environments (Michelutti et al. 2010), as reviewed by Michelutti and Smol (2016). Sedimentary spectral profiles were obtained using a FOSS NIRSystems Model 6500 series Rapid Content Analyzer, operating over the range of 400–2500 nm.

Elemental and isotope composition

Bulk organic carbon and nitrogen elemental and isotope composition were measured at 0.5-cm sediment intervals for both lakes. Samples were prepared for analysis following standard methods described by Wolfe et al. (2001). 1 M hydrochloric acid (8–10% by volume) was applied to samples in order to remove any carbonate material. The supernatant of the samples was then aspirated and samples were rinsed repeatedly with de-ionized water until a neutral pH was obtained. The samples were then freeze-dried and sieved to < 500 μm to remove microfossil plant debris. The remaining fine fraction was then analysed for organic carbon and nitrogen elemental and isotope composition using a continuous flow isotope ratio mass spectrometer (CF-IRMS) at the University of Waterloo Environmental Isotope Laboratory. Carbon and nitrogen ratios were calculated using percent dry weight organic carbon and nitrogen contents. Stable nitrogen isotope ratios were reported as $\delta^{15}\text{N}$ (‰) relative to atmospheric nitrogen (AIR).

Statistical analyses

Principal components analysis (PCA) was used to detect major patterns of variation in the diatom data and to facilitate comparisons in the magnitude and timing of changes between the two cores. The default settings in Canoco version 4.5 (ter Braak and Šmilauer 2002) were used to generate PCA sample scores on square-root transformed species data. For each sedimentary interval, diatom species diversity was calculated using Hill's N_2 (the number of very abundant taxa in a given sample) using Canoco version 4.5 (ter Braak and Šmilauer 2002). Stratigraphic zones in both the diatom and elemental/isotope data were determined by constrained hierarchical clustering, following the Constrained Incremental Sum of Squares (CONISS) methodology described in Grimm (1987), using the "rioja" package (Juggins 2009) in R v. 2.13.2.

Limnological changes were plotted against continuous temperature data (1943–2011) available from the Churchill meteorological station (Environment and Climate Change Canada: <http://www.cccma.ec.gc.ca/hccd/>). Churchill, Manitoba is the nearest climate station within the western HBL with a continuous climate record (located ~ 700 km from the study lakes) and, similar to our study sites, is located close to the Hudson Bay coast. Annual and seasonal temperature data from the Churchill record were significantly correlated to records from Winisk, ON, which is located much closer to the study sites (~ 90 km away), but where the climate record was interrupted and the station was re-located farther inland to Peawanuck in the 1980s because of flooding. Direct comparisons between annually resolved time series data and lake sediment proxy data are always difficult, as the time period represented by each sediment interval may vary with core compression and varying sedimentation rates. To help align these datasets, air temperature data were averaged to match the period of accumulation for each sediment interval based on ^{210}Pb dates, with 6–8 years of instrumental data averaged per sediment interval. Correlations of mean annual and seasonal air temperature anomalies with biological indices were performed using a Spearman rank correlation using the "rcorr" function of the "Hmisc" package (v. 3.9-2; Harrell Jr 2012) in R 2.13.2. Seasonal time periods were defined as: spring (March, April, and May); summer (June, July, and

August); fall (September, October, and November); and winter (December, January, and February). Following Rühländ et al. (2013), the Churchill annual and spring air temperature data are plotted as anomalies from the long-term (1971–2000) baseline.

Results

^{210}Pb dating

Background ^{210}Pb activities, estimated as the mean ^{214}Bi concentration from all dated samples, were reached at core depths of ~ 24 cm and ~ 15 cm in Wolfgang and Sam lakes, respectively (Figs. 2, 3). Neither lake followed an ideal exponential decline curve for ^{210}Pb . The dating profile for Wolfgang Lake (Fig. 2) showed a flattening of the ^{210}Pb activity curve from core depths of 8–20 cm, with a corresponding increase in inferred sedimentation rates. In Sam Lake (Fig. 3), the upper 3 cm of the sediment core showed variable ^{210}Pb activity, indicating possible physical or biological mixing near the sediment–water interface in this shallow lake (Appleby 2001). However, relatively well resolved peaks in the ^{137}Cs activity profiles from both cores provide independent support for the age-depth models, with ^{137}Cs peaks observed at inferred ages of ~ 1966 and 1969 for Wolfgang and Sam lakes, respectively.

Wolfgang Lake

Diatoms from both sediment cores were well preserved in all intervals counted with no obvious signs of silica dissolution or valve breakage. Prior to a marked taxonomic shift in the mid-1990s, diatom assemblages in Wolfgang Lake were dominated (up to 60%) by small benthic fragilarioid taxa (Fig. 4). Beginning in the mid-1990s, we recorded a concurrent increase in whole-lake primary production (approximated as chlorophyll *a* concentration) and diatom species diversity (Hill's N_2), which included increases in relative abundances of several periphytic taxa (from the genera *Cymbella* (sensu lato), *Brachysira*, *Achnanthes* (sensu lato) and *Nitzschia*; Fig. 4). Based on CONISS and broken-stick analysis, the diatom species assemblage change in the mid-1990s (4 cm) was the only notable taxonomic change recorded throughout the sediment core.

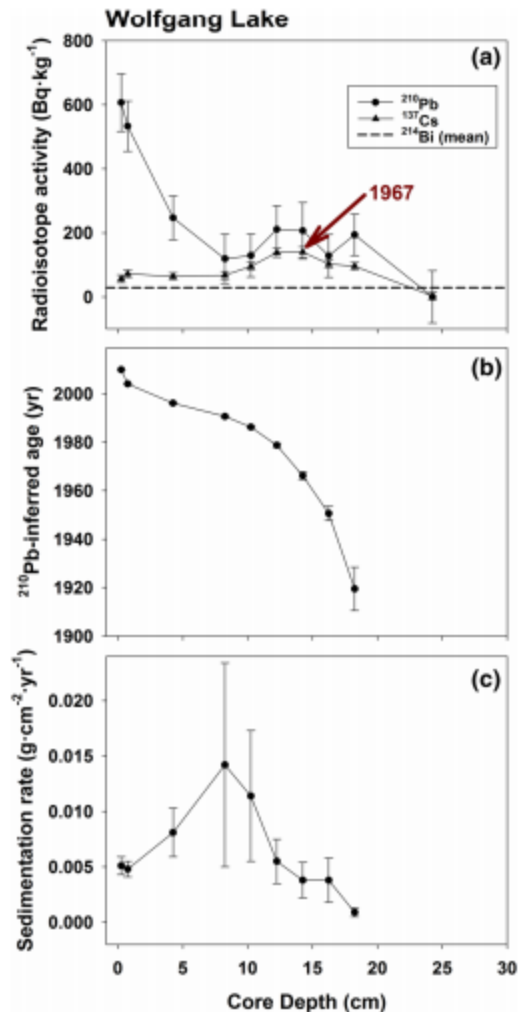


Fig. 2 Radiometric dating analysis of lake sediments from Wolfgang Lake showing **a** ^{210}Pb , ^{137}Cs activities (in Bq kg^{-1}), and the mean ^{214}Bi activity from all dated sections (dashed vertical line), plotted against core depth, **b** ^{210}Pb inferred year plotted against core depth, with dating errors associated with each dating interval, and **c** sedimentation rate (in $\text{g cm}^{-2}\text{year}^{-1}$) plotted against core depth, with estimated errors shown

In Wolfgang Lake, $\delta^{15}\text{N}$ and C/N records were stable throughout the duration of the sediment core (Fig. 6a). There was a gradual decline in %N in Wolfgang Lake, which began at a core depth of ~ 9 cm (ca. late 1980s).

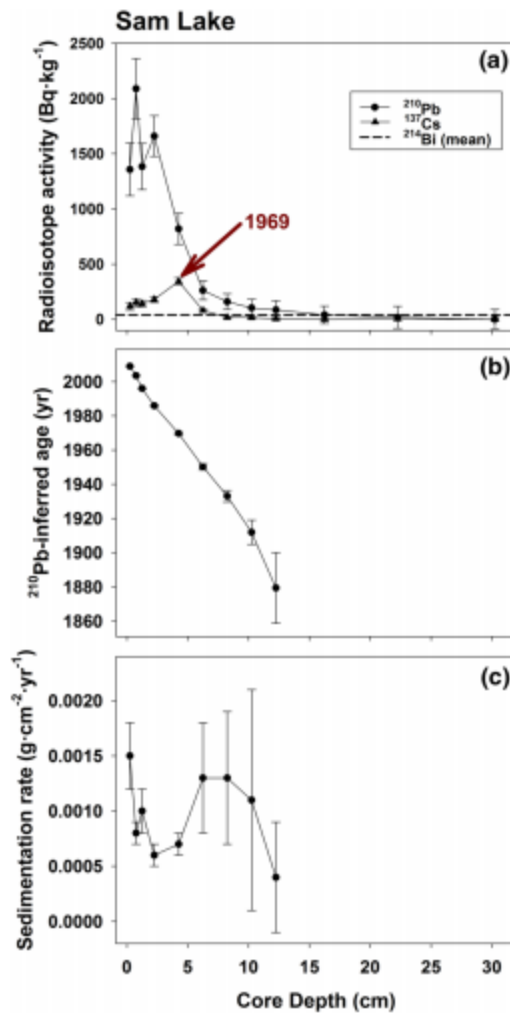


Fig. 3 Radiometric dating analysis of lake sediments from Sam Lake showing **a** ²¹⁰Pb, ¹³⁷Cs activities (in Bq kg⁻¹), and the mean ²¹⁴Bi activity from all dated sections (dashed vertical line), plotted against core depth, **b** ²¹⁰Pb inferred year plotted against core depth, with dating errors associated with each dating interval, and **c** sedimentation rate (in g cm⁻²·year⁻¹) plotted against core depth, with estimated errors shown

Sam Lake

Diatom species assemblage changes in Sam Lake were clear but muted relative to those described in Wolfgang Lake, with no apparent directional trend in species diversity (Fig. 5). The most pronounced taxonomic shift, as identified by CONISS, occurred

at ~ 4 cm depth in the sediment core (early 1970s) and was characterized by a decline in the relative abundance of several *Navicula (sensu lato)* taxa [e.g., *Eolimna minima* (Grunow) Lange-Bertalot and *Selaphora pupula* (Kützing) Mereschowsky] and contemporaneous increases in *Brachysira vitrea* (Grunow) R. Ross, *Encyonopsis falaisensis* (Grunow) Krammer and Lange-Bertalot, and several planktonic taxa [*Discostella stelligera* (Cleve and Grunow) Houk and Cleve, *Asterionella formosa* Hassall, and *Fragilaria crotonensis* Kitton; Fig. 5]. Concurrent with the ca. 1970 shift in the diatom species assemblage, we documented an increase in whole-lake primary production. However, a marked decline in spectrally-inferred chlorophyll *a* concentration occurred ca. 1980 and persisted until the most recent sediment interval (ca. 2011), at which time chlorophyll *a* increased sharply (Fig. 3). This decline in chlorophyll *a* coincides with variable ²¹⁰Pb activity noted near the surface of the Sam Lake core.

In Sam Lake, geochemical changes occurred in both the pre-industrial sediments (at ~ 40 cm core depth), and then again in the recent sediments (Fig. 6b). In the pre-industrial sediments, these changes were characterized by a ~ 1.25 ‰ increase in δ¹⁵N along with a concurrent decrease in sediment ‰N. Since ca. 1970, ‰N has increased and δ¹⁵N decreased, returning to levels observed in pre-industrial sediments (at core depths of > 40 cm) (Fig. 6b).

Inter-lake comparisons and climate correlations

In Wolfgang Lake, we observed significant correlations between the mean annual air temperature anomaly (relative to a 1970–2000 baseline) and increases in primary production ($r = 0.66, p < 0.01$; Fig. 7a) and diatom species diversity ($r = 0.56, p = 0.01$; Fig. 7a). We also found significant correlations between diatom assemblage changes (i.e., PCA axis 1 scores) and the mean annual ($r = 0.66, p < 0.01$; Fig. 7a), mean fall ($r = 0.56, p < 0.01$), and mean winter ($r = 0.59, p < 0.01$) air temperature anomalies.

Similarly, we found significant correlations between the changes observed in the diatom species assemblage of Sam Lake and recent climate change metrics. Specifically, we noted a positive correlation between diatom PCA axis 1 sample scores and the mean spring air temperature anomaly at Churchill

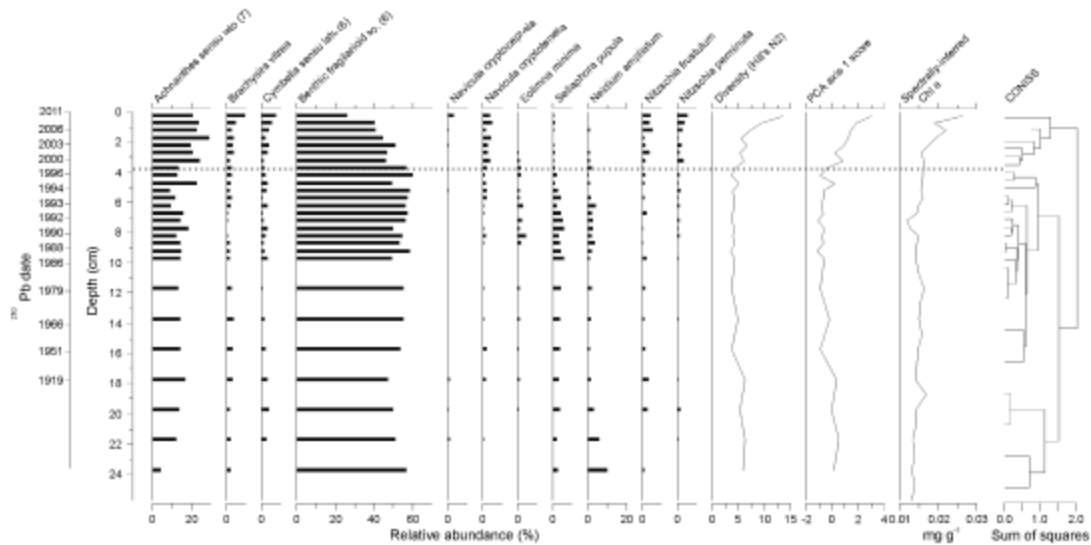


Fig. 4 Horizontal dashed line depicts zonation determined through constrained incremental sum of squares (CONISS) and deemed important by broken stick analysis. Diversity (as Hill's N_2), diatom species assemblage shifts (PCA axis 1 sample scores), and spectrally inferred chlorophyll *a* are also shown. The Benthic fragilarioid sp. category includes *Fragilaria capucina*, *F. capucina* var. *vaucheriae*, *Pseudostaurosira brevistriata*, *Staurosira construens* var. *venter*, *Staurosirella*

pinnata, and *S. pinnata* var. *intercedens*. *Cymbella* sensu lato includes *Encyonema hebridicum*, *E. minutum*, *Encyonopsis cestaii*, *E. descripta*, *E. microcephala*, and *E. falaisensis*. *Achnanthes* sensu lato includes *Achnanthes saccula*, *Achnantheidium minutissimum*, *A. macrocephalum*, *A. rosenstockii*, *Encocconeis flexella*, *Psammothidium curtissimum*, and *Rosithidium petersenii*

($r = 0.68$, $p < 0.01$, Fig. 7b). No significant correlations were observed between the biological metrics and annual or the other seasonal (summer, fall and winter) air temperature anomalies. However, an examination of the relationship between changes in planktonic diatom species and the mean spring air temperature anomaly revealed a significant correlation ($r = 0.70$, $p < 0.01$, Fig. 7b), as has been reported for deeper lakes in the HBL (Rühland et al. 2013; mean planktonic relative abundance versus mean annual air temperature anomaly).

Discussion

Changes in diatom assemblages

Our paleolimnological analyses provide evidence of biological and geochemical responses to recent warming in shallow sub-arctic lakes. However, consistent with previous studies (Smol and Douglas 2007a, b; Rühland et al. 2015), variability in the magnitude and

nature of the proxy changes was related to site and catchment-specific differences between these two shallow lakes. In Wolfgang Lake we documented an increase in the complexity and diversity of benthic/littoral taxa in the modern sediments, characterized by higher relative abundances of a number of periphytic forms, that was temporally coherent (mid-1990s) with increases in mean annual air temperature. These taxonomic changes, from a simple benthic assemblage towards a diversified and complex benthic community, coincided with increased primary production (i.e., spectrally inferred chlorophyll *a*). Diatom assemblage changes observed in Wolfgang Lake were consistent, taxonomically and temporally, with floristic changes observed in other shallow lakes in the HBL (Rühland et al. 2014), and throughout the Arctic where climate warming has resulted in increased availability and variety of littoral habitat (Douglas et al. 1994; Smol et al. 2005; Smol and Douglas 2007a; Roberts et al. 2015; Rühland et al. 2015).

Clear changes in relative abundances of benthic taxa were observed in the upper sedimentary intervals

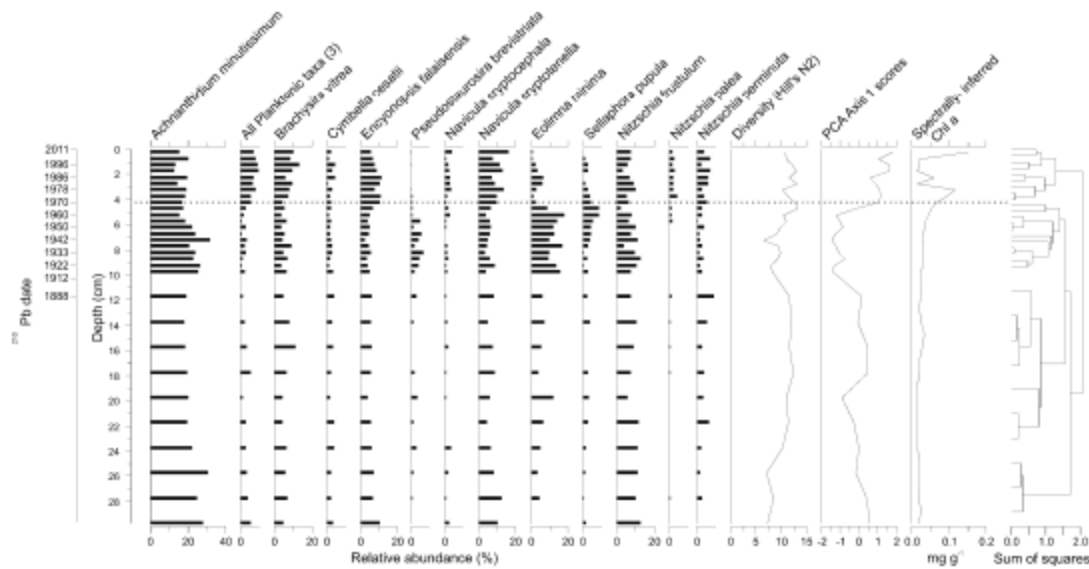


Fig. 5 Horizontal dashed line depicts zonation determined through contained incremental sum of squares (CONISS) and deemed important by broken stick analysis. Diversity (as Hill's N2), diatom species assemblage shifts (PCA axis 1 sample

scores), and spectrally inferred chlorophyll *a* are also shown. The Planktonic taxa group included *Discostella stelligera*, *Asterionella formosa*, and *Fragilaria crotonensis*

of Sam Lake, with some similarity to the taxonomic changes recorded in Wolfgang Lake. For example, both lakes underwent an increase in relative abundance of several periphytic forms [e.g., *Cymbella* (sensu lato), *Nitzschia* and large *Navicula*, and *Brachysira* taxa]. These benthic diatoms are commonly found attached to a variety of substrates (mud, rocks, mosses and macrophytes). Concurrent with these increases, declines in species reported as epipellic/epilithic (e.g., *Eolimna minima*, *Sellaphora pupula*: Mann et al. 1999; Cho 2000) were observed in both lakes. With climate warming, reduced ice cover and a lengthening of the growing season may promote the establishment and expansion of aquatic mosses and plants (Smol 1988), thus facilitating the diversification and growth of the epiphytic taxa that we have documented here. Similar taxonomic changes have also been observed in the Canadian High Arctic (Smol et al. 2005; Smol and Douglas 2007a, b), in other shallow lakes in the HBL (Stuart, Billbear, Julison, and Cassie lakes; Rühland et al. 2014), and elsewhere (Roberts et al. 2015; Rühland et al. 2015).

Contemporaneous with benthic species changes, planktonic diatom taxa in Sam Lake doubled in relative abundance to > 5%, a change that was

significantly correlated with trends in spring air temperature (Fig. 7b). Although this change was not observed in Wolfgang Lake, an increased importance of planktonic taxa in these polymictic, shallow systems is consistent with findings from other shallow lakes in the HBL. For example, Paterson et al. (2014) found evidence of blooms of planktonic algae in shallow HBL lakes when sampling phytoplankton during particularly warm temperatures in mid-summer, including relatively high biovolumes of the diatoms *Cyclotella* (sensu lato) and *Asterionella formosa*, and the presence of *Mallomonas*, a genus of unicellular, planktonic chrysophytes (Siver 1991). Likewise, a recent “top–bottom” paleolimnological survey of lakes in this HBL region, which included Sam and Wolfgang lakes, found higher relative abundances of several planktonic taxa in the modern sediments of all lakes studied including nine shallow lakes (Rühland et al. 2014). In the “Ring of Fire” region, ~ 250 km farther south but still within the HBL, Hargan et al. (2016) also reported the first arrival and increase in the relative abundances of planktonic diatoms during the past few decades in two shallow lakes ($Z_{max} \sim 2$ m), that were attributed to recent warming. Thus, while benthic taxa clearly dominate

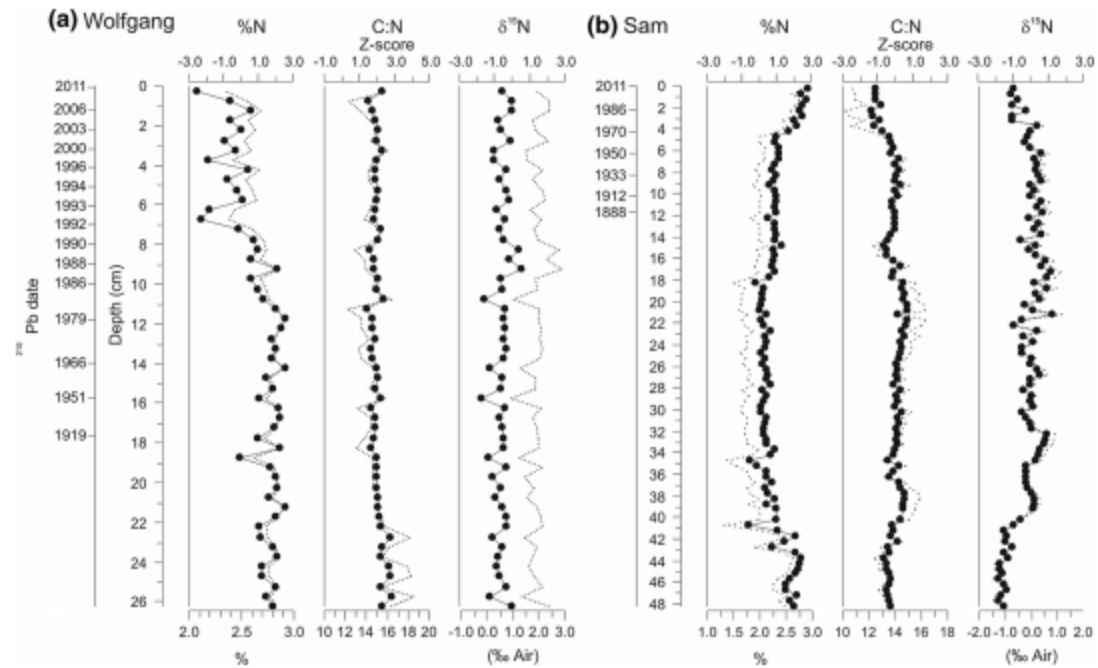


Fig. 6 Results of sedimentary elemental and isotope analysis (%N, C:N and $\delta^{15}\text{N}$) from **a** Wolfgang Lake and **b** Sam Lake presented as stratigraphic profiles against both sediment depth

and age (based on ^{210}Pb dating). Data are summarized as both measured values (black circles and solid lines) and standardized scores (dotted lines)

the diatom assemblages of shallow lakes in the HBL, widespread increases in the relative importance of planktonic taxa are now being reported in many lakes, indicating these changes are ecologically important. As reported elsewhere (Taranu et al. 2012), it is possible that these polymictic systems stratify for short periods of time (hours to days) during warm periods, allowing for the rapid proliferation of planktonic taxa.

Changes in geochemistry

Similar diatom responses to those we have documented in Sam Lake (i.e., the increased relative abundance of cyclotella and pennate planktonic taxa) have been attributed to the long-range transport and deposition of anthropogenic contaminants in some lakes (Wolfe et al. 2003, 2006). For example, in two ponds on Baffin Island, Wolfe et al. (2006) partially attributed diatom species changes to ^{15}N depletion and increased %N. They suggested that these isotopic signatures were indicative of nutrient enrichment from

atmospheric nitrogen deposition, which has increased globally by as much as 10% annually in the 20th century as a result of fertilizer production, cultivation of nitrogen-fixing legumes, and the release of nitrogen oxides associated with the burning of fossil fuels (Sheldrick 1987; Matthews 1994). However, global assessments by Vet et al. (2014) indicate that atmospheric nitrogen deposition in the HBL region is very low, and geochemical data from the Sam and Wolfgang Lake sediment cores offer little evidence that atmospheric nitrogen deposition is responsible for the diatom changes we document here (Fig. 4). In Wolfgang Lake, where notable changes in diatom assemblages have occurred since the mid-1990s, we document no directional change in $\delta^{15}\text{N}$ or C/N ratio. Furthermore, rather than an increase in %N that would be expected with increased inputs from deposition, we observed a decline since the mid-1990s (Fig. 3a). In Sam Lake, the geochemical changes throughout the core are subtle with current values falling within the range of long-term variability recorded in the sediment core, and representing a return to pre-industrial levels

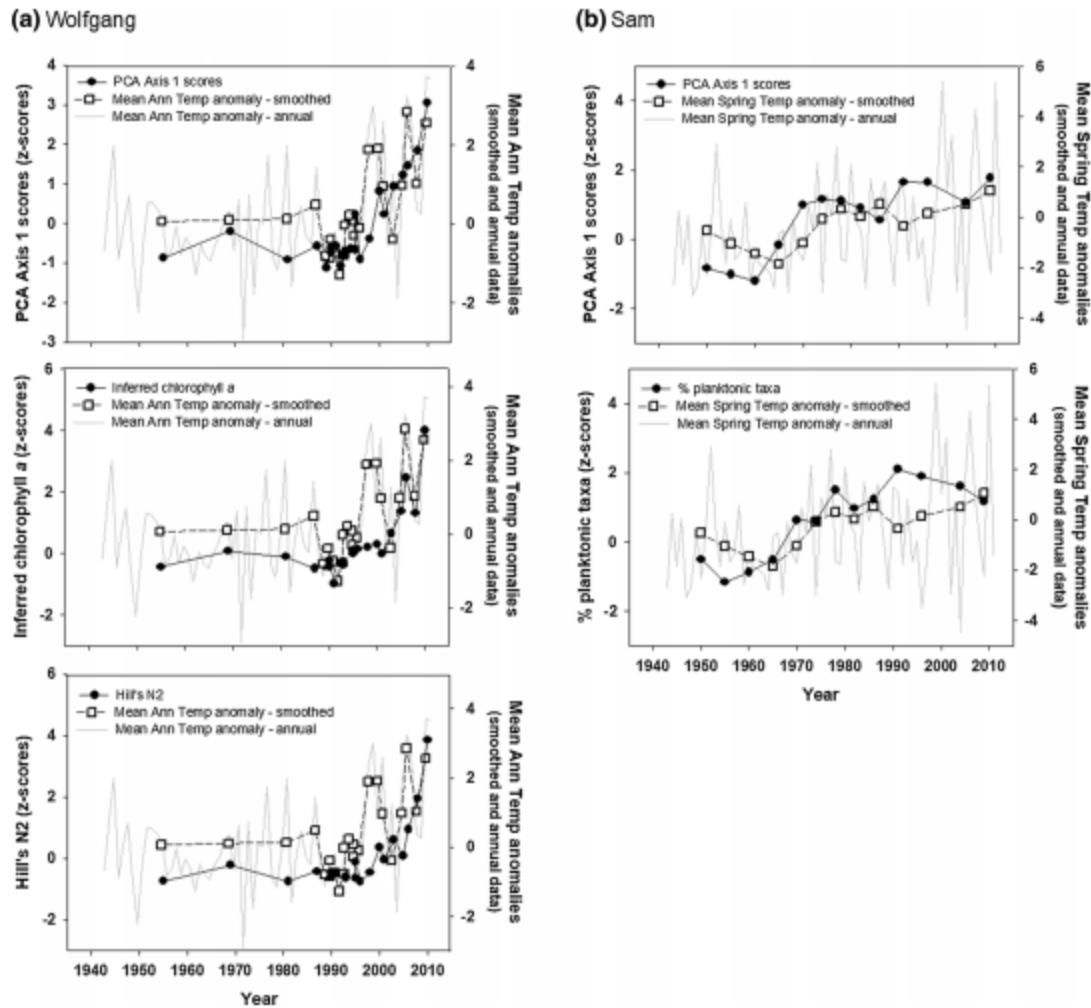


Fig. 7 **a** Trends in diatom assemblage composition (PCA axis 1 scores), primary production (inferred chlorophyll *a*, standardized as z-scores) and species diversity (Hills N2, standardized as z-scores) from Wolfgang Lake, plotted against mean annual temperature anomalies. Temperature anomalies are presented as both adjusted (open squares) and annual (solid grey line) data. **b** Trends in diatom assemblage composition (PCA Axis 1

scores), and % planktonic taxa (standardized as z-scores) from Sam Lake, plotted against mean spring temperature anomalies. Temperature anomalies are presented as both adjusted (open squares) and annual (solid grey line) data. Mean annual and mean spring air temperature anomalies were calculated relative to a 1971–2000 baseline, using data from the Churchill (Manitoba) climate station from 1953 to 2011

(Fig. 3b). Furthermore, nitrogen isotope changes in Sam Lake (ca. 1970) post-date the timing expected under an atmospheric deposition scenario.

With minimal supporting data in this remote region, it would be speculative to comment on the specific reasons for the differing geochemical signals over time in the study lakes, although it is worth noting that the timing of these changes correlates well with

diatom assemblage changes, suggesting a common driver. As described below, a number of factors may have contributed to differences in the observed geochemical signals, including differences in the organic matter supply related to variations in catchment vegetation and permafrost extent (Wolfe et al. 1999; Talbot 2001). Furthermore, lake-specific differences in hydrological connectivity may have

contributed to variability in the delivery of organic matter, and to the relative importance of precipitation in the lakes' water and nutrient budgets (Wolfe et al. 2011).

Variability in shallow lakes: local factors moderate biological and geochemical responses to warming

Diatom species assemblage changes in Sam Lake predated those observed in Wolfgang Lake by approximately two decades. The shift to an assemblage characterized by more planktonic taxa was comparable to changes reported for deeper lakes of the Sutton River region of the HBL, where temperature anomalies (both annual and seasonal) were significantly correlated to increased relative abundances of planktonic taxa, increased species diversity (Hill's N_2) and increased primary production (i.e., chlorophyll a concentration) (Rühland et al. 2013). Similar increases in planktonic taxa have also been noted in shallow lakes in the Ring of Fire, where the first records of planktonic species in McFaulds Lake and Symons lakes were recorded in the 1900s and the 1960s, respectively (Hargan et al. 2016). Temporal variation in the response of planktonic taxa in Wolfgang, Sam and other northern Ontario lakes suggest that local scale factors such as morphology, permafrost dynamics and hydrological connectivity likely mediate threshold responses to climate in these systems, and in shallow lakes in general.

For example, important morphometric differences exist between Sam and Wolfgang lakes. Wolfgang Lake is substantially larger than Sam Lake in both surface area (157 ha vs. 32 ha) and fetch (approx. 1.6 km vs. 0.6 km). These properties may significantly influence the thermal regimes of lakes, altering the strength and duration of thermal stratification (Gorham 1964; Timms 1975; Hanna 1990; Rühland et al. 2015). As noted above, it is possible that the smaller Sam Lake may be more thermally stable for longer periods in the summer as a result of its smaller fetch. This may account for the differences we observe in the nature (i.e., the presence of planktonic taxa in Sam Lake) and earlier timing of the diatom species assemblage changes.

In addition, previous research has also shown that the degree of permafrost development (continuous versus discontinuous) may influence the water chemistry of lakes in the HBL region (Paterson et al. 2014)

that, in turn, may have contributed to differences in diatom assemblage changes and geochemistry in Sam and Wolfgang lakes. These lakes reside very near the boundary between continuous and discontinuous permafrost and thus it is possible that recent climate change has altered permafrost conditions at a local scale. For example, it is well documented that the presence or absence of permafrost affects the infiltration of surface water and groundwater flow (MacLean et al. 1999; Carey 2003; Kawahigashi et al. 2004; Jones et al. 2005; O'Donnell and Jones 2006), and may result in the release of previously bound nutrients (Vincent et al. 2013); however, given the lack of ground-truthed data for our isolated lakes, we can only speculate on possible differences in their hydrological connectivity and permafrost dynamics within their surrounding catchments.

Climate and hydrological connectivity

As well as direct and indirect impacts on physical and chemical properties of lakes, climate warming may also alter the hydrology of sub-arctic freshwater systems. For example, changes in hydrological connectivity attributed to thawing permafrost and increased surface water-groundwater interaction likely contributed to divergent hydrological responses to recent warming in four HBL ponds near Churchill (Wolfe et al. 2011). Limnological characteristics of ponds in this region are likewise influenced by climatic and hydrological conditions (Bos and Pellatt 2012; White et al. 2014).

Visual inspection (Google Earth[®]; 2005 image) may further illustrate potential variability in limnological responses associated with hydrological connectivity. By constructing a simple schematic of water bodies around Sam and Wolfgang lakes, Sam Lake appears to currently be relatively isolated, while Wolfgang Lake is surrounded by several shallow water bodies within 250 m of its shoreline (Fig. 8). Thus, we speculate that some of these small ponds may become hydrologically connected to Wolfgang Lake during the ice-free season. In the northwestern HBL, hydrological connectivity in ponds, both temporary and permanent, has been shown to result in higher suspended sediment and total nitrogen concentrations, while lakes without connectivity generally show rising alkalinity and ionic content as evaporative concentration dominates the lake water balance

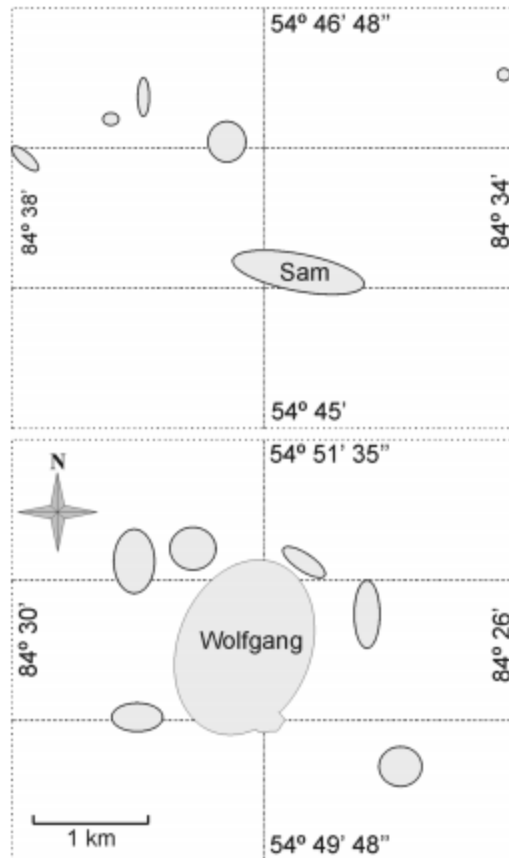


Fig. 8 Schematic diagram of Sam and Wolfgang lakes, showing the surrounding water bodies. The image is transcribed from a 2005 Google Earth™ image

(White et al. 2014). While it is not possible to determine the extent of hydrological connectivity in our study lakes with the information available, water chemistry data record higher nutrient concentrations in Wolfgang Lake, consistent with connectivity. Similarly, higher conductivity in Sam Lake (despite being 10 km farther inland from Hudson Bay) is consistent with potential evaporative concentration associated with its relative isolation (Table 1). A significant correlation between diatom species assemblage shifts (as PCA axis 1 scores) and spring precipitation in Sam Lake ($r = -0.65$, $p = 0.02$), which were not present in Wolfgang Lake, also suggests that it has responded to historical fluctuations in precipitation and may be less influenced by groundwater inputs. Furthermore, Wolfgang Lake

has a much higher sediment deposition rate than Sam Lake based on ^{210}Pb dating, supporting the notion of increased hydrological inputs.

Conclusions

Evidence provided by recent limnological and paleolimnological surveys of the HBL suggests that relatively deep lakes in this region have been altered by 20th century climate warming (Paterson et al. 2014; Rühland et al. 2013, 2014). We have presented detailed paleolimnological and geochemical results for two shallow sub-arctic lakes in the Sutton River region of the HBL. In both lakes we record abrupt, albeit subtle, shifts among benthic diatom taxa from assemblages predominantly associated with sediments to more diverse assemblages that include an increased abundance of epiphytic diatoms. In Wolfgang Lake, we recorded increases in whole-lake production and diatom diversity, changes that are consistent with a longer-ice free period and longer growing season. Unlike Wolfgang Lake, Sam Lake registered an increase in planktonic diatoms in the upper sediments that is similar to changes recorded in deeper lakes of this region (Rühland et al. 2013). The timing of limnological change in Wolfgang Lake supports other regional evidence (Rühland et al. 2014) that warming during the past ~ 20 years has led to notable biological responses in these aquatic systems. The timing of the limnological changes in Sam Lake pre-dates perturbations in mean annual temperature by ~ 20 years and suggests that a more complex mechanism, and seasonal warming, may be important. We speculate that differences in hydrological connectivity and permafrost dynamics, in part influenced by climate change, combined with differences in lake morphometry, likely contributed to the observed differences.

The paleolimnological examination of only two shallow lakes in the Sutton River region limits our ability to make broad statements about regional limnological change in the HBL, particularly given the temporal variability in the responses we have documented. Nevertheless, it is clear that the biological and geochemical responses to warming in shallow lakes may vary because of differences in local, catchment-scale factors, including permafrost extent and vegetation (Shinneman et al. 2016). This is true of

lakes located in the same geographic region and experiencing similar climatic forcing, emphasizing the need to understand the local context when interpreting long-term trends.

Acknowledgements This research was supported by the Ontario Ministry of the Environment and Climate Change through the Climate Change and Multiple Stressor Aquatic Research Program at Laurentian University, as well as the Natural Sciences and Engineering Research Council of Canada. We would also like to thank Albert and Gilbert Chookomolin for their assistance with field surveys, and Hearst Air for their professional service and safe access to these remote lakes.

References

- Antoniades D, Hamilton PB, Douglas MSV, Smol JP (2008) Diatoms of North America: The freshwater floras of Prince Patrick, Ellef Ringnes and northern Ellesmere Islands from the Canadian Arctic Archipelago. Koeltz Scientific Books, Koenigstein
- Appleby PG (2001) Chronostratigraphic techniques in recent sediments. In: Last WM, Smol JP (eds) Tracking environmental change using lake sediments: basin analysis, coring, and chronological techniques, vol 1. Kluwer Academic Publishers, Dordrecht, pp 171–203
- Battarbee RW, Jones VJ, Flower RJ, Cameron NG, Bennion H, Carvalho L, Juggins S (2001) Diatoms. In: Smol JP, Birks HJB, Last VM (eds) Tracking environmental change using lake sediments, vol 3. Terrestrial, algal, and siliceous indicators. Kluwer, Dordrecht, pp 155–202
- Bos DG, Pellatt MG (2012) The water chemistry of shallow ponds around Wapusk National Park of Canada, Hudson Bay Lowlands. *Can Water Res J* 37:163–175
- Bouchard F, Turner KW, MacDonald LA, Deakin C, White H, Farquharson N, Medeiros AS, Wolfe BB, Hall RI, Pienitz R, Edwards TWD (2013) Vulnerability of shallow subarctic lakes to evaporate and desiccate when snowmelt runoff is low. *Geophys Res Lett* 40:6112–6117
- Bramburger AJ, Reavie ED, Sgro GV, Estep LR, Shaw Chraïbi VL, Pillsbury RW (2017) Decreases in diatom cell size during the 20th century in the Laurentian Great Lakes: a response to warming? *J Plank Res* 39:199–210
- Carey SK (2003) Dissolved organic carbon fluxes in a discontinuous permafrost subarctic alpine catchment. *Perm Periglac Proc* 14:161–171
- Chapman WL, Walsh JE (1993) Recent variations of sea ice and air temperature in high latitudes. *Bull Am Meteor Soc* 74:33–47
- Cho K-J (2000) Epipsammic diatom flora of the Pukchong-Namdaechon River of North Korea. *Algae* 15:233–254
- Douglas MSV, Smol JP, Blake W Jr (1994) Marked post-18th century environmental change in high Arctic ecosystems. *Science* 266:416–419
- Dunn C, Freeman C (2011) Peatlands: our greatest source of carbon credits? *Carb Manage* 2:289–301
- Fallu MA, Pienitz R, Walker IR, Lavoie M (2005) Paleolimnology of a shrub-tundra lake and response of aquatic and terrestrial indicators to climate change in arctic Québec, Canada. *Palaeogeog Palaeoclim Palaeoecol* 215:183–203
- Gaston AJ, Smith PA, Provencher JF (2012) Discontinuous change in ice cover in Hudson Bay in the 1990s and some consequences for marine birds and their prey. *ICES J Mar Sci* 69:1218–1225
- Glew JR (1988) A portable extruding device for close interval sectioning of unconsolidated core samples. *J Paleolimnol* 1:235–239
- Glew JR (1989) A new trigger mechanism for sediment samplers. *J Paleolimnol* 2:241–243
- Gorham E (1964) Morphometric control of annual heat budgets in temperate lakes. *Limnol Oceanogr* 9:525–529
- Gough WA, Cornwell AR, Tsuji LJS (2004) Trends in seasonal sea ice duration in southwestern Hudson Bay. *Arctic* 57:299–305
- Grimm EC (1987) CONISS: A FORTRAN 77 program for stratigraphically constrained cluster analysis by the method of incremental sum of squares. *Comput Geosci* 13:13–35
- Hadley KR, Paterson AM, Stainsby EA, Michelutti N, Yao H, Rusak JA, Ingram R, McConnell C, Smol JP (2014) Climate warming alters thermal stability but not stratification phenology in a small north-temperate lake. *Hydrolog Proc* 28:6309–6319
- Hargan KE, Nelligan C, Jeziorski A, Rühland KM, Paterson AM, Keller W, Smol JP (2016) Tracking the long-term responses of diatoms and cladocerans to climate warming and human influences across lakes of the Ring of Fire in the Far North of Ontario, Canada. *J Paleolimnol* 56:153–172
- Hanna M (1990) Evaluation of models predicting mixing depth. *Can J Fish Aquat Sci* 47:940–947
- Harrell Jr FE (2012) Harrell Miscellaneous. <http://biostat.mc.vanderbilt.edu/wiki/Main/Hmisc>
- Hochheim KP, Barber DG (2010) Atmospheric forcing of sea ice in Hudson Bay during the fall period, 1980–2005. *J Geophys Res* 115:C05009. <https://doi.org/10.1029/2009JC005334>
- Hochheim KP, Barber DG (2014) An update on the ice climatology of the Hudson Bay system. *Arct Antarct Alp Res* 46:66–83
- Hoover C (2010) Hudson Bay ecosystem: past, present, and future. In: Ferguson SH, Loseto LL, Mallory ML (eds) A little less Arctic: top predators in the world's largest Northern Inland Sea, Hudson Bay. Springer, Dordrecht, pp 217–236
- Ingram RG, Girard RE, Paterson AM, Sutey P, Evans D, Xu R, Rusak J, Thomson C, Masters C (2013) Lake sampling methods. Ontario Ministry of the Environment, Dorset Environmental Science Centre, Dorset
- Jones JB Jr, Petrone KC, Finlay JC, Hinzman LD, Bolton WR (2005) Nitrogen loss from watersheds of interior Alaska underlain with discontinuous permafrost. *Geophys Res Lett*. <https://doi.org/10.1029/2004gl021734>
- Juggins S (2009) Analysis of Quaternary science data. <http://www.staff.ncl.ac.uk/staff/stephen.juggins/>
- Kawahigashi M, Kaiser K, Kalbitz K, Rodionov A, Guggenberger G (2004) Dissolved organic matter in small streams along a gradient from discontinuous to continuous permafrost. *Glob Change Biol* 10:1576–1586
- Krammer K, Lange-Bertalot H (1986–1991) Bacillariophyceae. In: Ettl H, Gerloff J, Heynig H, Mollenhauer D (eds)

- Stüßwasserflora von Mitteleuropa, vol 2. Gustav Fischer Verlag, Stuttgart/Jena, pp 1–4
- Laing TE, Pienitz R, Payette S (2002) Evaluation of limnological responses to recent environmental change and caribou activity in the Rivière George Region, northern Québec, Canada. *Arct Antarct Alp Res* 34:454–464
- MacLean R, Oswald MW, Irons JG, McDowell WH (1999) The effect of permafrost on stream biogeochemistry: a case study of two streams in the Alaskan (USA) taiga. *Biogeochemistry* 47:239–267
- Mallory ML, Loseto LL, Ferguson SH (2010) The future of Hudson Bay: new directions and research needs. In: Ferguson SH, Loseto LL, Mallory ML (eds) *A little less Arctic: top predators in the world's largest northern Inland Sea*, Hudson Bay. Springer, Dordrecht, pp 291–303
- Mann DG, Chepurnov VA, Droop SJM (1999) Sexuality, incompatibility, size variation, and preferential polyandry in natural populations and clones of *Sellaphora pupula* (Bacillariophyceae). *J Phycol* 35:152–170
- Martini IP (2006) The cold-climate peatlands of the Hudson Bay Lowland, Canada: brief overview of recent work. In: Martini IP, Martinez Cortizas A, Chesworth W (eds) *Peatlands: evolution and records of environmental and climate changes*. Elsevier, Amsterdam, pp 53–84
- Matthews E (1994) Nitrogenous fertilizers: global distribution of consumption and associated emissions of nitrous oxide and ammonia. *Glob Biogeochem Cyc* 8:411–439
- McLaughlin J, Webster K (2014) Effects of climate change on peatlands in the far north of Ontario, Canada: a synthesis. *Arct Antarct Alp Res* 46:84–102
- Michelutti N, Smol JP (2016) Visible spectroscopy reliably tracks trends in paleo-production. *J Paleolimnol* 56:253–265
- Michelutti N, Blais JM, Cumming BF, Paterson AM, Rühland KM, Wolfe AP, Smol JP (2010) Do spectrally inferred determinations of chlorophyll *a* reflect trends in lake trophic status? *J Paleolimnol* 43:205–217
- Nelligan C, Jeziorski A, Rühland KM, Paterson AM, Smol JP (2016) Managing lake trout lakes in a warming world: a paleolimnological assessment of nutrients and lake production at three Ontario sites. *Lake Reserv Manage* 32:315–328
- O'Beirne MD, Werne JP, Hecky RE, Johnson TC, Katsev S, Reavie ED (2017) Anthropogenic climate change has altered primary productivity in lake superior. *Nat Commun* 8:15713
- O'Reilly CM, Sharma S, Gray DK, Hampton SE, Read JS and 59 others (2015) Rapid and highly variable warming of lake surface waters around the globe. *Geophys Res Lett* 42. <https://doi.org/10.1002/2015gl066235>
- O'Donnell JA, Jones JB (2006) Nitrogen retention in the riparian zone of catchments underlain by discontinuous permafrost. *Freshw Biol* 51:854–864
- Obbard ME, Cattet MRL, Moody T, Walton LR, Potter D, Inglis J, Chenier C (2006) Temporal trends in the body condition of southern Hudson Bay polar bears. Climate change research information note, No 3. Applied Research and Development Branch, Ministry of Natural Resources, Sault Ste. Marie, Ontario
- Ontario Ministry of the Environment (1983) Handbook of analytical methods for environmental samples, vols. 1 and 2. Laboratory Services Branch, Ontario Ministry of the Environment and Energy, Sudbury, Ontario
- Paterson AM, Betts AA, Smol JP, Zeeb BA (2003) Diatom and chrysophyte algal response to long-term PCB contamination from a point-source in northern Labrador, Canada. *WASP* 145:377–393
- Paterson AM, Keller W, Rühland KM, Jones FC, Winter JG (2014) First assessment of regional water chemistry and plankton from lakes near the Sutton River, Hudson Bay Lowlands, Ontario, Canada. *Arct Antarct Alp Res* 46:121–138
- Paterson AM, Rühland KM, Anstey CV, Smol JP (2017) Climate as a driver of increasing algal production in Lake of the Woods, Ontario, Canada. *Lake Reserv Manage* 33:403–414
- Ponader K, Pienitz R, Vincent W, Gajewski K (2002) Limnological conditions in a subarctic lake (northern Québec, Canada) during the late Holocene: analyses based on fossil diatoms. *J Paleolimnol* 27:353–366
- Reavie ED, Sgro GV, Estep LR, Bramburger AJ, Shaw Chraïbi VL, Pillsbury RW, Cai M, Stow CA, Dove A (2017) Climate warming and changes in *Cyclotella* sensu lato in the Laurentian Great Lakes. *Limnol Oceanogr* 62:768–783
- Regehr EV, Lunn NJ, Amstrup SC, Stirling I (2007) Effects of earlier sea ice breakup on survival and population size of polar bears in western Hudson Bay. *J Wild Manage* 71:2673–2683
- Roberts KE, Lamoureux SF, Kyser TK, Muir DCG, Lafrenière Iqaluk D, Piefkowski AJ, Normandeau A (2017) Climate and permafrost effects on the chemistry and ecosystems of high Arctic Lakes. *Sci Rep* 7:13292
- Roberts S, Jones VJ, Allen JRM, Huntley B (2015) Diatom response to mid-Holocene climate in three small Arctic lakes in northernmost Finnmark. *Holocene* 25:911–920
- Rühland KM, Paterson AM, Smol JP (2008) Hemispheric-scale patterns of climate-related shifts in planktonic diatoms from North American and European lakes. *Glob Change Biol* 14:2740–2754
- Rühland KM, Paterson AM, Keller W, Michelutti N, Smol JP (2013) Global warming triggers the loss of a key Arctic refugium. *Proc Roy Soc Lond Ser B* 280:20131887
- Rühland KM, Hargan KE, Jeziorski A, Paterson AM, Keller W, Smol JP (2014) A multi-trophic exploratory survey of recent environmental change using lake sediments in the Hudson Bay Lowlands, Ontario. *Arct Antarct Alp Res* 46:139–158
- Rühland KM, Paterson AM, Smol JP (2015) Lake diatom responses to warming: reviewing the evidence. *J Paleolimnol* 54:1–35
- Schelske CL, Peplow A, Brenner M, Spence MCN (1994) Low-background gamma counting: applications for ²¹⁰Pb dating of sediments. *J Paleolimnol* 10:115–128
- Sheldrick WF (1987) World nitrogen survey, World Bank Technical Paper 59. The World Bank, Washington, DC
- Shinneman ALC, Umbanhowar CE Jr, Edlund MB, Hobbs WO, Camill P, Geiss C (2016) Diatom assemblages reveal regional-scale differences in lake responses to recent climate change at the boreal-tundra ecotone, Manitoba, Canada. *J Paleolimnol* 56:275–298
- Siver PA (1991) The biology of *Mallomonas*: morphology, taxonomy and ecology. Kluwer, Dordrecht

- Smol JP (1988) Paleoclimate proxy data from freshwater arctic diatoms. *Verh Int Verein Limnol* 23:837–844
- Smol JP (2016) Arctic and sub-Arctic shallow lakes in a multiple-stressor world: a paleoecological perspective. *Hydrobiologia* 778:253–272
- Smol JP, Douglas MSV (2007a) From controversy to consensus: making the case for recent climatic change in the Arctic using lake sediments. *Front Ecol Environ* 5:466–474
- Smol JP, Douglas MSV (2007b) Crossing the final ecological threshold in high Arctic ponds. *PNAS* 104:12395–12397
- Smol JP, Wolfe AP, Birks HJB, Douglas MSV, Jones VJ, Korhola A, Pienitz R, Ruhland KM, Sorvari S, Antoniades D, Brooks SJ, Fallu M-A, Hughes M, Keatley BE, Laing TE, Michelutti N, Nazarova L, Nyman M, Paterson AM, Perren B, Quinlan R, Rautio M, Saulnier-Talbot E, Siitonen S, Solovieva N, Weckstrom J (2005) Climate-driven regime shifts in the biological communities of Arctic lakes. *PNAS* 102:4397–4402
- Sorvari S, Korhola A, Thompson R (2002) Lake diatom response to recent Arctic warming in Finnish Lapland. *Glob Change Biol* 8:171–181
- Stainsby EA, Winter JG, Jarjanazi H, Paterson AM, Evans DO, Young JD (2011) Changes in the thermal stability of Lake Simcoe from 1980 to 2008. *JGLR* 37:55–62
- Talbot MR (2001) Nitrogen isotopes in paleolimnology. In: Last WM, Smol JP (eds) *Tracking environmental change using lake sediments: physical and geochemical methods*, vol 2. Kluwer, Dordrecht, pp 401–439
- Taranu ZE, Zurawell RW, Pick F, Gregory-Eaves I (2012) Predicting cyanobacterial dynamics in the face of global change: the importance of scale and environmental context. *Glob Change Biol* 18:3477–3490
- Tarnocai C (2006) The effect of climate change on carbon in Canadian peatlands. *Glob Planet Change* 53:222–232
- ter Braak CJF, Šmilauer P (2002) *CANOCO reference manual and CanoDraw for Windows user's guide: software for canonical community ordination v.4.5*. Microcomputer Power
- Timms BV (1975) Basic limnology of two crater lakes in Western Victoria. *Proc R Soc Victoria* 87:159–165
- Vet R, Artz RS, Carou S, Shaw M, Ro C-U, Aas W, Baker A, Bowersox VC, Dentener F, Galy-Lacaux C, Hou A, Pienaar JJ, Gillett R, Forti MC, Gromov S, Hara H, Khodzher T, Mahowald NM, Nickovic S, Rao PSP, Reid NW (2014) A global assessment of precipitation chemistry and deposition of sulfur, nitrogen, sea salt, base cations, organic acids, acidity and pH, and phosphorus. *Atmos Environ* 93:3–100
- Vincent WF, Laurion I, Pienitz R, Walter Anthony KM (2013) Climate impacts on Arctic lake ecosystems. In: Goldman CR, Kumagai M, Roberts RD (eds) *Climatic change and global warming of inland waters: impacts and mitigation for ecosystems and societies*. Wiley, New York, pp 27–42
- Weckström K, Weckström J, Huber K, Kamenik C, Schmidt R, Slavenmoser W, Rieradevall M, Weisse T, Psenner R, Kurmayer R (2016) Impacts of climate warming on Alpine lake biota over the past decade. *Arct Antarct Alp Res* 48:361–376
- White J, Hall RI, Wolfe BB, Light EM, Macrae ML, Fishback L (2014) Hydrological connectivity influences seasonal patterns of limnological conditions in shallow tundra ponds of the western Hudson Bay Lowlands. *Arct Antarct Alp Res* 46:218–235
- Wolfe AP, Van Gorp AC, Baron JS (2003) Recent ecological and biogeochemical changes in alpine lakes of Rocky Mountain National Park (Colorado, USA): a response to anthropogenic nitrogen deposition. *Geobiology* 1:153–168
- Wolfe AP, Cooke CA, Hobbs WA (2006) Are current rates of atmospheric nitrogen deposition influencing lakes in the eastern Canadian Arctic? *Arct Antarct Alp Res* 38:465–476
- Wolfe BB, Edwards TWD, Aravena R (1999) Changes in carbon and nitrogen cycling during tree-line retreat recorded in the isotopic context of lacustrine organic matter, western Taimyr Peninsula, Russia. *Holocene* 9:215–222
- Wolfe BB, Edwards TWD, Beuning KRM, Elgood RJ (2001) Carbon and oxygen isotope analysis of lake sediment cellulose: methods and applications. In: Last WM, Smol JP (eds) *Tracking environmental change using lake sediments*, vol 2. Physical and chemical techniques. Kluwer, Dordrecht, pp 373–400
- Wolfe BB, Light EM, Macrae ML, Hall RI, Eichel K, Jasechko S, White J, Fishback L, Edwards TWD (2011) Divergent hydrological responses to 20th century climate change in shallow tundra ponds, western Hudson Bay lowlands. *Geophys Res Lett*. <https://doi.org/10.1029/2011gl04976>

Publisher's Note Springer Nature remains neutral with regard to jurisdictional claims in published maps and institutional affiliations.

**SPRINGER NATURE LICENSE
TERMS AND CONDITIONS**

Apr 04, 2019

This Agreement between Wilfrid Laurier University -- Hilary White ("You") and Springer Nature ("Springer Nature") consists of your license details and the terms and conditions provided by Springer Nature and Copyright Clearance Center.

License Number	4557750113685
License date	Mar 28, 2019
Licensed Content Publisher	Springer Nature
Licensed Content Publication	Journal of Paleolimnology
Licensed Content Title	Biological and geochemical changes in shallow lakes of the Hudson Bay Lowlands: a response to recent warming
Licensed Content Author	Kristopher R. Hadley, Andrew M. Paterson, Kathleen M. Rühland et al
Licensed Content Date	Jan 1, 2019
Licensed Content Volume	61
Licensed Content Issue	3
Type of Use	Thesis/Dissertation
Requestor type	academic/university or research institute
Format	electronic
Portion	full article/chapter
Will you be translating?	no
Circulation/distribution	<501
Author of this Springer Nature content	yes
Title	Development and application of hydrological and limnological monitoring in pond-rich landscapes of Canada's subarctic National Parks
Institution name	n/a
Expected presentation date	May 2019
Requestor Location	Wilfrid Laurier University 75 University Ave W Department of Geography Arts Building Waterloo, ON N2L 3C5 Canada Attn: Hilary White
Total	0.00 CAD